

Glacier fluctuations and sediment transport at Vestre Blomsterskardsbreen, Folgefonna



Master's thesis in physical geography

Hella Wittmeier

Department of Geography

University of Bergen

Spring 2010



Front cover picture: Glacier snout of Vestre Blomsterskardsbreen. Picture is taken looking to the north.

Foreword

I would like to thank my supervisors, Dr. Jostein Bakke and Dr. Svein Olaf Dahl, for good supervising. Thank you for introducing me to the fascinating world of paleoclimate, I have learned so much from you.

Sunnhordland Kraftlag supported this work both financially and through providing cabin and boat during fieldwork; I would especially like to thank Bodil Øyre, Terje Sandvik and Egil Åkra.

Thank you to Bjørn Kvisvik, Reidar Løvlie and Ingelinn Aarnes for much help during lab work, and Hanne, Vigdis, Mareile and Tine for always being helpful and making the times spent in the lab good ones.

Thank you to Lisa, Eivind, Bjørn and Nick for joining the coring Lake Midtbotnvatn; and to Sigmund and Berit for providing a car.

Thank you to Franzi, Nina, Inga, Lars, Steffi and Stephan for joining me at field work, and for your enthusiasm on Norwegian nature. ☺

Friends and fellow students at the department were very important to me, thank you all for the nice times during the master studies, and for good discussions.

To my parents, Anne and Helge, thank you for all your support, and for always being there for me! You gave me the courage to study in Bergen. Thank you very much as well for joining me at field work.

Last but not least I want to thank Øystein for your great support and patience, without you this thesis would never have been possible.

Bergen, May 2010

Hella Wittmeier

Contents

Foreword	III
Contents	V
List of figures	IX
List of tables	XV
List of pictures	XVII
List of abbreviations	XIX
Abstract	XXI
1 INTRODUCTION AND APPROACH TO THE STUDY AREA	1
1.1 INTRODUCTION	1
1.2 PURPOSE OF THE STUDY	1
1.3 APPROACH TO THE STUDY AREA	2
1.4 DESCRIPTION OF THE STUDY AREA	3
1.5 BEDROCK GEOLOGY	5
1.6 CLIMATE	6
1.6.1 <i>Today's climate</i>	6
1.6.2 <i>Today's equilibrium line altitude</i>	8
1.6.3 <i>Precipitation</i>	9
1.6.4 <i>Temperature</i>	12
1.6.5 <i>Wind</i>	14
1.7 PREVIOUS RELEVANT INVESTIGATIONS IN THE STUDY AREA	14
2 QUATERNARY MAPPING OF THE STUDY AREA	19
2.1 QUATERNARY MAPPING - METHOD DESCRIPTION	19
2.1.1 <i>Aerial photographs</i>	19
2.1.2 <i>Base maps</i>	20
2.1.3 <i>Fieldwork equipment</i>	20
2.1.4 <i>Programs used for data handling (quaternary mapping)</i>	20
2.2 PRESENTATION AND INTERPRETATION OF LOCATIONS	20
2.2.1 <i>Glacial deposits</i>	21
2.2.1.1 <i>Marginal moraines</i>	21
2.2.1.2 <i>Till</i>	35
2.2.1.3 <i>Erratic blocks</i>	36
2.2.2 <i>Glacial erosion forms</i>	37
2.2.3 <i>Glaciofluvial deposits</i>	37
2.2.4 <i>Glaciolacustrine deposits</i>	39
2.2.5 <i>Glaciofluvial erosion forms</i>	40
2.2.6 <i>Rapid mass-movement deposits</i>	41
2.3 LICHENOMETRY	42
2.3.1 <i>Lichenometry – Method description</i>	42
2.3.2 <i>Lichenometry – Application</i>	44

2.3.3	<i>Lichenometry – Interpretation</i>	48
2.4	SUMMARY	52
3	ANALYSIS OF PROGLACIAL SEDIMENTS	53
3.1	PROGLACIAL SEDIMENTS	53
3.2	SEDIMENTATION AND AFFECTING FACTORS IN PROGLACIAL LAKES.....	55
3.3	CORING LOCATION IN A PROGLACIAL LAKE	56
3.4	ANALYSIS PARAMETERS	57
3.4.1	<i>Magnetic Susceptibility</i>	57
3.4.2	<i>Loss on ignition</i>	58
3.4.3	<i>Dry Bulk Density</i>	59
3.4.4	<i>Grain-size distribution</i>	60
3.4.5	<i>X-radiography and X-ray fluorescence</i>	62
3.4.6	<i>Dating</i>	63
3.4.6.1	<i>Radiocarbon dating</i>	63
3.4.6.2	<i>Lead dating</i>	65
3.5	LAKE MIDTBOTNVATN	66
3.5.1	<i>Site location Lake Midtbotnvatn</i>	66
3.5.2	<i>Core locations</i>	67
3.5.3	<i>Coring</i>	69
3.5.4	<i>Field observations and influencing factors on sedimentation in Lake Midtbotnvatn</i>	69
3.6	PRESENTATION OF DATA FROM LAKE MIDTBOTNVATN	72
3.6.1	<i>Programs used for data handling</i>	73
3.6.2	<i>Description of MIP-109 and presentation of analysis parameters</i>	73
3.6.3	<i>Description of MIP-209 and presentation of analysis parameters</i>	78
3.7	SEDIMENT PARAMETERS AS PROXY FOR GLACIAL ACTIVITY	83
3.8	SEDIMENTATION PROCESSES.....	86
3.9	INTERPRETATION	91
3.9.1	<i>Interpretation of MIP-109</i>	91
3.9.2	<i>Interpretation of MIP-209</i>	95
3.10	COMPARISON OF MIP-109 AND MIP-209	100
3.11	DATINGS	101
3.11.1	<i>Age-depth models</i>	105
3.11.2	<i>Sedimentation rates</i>	108
3.12	SUMMARY.....	110
4	CALCULATION AND RECONSTRUCTION OF PALAEOCLIMATE: EQUILIBRIUM LINE ALTITUDES AND RELATIVE GLACIAL ACTIVITY	111
4.1	EQUILIBRIUM LINE ALTITUDES –THEORY	111
4.1.1	<i>Accumulation Area Ratio (AAR)</i>	114
4.1.2	<i>Area Altitude Balance Ratio (AABR)</i>	114
4.2	RECONSTRUCTIONS OF FORMER ELAS	115

4.3	RECONSTRUCTED ELAS OF VESTRE BLOMSTERSKARDSBREEN.....	118
4.4	CORRECTION OF ISOSTATIC ADJUSTMENT.....	121
4.5	RECONSTRUCTION OF A RELATIVE GLACIAL ACTIVITY CURVE.....	123
4.6	VARIATIONS OF RELATIVE GLACIAL ACTIVITY OF VESTRE BLOMSTERSKARDSBREEN DURING THE LATE-HOLOCENE.....	125
5	DISCUSSION.....	127
5.1	SEDIMENTATION IN LAKE MIDTBOTNVATN.....	127
5.2	HOLOCENE VARIATIONS IN GLACIAL ACTIVITY OF VESTRE BLOMSTERSKARDSBREEN.....	128
5.2.1	<i>Early and mid-Holocene glacier and climate variations (earlier than 4235 cal. years BP).....</i>	<i>128</i>
5.2.2	<i>Late Holocene glacier and climate variations (the last 4235 cal. years BP).....</i>	<i>132</i>
5.2.2.1	The Medieval Warm Epoch.....	134
5.2.2.2	The Little Ice Age.....	135
5.2.2.3	Vestre Blomsterskardsbreen since the LIA.....	140
5.3	NATURAL CLIMATE VARIABILITY.....	141
5.4	VESTRE BLOMSTERSKARDSBREEN IN COMPARISON WITH OTHER GLACIER RECORDS IN THE NORTHERN HEMISPHERE.....	148
6	CONCLUSION.....	151
7	CLOSING REMARKS.....	153
	REFERENCES.....	155
	APPENDIX.....	167

List of figures

- FIGURE 1.1** 3D-ILLUSTRATION SHOWING THE FOLGEFONNA PENINSULA IN SOUTH-WESTERN NORWAY AND THE THREE PARTS OF FOLGEFONNA GLACIER: NORTHERN, MIDDLE AND SOUTHERN FOLGEFONNA. THE RED LINE INDICATES THE STUDY AREA, LOCATED AT THE SOUTH SIDE OF SOUTHERN FOLGEFONNA. (ILLUSTRATION: KJELL HELGE SJØSTRØM, UNIVERSITY OF BERGEN) 2
- FIGURE 1.2** GENERAL MAP OF THE STUDY AREA THAT IS INDICATED WITH RED LINE (UTM GRID SYSTEM WGS84, ZONE 32V) AND LOCATION OF THE STUDY AREA IN A MAP OF SOUTH NORWAY. 4
- FIGURE 1.3** GEOLOGICAL MAP OF THE STUDY AREA (RED LINE) (MODIFIED FROM LUTRO 2005)..... 6
- FIGURE 1.4** MAP OF THE MODERN NORTH ATLANTIC REGION. STUDY AREA AT THE FOLGEFONNA PENINSULA IS SHOWN IN THE RED FRAME. THE AVERAGE POSITION OF THE ATMOSPHERIC POLAR FRONT IS INDICATED BY RED ARROWS. THE LOW-PRESSURE FIELD NEAR ICELAND AND THE HIGH-PRESSURE-FIELD OVER SCANDINAVIA OR WESTERN RUSSIA HAVE IMPORTANT IMPACT ON THE CLIMATE OF NORWAY’S WEST COAST. THE BLACK ARROWS INDICATE THE MEAN OCEAN CURRENTS OF TODAY’S NORTH ATLANTIC REGION. (MODIFIED FROM BAKKE 2004, 3) 8
- FIGURE 1.5** A) MEAN ANNUAL PRECIPITATION (MM/YEAR) IN SOUTH NORWAY DURING THE NORMAL PERIOD 1961-1990. THE PRECIPITATION VALUES AT THE SOUTHWEST COAST OF NORWAY ARE VERY HIGH COMPARED TO THE INLAND. THE STUDY AREA IS MARKED WITH RED FRAME (MODIFIED FROM DET NORSKE METEOROLOGISKE INSTITUTT 2009A). B) DIAGRAM OF THE MEASURED MEAN MONTHLY PRECIPITATION RATES IN THE NORMAL PERIOD 1961-1990 AT THE CLIMATE STATIONS INDRE MATRE AND ULLENSVANG FORSØKSGÅRD (DET NORSKE METEOROLOGISKE INSTITUTT 2008) 10
- FIGURE 1.6** BASED ON TEN AT PRESENT EXISTING NORWEGIAN GLACIERS IN BOTH MARITIME AND CONTINENTAL CLIMATE REGIMES, A CLOSE NON-LINEAR (EXPONENTIAL) RELATIONSHIP BETWEEN MEAN ABLATION-SEASON TEMPERATURE (T) (1. MAY – 30. SEPTEMBER) AND ANNUAL WINTER PRECIPITATION (A) AT THE ELA IS DEMONSTRATED. (1. ÅLFOTBREEN, 2. ENGABREEN, 3. FOLGEFONNA, 4. NIGARDSBREEN, 5. TUNBERGDALS BREEN, 6. HARDANGERJØKULEN, 7. STORBREEN, 8. AUSTRE MEMURUBREEN, 9. HELLSTUGUBREEN, 10. GRÅSUBREEN) (DAHL ET AL. 1997, 170)..... 11
- FIGURE 1.7** A) MEAN ANNUAL TEMPERATURE (°C) IN SOUTH NORWAY DURING THE NORMAL PERIOD 1961-1990. THE STUDY AREA IS MARKED WITH BLACK FRAME (MODIFIED FROM DET NORSKE METEOROLOGISKE INSTITUTT 2009B). B) DIAGRAM OF THE MEASURED MEAN MONTHLY TEMPERATURE VALUES (°C) IN THE NORMAL PERIOD 1961-1990 AT THE CLIMATE STATIONS INDRE MATRE AND ULLENSVANG FORSØKSGÅRD (DET NORSKE METEOROLOGISKE INSTITUTT 2008)..... 13
- FIGURE 2.1** MAP OF THE MARGINAL MORAINES (M-1 TO M-32) IN THE STUDY AREA. M-1 TO M-22 ARE INTERPRETED TO BE DEPOSITED BY VESTRE BLOMSTERSKARDSBREEN, M-23 TO M-32 ARE INTERPRETED TO BE DEPOSITED BY MØSEVASSBREEN..... 22
- FIGURE 2.2** THE LICHEN GROWTH CURVE FOR *RHIZOCARPON GEOGRAPHICUM* “FOLGEFONNA – COMPILED DATA”, BASED ON SEVERAL CONTROL POINTS AROUND FOLGEFONNA GLACIER (BLUE RHOMBUSES), WAS USED TO DATE MORAINES OF VESTRE BLOMSTERSKARDSBREEN, MARKED WITH RED TRIANGLES (MODIFIED FROM BAKKE ET AL. 2005A, 184). DATES FROM MØSEVASSBREEN ARE INCLUDED (GREEN RECTANGLES) (BJØNNES 2006). SCIENTIFIC STUDIES INDICATE AN EARLY LIA GLACIAL ADVANCE AT MANY GLACIER OUTLETS OF

FOLGEFONNA CLOSE TO AD 1750, AND LATER READVANCES BETWEEN AD 1870 AND 1890 AND DURING THE 1930S (BAKKE ET AL. 2005A AND REFERENCES THEREIN)..... 46

FIGURE 3.1 THE RELATIONSHIP BETWEEN WATER CONTENT AND BULK DENSITY RELATED TO THE TYPE OF SEDIMENT. THE POROSITY OF SEDIMENT DOMINATED OF ANGULAR MINEROGENIC PARTICLES IS HIGHER THAN THE ONE DOMINATED OF ROUNDED GLACIALLY DERIVED MINEROGENIC PARTICLES; LOWEST BULK-DENSITY VALUES ARE OBTAINED FROM SEDIMENTS CONSISTING OF GYTTJA AND ANGULAR MINEROGENIC PARTICLES (BAKKE ET AL. 2005C, 171)..... 60

FIGURE 3.2 THE HJULSTRÖM DIAGRAM SHOWS THE RELATIONSHIP BETWEEN FLOW VELOCITY OF WATER AND THE TRANSPORT OF LOOSE GRAINS. TO ERODE A GRAIN PARTICLE ALREADY SETTLED, MORE ENERGY IS NEEDED THAN TO TRANSPORT IT WHEN IT ALREADY IS IN MOTION (NICHOLS 1999, 42) 61

FIGURE 3.3 BATHYMETRIC MAP OF MIDTBOTNVATN. WATER DEPTHS IN COLOUR SCALE, DAM, CORING LOCATIONS, INLET, OUTLET, AND INFLOWING STREAMS ARE SHOWN. 68

FIGURE 3.4 DESCRIPTION OF MIP-109. FIGURE SHOWS PICTURE, X-RAY PICTURE, VISUAL STRUCTURE, SEDIMENT TYPE, DESCRIPTION AND SECTION DIVISION. THE SEDIMENT STRUCTURE WAS QUITE DISTURBED DURING THE CORING PROCESS. 76

FIGURE 3.5 ILLUSTRATION OF SEDIMENT PARAMETERS OF MIP-109: MEAN, SORTING, DBD, MS, LOI, WC, Tl, Sl, Rb, Fe/Tl, INC/COH. IN ADDITION, CORE DEPTH, PICTURE, VISUAL STRUCTURE AND SECTIONS ARE INCLUDED. DIVISION INTO SECTIONS IS MAINLY BASED ON VARIATIONS IN ANALYSIS PARAMETERS, ONLY TO A MINOR EXTEND ON VISUAL DIFFERENCES..... 77

FIGURE 3.6 PERCENTAGE DISTRIBUTION OF THE GRAIN SIZES OF MIP-109. MEASUREMENTS WERE PERFORMED IN 1 CM INTERVALS FROM 0-50 CM, AND THEREAFTER IN 5 CM INTERVALS. VALUES OF EACH GRAIN SIZE ARE PRESENTED IN PERCENT OF THE WHOLE SAMPLE. 78

FIGURE 3.7 DESCRIPTION OF MIP-209. FIGURE SHOWS PICTURE, X-RAY PICTURE, VISUAL STRUCTURE, SEDIMENT TYPE, DESCRIPTION AND SECTION DIVISION. THE SEDIMENT STRUCTURE WAS QUITE DISTURBED DURING THE CORING PROCESS. 81

FIGURE 3.8 ILLUSTRATION OF SEDIMENT PARAMETERS OF MIP-209: MEAN, SORTING, DBD, MS, LOI, WC, Tl, Sl, Rb, Fe/Tl, INC/COH. IN ADDITION, CORE DEPTH, PICTURE, VISUAL STRUCTURE AND SECTIONS ARE INCLUDED. DIVISION INTO SECTIONS IS MAINLY BASED ON VARIATIONS IN ANALYSIS PARAMETERS, ONLY TO A MINOR EXTEND ON VISUAL DIFFERENCES..... 82

FIGURE 3.9 PERCENTAGE DISTRIBUTION OF THE GRAIN SIZES OF MIP-209. MEASUREMENTS WERE PERFORMED IN 1 CM INTERVALS. VALUES OF EACH GRAIN SIZE ARE PRESENTED IN PERCENT OF THE WHOLE SAMPLE. 83

FIGURE 3.10 SECTIONS IN MIP-209 INTERPRETED AS BEING DEPOSITED DURING DIFFERENT HYDROLOGICAL CONDITIONS IN THE DRAINAGE AREA: INCREASED GLACIAL ACTIVITY, DECREASED GLACIAL ACTIVITY, FLOOD, GRAVITATIONAL PROCESS. DIVISION PRESENTED HERE IS ACCORDING TO DIFFERENCES IN GRAIN SIZE DISTRIBUTION..... 90

FIGURE 3.11 MIP-109: SECTIONS A TO D WITH RESPECTIVE SUBSECTIONS, AND THEIR INTERPRETATIONS. SECTIONS INTERPRETED AS INCREASED GLACIAL ACTIVITY ARE MARKED GREEN, DECREASED GLACIAL ACTIVITY IS MARKED YELLOW, SUBSECTIONS INTERPRETED AS FLOODS AND GRAVITATIONAL PROCESSES ARE MARKED BLUE AND RED, RESPECTIVELY. THE PROGLACIAL SEDIMENT PARAMETERS DBD, VERY COARSE SILT, VERY FINE SILT (INVERS INDICATOR) AND THE DETRITAL XRF PARAMETERS Tl, Sl, AND Rb

WERE USED TO INTERPRETE GLACIAL ACTIVITY. THE PARAMETERS MEAN AND SORTING AS WELL AS THE XRF RATIOS Fe/Ti AND INC/COH WERE USED FOR INTERPRETATION OF EPISODIC EVENTS. IN ADDITION, RADIOCARBON DATINGS ARE INCLUDED, RELIABLE ONES ARE MARKED RED..... 94

FIGURE 3.12 MIP-209: SECTIONS A TO E WITH RESPECTIVE SUBSECTIONS, AND THEIR INTERPRETATIONS. SECTIONS INTERPRETED AS INCREASED GLACIAL ACTIVITY ARE MARKED GREEN, DECREASED GLACIAL ACTIVITY IS MARKED YELLOW, SUBSECTIONS INTERPRETED AS FLOODS AND GRAVITATIONAL PROCESSES ARE MARKED BLUE AND RED, RESPECTIVELY. THE PROGLACIAL SEDIMENT PARAMETERS DBD, VERY COARSE SILT, VERY FINE SILT (INVERS INDICATOR) AND THE DETRITAL XRF PARAMETERS Ti, Si, AND Rb WERE USED TO INTERPRETE GLACIAL ACTIVITY. THE PARAMETERS MEAN AND SORTING AS WELL AS THE XRF RATIOS Fe/Ti AND INC/COH WERE USED FOR INTERPRETATION OF EPISODIC EVENTS. IN ADDITION, RADIOCARBON AND LEAD DATINGS ARE INCLUDED, RELIABLE ONES ARE MARKED RED..... 99

FIGURE 3.13 COMPARISON OF THE CORES MIP-109 AND MIP-209; THE SEDIMENT PARAMETERS DBD AND LOI ARE USED. DOTTED LINE INDICATES INTERPRETED BEGINNING OF THE REGULATION OF LAKE MIDTBOTNVATN, DASHED LINES A AND B INDICATE INTERPRETED CHANGES IN GLACIAL ACTIVITY OBSERVABLE IN BOTH CORES. VISUAL SEDIMENT STRUCTURES OF BOTH CORES ARE INCLUDED. 100

FIGURE 3.14 ¹³⁷Cs CHRONOLOGY OF CORE MIP-209 WITH CORRECTED CORE DEPTH. THE CHERNOBYL PEAK IN 1986 IS CLEARLY OBSERVABLE. 105

FIGURE 3.15 AGE-DEPTH MODEL OF CORE MIP-109, BASED ON ONE RADIOCARBON DATE (4405 ± 130 CAL. YEARS BP) AND THE INTERPRETED DATE OF THE BEGINNING OF THE LAKE REGULATION IN 1953. DBD VALUES AND CALCULATED SEDIMENTATION RATES ARE ILLUSTRATED AS WELL. A SEDIMENT LOSS OF CA. 20 CM AT THE TOP OF THE CORE IS ASSUMED, TRANSFERRED FROM LEAD DATING RESULTS OF CORE MIP-209. EPISODIC EVENTS ARE EXCLUDED BEFORE CREATING THE MODEL, CALCULATING THE SEDIMENTATION RATES, AND AS WELL FROM THE DBD GRAPH..... 106

FIGURE 3.16 AGE-DEPTH MODEL OF CORE MIP-209, BASED ON TWO RADIOCARBON DATES (2360 ± 105 AND 4235 ± 175 CAL. YEARS BP), ONE LICHENOMETRIC DATING OF MARGINAL MORAINES ORIGINATED FROM THE INTERPRETED MAXIMUM GLACIER ADVANCE DURING THE LIA (AD 1735 ± 25; DASHED LINE INDICATES CORRELATION TO DBD) AND THE INTERPRETED DATE OF THE BEGINNING OF THE LAKE REGULATION IN 1953. DBD VALUES AND CALCULATED SEDIMENTATION RATES ARE ILLUSTRATED AS WELL. A SEDIMENT LOSS OF 22 CM AT THE TOP OF THE CORE IS ASSUMED, BASED ON LEAD DATING RESULTS. EPISODIC EVENTS ARE EXCLUDED BEFORE CREATING THE MODEL, CALCULATING THE SEDIMENTATION RATES, AND AS WELL FROM THE DBD GRAPH. THE LOWER FIGURE SHOWS THE AGE-DEPTH MODEL OF THE UPPER PART OF MIP-209, BASED ON 18 LEAD DATES (2009 TO 1967); CORE DEPTH WAS CORRECTED FOR A 22CM LOSS AT THE CORE TOP..... 107

FIGURE 4.1 IDEALIZED SCHEMATIC OVERVIEW OF THE DIFFERENCES IN ALTITUDE BETWEEN THE REGIONAL TP-ELA OF A PLEATEAU GLACIER AND THE TPW-ELAS AT CIRQUE GLACIERS DEPENDING ON LOCAL TOPOGRAPHY (DAHL ET AL. 2003, 279)..... 112

FIGURE 4.2 FLOW LINES AND CONTOURS ON AN IDEALIZED CIRQUE GLACIER SEEN FROM ABOVE AND SIDE VIEW. DUE TO THE FACT THAT LATERAL MORAINES NORMALLY DO NOT FORM ABOVE THE STEADY-STATE ELA, THEY CAN BE USED TO ESTIMATE FORMER ELAS (DAHL ET AL. 2003, 281) 113

FIGURE 4.3 DRAINAGE AREAS OF SEVERAL GLACIER OUTLETS OF SOUTHERN FOLGEFONNA; DIVISION FOLLOWS THE “ATLAS OF GLACIERS IN SOUTH NORWAY” (ØSTREM ET AL. 1988, 38). 1= GLACIER OUTLET DRAINING DOWN TO LAKE FONNAVATN, 2= MØSEVASSBREEN, 3= VESTRE BLOMSTERSKARDSBREEN, 4= ØSTRE BLOMSTERSKARDSBREEN, 5= SAUABREEN.	117
FIGURE 4.4 RECONSTRUCTIONS OF VESTRE BLOMSTERSKARDSBREEN FOR SPECIFIC TIMES IN THE PAST (CONTOUR INTERVALS 100 M; ELAS MARKED RED): 2007 (BASED ON DIGITAL CONTOUR INTERVALS FROM LASERSCANNING IN 2007, NVE), LIA MAXIMUM ADVANCE (BASED ON DATED MARGINAL MORAINES M-1, M-2, M-4, M-19), GLACIER ADVANCE THAT DEPOSITED MORAINES M-20 AND M-21, GLACIER ADVANCE THAT DEPOSITED MORaine M-22. DATED MARGINAL MORAINES USED FOR RECONSTRUCTIONS ARE SHOWN IN THE 2007 ILLUSTRATION.	119
FIGURE 4.5 AREA DISTRIBUTION AND ACCUMULATIVE AREA DISTRIBUTION PER 100 M CONTOUR INTERVAL OF VESTRE BLOMSTERSKARDSBREEN FOR THE RECONSTRUCTED SPECIFIC TIMES IN THE PAST: 2007, 1986, 1959, LIA MAXIMUM GLACIER ADVANCE, GLACIER ADVANCE THAT DEPOSITED M-20 AND M-21, GLACIER ADVANCE THAT DEPOSITED M-22. METHODS AAR 0.65 AND AAR 0.70 ARE USED FOR THE CALCULATIONS (CP. BENN AND GEMMELL 1997).	120
FIGURE 4.6 ISOSTATIC ADJUSTMENT CURVE FOR ISOBASE 26 (MØLLER AND HOLMESLET 1998).....	121
FIGURE 4.7 RELATIVE GLACIAL ACTIVITY CURVE OF VESTRE BLOMSTERSKARDSBREEN FOR THE LAST 4235 CAL. YEARS BP. SINCE LAKE MIDTBOTNVATN HAS BEEN REGULATED SINCE AD 1953, ANY CONCLUSIONS ON GLACIAL ACTIVITY SINCE THEN ARE NOT POSSIBLE. THEREFORE, THE CURVE STARTS AS LATE AS AD 1953; THE GLACIER’S EXTENT AND ACTIVITY ACCORDING TO THE DBD RECORD OF THAT YEAR HENCE IS THE ONE PAST GLACIAL ACTIVITY IS COMPARED TO. PERIODS INTERPRETED AS INCREASED GLACIAL ACTIVITY ARE MARKED GRAY. RADIOCARBON DATES AND THE BEGINNING OF THE LAKE REGULATION ARE ILLUSTRATED IN RED.....	124
FIGURE 5.1 RELATIVE GLACIAL ACTIVITY CURVE OF VESTRE BLOMSTERSKARDSBREEN FOR THE TIME SPAN AD 1953 TO 4235 CAL. YEARS BP. PERIODS INTERPRETED AS INCREASED GLACIAL ACTIVITY ARE MARKED GRAY. RADIOCARBON DATES AND THE BEGINNING OF THE LAKE REGULATION ARE ILLUSTRATED IN RED.	134
FIGURE 5.2 THE RELATIVE GLACIAL ACTIVITY CURVE COMPILED FOR VESTRE BLOMSTERSKARDSBREEN OVER THE PAST 1200 YEARS COMPARED TO THE MULTI-PROXY RECONSTRUCTION OF THE WINTER NAO INDEX BACK TO AD 1400 (COOK 2003, 73), SEA SURFACE TEMPERATURE IN °C (AUGUST) AT THE VØRING PLATEAU IN THE NORTH ATLANTIC (ANDERSSON ET AL. 2003, 22.5), WINTER PRECIPITATION IN % OF PRESENT (AD 1961-1990) AT FOLGEFONNA (BAKKE ET AL. 2008, 34), SUMMER TEMPERATURE IN °C (JULY) AT VESTRE ØYKJAMYRTJØRN IN SOUTH-WESTERN NORWAY (BJUNE ET AL. 2005, 184) AND THE TOTAL SOLAR IRRADIANCE IN W/M ² (BARD ET AL. 2000, 989). THE TIME PERIODS OF THE LITTLE ICE AGE (LIA) AND THE MEDIEVAL WARM EPOCH (MWE) ARE MARKED GRAY, FOR COMPARISONS OF THE PARAMETERS DURING THESE TIMES SEE TEXT. DASHED LINES INDICATE PEAKS IN WINTER PRECIPITATION AND SST FOLLOWED BY SUBSEQUENT PEAKS IN RELATIVE GLACIAL ACTIVITY; ACCORDING TO THIS THE REFERENCE TIME OF VESTRE BLOMSTERSKARDSBREEN AVERAGES OUT AROUND 30 YEARS.	143
FIGURE 5.3 THE RELATIVE GLACIAL ACTIVITY CURVE COMPILED FOR VESTRE BLOMSTERSKARDSBREEN COMPARED TO SELECTED RECONSTRUCTIONS OF RELATIVE GLACIER EXTENTS AND PHASES WITH MAJOR MORaine FORMATIONS FROM THE NORTHERN HEMISPHERE: 78°N SVALBARD (HUMLUM ET AL. 2005;	

JANSEN ET AL. 2007, 461), 65-73°N BAFFIN ISLAND (BRINER ET AL. 2009, 2084), 65°N OKSTINDAN (BAKKE ET AL. 2010, 1259), 64°N ICELAND (KIRKBRIDE AND DUGMORE 2008 IN BAKKE ET AL. 2010; GEIRSDÓTTIR ET AL. 2009 IN BAKKE ET AL. 2010), 50°N EUROPEAN ALPS (IVY-OCHS ET AL. 2009, 2143), 30°N HIMALAYA (OWEN 2009 IN BAKKE ET AL. 2010). GRAY MARKING INDICATES COMMON GLACIER ADVANCES MENTIONED IN THE TEXT. FIGURE BASED ON BAKKE ET AL. (2010, 1260)..... 148

List of tables

TABLE 1 NORMALS OF PRECIPITATION IN MM 1931-1960 AND 1961-1990, FOR STATION NO. 47900 INDRE MATRE (DET NORSKE METEOROLOGISKE INSTITUTT 2008)	9
TABLE 2 NORMALS OF PRECIPITATION IN MM 1931-1960 AND 1961-1990, FOR STATION NO. 49490 ULLENSVANG FORSØKSGÅRD (DET NORSKE METEOROLOGISKE INSTITUTT 2008).....	9
TABLE 3 NORMALS OF TEMPERATURE IN °C 1931-1960 AND 1961-1990, FOR STATION NO. 47900 INDRE MATRE (DET NORSKE METEOROLOGISKE INSTITUTT 2008)	12
TABLE 4 NORMALS OF TEMPERATURE IN °C 1931-1960 AND 1961-1990, FOR STATION NO. 49490 ULLENSVANG FORSØKSGÅRD (DET NORSKE METEOROLOGISKE INSTITUTT 2008).....	12
TABLE 5 LICHENOMETRIC MEASUREMENTS (MM) AT OBSERVED MORAINES IN FRONT OF VESTRE BLOMSTERSKARDSBREEN; CALCULATIONS ARE BASED ON WINKLER (2003, 89). DATINGS INTERPRETED AS RELIABLE ARE MARKED BOLD.	45
TABLE 6 DATING RESULTS OF OBSERVED MORAINES IN FRONT OF VESTRE BLOMSTERSKARDSBREEN BASED ON THE LICHENOMETRIC DATING CURVE “FOLGEFONNA – COMPILED DATA” (BAKKE ET AL. 2005A, 184). DATES INTERPRETED AS RELIABLE ARE MARKED BOLD.	46
TABLE 7 CORRELATION VALUES OF THE SEDIMENT PARAMETERS USED TO ANALYZE MIP-109. CORRELATIONS MENTIONED IN THE TEXT ARE MARKED BOLD.	84
TABLE 8 CORRELATION VALUES OF THE SEDIMENT PARAMETERS USED TO ANALYZE MIP-209 CORRELATIONS MENTIONED IN THE TEXT ARE MARKED BOLD.	85
TABLE 9 RADIOCARBON DATES OBTAINED FROM THE CORES MIP-109 AND MIP-209. DATES ASSUMED AS RELIABLE ARE MARKED BOLD.	103
TABLE 10 LEAD DATING RESULTS OF CORE MIP-209.....	104
TABLE 11 RECONSTRUCTED AREAS (KM ²) AND ELAS (M A.S.L.) OF VESTRE BLOMSTERSKARDSBREEN FOR SPECIFIED TIMES IN THE PAST, CALCULATED USING DIFFERENT METHODS, BASED ON MARGINAL MORAINES AND OLD MAPS. METHODS USED ARE AAR 0.65 AND 0.7 (BENN AND GEMMELL 1997) AND AABR WITH A BALANCE RATIO OF 1.0 AND 2.0 (OSMASTON 2005). ELAS CALCULATED WITH A BALANCE RATIO OF 2.0 ARE CONSIDERED AS THE MOST RELIABLE ONES, THE ELA LOWERING COMPARED TO TODAY’S ELA (2007) IS BASED ON THIS CALCULATION.	118
TABLE 12 CALCULATED ELAS CORRECTED FOR ISOSTATIC ADJUSTMENT; LOWERING OF CORRECTED ELAS COMPARED TO TODAY. CORRECTIONS ARE BASED ON ISOBASE 26 (MØLLER AND HOLMESLET 1998).....	122

List of pictures

PICTURE 1 MARGINAL MORaine M-1, WHICH IS STRONGLY MODIFIED BY RIVER BLÅDALSEV. PICTURE IS TAKEN LOOKING TO THE NORTH.....	23
PICTURE 2 MARGINAL MORaine M-2 AT THE SOUTHERN END OF THE SMALL LAKE, WHICH IS LOCATED APPROXIMATELY ONE KM SOUTH OF THE GLACIERS' TERMINUS. PICTURE IS TAKEN LOOKING TO THE SOUTH.	24
PICTURE 3 SOUTHERN PART OF MARGINAL MORaine M-5, WHICH IS LOCATED IN THE AREA OF INSTA BOTNANE AND HAS BEEN MODIFIED BY MELTWATERS. PICTURE IS TAKEN LOOKING TO THE WEST.....	26
PICTURE 4 MARGINAL MORaines M-7, M-8, AND M-9, LOCATED IN A VALLEY SIDE IN THE AREA OF INSTA BOTNANE. PICTURE IS TAKEN LOOKING TO THE NORTH.....	28
PICTURE 5 MARGINAL MORaine M-21, DIVIDED BY RIVER BLÅDALSELV. PICTURE IS TAKEN LOOKING TO THE WEST.	32
PICTURE 6 ERRATIC BLOCK OF CA. 2 M IN DIAMETER LOCATED NORTH OF LAKE MIDTBOTNVATN; PERSON FOR SCALE. PICTURE IS TAKEN LOOKING TO THE SOUTH. (PICTURE: STEPHANIE WEGSCHEIDER).....	36
PICTURE 7 GLACIOLACUSTRINE DEPOSITS IN FRONT OF THE GLACIER TONGUE OF VESTRE BLOMSTERSKARDSBREEN; MODIFIED BY MELTWATERS. PICTURE IS TAKEN LOOKING TO THE NORTH-WEST.	40
PICTURE 8 AERIAL PHOTOGRAPH OF ØSTRE AND VESTRE BLOMSTERSKARDSBREEN TAKEN IN MID-OCTOBER 2005; SNOW LINE IS LOCATED AT AROUND 1300-1320 M. (PICTURE: JAN RABBEN)	116

List of abbreviations

±	Error deviation; plus and minus
AD	Anno Domini
AABR	Area Altitude Balance Ratio
AAR	Accumulation Area Ratio
B _n	Net mass balance
BP	Before present
BR	Balance Ratio
B _w	Winter mass balance
¹⁴ C	Carbon isotope 14
°C	Degree Celsius
cp.	compare
DBD	Dry Bulk Density
ELA	Equilibrium Line Altitude
et al.	Latin: and others
GPS	Global Positioning System
cal.	Calendar
cm	Centimeter
km ²	Square kilometers
LIA	Little Ice Age
LOI	Loss on ignition
m	Meter
MEG	Median elevation of glaciers
MELM	Maximum elevation of lateral moraines
mm	Millimeter
m a.s.l.	Meter above sea level
MS	Magnetic Susceptibility
µm	Micrometer
NAO	North Atlantic Oscillation
NGU	Norwegian: Norges Geologiske Undersøkelse (Geological Survey of Norway)
NVE	Norwegian: Norges vassdrags- og energidirektorat (Norwegian Water Resources and Energy Directorate)
σ	Greek: sigma; standard deviation
THAR	Toe to Headwall Altitude Ratio
THC	Thermohaline Circulation
TP-ELA	Temperature-Precipitation ELA
TPW-ELA	Temperature-Precipitation-Wind ELA
UTM	Universal Transverse Mercator
XRF	X-ray fluorescence

Abstract

Vestre Blomsterskardsbreen is the southernmost glacier outlet of southern Folgefonna, a maritime temperate plateau glacier located on the Folgefonna peninsula in western Norway. It drains into Lake Midtbotnvatn, which is located approximately 5 km from the present glacier terminus.

Vestre Blomsterskardsbreen is an adequate area to reconstruct glacier fluctuations based on interpretation of proglacial sediments. A limiting factor is the fact that Lake Midtbotnvatn is regulated for the development of hydroelectrical power since AD 1953, which enlarged the sedimentation rate many times over normal and hence prevents any interpretation of the sediment with respect to glacial activity since then.

A continuous record of the relative glacial activity of the glacier outlet has been compiled for the time period AD 1953 to 4235 cal. years BP, based on the DBD record of proglacial sediments and according radiocarbon datings. The reliability of the results was limited by the greatly disturbed sediment structure of the core.

Proglacial sediment studies revealed that Vestre Blomsterskardsbreen has been present in the catchment at least during the past 4235 cal. years BP, with remarkable peaks in relative glacial activity around 4200, 2650, 2150, 1800, 1600, 1100 and 140 cal. years BP. Lichen-dated marginal moraines indicate, that the Little Ice Age (LIA) maximum advance occurred during the first half of the 18th century. The latest LIA glacier expansion was dated to AD 1945.

The relative glacial activity record of Vestre Blomsterskardsbreen was linked to natural climate archives. As a result, the glacier outlet is considered an indicator for winter climate variability, the winter NAO index and the strengths of the westerlies at the west coast of Norway. Furthermore the glacial record was compared to several selected glacier sites in the Northern Hemisphere; four common glacier advances correspond to the overall relative glacial activity pattern of Vestre Blomsterskardsbreen.

1 Introduction and approach to the study area

1.1 Introduction

During the last decades, modern climate change has been receiving more and more public attention, as has the fact that it has anthropogenic causes, mainly in form of steadily increasing greenhouse gas emissions. To understand past natural climate variations and present global warming, and to be able to model future natural climate developments and the human impact on those, it is important to achieve as much knowledge as possible about past climates.

Glaciers in general are good climate indicators, reacting on changes in summer temperature and winter precipitation of different scales. Folgefonna glacier in southern Norway is, due to its maritime setting, considered as a very sensitive indicator for climate variations in this part of the North Atlantic region.

My supervisor, Dr. Jostein Bakke, has performed much research work at Folgefonna with focus on glacier fluctuations and climate variations. The theme of this Master's thesis was his suggestion: glacier fluctuations and sediment transport of Vestre Blomsterskardsbreen, which is the southernmost glacier outlet of southern Folgefonna.

1.2 Purpose of the study

The purpose of this study is to reconstruct Holocene glacier fluctuations at Vestre Blomsterskardsbreen. Reconstructions are based on quaternary mapping of the study area including lichenometric dating of marginal moraines, and, more importantly, analyses of proglacial sediments brought up from Lake Midtbotnvatn, which is the lake Vestre Blomsterskardsbreen drains into. The main research questions in this study are

1. Can sediment from the distal glacier-fed lake Lake Midtbotnvatn be used to reconstruct past glacier fluctuations at Vestre Blomsterskardsbreen?
2. How did the glacier Vestre Blomsterskardsbreen fluctuate during the Late Holocene?
3. What is the timing of the LIA maximum extent of the glacier Vestre Blomsterskardsbreen, and how is this glacier behaving compared to other glaciers in the Northern Hemisphere?
4. How does a maritime glacier outlet like Vestre Blomsterskardsbreen respond to climate variations, also compared to other glacier sites of the Northern Hemisphere?

1.3 Approach to the study area

Folgefonna glacier in western Norway is located on the Folgefonna peninsula in the area of high mountains between the Sjørfjord, the Åkrafjord and the Hardangerfjord, oriented in a north-south direction. The temperate plateau glacier, with its location close to the west coast of Norway, is maritime, which indicates that precipitation, not temperature, is the decisive factor for the glacier's existence (Ryvarden and Wold 1991; Bakke et al. 2005c). The winter precipitation in turn is strongly related to the North Atlantic Oscillation index; therefore maritime glaciers in southwestern Norway are considered important indicators for the winter climate variation patterns in the North Atlantic region back in time (Six et al. 2001; Hurrell et al. 2003; Bakke 2004). Today Folgefonna is separated into three parts: northern, middle and southern Folgefonna, covering a total area of 219 km² (as of 1988) (Østrem et al. 1988). Southern Folgefonna is the third largest glacier in Norway; it has 17 glacier tongues, covers an area of 185 km² (as of 1988) and ranges between 490 m and 1660 m in altitude a.s.l. (Østrem et al. 1988). The ice thickness of southern Folgefonna is around 155 m on average (Tvede 2008, 27).

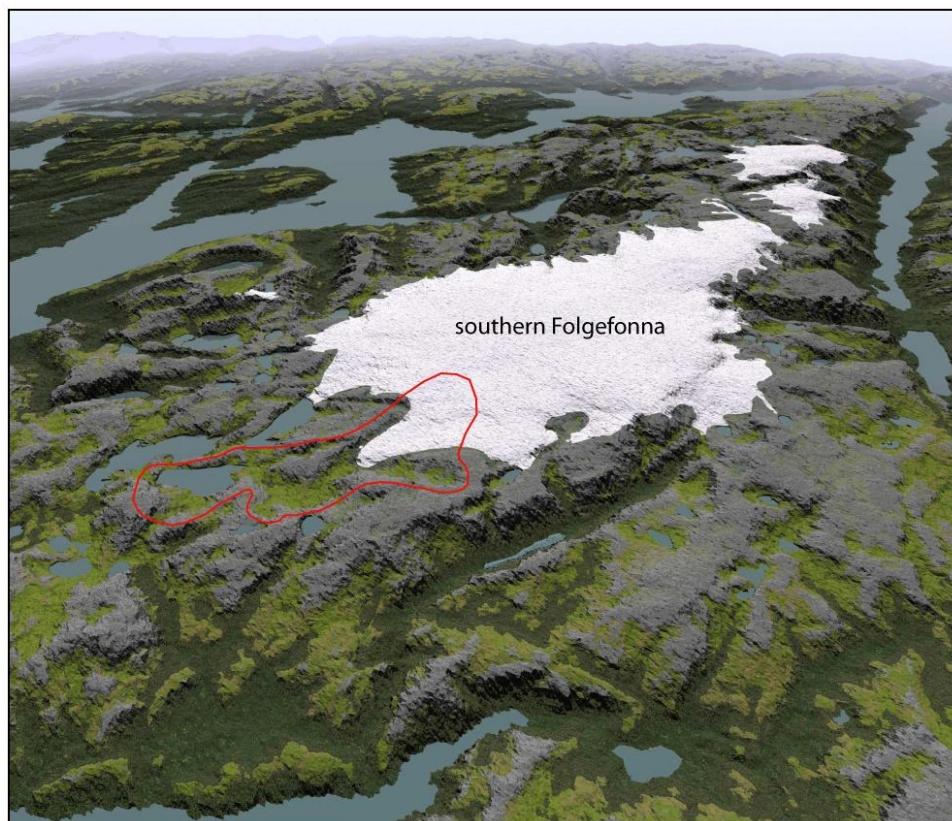


Figure 1.1 3D-illustration showing the Folgefonna peninsula in south-western Norway and the three parts of Folgefonna glacier: northern, middle and southern Folgefonna. The red line indicates the study area, located at the south side of southern Folgefonna. (Illustration: Kjell Helge Sjøstrøm, University of Bergen)

1.4 Description of the study area

The study area is located at the southern part of southern Folgefonna, covering the drainage basin of Lake Midtbotnvatn, which is located in front of the glacier tongue Vestre Blomsterskardsbreen, also called Svelgabreen (Helleland 2008, 425).

The geographical coordinates of the study area are N59°54'20'' to N59°57'10'' in north-south direction and E06°10'40'' to E06°19'30'' in east-west direction. The study area covers approximately 45 km², around 26 km² of this is covered by glacier ice.

Vestre Blomsterskardsbreen is an outlet glacier of southern Folgefonna, reaching up to 1640 m a.s.l. in elevation, while its lowest point at the terminus is 820 m a.s.l. (Tvede and Liestøl 1977). The aspect of the accumulation area slope of the glacier tongue is south, the one of the ablation area is south-west (Østrem et al. 1988). In 2007, Vestre Blomsterskardsbreen covered an area of 22.5 km² (Kjøllmoen 2009); due to its size and its comparative shallowness the glacier tongue is considered to have a longer response time than other, smaller outlets of southern Folgefonna.

Vestre Blomsterskardsbreen drains into Lake Midtbotnvatn (2 km² lake area), which is located approximately 5 km southwest of the glaciers' terminus, in between partly steep rock faces; the highest point in the surroundings is Blådalsborga in the south, with an elevation of 1302 m a.s.l. (see Figure 1.2).

The glacier outlet of Blomsterskardsbreen is divided into two tongues and as such into two hydrological units, Vestre Blomsterskardsbreen (22.5 km² in 2007) and Østre Blomsterskardsbreen (22.8 km² in 2007) (Tvede and Liestøl 1977; Smith-Meyer and Tvede 1996; Kjøllmoen 2009). With the development of hydroelectric power since the middle of the 20th century in the Folgefonna area, the drainage system of Vestre Blomsterskardsbreen was regulated. In 1970, a tunnel was constructed to lead the drainage water from Østre Blomsterskardsbreen, which previously flowed into river Londalselv, to river Blådalselv, Insta Botnane, where the meltwaters from both glacier tongues coalesce. Today the drainage system of Vestre and Østre Blomsterskardsbreen can therefore be seen as that of one glacier unit (Tvede and Liestøl 1977). Further regulations were implemented since the early 1950s. In 1953 a 650 m long tunnel to Lake Blådalsvatn was built to drain water. That way, Lake Midtbotnvatn could be drained down 40 m (Tjelmeland 1992). In 1958 Lake Midtbotnvatn was dammed to keep the large amount of water which came as meltwater from the glacier in summer, in order to have enough water in winter time for the production of hydroelectric power (Tjelmeland 1992). This dam was enlarged and amplified in 1967, 1983 and 1992; today Lake Mitdbotnvatn has a capacity of 102 million m³ water between highest and lowest

water level. The total height of regulation of Lake Midtbotnvatn is 70 m (Tjelmeland 1992); the regulated minimum and maximum values of elevation of Lake Midtbotnvatn are 700-770 m a.s.l. The maximum water depth is approximately 100 m.

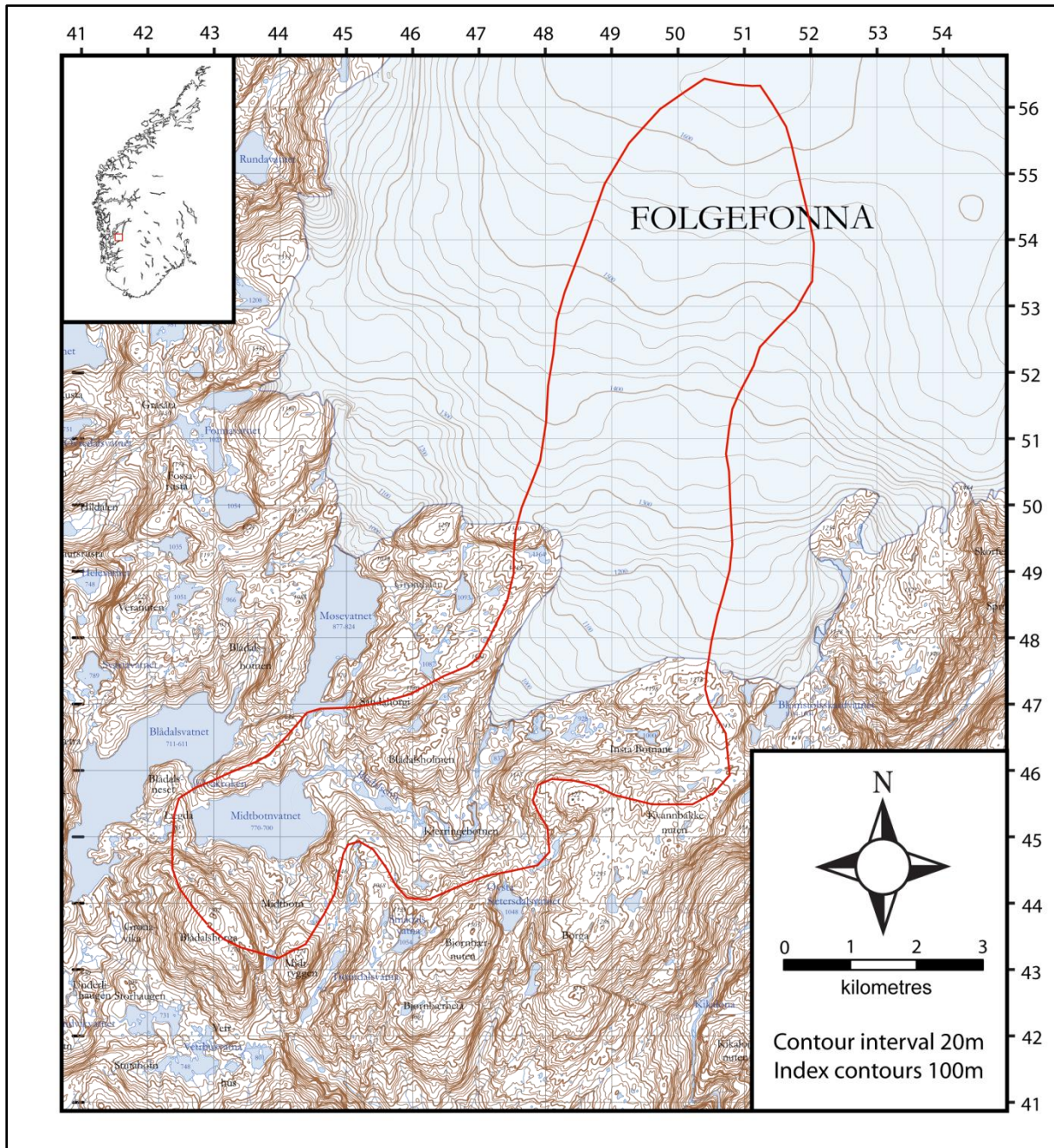


Figure 1.2 General map of the study area that is indicated with red line (UTM grid system WGS84, Zone 32V) and location of the study area in a map of south Norway.

1.5 Bedrock geology

Two orogenic phases influenced the bedrock geology of the Folgefonna peninsula: the Sveconorwegian orogeny (1250-900 million years BP) and later the Caledonian orogeny (600-400 million years BP) (Askvik 1995).

Of those, the Caledonian orogeny is the one that had the greatest geologic impact. In the beginning of this period the large continent broke apart; America and Eurasia started to drift apart from each other, so that the first Atlantic sea, the so-called Iapetus Sea, developed between them (Askvik 1976, 1995; Fossen 2004a). This sea also covered the flat land which is today's Norway, depositing huge amounts of sediments which in the course of time became rock. Due to the tectonic plate movement the American and Eurasian plates closed the Atlantic sea again and collided with each other. Bedrock was folded and metamorphosed, parts of the bedrock slid to some extent over the remainder, and additionally, there was volcanic activity (Askvik 1976; Fossen 2004a). Today metamorphosed and volcanic bedrocks dominate the geology of Folgefonna peninsula, accompanied by reams of foldings and downthrows; and due to various metamorphological and intrusive processes a large amount of different bedrock exists (Askvik 1976; Fossen 2004a).

The Caledonian orogeny influenced mainly the northern part of the Folgefonna peninsula, where the bedrock geology is linked with the geology of the Telemark Supergroup, which to a great extent is in the Telemark area, and whose deposition started around 1250 million years BP (Askvik 1976, 1995).

In the southern part of the Folgefonna peninsula, older orogenies than the Caledonian orogeny probably had the most decisive influence (Fossen 2004b). Precambrian rocks, formed deep within the Earth's crust during the time period 1000-1500 million years BP, dominate the bedrock geology in the study area, which more precisely is basically composed of granite, gneiss and, to a minor extent, gabbro and amphibolite. This can be gleaned from the geological map of the Geological Survey of Norway (NGU), (Lutro 2005); cp. Figure 1.3.

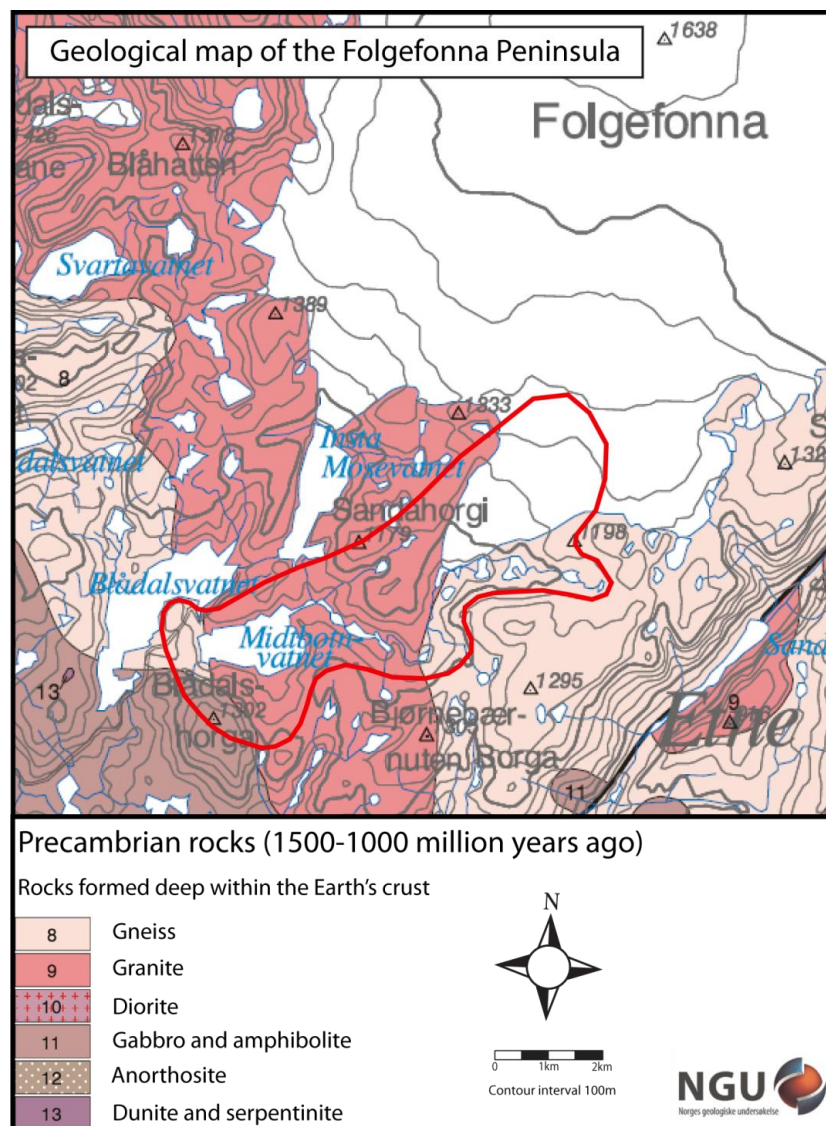


Figure 1.3 Geological map of the study area (red line) (Modified from Lutro 2005)

1.6 Climate

1.6.1 Today's climate

Today's climate in the study area is exemplary for the climate at the west coast of Norway, where the influences of the warm water masses of the Gulf stream and the position of the atmospheric polar front are essential (see Figure 1.4) (Bakke 2004; Bakke et al. 2005c). The polar front is the front zone between the warm and humid air masses coming from the south and the cool and dry air from the north, appearing around 60°N (Bakke 2004; Utaaker 2004). When pressed against each other, the lighter warm and moist air masses move above the heavier cold air and cool off, resulting in front precipitation when the dew-point temperature is reached (Skaar 2004). Large temperature anomalies within the polar front, which have their

cause in the heat transport of the sea at Norway's west coast, generate cyclones within the North Atlantic zone of westerlies, which, migrating across Scandinavia, cause the prevailing westerly and south-westerly winds (Broecker 1991 in Bakke et al. 2004; Hopkins 1991 in Bakke et al. 2004; Bakke 2004; Utaaker 2004). Accordingly, the precipitation rate at the west coast of Norway is dominated by strong westerlies in autumn and winter times (Skaar 2004; Nordli et al. 2005). The westerlies, characterized as mostly wet air masses coming from a western and south-western direction, release large amounts of precipitation when forced uphill by the range of mountains trending in a north-south direction in south-western Norway (Bakke 2004; Skaar 2004). Much of the precipitation, especially the winters, in the Folgefonna area is thereby the result of orographically intensified front precipitation (Bakke 2004; Skaar 2004). The precipitation amount at the Folgefonna peninsula mainly depends on the position of the atmospheric polar front with respect to quantity and strengths of the cyclones within the westerlies, and on the temperature of sea surface (SST) of the North Atlantic Sea (Bakke 2004; Nesje et al. 2004). The high winter precipitation rates at Folgefonna, which bring enough snow to compensate for what melts away due to higher temperatures during summer, are the reason for the glacier's existence (Nesje et al. 2004).

The intensity of the westerlies is strongly related to the North Atlantic Oscillation index (NAO index), which reflects the winter climate variation patterns in the North Atlantic region (Six et al. 2001; Hurrell et al. 2003; Bakke 2004). The NAO index is defined by the pressure difference between a subpolar low-pressure system near Iceland and a subtropical high-pressure system near the Azores, calculated on mean centered pressures (Six et al. 2001; Bakke 2004). A positive NAO index corresponds to mild and wet winter weather conditions in northern Europe, while a negative NAO index corresponds to anticyclonic cold and dry conditions, respectively (Six et al. 2001). The existence of a high-pressure field over Scandinavia or western Russia can have a blocking impact on the prevailing westerlies, which in that case are directed either north or south of south-western Norway; in south-western Norway the zonal atmospheric winter circulation of the North Atlantic is in such cases replaced by a quasimeridional circulation, and hence anticyclonic impact then dominates the weather (Bakke 2004).

The net mass balances of the maritime glaciers in south-western Norway generally correlate best with their winter net balance, and both the glacier mass balances and the winter precipitation in the area are strong positively correlated to the NAO index (Bjune et al. 2005; Nesje et al. 2008). Accordingly, long-term changes in atmospheric and oceanic circulation are reflected in glacier variations in south-western Norway (Bakke 2004).

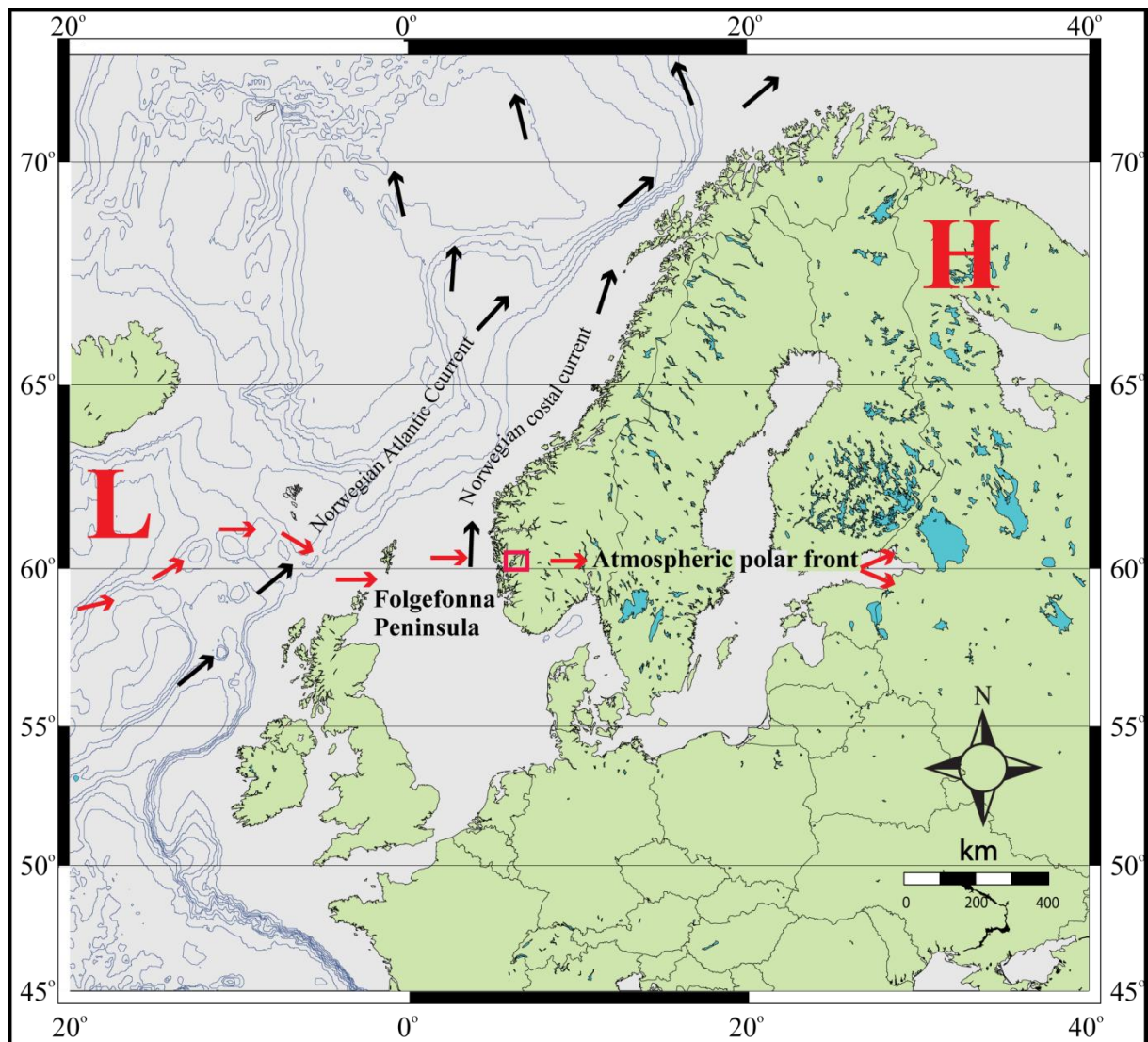


Figure 1.4 Map of the modern North Atlantic region. Study area at the Folgefonna peninsula is shown in the red frame. The average position of the atmospheric polar front is indicated by red arrows. The low-pressure field near Iceland and the high-pressure-field over Scandinavia or western Russia have important impact on the climate of Norway's west coast. The black arrows indicate the mean ocean currents of today's North Atlantic region. (Modified from Bakke 2004, 3)

1.6.2 Today's equilibrium line altitude

Today's equilibrium line altitude of Vestre Blomsterskardsbreen was calculated to be at 1328 m a.s.l. (in 2007). The calculation was based on digital contour intervals of Vestre Blomsterskardsbreen received from laserscanning in 2007 (Sylvia Smith-Meyer, NVE, personal communication, 2010) (see Chapter 4).

1.6.3 Precipitation

The high amounts of winter precipitation, mainly appearing as orographically enhanced front precipitation, are the main reason for the existence of Folgefonna glacier (Bakke 2004; Nesje et al. 2004; Skaar 2004). On annual terms, approximately 70% of the precipitation is snow, while 30% falls as rain (Nesje et al. 2004). The western and the highest southern parts of Folgefonna, including Vestre Blomsterskardsbreen, receive most of the precipitation (Nesje et al. 2004). Annual precipitation values of up to 5500 mm at Blomsterskardsbreen are the maximum values for the entire Folgefonna glacier (Tvede 1973; Tvede and Liestøl 1977; Nesje et al. 2004). With such large winter precipitation at Blomsterskardsbreen, raising summer temperatures due to climate change could until the 1970s not induce the significant retreat of the glacier tongue, as could be observed at all other tongues of Folgefonna glacier, and generally at most Norwegian glaciers (Tvede 1973; Jansen et al. 2007; Nesje et al. 2008). For precipitation data, the measurements over the normal periods 1931-1960 and 1961-1990 of two climate stations, no. 47900 Indre Matre and no. 49490 Ullensvang Forsøksgård, are used (see Table 1 and Table 2; accumulation season is from October to April, ablation season from May to September (Paterson 1994)); data source is the Norwegian Meteorological Institute (Det Norske Meteorologiske Institutt 2008).

Climate station no. 47900 Indre Matre is located 24 m a.s.l., at about 17 km air-line distance from Vestre Blomsterskardsbreen in a southwesterly direction. Climate station no. 49490 Ullensvang Forsøksgård is located 12 m a.s.l., ca. 30 km in air-line distance northeast of the study area.

Table 1 Normals of precipitation in mm 1931-1960 and 1961-1990, for station no. 47900 Indre Matre (Det Norske Meteorologiske Institutt 2008)

INDRE MATRE															
Normals	Jan	Feb	Mar	Apr	May	Jun	Jul	Aug	Sep	Oct	Nov	Dec	Abl.	Acc.	Year
1931-1960	275	233	168	194	110	180	172	229	305	353	311	316	996	1850	2846
1961-1990	284	204	247	126	136	185	195	223	370	389	355	356	1109	1961	3070

Table 2 Normals of precipitation in mm 1931-1960 and 1961-1990, for station no. 49490 Ullensvang Forsøksgård (Det Norske Meteorologiske Institutt 2008)

ULLENSVANG FORSØKSGÅRD															
Normals	Jan	Feb	Mar	Apr	May	Jun	Jul	Aug	Sep	Oct	Nov	Dec	Abl.	Acc.	Year
1931-1960	143	110	69	96	44	67	68	83	130	160	132	150	392	860	1252
1961-1990	144	94	110	51	50	64	75	92	157	181	163	169	438	912	1350

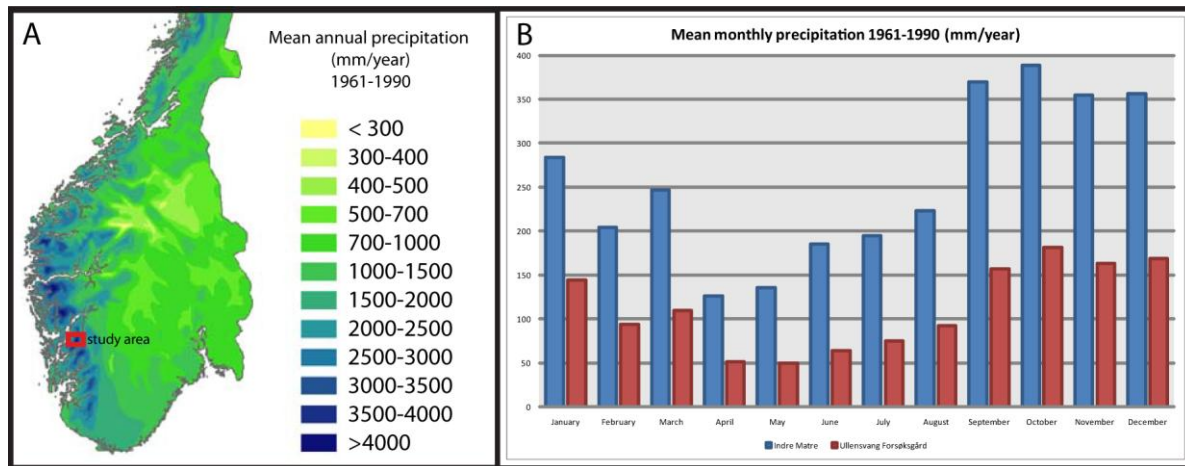


Figure 1.5 A) Mean annual precipitation (mm/year) in south Norway during the normal period 1961-1990. The precipitation values at the southwest coast of Norway are very high compared to the inland. The study area is marked with red frame (Modified from Det Norske Meteorologiske Institutt 2009a). B) Diagram of the measured mean monthly precipitation rates in the normal period 1961-1990 at the climate stations Indre Matre and Ullensvang Forsøksgård (Det Norske Meteorologiske Institutt 2008)

In the normal period 1931-1960, the mean annual precipitation rate at Indre Matre was 2846 mm. In the normal period 1961-1990, increased values of mean annual precipitation were measured, 3070 mm.

The mean annual precipitation rate at Ullensvang Forsøksgård in the 1931-1960 normal period was 1252 mm, which was less than half of the value of Indre Matre. For the normal period 1961-1990, the measured mean annual precipitation value at Ullensvang Forsøksgård was 1350 mm, which represents a slight increase compared to 1931-1960, but still remarks a great difference compared to the Indre Matre precipitation values.

The remarkable lower mean annual precipitation rates at Ullensvang Forsøksgård have their main reason in the fact that the majority of the annual precipitation at Folgefonna results from orographically intensified front precipitation (Bakke 2004; Nesje et al. 2004; Skaar 2004), which causes high precipitation rates at the windward areas located to the western and southwestern parts of Folgefonna, and lower ones at the leeward areas located to the eastern side. A minor contributing explanation for the differing precipitation values is the height above sea level of the two climate stations; Indre Matre is located 12 m higher and, according to the fact that precipitation values increase with altitude (Haakensen 1989), Indre Matre would be expected to receive more precipitation than Ullensvang Forsøksgård. Due to the study area's location at the southwestern side of Folgefonna, the climate station Indre Matre is expected to indicate most closely the local mean annual precipitation there.

The exponential increase of precipitation with 8%/100 m altitude also causes that mean annual precipitation values on the Folgefonna glacier itself differ from the climate stations

Indre Matre and Ullensvang Forsøksgård (Haakensen 1989). The measured mean accumulation season precipitation value at Indre Matre climate station in the normal period 1961-1990 was 1961 mm. Calculations from the assumption of an exponential increase of precipitation with 8%/100 m altitude indicate a mean winter precipitation rate of 3361 mm at Lake Midtbotnvatn (700 m a.s.l.) and of 5333 mm at today's ELA (1328 m a.s.l. in AD 2007)

Based on a study of ten Norwegian glaciers that exist at present in both maritime and continental climate regimes, a close non-linear (exponential) relationship (Liestøl relationship) between mean ablation-season temperature (1. May – 30. September) and annual winter precipitation at the ELA was proved (Figure 1.6) (Liestøl in Sissons 1979; Sutherland 1984; Dahl et al. 1997, 170).

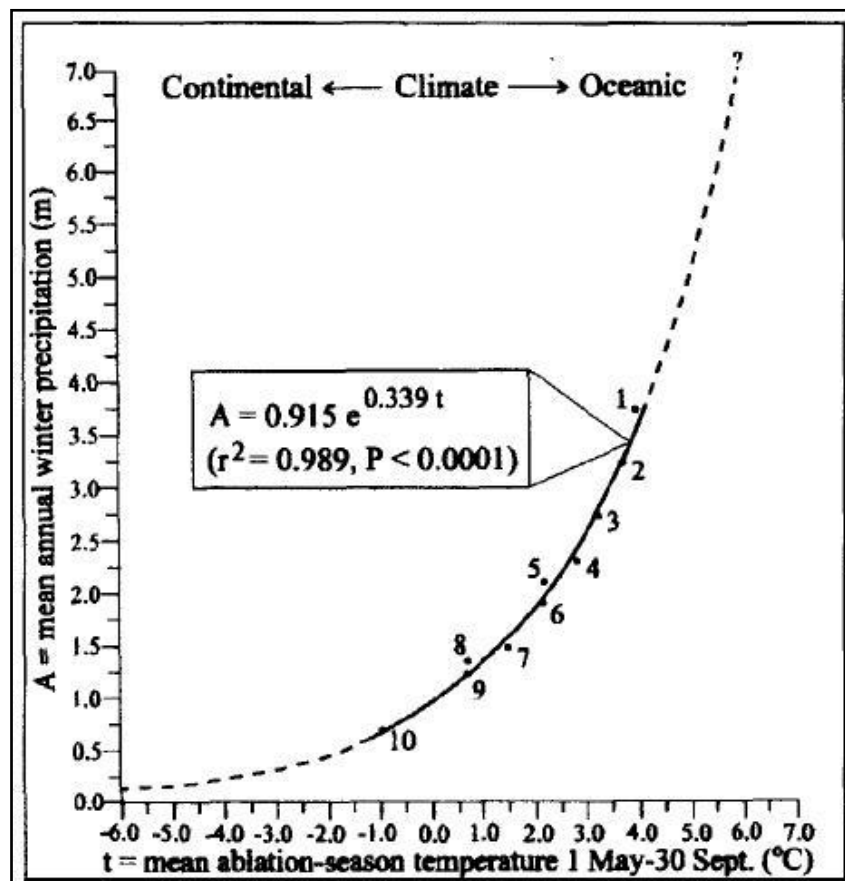


Figure 1.6 Based on ten at present existing Norwegian glaciers in both maritime and continental climate regimes, a close non-linear (exponential) relationship between mean ablation-season temperature (t) (1. may – 30. september) and annual winter precipitation (A) at the ELA is demonstrated. (1. Ålfotbreen, 2. Engabreen, 3. Folgefonna, 4. Nigardsbreen, 5. Tunsbergdalsbreen, 6. Hardangerjøkulen, 7. Storbreen, 8. Austre Memurubreen, 9. Hellstugubreen, 10. Gråsubreen) (Dahl et al. 1997, 170)

This relationship corresponds to the following regression equation:

$$A = 0.915e^{0.339t}$$

$$(r^2 = 0.989; P < 0.0001)$$

Equation 1 The regression equation for the relationship between mean ablation-season temperature and annual winter precipitation (Ballantyne 1989, 105)

A is winter precipitation expressed in meters water equivalent and t is temperature in °C; r is a measure of correlation, r^2 is the coefficient of determination and P is a measure of probability (Ballantyne 1989; Dahl et al. 1997).

Based on the Liestøl relationship, the mean annual accumulation season precipitation at today's ELA (1328 m a.s.l.) is calculated to 4346 mm. The differences between the calculated winter precipitation at today's ELA based on the Liestøl relationship (4346 mm) and the one based on the assumed exponential increase with 8%/100 m altitude (5333 mm) are attributed to local topographical variations.

1.6.4 Temperature

The location of the Folgefonna glacier at the west coast of Norway, so close to the North Atlantic sea and the Gulf Stream which transports warm water masses northwards, causes a maritime climate of the setting (Ryvarden and Wold 1991; Bakke et al. 2005c).

As for precipitation data, the temperature data of the climate stations no. 47900 Indre Matre and no. 49490 Ullensvang Forsøksgård are used (Table 3 and Table 4); data source is the Norwegian Meteorological Institute (Det Norske Meteorologiske Institutt 2008).

Table 3 Normals of temperature in °C 1931-1960 and 1961-1990, for station no. 47900 Indre Matre (Det Norske Meteorologiske Institutt 2008)

INDRE MATRE															
Normals	Jan	Feb	Mar	Apr	May	Jun	Jul	Aug	Sep	Oct	Nov	Dec	Abl.	Acc.	Year
1931-1960	0.7	0.6	2.7	5.8	10.3	12.7	14.8	14.2	11.3	7.7	4.9	2.6	12.7	3.6	7.4
1961-1990	1.1	0.8	2.6	5.8	10.3	13.2	14.2	13.6	10.8	8	4.3	2	12.4	3.5	7.2

Table 4 Normals of temperature in °C 1931-1960 and 1961-1990, for station no. 49490 Ullensvang Forsøksgård (Det Norske Meteorologiske Institutt 2008)

ULLENSVANG FORSØKSGÅRD															
Normals	Jan	Feb	Mar	Apr	May	Jun	Jul	Aug	Sep	Oct	Nov	Dec	Abl.	Acc.	Year
1931-1960	-0.7	-0.6	1.6	5.5	10.4	13.4	15.7	14.7	10.9	6.7	3.8	1.3	13	2.5	6.9
1961-1990	-0.2	-0.4	1.7	5.2	10.2	13.8	15	14.1	10.5	7.1	3.1	0.9	12.7	2.5	6.8

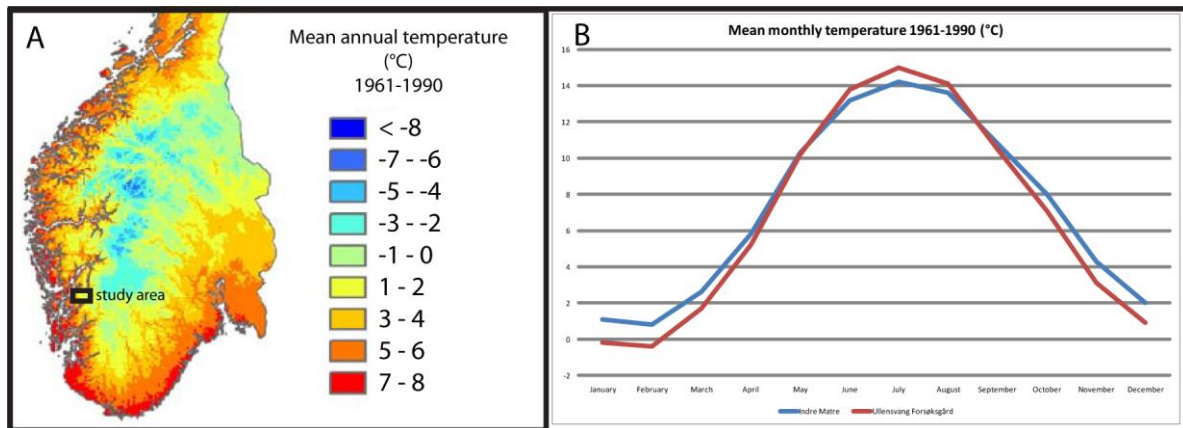


Figure 1.7 A) Mean annual temperature ($^{\circ}\text{C}$) in south Norway during the normal period 1961-1990. The study area is marked with black frame (Modified from Det Norske Meteorologiske Institutt 2009b). **B)** Diagram of the measured mean monthly temperature values ($^{\circ}\text{C}$) in the normal period 1961-1990 at the climate stations Indre Matre and Ullensvang Forsøksgård (Det Norske Meteorologiske Institutt 2008)

The average annual temperature value at Indre Matre in the 1931-1960 normal period was 7.4°C . In the 1961-1990 normal period, the average annual temperature value was slightly lower, 7.2°C .

At Ullensvang Forsøksgård the average annual temperature value was 6.9°C in the normal period 1931-1960; and 6.8°C slightly lower in the normal period 1961-1990.

Higher ablation-season temperatures and lower accumulation-season temperatures compared to the Indre Matre climate station indicate less maritime influence at the Ullensvang Forsøksgård climate station, which is located at the lee side east of Folgefonna glacier. Due to the south-western location of Vestre Blomsterskardsbreen, the Indre Matre climate station is assumed to be the most reliable one for the study area.

The temperature on the Folgefonna glacier is due to increased altitude lower than the measured values at the climate stations Indre Matre and Ullensvang Forsøksgård. Based on comprehensive research work in western Norway, Dahl and Nesje (1992) indicate the adiabatic lapse rate being $0.6^{\circ}\text{C}/100\text{ m}$ altitude. The mean ablation-season temperature of the normal period 1961-1990 was 12.42°C , which, assuming a decrease in temperature of $0.6^{\circ}\text{C}/100\text{ m}$ altitude, indicates a mean summer temperature of 8.36°C at Lake Midtbotnvatn (700 m a.s.l.) and 4.60°C at today's ELA (1328 m a.s.l.).

1.6.5 Wind

The westerlies are the most important influencing factor for prevailing wind directions and strengths at the Folgefonna peninsula. Cyclones, generated mainly in the area southwest of Iceland within the atmospheric polar front, migrate from the North Atlantic Sea inland across south-western Norway (Utaaker 2004). The prevailing wind direction at the Folgefonna peninsula are southerly, westerly, and southwesterly winds (Børresen 1987; Bakke 2004; Utaaker 2004); and especially in autumn and winter times the westerlies dominate the precipitation rate at the west coast of Norway (Skaar 2004; Nordli et al. 2005). Local topography has a strong influence on the prevailing wind directions and strengths (Utaaker 2004). Moreover, Folgefonna glacier causes katabatic winds. Air upon the glacier is cooled by the ice and thus gets heavier, resulting in downhill winds. In the valleys, the air then re-warms and ascends (Nesje et al. 2004). According to the aspect of the glacier tongue, the katabatic winds blowing down from Vestre Blomsterskardsbreen have prevailing north-eastern directions.

During the accumulation seasons between 1970 and 1990 the strength of the average westerlies in the North Atlantic region steadily increased (Tvede and Laumann 1996 in Smith-Meyer and Tvede 1996). The result of this was an increase in the amount of snow accumulation in the accumulation area of Blomsterskardsbreen during that period due to higher snow blow-out from the west and southwest orientated parts of Møsevassbreen. The strengthened winds from west to east were, next to the precipitation rates, one of the main contributing factors to the volume steadiness of Blomsterskardsbreen during the last century, in contrast to many other glacier outlets at Folgefonna (Smith-Meyer and Tvede 1996).

1.7 Previous relevant investigations in the study area

The first person who wrote about Folgefonna was priest Peder Claussøn Friis in the year 1600. In 1752 Erich Pontoppidan mentioned the glacier in his book "*Det første forsøg paa Norges Naturlige Historie*" (Ryvarden and Wold 1991). The first explicit description including scientific mapping, basically of the main glacier tongues Bondhusbreen, Buerbreen and Blåbreen, was created by priest S.A. Sexe within his book "Sneebreen Folgefond" in 1864 (Sexe 1864).

In the second half of the 19th century the photographer Knut Knutsen took pictures of Folgefonna, which were later useful for scientific work in the region in order to reconstruct the last great glacier advance (Bakke et al. 2000).

Geologist Rekstad (1905) made observations of some of the largest glacier tongues of Folgefonna in the very beginning of the 20th century. He described and took pictures of Bondhusbreen, Pyttabreen, Buerbreen and Blomsterskardsbreen.

In the 20th century Folgefonna was mentioned and described in many yearbooks of the Norwegian Tourist Association (Den Norske Turistforening) and in local village books (bygdebøker) (Bakke et al. 2000).

Several Master's theses about areas around Folgefonna were written. Risan (1950) created a quaternary map of the Kvinnherad region. Among other areas, Blådalen was described. The moraines that were located along the earlier rivers, which went down from Lake Møsevatn and Lake Midtbotnvatn, were supposed to be of the same stage since they were so close together. They probably came from two glaciers that were calving into Lake Blådalsvatn contemporaneously. Furthermore there were moraines located around Lake Midtbotnvatn, so it seems likely that there was a glacier calving in here as well at some time.

Follestad (1970) described the ice movement and deglaciation history of the southwestern Folgefonna peninsula after the Weichselian ice age. His research work was based on dates from earlier studies in that area, air photographs, and on his own geomorphological investigations.

As a result of an extensive development of hydroelectric power since the 1960s, Folgefonna and the region around were the subject of many research studies containing among other things mass balance and volume variation measurements, meltwater measurements, water mass calculations and mapping (Pytte 1969; Tvede 1972, 1973; Tvede and Liestøl 1977; Hagen et al. 1993; Tvede 1994). Many of the scientific works in that time period were connected to the Norwegian Water Resources and Energy Directorate (Norges Vassdrags- og Energidirektorat NVE). The research area in most of the studies was southern Folgefonna (Kennett and Sætrang 1987; Tvede 1994; Smith-Meyer and Tvede 1996; Elvehøy 1997, 1998).

In the 1970s and 90s the scientific works from Tvede (Tvede 1972, 1973; Tvede and Liestøl 1977; Tvede 1994) gave a comprehensive picture of Folgefonna. In his Master's thesis in 1972, he made mass balance measurements of two balance years on different parts at middle Folgefonna and on Blomsterskardsbreen, and compared the results. There were differences in mass balances and in the height of the equilibrium line altitude for different parts of the glacier area. Tvede concluded that the differences in regional glacio-climatic conditions in the Folgefonna area were primarily driven by variations in precipitation. Moreover fluctuation histories since the "Little Ice Age" (LIA) of different glacier tongues at Folgefonna were

reconstructed, using methods such as lichenometry and interpretation of air photographs. According to Tvede (1972), the northern parts of Folgefonna had their maximum expansion around 1750, but the more southerly the glacier tongues are located, their maximum expansion took place later. Some glacier tongues at the southern part of southern Folgefonna had their maximum expansion during the LIA not before 1930, as for example Østre Blomsterskardsbreen, which did not retreat significantly until 1972 (Tvede 1972). These differences led to his conclusion that the recent glacial history of Folgefonna is different compared to other southern Norwegian glaciers. In his study in 1973, Tvede confirmed this and explained the phenomenon with higher winter precipitation rates because of the maritime location and in case of Blomsterskardsbreen the south-western slope direction.

Tvede and Liestøl (1977) made a detailed study on Blomsterskardsbreen concerning mass balance measurements and reconstructions of recent fluctuations. They came to the conclusion that Blomsterskardsbreen had its LIA maximum expansion in 1940, which is in strong contrast to other southern Norwegian glacier tongues that had earlier maximums.

During the last decade, a couple of Master's theses and one dissertation with focus on the Folgefonna area were written at the University of Bergen. In 1997 the HOLSCATRANS-project (Holocene glacier and climate variations along a north-south Scandinavian transect) was established with the goal to get continuous high resolution reconstructions of glacier variations along a north-south transect in Scandinavia (Simonsen 1999). Connected to this project, three Master's theses in the Folgefonna area were completed, in order to reconstruct glacier and climate variations during the Holocene. The studies included, among other things, quaternary mapping, proglacial and terrestrial sediment studies and dating through lichenometry. Bjelland (1998) worked in Buerdalen, southern Folgefonna, Simonsen (1999) in Bondhusdalen, southern Folgefonna, and Bakke (1999) at northern Folgefonna.

In his dissertation, Bakke (2004) made a continuous reconstruction of the equilibrium line altitude at northern Folgefonna during the Lateglacial and Holocene. Furthermore, glacier size variations along a north-south transect in Norway were evaluated and implicated with atmospheric circulation patterns. Glaciers along the west coast of Norway, including Folgefonna, were used as paleoclimatic indicators for the development of the climate in the western part of the North Atlantic region. In this connection the atmosphere-ocean interaction is essential, for example fluctuations in the Atlantic Meridional Overturning Circulation (AMOC) can influence the climate significantly (Bakke et al. 2005a). Further articles about Folgefonna followed (for example Bakke et al. 2008).

In 2006 Edvardsen and Bjønnes completed their Master's theses (Bjønnes 2006; Edvardsen 2006). Both had study areas located at southern Folgefonna. Edvardsen (2006) reconstructed the paleoclimate of Sauabreen. Bjønnes (2006) worked at Møsevassbreen and reconstructed glacier fluctuations and climate variations during the Holocene, based on analyses of glaciolacustrine sediments and quaternary mapping. Moreover she linked the results of her study to the influence of the sea surface temperature (SST) of the western part of the Atlantic Ocean on maritime glaciers like Folgefonna.

Voster (2007) wrote a Master's thesis about variations of the mountain vegetation and tree line in Raunsdalen, northern Folgefonna, as a result of land use and climate changes.

In 2008 Tolo finished her Master's thesis. She investigated glacier fluctuations and climate changes of Dettebreen, northern Folgefonna, during the late Holocene, based on quaternary mapping and analyses of glaciolacustrine sediments; and she compared the results amongst other things with the NAO index, the SST of the North Atlantic of the last 3000 years, and temperature data from Greenland ice cores (Tolo 2008).

Two definitive books, "*Naturhistorisk Vegbok Hordaland*" and "*Folgefonna og Fjordbygdene*", were published in 2004 and 2008, respectively. Both works contain comprehensive information about the Folgefonna peninsula with respect to topics such as geomorphology, geology, history, ecology, climatology, glaciology, and hydrology (Helland-Hansen 2004; Brekke et al. 2008).

2 Quaternary mapping of the study area

This chapter contains the description of the method of quaternary mapping, and of the equipment used in the preparation for and during fieldwork in the study area, and for subsequent data handling. The results are presented in the quaternary map of Blomsterskardsbreen and Midtbotnvatn (see Appendix 1) and interpreted in this chapter. Finally, the dating method of lichenometry is described and applied on marginal moraines in the field area.

2.1 Quaternary mapping - method description

Quaternary mapping is a method used to investigate superficial deposits that have their origin in the time period of the Quaternary. There are two main purposes of quaternary mapping in this study. The first one is to give an overview of the deposits in the study area. Here are type, form, expansion and thickness of the superficial deposits relevant. The second purpose is to interpret the results and that way to understand the processes that formed the landscape in the past and the ones that are still active in present. Moreover, the quaternary map is an important feature when it comes to the interpretation of proglacial sediments of Lake Midtbotnvatn. Firstly with regard to distinguishing between glacial and non-glacial origins of the lake sediments, and secondly to correctly link the signals achieved from analysis of the proglacial sediments to paleoclimatic conditions (cp. Støren 2006; Tolo 2008).

Special emphasis is moreover laid on mapping and lichenometric dating of marginal moraines in front of Vestre Blomsterskardsbreen, in order to reconstruct the glacier's positions during different time periods of the LIA and former ELAs. (cp. Bakke et al. 2005a).

Fieldwork for the quaternary map was done in August and September 2008 and August 2009. The data obtained then formed the basis for the quaternary map of Blomsterskardsbreen and Midtbotnvatn (see Appendix 1). The legend, including colours and symbols for the superficial deposits, follows the standard of the Geological Survey of Norway (Bergstrøm et al. 2001).

2.1.1 Aerial photographs

A Wild Heerbrugg mirror stereoscope and aerial photographs were used in the preparation for the fieldwork to get an overview of the study area, and afterwards while drawing the map. The aerial photographs were black-and-white ones by Fjellanger Widerøe a/s, scale 1:40 000, series 7083, NFL 81 01 14-8 photography 06-07, and NLF 81 01 14-7 photography 08-10, date 07.08.1981.

Geometrically corrected digital aerial photographs (Statens Vegvesen et al. 2006) were helpful to ascertain the extents of different deposits while drawing the map.

2.1.2 Base maps

The following maps provided the basis for the fieldwork:

- The Norwegian Mapping Authority (Statens Kartvesen) (2003): series M711, map sheet 1314 IV (Fjæra), edition 5-NOR, scale 1:50 000, contour interval 20 m; and prints from the digital issue.
- The Norwegian Mapping Authority (Statens Kartvesen) (2003): series M711, map sheet 1214 I (Rosendal), edition 5-NOR, scale 1:50 000, contour interval 20 m; and prints from the digital issue.
- Uglund IT Group (2006): turkart Folgefonna nasjonalpark, scale 1:50 000, contour interval 20 m. This hiking map is based on the map database N50 KARTDATA.

2.1.3 Fieldwork equipment

Equipment used during fieldwork was composed of a slide calliper, a scraper, a digital camera, binoculars, a mirror compass with inclinometer, measuring tape and coloured pencils. A GPS (Garmin Oregon 300) was used to outline and log the different deposits.

2.1.4 Programs used for data handling (quaternary mapping)

The data obtained during fieldwork was digitised and processed with the computer program Adobe Illustrator CS3. Digital orthophotos (Statens Vegvesen et al. 2006) were also processed with Adobe Photoshop CS3.

2.2 Presentation and interpretation of locations

The glacial activity of Folgefonna has had a significant impact on the study area in the course of the Quaternary. The glacier is temperate, which implies that it erodes the ground surface that lies beneath it (Paterson 1994). Thus all superficial deposits that are located in the study area at present must have been deposited after the glacier's last retreat.

Exposed bedrock, exhibiting small-scale forms of glacial erosion and to a small extent covered by superficial deposits, dominates the study area. In the following, the deposits are presented and interpreted according to the agents that deposited them.

2.2.1 Glacial deposits

2.2.1.1 Marginal moraines

Marginal moraines are ridges of moraine material (see Chapter 2.2.1.2) that are formed along the present or past margins of glaciers (Benn and Evans 1998). They evolve when moraine material is either pushed by an advancing glacier, or they form during a steady-state phase of the glacier which is in a general retreat period (Nesje 1995). They can appear as distinct formed ridges or as non-coherent ridges in belts and zones. In some areas, only small belts of moraine material or just boulders mark an earlier position of a glacier tongue (Nesje 1995). Meltwater can subsequently modify or even destroy marginal moraines (Summerfield 1991).

Marginal moraines are formed below the steady-state ELA of the glacier, a fact that enables these forms to be used to reconstruct former ELAs (Dahl et al. 2003) (cp. Chapter 4.1.).

Marginal moraines deposited along the side of a glacier are named lateral moraines, the ones formed along a glacier's terminus are named end- or terminal moraines (Nesje 1995).

Complex interactions of different paraglacial and glacial processes are the cause of numerous deposition forms that characterize and term different types of marginal moraines (Benn and Evans 1998).

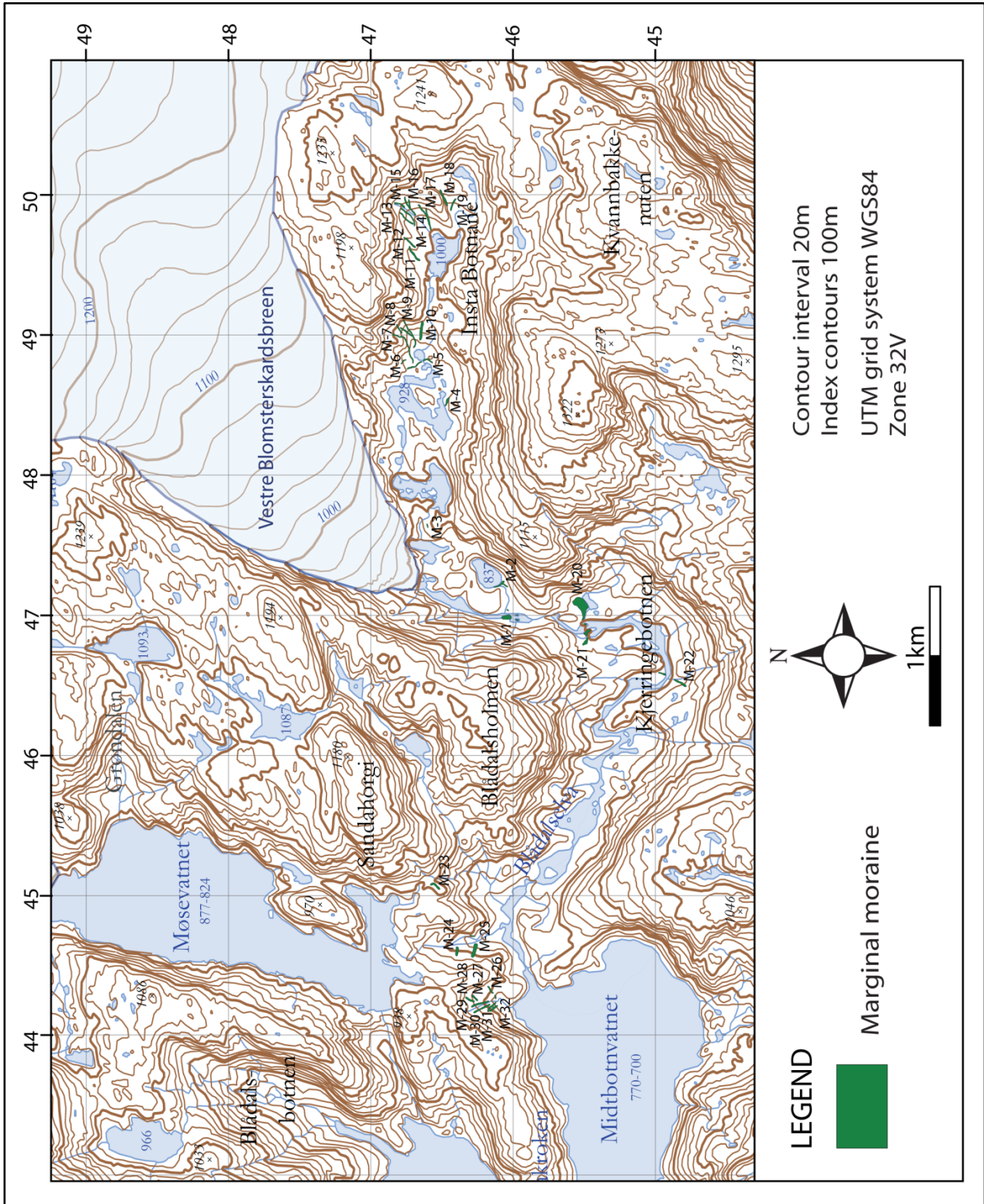


Figure 2.1 Map of the marginal moraines (M-1 to M-32) in the study area. M-1 to M-22 are interpreted to be deposited by Vestre Blomsterskardsbreen, M-23 to M-32 are interpreted to be deposited by Møsevassbreen.

M-1 Observation

Ridge-formed depositions close to river Blådalselv south of the terminus of Vestre Blomsterskardsbreen, UTM 469777 to UTM 470255, 835 m a.s.l.

M-1 consists of ridge-formed depositions on three close to each other located islets in the river Blådalselv. Only the main islet was reachable during fieldwork, here the ridge-form is most distinctive. It consists of boulders of up to 1.5 m in diameter, which are partly covered by vegetation. The river has washed out the fine fractions and considering the amount of meltwater available in the area today, which must have been even more during past deglaciation periods after glacier advances, downstream transport of bigger blocks of more than 1 m in diameter is seen as a realistic assumption. This explains the distribution over three islands downstream the river. The ridge form on the biggest islet is 120 m long and up to 1.5 m high. It is orientated north-south. The proximal angle is 25° , and the distal angle is 20° . The deposition can be followed up the two smaller islets downstream in the river, and on the eastern side of river Blådalselv, where it consists of some spread individual boulders of 0,5 m to 1.5 m in diameter.



Picture 1 Marginal moraine M-1, which is strongly modified by river Blådalsev. Picture is taken looking to the north.

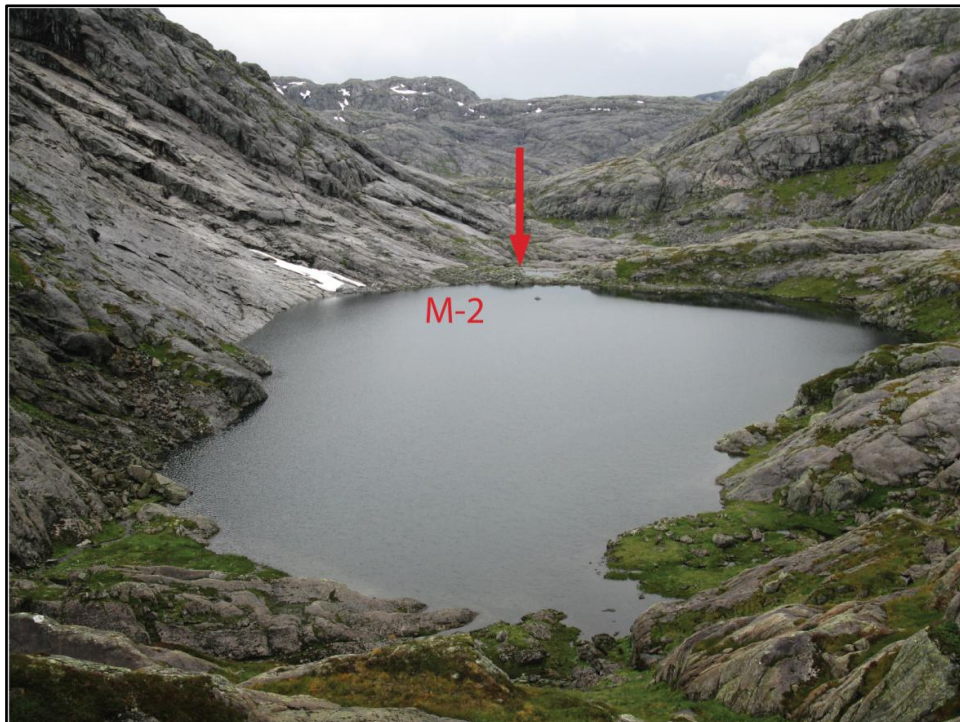
M-1 Interpretation

M-1 is interpreted as a terminal moraine representing the maximum glacier advance during the Little Ice Age (LIA). Lichenometric measurements were performed; datings are presented in Chapter 2.3.2. River Blådalselv must have worked on the moraine a long time, and has drastically modified and reduced it. Directly after deposition, the moraine was probably much higher, orientated in a general east-west direction.

M-2 Observation

Ridge located south of the terminus of Vestre Blomsterkardsbreen, UTM 471200, 838 m a.s.l.

M-2 is a ridge located at the southern end of the small lake located approximately one km south of the terminus of Vestre Blomsterskardsbreen. The ridge is 230 m long, 3-4 m high, and its length axis is orientated in a north-west to south-east direction. The material is not sorted and consists of sub-angular and rounded blocks of up to 2 m in diameter; the smallest grain size observed is gravel. Since the ridge material was very coarse, angle measurements were difficult to perform; proximal and distal angles are approximately 40°. No vegetation was discovered on the ridge. On the south-eastern part, the ridge borders an area of rapid mass-movement deposits. This material is angular to sub-angular, and can partly be observed also on the ridge itself.



Picture 2 Marginal moraine M-2 at the southern end of the small lake, which is located approximately one km south of the glaciers' terminus. Picture is taken looking to the south.

M-2 Interpretation

M-2 is interpreted as a terminal moraine representing the maximum glacier advance during the LIA. Lichenometric measurements were performed; care was taken not to measure lichen thalli on boulders interpreted as rapid mass-movement deposit. Datings are presented in Chapter 2.3.2.

M-3 Observation

Four blocks in a row deposited south of Vestre Blomsterskardsbreen, in Insta Botnane, UTM 476244, 890 m a.s.l.

M-3 is a deposit of four blocks in east-west direction; each block has a diameter of approximately 1 m. Angle measurements were not performed due to the coarse character of the deposit. The blocks are not covered by vegetation, nor are the surroundings, which is mainly pure bedrock.

M-3 Interpretation

The deposit is interpreted as part of a crucially washed-out lateral moraine deposited by the last glacier advance during the LIA. Lichenometric measurements were performed on the four blocks; datings are presented in Chapter 2.3.2.

M-4 Observation

Ridge located southeast of Vestre Blomsterskardsbreen, in Insta Botnane, UTM 485100, 935 m a.s.l.

M-4 is a 120 m long ridge orientated west – east. It borders exposed bedrock in the south. The unsorted material ranges in size from gravel to many rounded and sub-angular blocks of up to 2 m in diameter. Within, angular blocks can be observed, which is interpreted as rapid mass-movement deposit originated from a small tear-off edge above the moraine. The material is too coarse for angle measurements. The ridge is not covered by vegetation.

M-4 Interpretation

M-4 is interpreted as a lateral moraine representing the maximum glacier advance during the LIA. Lichenometric measurements were performed; care was taken not to measure lichen thalli on boulders interpreted as rapid mass-movement deposit. Datings are presented in Chapter 2.3.2.

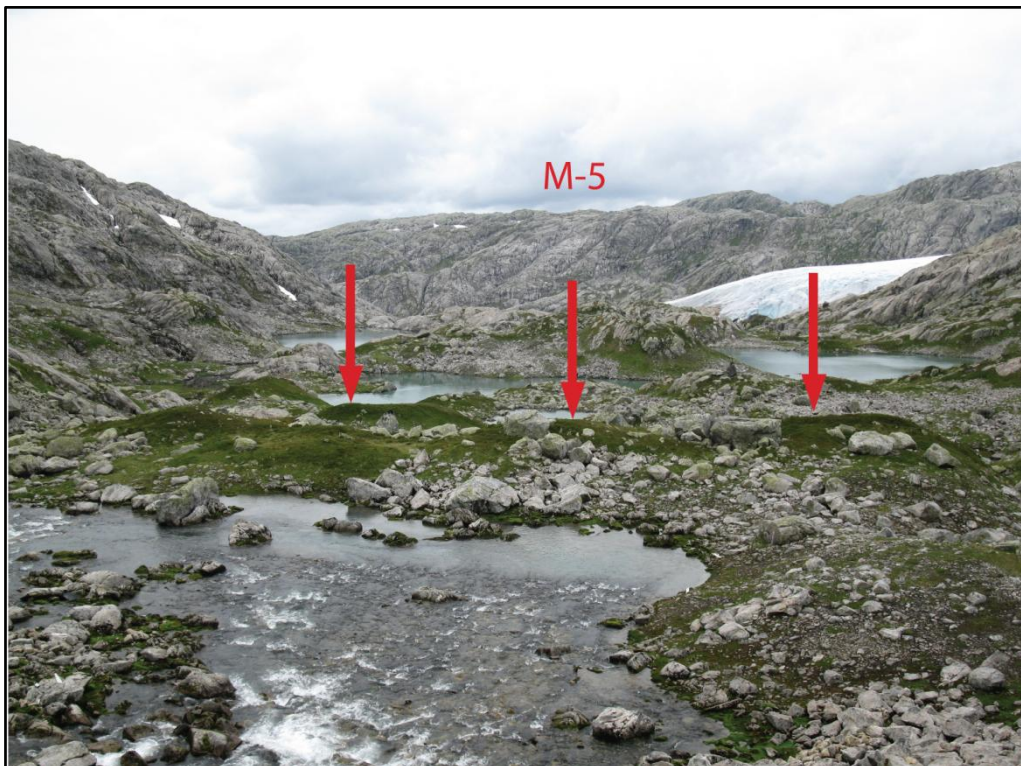
M-5 Observation

Ridge located southeast of Vestre Blomsterskardsbreen, in Insta Botnane, UTM 487397, 927 m a.s.l.

M-5 is a 250 m long ridge with a length axis orientated in north-northwest – south direction. The height is 5-6 m, the proximal angle is 40° and the distal angle is 30°. The material is unsorted and consists of grain sizes from sand up to large blocks with 1-5 m in diameter, which are angular or sub-angular. There is well-established vegetation on the ridge, mainly mosses, blueberries and grasses. Many single big blocks are free of vegetation. The ridge can be followed up at the southern side of the meltwater stream, where it is approximately 110 m long, showing the same characteristics as the northern part.

M-5 Interpretation

The ridge is interpreted as a lateral moraine originated by a glacier advance or steady-state position during the LIA, later divided into two parts by the glacial meltwater stream, which flows through it. Lichenometric measurements were performed on the parts of the ridge without vegetation; datings are presented in Chapter 2.3.2.



Picture 3 Southern part of marginal moraine M-5, which is located in the area of Insta Botnane and has been modified by meltwaters. Picture is taken looking to the west.

M-6 Observation

Ridge located southeast of Vestre Blomsterskardsbreen, in Insta Botnane, UTM 487955, 929 m a.s.l.

M-6 is a ridge formed deposit of 80 m length, with a northwest – southeast length axis orientation. It is around 4 m high, the proximal angle is 35° and the distal angle is 30°. Grain sizes ranging from sand up to rounded and sub-angular and partly angular large blocks with 1-5 m in diameter could be observed. There is well-established vegetation on the ridge, mainly consisting of mosses, blueberries and grasses. Many single big blocks upon are free of vegetation.

M-6 Interpretation

The ridge is interpreted as a lateral moraine, reflecting a glacier advance or steady-state position during the LIA. Lichenometric measurements were not performed.

M-7, M-8, M-9 Observation

Three ridges located in a valley side southeast of Vestre Blomsterskardsbreen, in Insta Botnane, UTM 489971, 940 m to 960 m a.s.l.

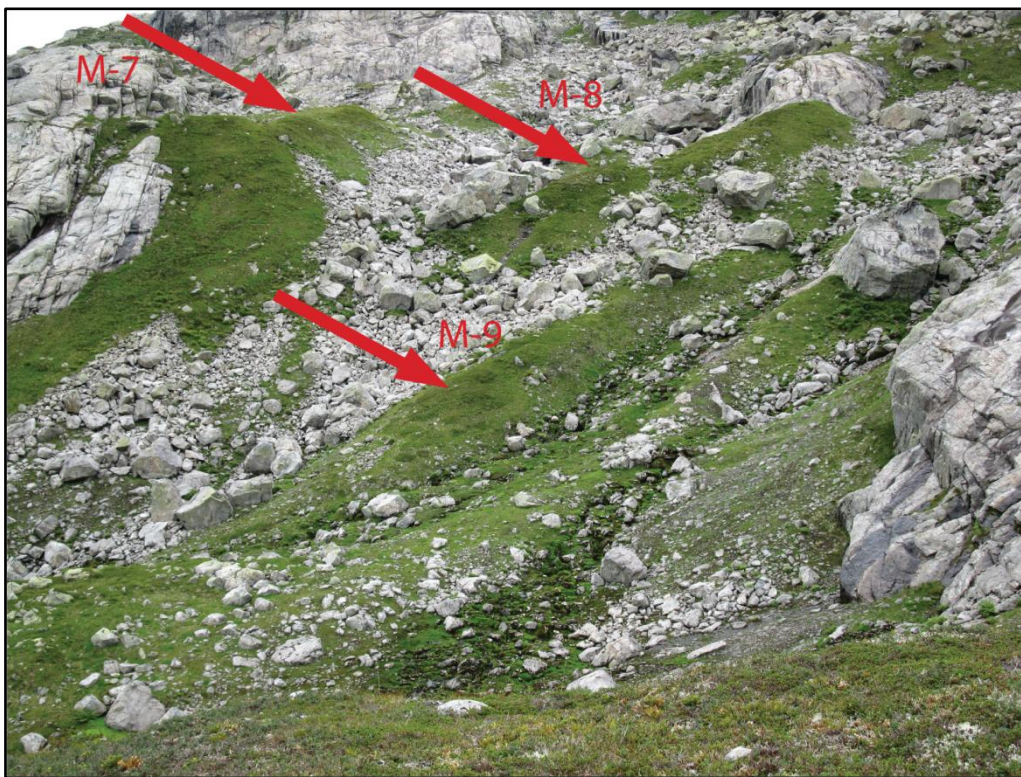
M-7, M-8 and M-9 are three ridges located downhill in a valley side.

M-7 is located from ca.1000 m down to 930 m a.s.l. It is orientated northeast – southwest, in the west it is bordered by exposed bedrock. This ridge is approximately 470 m long and up to 6 m high, the distal angle is 35°. It consists of sub-angular to rounded unsorted material with grain sizes from sand to big, angular to sub-angular boulders of up to 2 m in diameter. The surroundings are steep, and many big blocks with diameters of up to 3 m are located at the eastern bottom line of the ridge; those probably fell or rolled down after deposition. Some smaller, angular blocks can be observed within the ridge material, assumed to be originated from rapid mass-movement, mainly rockfall. The ridge itself is completely covered by vegetation, only some large blocks are partly uncovered.

M-8 is located east of M-7 at ca. 1000 m to 980 m a.s.l. The ridge is 110 m long, 4-5 m high, and north-east – southwest orientated. The proximal angle is 35° and the distal angle is 30°. As M-7, it consists of sub-angular to rounded unsorted material with grain sizes from sand to big boulders, and it is covered by well-established vegetation, but on some parts with large angular to sub-angular boulders of up to 1 m in diameter on top. Angular rapid mass-movement deposits can be observed in between.

M-9 is located at the east side of the valley, consisting of two parts in the beginning, coalescing to one ridge further downhill. The western ridge starts at a height of 980 m a.s.l., the eastern one at a height of ca. 995 m a.s.l.; the two ridges coalesce at a height of 950 m a.s.l. and can be followed down to ca. 935 m a.s.l. The total length of M-9 is approximately 380 m, and shows the same characteristics as M-7 with respect to material, orientation of length axis and proximal and distal angle.

Between the three ridges, angular and sub-angular boulders of up to 2 m in diameter can be observed, which are not covered by vegetation. This is interpreted as till and rapid mass-movement deposit.



Picture 4 Marginal moraines M-7, M-8, and M-9, located in a valley side in the area of Insta Botnane. Picture is taken looking to the north.

M-7, M-8, M-9 Interpretation

In the whole study area it can be observed that there is much more material deposited in valley sides than on the peaks; the latter often appear almost free of any vegetation and deposits. Based on investigations of landforms in Norway formed by the impacts of the last ice age and the following deglaciation, Gjessing (1978) points out that smaller glacier advances could form marginal moraines in valleys where enough material was available to be pushed up, whereas on heights either discontinuous or no moraines were deposited. This as a

result of material availability and the fact that glaciers often are located further back on heights than in valleys (Gjessing 1978, 95).

M-7, M-8 and M-9 are interpreted as a set of lateral moraines pushed up and deposited by glacier advances or steady-state positions of close temporal proximity during the LIA. Lichenometric measurements were performed on the eastern and the coalesced part of M-9, emphasis was put on not measuring lichen thalli on boulders originated from rapid mass-movement deposit; datings are presented in Chapter 2.3.2.

M-10 Observation

Ridge located southeast of Vestre Blomsterskardsbreen, in Insta Botnane, UTM 490011 956 m a.s.l.

M-10 is a 220 m long and up to 6 m broad ridge. It is orientated in a west-east direction. The proximal angle is 45°, as is the distal angle. It consists of sub-angular to rounded unsorted material with grain sizes from silt to big sub-angular boulders of 0,5 m to 2.5 m in diameter. The ridge is overgrown by mosses, blocks upon are few.

M-10 Interpretation

M-10 is interpreted as a lateral moraine formed by a glacier advance or steady-state position during the LIA. This moraine originated probably in close temporal proximity to M-7, M-8 and M-9. Lichenometric measurements were performed; datings are presented in Chapter 2.3.2.

M-11 and M-12 Observation

Two ridges located in a small valley side, southeast of Vestre Blomsterskardsbreen, in Insta Botnane, UTM 496047 1010 m to 1040 m a.s.l.

M-11 and M-12 are two ridges located downhill in a valley side; their length axes have a north-east – south-west orientation. M-11 is 235 m long, ranging from 1010 m to 1025 m a.s.l.; M-12 is 200 m long and located in a height of 1020 m to 1040 m a.s.l. They are up to 10 m in height, the proximal angle of M-11 is 45°, and the one of M-12 is 40°. The distal angles of M-11 and M-12 are 40°. The two ridges consist of grain sizes ranging from sand to large rounded and sub-angular blocks of 0,5 m to 12 m in diameter; the material is unsorted. Angular rapid mass-movement deposits could be observed some places. Well established gramineous vegetation covers the ridges, huge blocks upon are free of vegetation. The rest of

the valley is covered by till, many huge boulders could be observed; rapid mass-movement deposits could be identified in between.

M-11 and M-12 Interpretation

Being located in a till-rich valley, M-11 and M-12 are interpreted as lateral moraines pushed up and deposited by glacier advances or during steady-state positions during the LIA. Lichenometric measurements were performed, taking care not to include lichens located on rapid mass-movement deposits; datings are presented in Chapter 2.3.2.

M-13, M-14, M-15, M-16 and M-17 Observation

Five ridges located in a broad valley side, southeast of Vestre Blomsterskardsbreen, in Insta Botnane, UTM 498782, 1010 m to 1060 m a.s.l.

M-13 to M-17 are five ridges located in a broad valley at the eastern end of Insta Botnane. The ridges are all between 5 m and 10 m high; the orientation of their length axes is north-east – south west. They are all of the same composition: sub-angular to rounded unsorted material with grain sizes from sand to big boulders, covered by well established gramineous vegetation with numerous large angular and sub-angular boulders of 1 m to 8 m in diameter upon. Angular rapid mass-movement deposits can be observed some parts in between, especially upon M-13, the eastern part of M-16, and upon M-17, which border rapid mass-movement deposit areas in the west and in the east, respectively. The areas between the ridges are covered by till including boulders with diameters of 1 m and up to 15 m, not covered by vegetation.

M-13 is the westernmost ridge, bordering an area of rapid mass-movement deposits in the west. It is 230 m long, and ranges from 1020 m to 1050 m a.s.l. The proximal angle is 35°, and the distal angle is 40°.

M-14 is located east of M-13, 290 m long, from 1010 m up to 1050 m a.s.l. The proximal angle is 40°, as is the distal angle.

M-15 is a ridge north-east of M-12 with a length of 170 m, 1050 m to 1070 m a.s.l. Proximal and distal angles are 40°.

M-16 starts as two ridges on ca. 1070 m a.s.l., coalescing on 1025 m a.s.l, and reaching down to 1015 m a.s.l. The western part is 270 m long, the eastern 210 m; 120 m of this is together. Proximal and distal angles are 40°.

M-17 is the easternmost ridge in the valleyside, surrounded and partly covered by huge amounts of rapid mass-movement deposits which are in general more angular than the

material the ridges consist of. As M-16, the ridge starts as two, coalescing further downhill and continuing as one ridge. The western part is in total 360 m long, ranging from 1050 m down to 1005 m a.s.l., the eastern part is 270 m long, 1040 m to 1005 m a.s.l. They coalesce at a height of 1020 m a.s.l., continuing 190 m further down. Proximal and distal angles are 40°.

M-13, M-14, M-15, M-16 and M-17 Interpretation

The ridges M-13 to M-17 are interpreted as a set of lateral moraines, formed by glacier advances that pushed up the valley material or steady-state positions of close temporal proximity during the LIA.

Lichenometric measurements were performed on all of the ridges, lichen thalli located on rapid mass-movement depositions were avoided, though the huge amounts of rapid mass-movement deposits made lichenometric measurements difficult, especially on M-13 and M-17. Datings are presented in Chapter 2.3.2.

M-18 and M-19 Observation

Two ridges located in a valley side, southeast of Vestre Blomsterskardsbreen, in Insta Botnane, UTM 498930, 1015 m to 1040 m a.s.l.

M-18 and M-19 are two ridges in the easternmost valley of Insta Botnane. Their location is of difficult accessibility, for time reasons they could not be reached during fieldwork. Angle measurements and lichen measurements were therefore not performed on these ridges. But they could clearly be seen from the valley entrance. Based on aerial photographs (Statens Vegvesen et al. 2006), the following observations could be made: M-18 is approximately 200 m long, ranging from ca. 1020 to 1040 m a.s.l. M-19 is approximately 150 m long, ranging from ca. 1015 m to 1030 m a.s.l. They are covered by vegetation with a few larger boulders upon; and the ridges are surrounded by till.

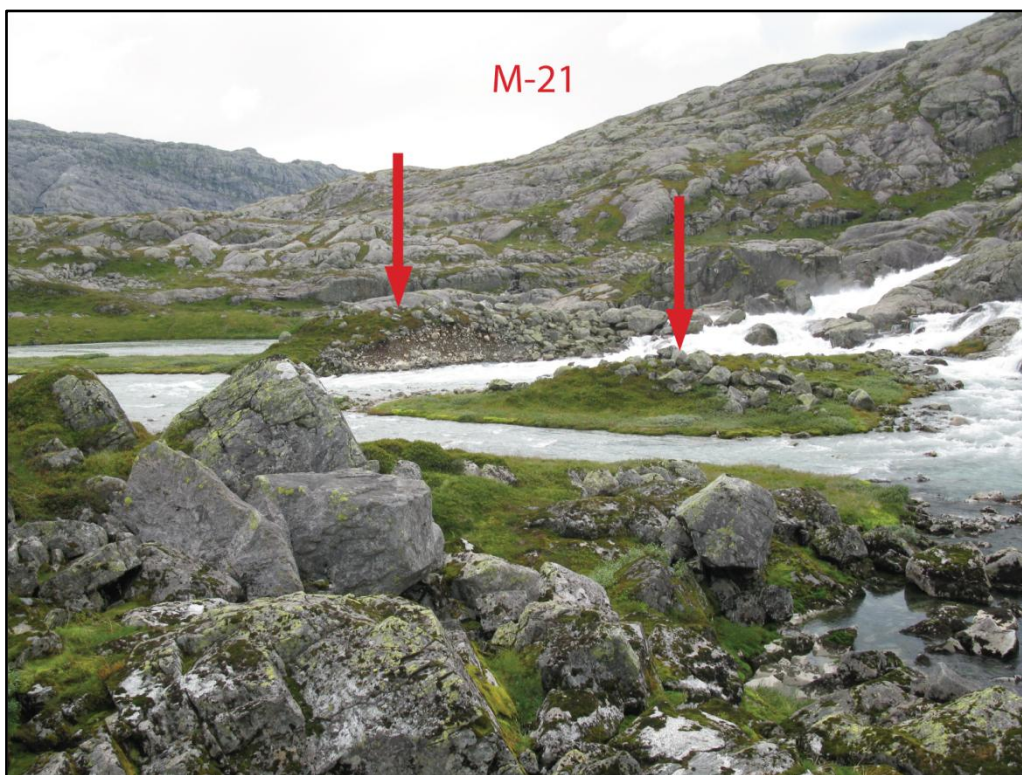
M-18 and M-19 Observation

M-18 and M-19 are due to their ridged forms and their locations interpreted as lateral moraines. The temporal origin of the easternmost moraine, M-19, is interpreted as being linked to the origin of M-1, M-2 and M-4, representing the maximum glacier advance during the LIA. Since lichenometric measurements were not performed, this assumption cannot be verified.

M-20 and M-21 Observation

Ridge system located in the north of Kjerringebotn, UTM 468100 to UTM 470475, 795 m to 812 m a.s.l.

M-20 is a large, ridge-formed deposition located in the north of Kjerringebotn. It is 270 m long, 110 m at its broadest, and around 10 m in height. Its length axis is orientated (north-) east to (south-) west. All grain sizes from silt to large sub-angular and rounded boulders could be observed, the material is unsorted. The ridge is covered by vegetation of mainly mosses, grass and blueberries, and many huge boulders of up to 5 m in diameter are located upon it. It is bordered by exposed bedrock in the north and a lake in the south, which made angle measurements not possible. The ridge can be followed through the river Blådalselv, where boulder depositions could be observed on islets within the river, probably washed out in the course of time. On the western side of the river, the ridge form carries on, numbered as M-21. Here, it appears as a 110 m long ridge form; the length axis is orientated in (north-)west to (south-)east direction. M-21 consists of large sub-angular to rounded boulders not covered by vegetation. They reach heights of up to 2.5 m. The material was too coarse for angle measurements.



Picture 5 Marginal moraine M-21, divided by river Blådalselv. Picture is taken looking to the west.

M-20 and M-21 Interpretation

M-20 and M-21 are interpreted as one terminal moraine, deposited during a glacier advance earlier than the LIA. Lichenometric measurements were performed on both M-20 and M-21; datings are presented in Chapter 2.3.2. Right after deposition, it was probably arch-formed, with a general east - west orientation, and much higher than today, containing all grain sizes. River Blådalselv modified it in the course of time; the moraine was washed out, and today only remnants of the moraine can be observed.

M-22 Observation

Ridge system located in the southwest of Kjerringebotn, UTM 465405, 805 m to 830 m a.s.l.

M-22 is a huge ridge located at the southwestern end of Kjerringebotn. It is surrounded by a thick layer of till in Kjerringebotn. The ridge is 180 m long, 15 m high, and the length axis is orientated in a north-northeast to south-southwest direction. It is covered by a thick layer of humus and well-established vegetation, mainly grasses and blueberries. On top of the ridge, many big, rounded blocks of up to 2 m in diameter are located, which are not covered by vegetation. All grain sizes could be observed, ranging from silt to huge, rounded or sub-angular boulders; the material is unsorted. The proximal angle is 45°, and the distal angle is approximately 35°. At the southeastern part of the ridge, an area of angular rapid mass-movement deposits is located. The ridge can be followed up on the northern riverbank of the river Blådalselv, where huge blocks are spread over an area of ca. 80 m downstream.

M-22 Interpretation

Due to the fact that no bedrock exposures could be observed that could have decisive impact on the form of the ridge, it is interpreted as a terminal moraine deposited earlier than the LIA, and earlier than M-20/M-21. The river Blådalselv cut into the moraine after deposition and washed out the northern part of it, which originally must have been orientated in a more north-east to south-west direction. Lichenometric measurements were performed on the ridge part located south of the river; the area of rapid mass-movement deposits in the southern part of the ridge was excluded. Datings are presented in Chapter 2.3.2.

M-23 Observation

Ridge located south of Lake Møsevatn, UTM 450919, 901 m a.s.l.

M-23 is a 110 m long and up to 2 m high ridge located south of Lake Møsevatn. The length axis is orientated north-east to south-west. It consists of rounded to sub-angular blocks of 0,5

to 2 m in diameter, individual blocks up to 5 m; it is in some parts covered by mosses. The ridge is surrounded by till and block-rich surface.

M-24 and M-25 Observation

Two ridges located south of Lake Møsevatn, UTM 446282, 775 m to 810 m a.s.l.

M-24 and M-25 are two ridges located in a valley side south of Lake Møsevatn close to river Blådalselv. The ridges are up to 4 m high; the observed material is unsorted and ranging from gravel to blocks of up to 1.5 m in diameter. M-25 could be followed up on the eastern side of the river, where the deposits consists of only blocks, while finer fractions were washed out. The orientation of ridges M-24 and M-25 is north-west to south-east; the loose depositions on the eastern riverside are orientated north-east to south-west. M-24 and M-25 are covered by a well-established layer of gramineous vegetation. The ridges are surrounded by till depositions.

M-26, M-27, M-28, M-29, M-30, M-31 and M-32 Observation

Seven ridges located in a valley side south of Lake Møsevatn, UTM 442400, 780 m to 840 m a.s.l.

M-26 to M-32 are seven ridges located within one valley side. The individual height of the ridges is up to 6 m. Unsorted material of all grain sizes could be observed; the ridges are covered by a thick layer of well-established vegetation, consisting of mainly ling, blueberries and grasses. The length axes of M-26 to M-28 are north-east to south-west orientated, the ones of M-29 to M-32 north-west to south-east. In between the ridges flow small streams, which indicate that the ridges once were connected in an east-west direction across the valley side, but then were washed out.

M-23 to M-32 Interpretation

M-23 to M-32 are interpreted as marginal moraines formed by glacier advances of Møsevassbreen.

Due to their close location to each other within one valley side, M-24 and M-25 and the loose depositions in the east of the valley are interpreted as to represent one moraine, which was washed out by the river that connects Lake Møsevatn and river Blådalselv. The morain is assumed to have been higher right after deposition, but afterwards reduced and modified by the river.

Due to their location so close to each other within one valley side, M-26 to M-32 are interpreted as one moraine set.

Based on ELA reconstructions of Mosevassbreen from these moraines, Bjønnes (2006) assumed that the moraines M-23 to M-32 were deposited during the preboreal and in the time period 10 550 – 10 450 cal. years BP. Within these two time periods two glacier advances could be proved at northern Folgefonna, “Jondal 1 event” and “Jondal 2 event”. “Jondal 1 event” corresponds with a time period of lower summer temperatures during the preboreal, and “Jondal 2 event” is a result of increased winter precipitation in the time period 10 550 – 10 450 cal. years BP. Moraines M-23 up to and including M-32 are interpreted as being formed during “Jondal 1 event” and “Jondal 2 event” (Bjønnes 2006 and references therein).

2.2.1.2 Till

Material transport within a glacier can take place subglacially, englacially and supraglacially (Nesje 1995). Most of the material transported within a temperate glacier is located at the glacier base, where a layer of dirty ice often forms the interface between clean ice and solid rock (Paterson 1994; Nesje 1995). This basal layer, which can have a thickness of up to several meters, is an important feature with respect to the glacier’s ability of eroding its bed, and transporting and crushing the material between the glacier ice and the glacier bed (Paterson 1994; Nesje 1995). When the glacier retreats, this material is deposited as till (Sulebak 2007). Till, also referred to as ground moraine, is moraine material which is characterized as unsorted material of all grain sizes ranging from clay to large boulders deposited by a glacier (Gjessing 1978). Depositions of till may allow conclusions about where within a glacier material was transported and finally deposited (Nesje 1995).

Till can appear as continuous cover (thickness greater than 0,5 m and up to several tens of meters), or as discontinuous or thin cover on bedrock (thickness of deposit normally smaller than 0,5 m, occasionally thicker) (Bergstrøm et al. 2001).

Observation and interpretation of till

Till is observed at multiple places in the study area. Amongst others in Midtbotn (UTM 439259, 770-940 m a.s.l.), Kjerringebotn (UTM 469655, 790-880 m a.s.l.) and parts of Insta Botnane (UTM 487768 and UTM 498610, 930-1080 m a.s.l.). Thickness and size of the moraine material vary. On the quaternary map, till is marked as discontinuous or thin cover on bedrock, because the thickness of the deposits observed are normally smaller or only at some locations a little thicker than 0,5 m; the form of the underlying bedrock is generally apparent, and often small bedrock exposures are observed within areas of till deposits, as for example in Insta Botnane.

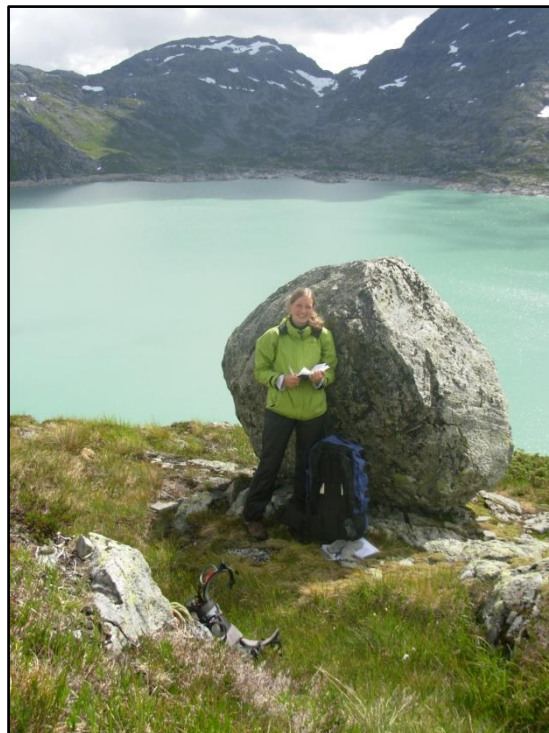
The till observed in the study area contains boulders of all grain sizes, rounded or with sub-angular; the material is unsorted. All areas where till is observed are marked on the quaternary map of Blomsterskardsbreen and Midtbotnvatn (see Appendix 1).

2.2.1.3 Erratic blocks

Erratic blocks are large boulders (size exceeding 10 m^3) transported and deposited by glacier ice during melt off, and therefore often rounded or sub-angular (Gjessing 1978; Bergstrøm et al. 2001; Ahnert 2003). When they consist of different rock than the bedrock they are deposited on, this is an indicator of their area of origin, which may give evidence on the direction of the glacier ice movement (Ahnert 2003; Sulebak 2007).

Observation and interpretation of erratic blocks

Erratic blocks ranging in diameter size between approximately 1 m and 20 m, can be observed at multitudinous places all over the study area, mostly deposited on bedrock or till (one example is located at UTM 454055, 785 m a.s.l.). Mapping all of them would exceed the framework of the master's thesis, but some of them are marked in the quaternary map of Blomsterskardsbreen and Midtbotnvatn (see Appendix 1).



Picture 6 Erratic block of ca. 2 m in diameter located north of Lake Midtbotnvatn; person for scale. Picture is taken looking to the south. (Picture: Stephanie Wegscheider)

2.2.2 Glacial erosion forms

The glacial erosion process has two constituent parts, plucking and abrasion (Nesje 1995). Plucking is when moving glacier ice lifts out boulders of any grain size from the underlying bedrock, previous loosening by freezing and accompanied expansion of water within joint fractures is decisive (Nesje 1995). Abrasion is when glacier ice moves over the underlying bedrock, transporting all plucked abundant rock fragments, which cause friction and that way scrape and grind the bedrock surface in the direction of the ice-movement (Nesje 1995; Strahler and Strahler 2006). Resulting forms on the bedrock are for example glacial striae, crescentic fractures and crescentic gouges, which, in addition to others, may indicate the direction of the ice-movement (Nesje 1995; Bergstrøm et al. 2001). Glacial striae are defined as (sub)parallel stripes at the bedrock surface evolved through abrasion (Nesje 1995). Crescentic gouges and fractures develop when glacier ice presses a boulder against a point on the bedrock surface, so that the pressure spreads out to surrounding parts of the bedrock. Crescentic gouges are induced by yield stress in front of the pressure point, resulting in arc-shaped gouges facing downwards. Crescentic fractures evolve when the yield stress behind the pressure point causes parabola-formed fractures concave in the direction of the ice-movement (Nesje 1995).

Observation and interpretation of glacial erosion forms

Glacial striae, crescentic gouges and crescentic fractures are observed at innumerable locations within the study area. They are orientated in south-western (for example UTM 472891, 847 m a.s.l.), southern (for example UTM 469983, 818 m a.s.l.) and western (for example UTM 466405, 805 m a.s.l.) directions. Mapping all of them would exceed the framework of the master's thesis, but some of them are marked in the quaternary map of Blomsterskardsbreen and Midtbotnvatn (see Appendix 1).

2.2.3 Glaciofluvial deposits

Glaciofluvial deposits are material transported and deposited by glacial meltwater streams (Thoresen 1991; Nesje 1995). Within a glacier, meltwater can flow subglacially, supraglacially and englacially (Menziés 1995). Depending on the individual characteristics of a glacier, such as amongst others type, topographic setting and mass balance, and moreover on the thermal conditions within a glacier and on climatic conditions and seasons, the flow conditions of meltwaters within a glacier vary temporally (for example daily, seasonally and

on long-period-scales), in flow velocity and amount of discharge (Summerfield 1991; Paterson 1994; Menzies 1995). Reaching the margins of a glacier and flowing out, meltwaters develop into glacial meltwater streams, which have a typical green-greyish-white colour due to their high amount of fine sediment originated by glacial abrasion (Summerfield 1991; Menzies 1995; Ahnert 2003). Because of the eroding activity of glaciers, glacial meltwater streams transport and thus deposit more sediment than normal rivers (Summerfield 1991). Glaciofluvial sediments can be deposited either in direct contact with the glacier, or in the proglacial environment beyond the ice front (Leeder 1982; Summerfield 1991). Glaciofluvial deposits are often less rounded than fluvial depositions, and generally more rounded than for example moraine material, the latter characteristic increases the longer the material is transported (Nesje 1995). Glaciofluvial deposits can generally be observed as sorted layers of different grain sizes, the so-called stratification is a key characteristic (Summerfield 1991; Nesje 1995). Varying properties concerning thickness and grain sizes of the layers reflect variations in the flow conditions of glacial meltwater streams (Nesje 1995).

Observation and interpretation of glaciofluvial deposits

Glaciofluvial deposits can be observed in some places in the study area, mostly in connection with the glacial meltwater stream Blådalselv. The dam built at the north-eastern end of Lake Midtbotnvatn has impacts on the stream, such as amongst others an increase in water level and a decrease in flow velocity. Result is that glaciofluvial deposits can be observed at many parts of the riverside (one example is in Kjerringebotn UTM 467917, 800 m a.s.l.), characterized by sorted layering and small grain sizes. In other parts, the glaciofluvial deposits are more scattered, thinner, and partly very discontinuous (as for example south of the river mouth at UTM 446712, 777 m a.s.l.).

Glaciofluvial deposits can as well be observed north-west of the small lake in front of the glacier tongue of Vestre Blomsterskardsbreen (UTM 474613, 869 m a.s.l.). These are interpreted to represent sediments transported and deposited while the glacier tongue of Vestre Blomsterskardsbreen was greater than today, having passed a local overflow gap (spillway) and sending glacial meltwater streams more easterly and through the small lake. These sediments may have originated in connection with the outflow of a proglacial lake that deposited the terrace that is today located in front of the glacier's terminus, consisting of glaciolacustrine sediments deposited during the LIA (cp. Chapter 2.2.4).

All areas where glaciolacustrine deposits can be observed are marked in the quaternary map of Blomsterskardsbreen and Midtbotnvatn (see Appendix 1).

2.2.4 Glaciolacustrine deposits

Glaciolacustrine deposits are sediments deposited within a proglacial lake (Leeder 1982). Incoming water is rich in suspended fine-grained material (cp. Chapter 2.2.3), which then is deposited in laminations at the lake bottom (Leeder 1982; Thoresen 1991). Variations in sedimentation rates in proglacial lakes, observed through differences in layering structures and grain sizes, can reflect changing glacier and melt water conditions (Leeder 1982); though there are many controlling factors regarding capacity of meltwater streams and sediment disposal (Leonard 1985). See Chapters 3.1 and 3.2 for a more detailed description of glaciolacustrine sediments and deposition factors.

Observation and interpretation of glaciolacustrine deposits

Glaciolacustrine deposits can be observed in some places in the study area, where they reflect the former presence of proglacial lakes. A terrace in front of the terminus of the glacier tongue of Vestre Blomsterskardsbreen is interpreted as glaciolacustrine sediments (UTM 474832, 860 m a.s.l., Picture 7), originated during the time period of the late LIA, when the glacier's terminus was located further south than today (see also Helleland 2008, 434f). The location of moraine M-3, dated to 1945 (cp. Chapter 2.3), is interpreted to reflect the position of the terminus of Vestre Blomsterskardsbreen which enabled the presence of a proglacial lake by blocking the meltwaters flowing in the western part of the valley and instead leading those more eastwards creating the proglacial lake. The meltwater then ran further southwards, depositing glaciofluvial sediments and later creating a glaciofluvial drainage channel (cp. Chapter 2.2.3 and 2.2.5); these features are all marked in the Quaternary map of Blomsterskardsbreen and Midtbotnvatn (see Appendix 1). The material of the glaciolacustrine sediments is fine-grained and laminated, and several meters thick. After deposition, it has been modified and partly been washed out by meltwaters from the glacier.

Another place where glaciolacustrine material can be observed is south of Lake Møsevatn (UTM 449653, 881 m a.s.l.); for a closer description see Bjønnes (2006).

Due to the varying water level of Lake Midtbotnvatn, scattered, thin and discontinuous glaciolacustrine deposits can also be observed in some parts around the lakefront.

All areas where glaciolacustrine deposits can be observed are marked in the quaternary map of Blomsterskardsbreen and Midtbotnvatn (see Appendix 1).



Picture 7 Glaciolacustrine deposits in front of the glacier tongue of Vestre Blomsterskardsbreen; modified by meltwaters. Picture is taken looking to the north-west.

2.2.5 Glaciofluvial erosion forms

Due to high flow velocities, especially high peak discharges and huge contents of fine and coarse suspended materials, glacial meltwater streams can have strongly erosive impact on both superficial deposits and exposed bedrock (Summerfield 1991). Glaciofluvial drainage channels, meltwater channels and glaciofluvially eroded canyons are examples for the erosive effect of glaciofluvial streams on landforms (Bergstrøm et al. 2001).

Observation and interpretation of glaciofluvial erosion forms

Glaciofluvial erosion plays an important role in the study area. The huge amount of meltwaters that annually naturally flow from Vestre Blomsterskardsbreen through river Blådalselv and into Lake Midtbotnvatn has been intensified by the development of hydroelectric power, in 1970 by the construction of a tunnel leading the drainage water from Østre Blomsterskardsbreen also into the river Blådalselv, and in 1983 by damming Lake Midtbotnvatn and river Blådalselv and enlarging the dam in 1992, resulting in a total height of

regulation of 70 m (Tvede and Liestøl 1977; Tjelmeland 1992). Also in the area of Insta Botnane small dams and a tunnel were constructed.

The area in front of the glacier tongue of Vestre Blomsterskardsbreen is therefore extremely washed-out (UTM 473056, 860 m a.s.l.), as are many parts of the study area located close to the river Blådalselv.

A glaciofluvial drainage channel can be observed, leading from the glaciolacustrine deposits in front of today's glacier front down to the small lake (from UTM 474930, 860 m a.s.l. to UTM 473981, 839 m a.s.l.), indicating a former drainage pattern during the LIA, which was located more easterly than today's (cp. Chapter 2.2.4). This glaciofluvial drainage channel is marked in the quaternary map of Blomsterskardsbreen and Midtbotnvatn (see Appendix 1).

2.2.6 Rapid mass-movement deposits

Rapid mass-movement deposits can be originated by rock falls, snow avalanches or debris avalanches (Thoresen 1991; Bergstrøm et al. 2001; Ahnert 2003).

Rock fall is the fall of individual blocks with a mass of up to 100 m³ from vertical faces steeper than 40-45°; the material is angular and contains grain sizes from silt to large boulders (Summerfield 1991, 169; Sulebak 2007). The fallen material has a sorted grain size distribution, forming a talus built up at the foot of the face, with a slope angle of 35-40°; the smallest grain sizes are at the top of the talus and the bigger blocks, which have the highest kinetic energy during the rock fall, can be found at the bottom (Gjessing 1978; Sulebak 2007).

A snow avalanche is the catastrophic low friction movement of snow and ice, in some cases with rock debris, precipitated by fall or slide (Summerfield 1991, 169).

A debris avalanche is a catastrophic low friction movement of rock debris of up to several kilometers, in some cases with ice and snow, usually precipitated by a major rock fall and capable of overriding significant topographic features (Summerfield 1991, 169).

Avalanche tracks can develop on rock faces that exhibit steep zones that are marked by joint fractures where weathering efficiently can affect the bedrock (Gjessing 1978).

Observation and interpretation of rapid mass-movement deposits

Rapid mass-movement deposits can be observed multitudinous places in the study area. The deposits have a thickness between approximately 0,3 m and several meters, though they are discontinuous and scattered in some parts. The material can be located on bedrock or above other superficial deposits, for example till. Some places, clear avalanche tracks can be seen in the rock faces above the deposits. Some examples for locations of rapid mass-movement

deposits are presented: At the northern foot of Blådalshorga (UTM 427800, 775 m to 850 m a.s.l.) there is a huge area covered by rapid mass-movement deposits, the boulders, mainly originated from rockfall, are very angular and range in sizes from a few cm to approximately 15 m. The absence of vegetation in this area indicates the activeness of the process there. At the steep rock face in the eastern part of Lake Midtbotnvatn (UTM 447381, 770 m up to 980 m a.s.l.), avalanche tracks can be seen, and during fieldwork in April 2008, traces of snow avalanches including debris could be observed. The material falling down here ends up in Lake Midtbotnvatn in the majority of cases. How rapid mass-movements may influence the sedimentation is discussed in detail in Chapter 3.5.4. A talus with avalanche track above can be observed in the area of Insta Botnane (UTM 485447, 974 m a.s.l.).

On the quaternary map, there is no distinction made between the different processes that deposit mass-movement material. All mass-movement deposits with sufficient extent are marked in the quaternary map of Blomsterskardsbreen and Midtbotnvatn (see Appendix 1).

2.3 Lichenometry

2.3.1 Lichenometry – Method description

Lichenometry is a biological dating method that uses the size of lichens to obtain the minimum age of the rock substrate it grows on, using the numerical relationship between the two factors (Karlén 1979; Matthews 1994; Bradley 1999; Matthews 2005). Lichenometry can be used to date surfaces of up to 500 years of age (Innes 1985a; Winkler 2003).

Knowing the growth rate of the investigated lichen species in the study area, the minimum age of the surface of rock deposits can be estimated through the largest lichen on it (Matthews 1994; Bradley 1999; Matthews 2005). In areas that earlier were covered by ice, lichenometry thus makes it possible to date the time rock substrate became deglaciated (Bradley 1999). Continuous glacier chronologies for the time period of the LIA can be reconstructed using this method (Beschel 1950; Winkler 2003), as Bakke et al. (2005a) did in the forelands of northern Folgefonna glacier, where a sufficient number of terminal moraines enabled the successful establishment of relative-age chronologies for the investigated moraine sets.

The growth rate of lichen is not linear with time, it varies for each lichen species with different climate conditions and rock types (Matthews 1994, 2005); and generally it is rather fast at the beginning, becoming slower and slower with time, until it reaches a more or less constant rate (Beschel 1950). That's why a lichenometric growth curve should be established for each study area, using points of known age in or as close as possible to the study area,

which is the “indirect approach” of lichenometry (Matthews 1994; Winkler 2003; Matthews 2005). So-called control points are used to achieve this (Matthews 1994); by measuring the largest lichen on a rock with known age, where other dating methods were applied, or where historical writings, photographs or paintings report the age (Bradley 1999; Winkler 2003; Matthews 2005).

There is also a “direct approach” that can be used to construct a lichenometric dating curve in a study area. Hereby, a lichen growth curve is established by directly measuring lichen growth over several years (Matthews 1994). This method must be applied on a long-term basis with a minimum requirement of measurements being done over several years, and even then the non-linearity of lichen growth over time cannot adequately be taken into account; the impact of this fact increases with the increasing age of the investigated surface (Matthews 1994). Matthews (1994) means that the “indirect approach” gives the best results when the lichenometric dating technique is applied on short time-scales over not more than five centuries, as long as sufficient independent dating control is provided. These are the reasons why in many studies the “indirect approach” is preferred to the “direct” one (Matthews 1994), as it is also done in this study. In southern Norway, lichenometry has been successfully applied several times by several authors, especially with respect to the time period of the LIA (cp. Matthews 1975; Erikstad and Sollid 1986; Innes 1986; Bickerton and Matthews 1992, 1993; Matthews 1994; McCarroll 1994, 2001; Bakke et al. 2005a; Matthews 2005).

There are some sources of error that may affect the results of lichenometry. It is important that the measured lichens are all of one species, and that the largest ones are measured (Bradley 1999; Winkler 2003). Both quantity and quality of the control points must be adequate: there should be the same environmental conditions, especially concerning moisture supply, at the control points and at the surfaces that are to be dated (Matthews 1994, 2005). Further important influencing environmental factors on lichen growth, that increase the environmental heterogeneity of an area, are temperature, light intensity, substrate lithology, substrate stability, snow cover, wind exposure, altitude, aspect, continentality and competition with other plant groups, which should be taken into account when constructing a dating curve (Innes 1985a; Matthews 1994). The greater the distance between study area and control points, the more environmental differences are to be expected, which makes the results less accurate (Matthews 1994, 2005). The reliability of dating results decreases generally as the age of the surfaces to be dated increases, since fewer control points are available further back in time (Matthews 1994).

The non-linear growth rate may also have been influenced by long-term climatic fluctuations, such that there were most likely times when lichen growth was quite fast and times where it was interrupted, for example when the rock substrate was covered by snow (Bradley 1999; Winkler 2003). Furthermore, the dating of the reference points can be inaccurate. These two factors may cause uncertainties in the growth curve (Bradley 1999).

The sometimes quite significant delay between exposure of the rock surface and colonisation of the surface by lichens can vary between study areas (Bradley 1999).

Rock substrate movement, for example through rockfall or snow avalanches, which leads to mixtures of older and younger rocks, can falsify results (Bradley 1999).

Measurements themselves are affected by subjective interpretations of the person performing; concerning, for example, ability to discover the largest lichen thalli, the choice of measuring or rejecting a lichen thallus, and accuracy in measurement (Erikstad and Sollid 1986).

Bickerton and Matthews (1992) dated LIA moraines at Nigardsbreen in Norway to an accuracy of 10%, which means an error between ± 5 and ± 20 years depending on the age of the moraines.

2.3.2 Lichenometry – Application

Measurements of lichen thalli were performed on marginal moraines in front of the glacier tongue of Vestre Blomsterskardsbreen in the summers of 2008 and 2009. The yellow-green lichens of the subgenus *Rhizocarpon*, species *Rhizocarpon geographicum*, were subject of investigation (cp. Innes 1985b; Bickerton and Matthews 1992). The longest diameters of the largest lichen thalli observed were measured with a slide calliper and a measuring tape, with accuracy to the nearest millimeter. Up to 40 measurements were performed within up to four ca. 4×10 m (40 m^2) rectangles (sites) on each moraine. On some smaller moraines the number and size of the rectangles were reduced. The rectangles were placed from the moraine tops down the proximal side, the side facing towards the glacier, to ensure the closest possible approximation to the minimum date of each moraine (cp. Innes 1985a; Bickerton and Matthews 1992). Due to the fact that snow stays longest in the lowest parts of a moraine, where it is better protected from sun and wind, the rectangles were located closer to the top than to the bottom of the moraines. Longer lasting snow layers reduce the length of the growing season and can decrease the growth of lichens, which in extreme cases, when several years pass without significant snowmelt, can culminate in “snow kill”, the dieback of lichens (Innes 1985a).

A prerequisite for a successful application of lichenometry is that the maximum diameter of the largest lichen, which grew as uniformly radial as possible, is measured (Bradley 1999).

This is based on the assumption that the largest lichen represents the most optimum environmental conditions of the study area and thus can give the best minimum dating result (Matthews 1994; Bradley 1999; Winkler 2003; Matthews 2005). Since it never can be guaranteed that the largest lichen could be found, normally the average of the five largest lichens is taken (e.g. Karlén 1979; Bickerton and Matthews 1992; Winkler 2003, 2004; Matthews 2005). Karlén (1979) points out that the five largest lichens can be useful to evaluate the quality of the measurements: the smaller the differences in size of the five largest lichens are, the higher is the reliability of the dating results.

The mean of the single largest lichens of each site on the moraines was used to date the moraines in the study area, based on the lichen growth curve for *Rhizocarpon geographicum* “Folgefonna – compiled data”, which was established through several control points around Folgefonna glacier (Figure 2.2, Table 5, Table 6) (Bakke et al. 2005a).

Table 5 Lichenometric measurements (mm) at observed moraines in front of Vestre Blomsterskardsbreen; calculations are based on Winkler (2003, 89). Datings interpreted as reliable are marked bold.

Moraine	Largest lichen (max) ¹	Largest lichen (mean) ²	Mean of five largest lichens (max) ³	Mean of five largest lichens (mean) ⁴	Sites per moraine
M-1	116	111	105	103	3
M-2	118	115	113	110	4
M-3	27	25	24	24	1
M-4	131	121	115	113	3
M-5	114	108	109	104	4
M-9	113	106	108	101	4
M-10	111	105	106	100	4
M-11	102	96	98	92	4
M-13	114	109	110	105	4
M-14	115	110	109	104	4
M-15	94	90	90	86	4
M-16	108	103	102	98	4
M-17	116	112	112	108	4
M-20 ⁵	300	219	217	196	4
M-21 ⁵	134	128	120	118	3
M-22 ⁵	282	259	254	249	4

1 Single largest lichen of all sites on the moraine (mm)

2 Mean of the single largest lichens of every site on the moraine (all sites, up to 4, included) (mm)

3 Highest value for the mean of the five largest lichens of all sites on the moraine (mm)

4 Mean of the means of the five largest lichens of every site on the moraine (all sites, up to 4, included) (mm)

5 Assumed pre-‘Little Ice Age’ moraine (see text). Dating by lichenometry was not applied for methodological reasons

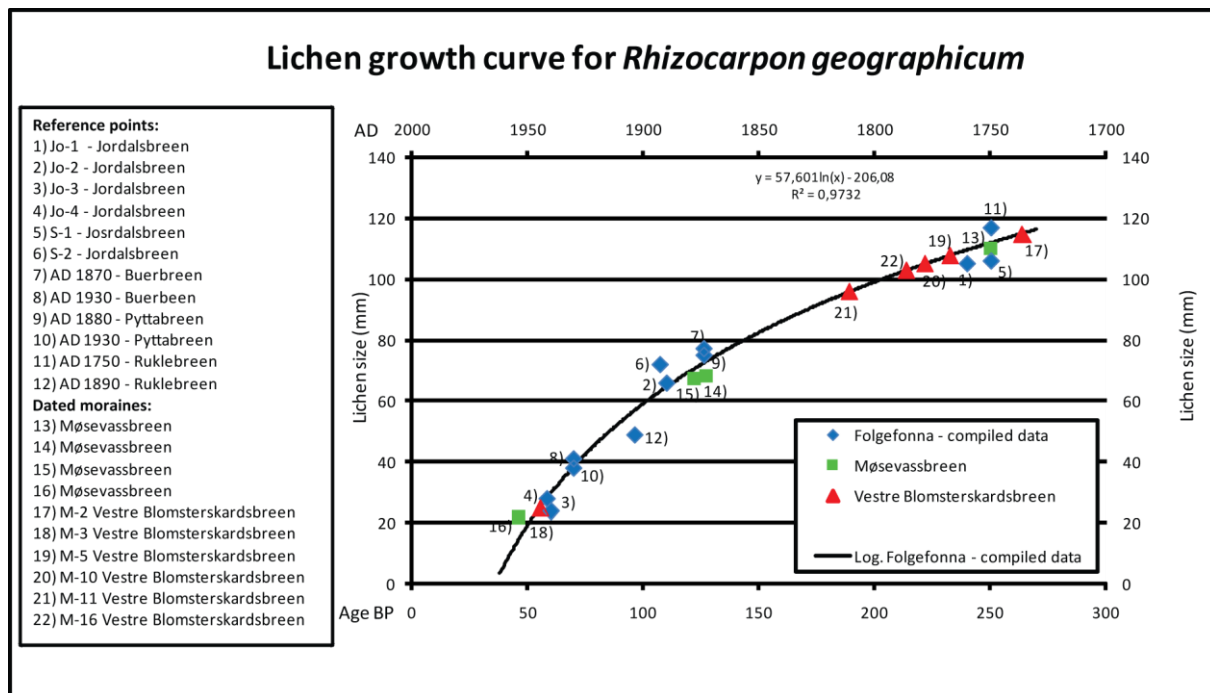


Figure 2.2 The lichen growth curve for *Rhizocarpon geographicum* “Folgefonna – compiled data”, based on several control points around Folgefonna glacier (blue rhombuses), was used to date moraines of Vestre Blomsterskardsbreen, marked with red triangles (Modified from Bakke et al. 2005a, 184). Dates from Møsevasbreen are included (green rectangles) (Bjønnes 2006). Scientific studies indicate an early LIA glacial advance at many glacier outlets of Folgefonna close to AD 1750, and later readvances between AD 1870 and 1890 and during the 1930s (Bakke et al. 2005a and references therein)

Table 6 Dating results of observed moraines in front of Vestre Blomsterskardsbreen based on the lichenometric dating curve “Folgefonna – compiled data” (Bakke et al. 2005a, 184). Dates interpreted as reliable are marked bold.

Moraine	Lichen size (mm)	Age BP	AD ± 10% (years)
M-1	111	246	1754 ± 25
M-2	115	264	1736 ± 26
M-3	25	55	1945 ± 6
M-4	121	292	1708 ± 30
M-5	108	233	1767 ± 23
M-9	106	225	1775 ± 23
M-10	105	222	1778 ± 22
M-11	96	189	1811 ± 19
M-13	109	237	1763 ± 24
M-14	110	242	1758 ± 24
M-15	90	171	1829 ± 17
M-16	103	214	1786 ± 21
M-17	112	250	1750 ± 25
M-20	219	> 300	before 1700
M-21	128	> 300	before 1700
M-22	259	> 300	before 1700

There are several factors that especially may reduce the reliability of the dating results in the study area.

First, rapid mass-movement deposits, mainly originated from rockfall, could be observed many places in the study area close to or upon several moraines, especially on those located within valley sides. In particular, this feature was sporadically observed at M-2, M-4, M-9, M-11, M-12, M-14, M-15, M-16, and at M-22, and very distinct at M-7, M-8, M-13, and M-17. Rapid mass-movement processes can transport material of older or younger age to the moraine, which, if it remains unidentified, can falsify the lichenometric dates. Therefore, care was taken not to measure lichen thalli on boulders interpreted as rapid mass-movement deposit. On M-2, M-4, M-16 and M-22, only limited parts of the moraine ridges were affected by sporadic or distinct rapid mass-movement deposits, these parts were carefully excluded from lichenometric measurements.

Second, well-established vegetation is present on many moraine ridges in the study area, complicating lichen thalli growth, observations and measurements. M-5, M-6, M-7, M-8, M-9, M-10, M-11, M-12, M-13, M-14, M-15, M-16, M-17, M-18, M-19, M-20, M-22 were, to different extends, covered by mainly gramineous vegetation, mosses, and small bushes like blueberries and ling. At these ridges, lichen growth is in competition with or covered by the vegetation, and therefore natural lichen growth rate is restrained; lichenometric dating results may be younger than the real age of the moraine.

Third, the huge amounts of melt- and run-off water in the study area impact many moraines, modifying the ridges and restraining the natural lichen growth in past and present. M-1, M-3, M-5, M-20, M-21 and M-22 were heavily washed-out and modified by running water. The high annual precipitation rate in form of rain and especially snow, and the hence resulting long annual snow cover also can have negative influence on the natural lichen growth.

Less measurement sites due to small sizes of the moraines reduced the reliability of the dating results at M-1, M-3, M-4 and M-21.

The moraines interpreted to have reliable dating results are M-2, M-3, M-5, M-10, M-11 and M-16.

M-20, M-21, M-22 and M-23-32 have lichen thalli diameter larger than 150 mm, for methodological reasons dating by lichenometry could therefore not be applied (cp. Winkler 2003).

2.3.3 Lichenometry – Interpretation

Observed moraine ridges of Vestre Blomsterskardsbreen in the study area were dated by the use of the lichen growth curve for *Rhizocarpon geographicum* “Folgefonna – compiled data”, which is based on several control points around Folgefonna glacier (Figure 2.2) (Bakke et al. 2005a). The fact that the control points are located in several regions around Folgefonna indicates that some environmental factors which influence lichen growth, such as temperature, moisture supply, light intensity, substrate lithology, substrate stability, snow cover, wind exposure, altitude, aspect, continentality or competition with other plant groups, may be different in the study area (cp. Innes 1985a; Matthews 1994). The lichen growth curve “Folgefonna – compiled data” thus is an approximation to the real conditions in the study area, a fact that may affect the accuracy of the dates. The limited time period covered by the control points is another limiting factor for the reliability of the dating results, the growth curve had to be interpolated for the time before AD 1750 and after AD 1942 (cp. Bakke et al. 2005a).

The outermost moraines which lichenometric dating successfully could be applied on were M-1, M-2, and M-4. M-1 and M-2, with mean diameters of the five largest lichens of 111 mm and 115 mm, were dated to an age of 246 and 264 years BP, respectively, which corresponds to an origin in AD 1754 and AD 1736. M-4, with a mean lichen diameter of 121 mm, reflecting an age of 292 years BP, is according to lichenometric measurements assumed to be deposited in AD 1708. Since M-1 to a great extent was reworked by river Blådalselv, and M-4 was influenced by rapid mass-movement deposits, lichenometric measurements on M-2 seem the most reliable. M-1, M-2 and M-4 are interpreted as reflecting the maximum glacier advance of the LIA in the first half of the 18th century, dated to AD 1736. M-19, on which lichenometric dating was not applied, is due to its location interpreted as being part of this set. The spatial closeness of M-18 indicates that the retreat from M-19 to M-18 must have gone comparatively fast. This cannot be verified since neither M-18 nor M-19 could be subject to lichenometric measurements during fieldwork.

M-5 and M-17, with mean lichen thalli diameters of 108 mm and 112 mm, are dated to an age of 233 and 250 years BP, which indicates a deposition in AD 1767 and AD 1750, respectively. The distinct impact of rapid mass-movement deposit may falsify the dating results of M-17; M-5 and M-17 are therefore interpreted as one moraine set reflecting a

glacier re-advance or steady-state position of Vestre Blomsterskardsbreen during the LIA in AD 1767.

M-10 and M-16 have mean lichen diameters of 105 mm and 103 mm, which results in an age of 222 and 214 years BP, indicating an origin in AD 1778 and AD 1786, respectively. Due to the fact that lichenometry in general is assumed to have an error of up to 10% (Bickerton and Matthews 1992), and the somewhat limited accuracy of the applied growth curve, these moraines are interpreted as to be one set, deposited by a glacier re-advance or a phase of steady-state during the LIA around AD 1780. According to the lichenometric dating results, the glacier retreated comparatively fast from the moraine set M-5 and M-17 (AD 1767) to M-10 and M-16 (AD 1780).

Rapid mass-movement deposits and vegetation cover made lichenometric measurements difficult or even impossible at M-7, M-8, M-9, M-13, M-14 and M-15, reliable dating results could not be achieved for these moraines. M-11, with a mean lichen thalli diameter of 96 mm, is interpreted as reliable, dated to an age of 189 years BP, which corresponds to an origin in AD 1811. Smaller glacier (re-)advances are assumed to be able to form marginal moraines in valleys where enough material was available to be pushed up, whereas on heights either discontinuous or no moraines were deposited; this is a result of material availability and the fact that glaciers often are located further back on heights than in valleys (Gjessing 1978, 95). Based on this assumption, M-11 is assumed to reflect the innermost and thus youngest moraine ridge in the sets of M-6 to M-9 and M-11 to M-15, located within three adjacent valley sides, which all were deposited contemporaneously or in close temporal proximity, reflecting small glacier re-advances or steady-state positions in a general phase of glacial retreat during the LIA in the time span after 1780 to around 1811.

The mean size of the five largest lichen thalli on M-3 is 25 mm, which corresponds to an age of 55 years BP. M-3 is thus dated to AD 1945. During the 1930s and 1940s, several glacier tongues of Folgefonna advanced (Tvede 1972; Bjelland 1998; Bakke 1999; Simonsen 1999; Bakke et al. 2005c; Edvardsen 2006). Since Vestre Blomsterskardsbreen, due to its size and its comparatively shallowness, is expected to have a longer response time than other, smaller and steeper glacier tongues of southern Folgefonna, the dating to AD 1945 is interpreted as reliable. M-3 hence is interpreted to represent the last glacier advance during the LIA; this moraine is the one observed closest to today's glacier tongue position, and since then the

glacier is interpreted as retreating until today. Furthermore, M-3 is interpreted to reflect the position of the terminus of Vestre Blomsterskardsbreen which enabled the presence of the proglacial lake that deposited the glaciolacustrine terrace (UTM 474832, 860 m a.s.l.) which can be observed in front of today's terminus of the glacier tongue (cp. Chapter 2.2.4).

Tvede (1972) and Tvede and Liestøl (1977) assume that Østre Blomsterskardsbreen had its maximum LIA glacier advance as late as during AD 1920 and AD 1940, probably mainly in the AD 1930's. According to this assumption, the maximum LIA glacier advance at Vestre Blomsterskardsbreen would be expected to be analogous. But based on the observed moraine ridges in the study area and the obtained lichenometric dates, the maximum LIA glacier advance for Vestre Blomsterkardsbreen is presumed to have occurred earlier, during the first half of the 18th century. Since Østre and Vestre Blomsterskardsbreen are two glacier tongues of the same glacier unit, this is difficult to explain. Important factors are slope aspect, precipitation rate, prevailing wind direction and topographic conditions. A detailed discussion is presented in Chapter 5.

Scientific studies indicate an early LIA glacial advance at many glacier outlets of Folgefonna close to AD 1750, and later re-advances between AD 1870 and 1890 and during the 1930s (Bakke et al. 2005a and references therein). Based on the observed moraine ridges in the study area and the obtained lichenometric dates, both glacial advances during the mid-18th and early 20th century were proved at Vestre Blomsterskardsbreen. In contrary, an advance between AD 1870 and AD 1890 could not be observed in the study area. This can be ascribed to several explanations. First, a glacial advance of Vestre Blomsterskardsbreen may not have occurred during the late 19th century. Another explanation is that there was a glacier advance during this period, but no moraines were deposited, or later eroded. Third, a glacier advance occurred and moraines were deposited, but could not be observed during fieldwork. North-east of Insta Botnane is a mountain area which is very difficult to access. The rough terrain prevented this plateau area to be investigated. Assumed AD 1870/1890 moraines would probably be deposited in that area, between the glacier and the moraines M-4 to M-19 observed and dated to AD 1811 or earlier in Insta Botnane. Moreover, huge amounts of meltwater may have prevented or washed out any moraine depositions around the glacier's terminus in the area without significant high terrain.

M-20 and M-21, interpreted as one moraine modified by river Blådalselv, were covered by lichen thalli with diameters larger than 150 mm, therefore lichenometric dating could not be applied. This moraine is interpreted to reflect a glacier advance earlier than the LIA.

On M-22, as well modified by river Blådalselv, also lichen thalli larger than 150 mm could be observed, therefore this moraine is interpreted to reflect a glacier advance earlier than the LIA. Due to its location further downvalley from today's terminus of Vestre Blomsterskardsbreen, M-22 is interpreted as being deposited earlier than M-20/M-21.

M-23 to M-32 are interpreted as marginal moraines formed by glacier advances of Møsevassbreen deposited during the preboreal and in the time period 10 550 – 10 450 cal. years BP (see Chapter 2.2.1.1) (Bjønnes 2006 and references therein).

2.4 Summary

- Quaternary mapping of the study area indicates that rapid mass-movement processes are active in many places in the study area. The impact of such processes on the sedimentation of Lake Midtbotnvatn is presented and discussed in Chapter 3.5.4.
- Several moraines originated by past glacier advances of Vestre Blomsterskardsbreen could be observed in the study area.
- M-1, M-2, M-4 and M-19/M-18 are interpreted to represent the maximum glacial advance of Vestre Blomsterskardsbreen during the LIA.
- M-5 and M-17 are interpreted as one moraine set reflecting a glacier readvance or steady-state position of Vestre Blomsterskardsbreen during the LIA in AD 1767.
- M-10 and M-16 are interpreted to be one set, deposited by a glacier readvance or a phase of steady-state during the LIA around AD 1780. According to the lichenometric dating results, the glacier retreated comparatively fast from the moraine set M-5 and M-17 (AD 1767) to M-10 and M-16 (AD 1780).
- M-11, dated to AD 1811, is assumed to reflect the innermost and thus youngest moraine ridge in the sets of M-6 to M-9 and M-11 to M-15, located within three adjacent valley sides, which all were deposited contemporaneously or in close temporal proximity, reflecting small glacier re-advances or steady-state positions in a general phase of glacial retreat during the LIA in the time span after 1780 to around 1811.
- M-3 is interpreted to represent the last glacier advance during the LIA, dated to AD 1945. This moraine is the one observed closest to today's glacier tongue position, and since then the glacier is interpreted as retreating until today.
- Moraines M-20, M-21 and M-22 are interpreted to represent glacier advances earlier than the LIA. These moraines are too old to be dated by lichenometry. M-20 and M-21 are interpreted as one moraine, washed out by river Blådalselv; M-22 was deposited earlier than M-20/M-21.
- M-23 to M-32 are moraines interpreted to be deposited by Møsevassbreen during the preboreal and in the time period 10 550 – 10 450 cal. years BP (“Jondal 1 event” and “Jondal 2 event”) (Bjønnes 2006).

3 Analysis of proglacial sediments

The second and central part of the study is the analysis and interpretation of proglacial (glaciolacustrine) sediments in order to reconstruct past glacier activities, continuous ELA fluctuations and with that climate variations.

This chapter gives an overview of the theory behind proglacial sediments used as proxies for past glacier fluctuations and climate variations; and it contains the description of the sediment parameters used to analyze the sediment cores. Finally the analyses data are presented and interpreted, age-depths models are created and sedimentation rates calculated.

3.1 Proglacial sediments

Proglacial sediments have their origin almost exclusively in glacial erosion and subsequent meltwater transport (Karlén 1981; Bakke 2004). Especially temperate glaciers, having a several meters thick basal ice layer containing rocks and debris particles, have high abrasive effects on bedrock, which results in typical clay-silt size fractions transported downstream by meltwaters and finally being deposited in proglacial lakes (Østrem 1975 in Bakke 2004; Haldorsen 1983; Leemann and Niessen 1994; Paterson 1994). A glacier produces all grain-sizes, ranging from large boulders to clay (Vorren 1977 in Bakke et al. 2005c; Ashley 1995). Depending on the power of the transporting meltwater stream to hold particles in suspension, there is a downstream decline in sediment size, and fine-grained particles are carried longest (Sundborg 1956 in Bakke 2004; Karlén 1981; Ashley 1995; cp. Chapter 3.4.4.).

The erosion rate of temperate glaciers, and with that the sediment delivery rate, is many times higher than of rivers with comparable water discharge, and can vary significantly from glacier to glacier and from year to year (Church and Ryder 1972; Embleton and King 1975 in Hicks et al. 1990; Ashley 1995). Influencing factors are topography and bedrock type, but both being constant for every glacier, erosion, transport, and sedimentation rate vary only with size, thickness and activity of the glacier, and with the water discharge (Østrem 1975 in Karlén 1981; Boulton 1979 in Leemann and Niessen 1994; Leonard 1985).

Leonard (1985) assumes that variations in sedimentation rates in proglacial lakes are complex, but on a long term basis high sedimentation rates are caused by high glacial activity. Osborn et al. (2007) agree with the fact that increased minerogenic sedimentation in a proglacial lake is linked to an increased erosion and production rate of a glacier. During which phase of activity (advance, maximum or rapid retreat) most material is produced has not been

completely clarified yet (Karlén 1981; Leonard 1985). Release and transport of the eroded material is probably greatest during the retreating phase, when water discharge is high due to numerous and increased meltwater streams (Karlén 1981).

For research works with the goal of paleoclimate reconstruction, the proportion of minerogenic material in the sediments is decisive, being related to the occurrence of a glacier in the catchment (Karlén 1981; Dahl et al. 2003; Bakke et al. 2005c). The minerogenic content can vary considerably in the composition of proglacial sediments, which is in contrast to lakes without glacial meltwater inflow (Karlén 1981; Bakke et al. 2005c). These variations can be linked to fluctuations in glacial activity (Karlén 1981; Haldorsen 1983; Karlén and Matthews 1992; Matthews and Karlén 1992; Leemann and Niessen 1994; Souch 1994; Bakke et al. 2005c; Osborn et al. 2007). Besides the organic and minerogenic content, also particle size and sediment thickness can give information about glacier fluctuations (Nesje and Dahl 2000). Glacial activity in association with erosion, transport and deposition of sediments vary with the size of the glacier in the drainage basin, its retreat or advance, and hence with climate conditions (Karlén 1976, 1981; Leonard 1985, 1986b, 1986a; Karlén and Rosqvist 1988; Benn and Evans 1998; Dahl et al. 2003; Bakke 2004; Bakke et al. 2005b; Bakke et al. 2005c; Osborn et al. 2007; Nesje et al. 2008). This enables reconstruction of glacier fluctuations through analysis and interpretation of proglacial sediments, through which a continuous high-resolution record on climatic change can be obtained (Karlén 1976, 1981; Bakke et al. 2005c). Dahl et al. (2003) gave an overview of former approaches on proglacial sediment studies (the earliest by Karlén 1976; Karlén 1981 in northern Sweden; and Leonard 1985; Leonard 1986a; 1986b in western Canada) and proved in their studies that proglacial sediment parameters are suitable to reconstruct past continuous variations of ELAs and glacial activity in Norway. The approach of using proglacial lake sediments to reconstruct former ELAs extends works based on lateral moraines that reflected ELAs only for certain time periods during a steady state of a glacier. In addition, earlier studies were limited by a lack of historical records and measurements, and the fact that many lateral moraines formed during the Holocene were erased through advancing glaciers during the LIA around AD 1750 (Dahl et al. 2003).

The positive correlation between the minerogenic content of proglacial sediments, glacial activity and hence climate fluctuations is also proven by a large amount of other Sandinavian research studies (e.g. Roland and Haakensen 1985; Nesje and Kvamme 1991; Nesje et al. 1991; Karlén and Matthews 1992; Matthews and Karlén 1992; Dahl and Nesje 1994; Nesje et al. 1995; Dahl and Nesje 1996; Matthews et al. 2000; Nesje et al. 2000a; Nesje et al. 2001;

Sandgren and Snowball 2001; Rosqvist et al. 2004; Bakke et al. 2005a; cp. references in Dahl et al. 2003, Bakke 2004, Bakke et al. 2005c).

In contrast to these approaches, Hicks et al. (1990) proved that in some environments the sedimentation in proglacial lakes both in amount and variation as well can be dominated by the erosion rates of precipitation and runoff, where the intensity is the determinant, and less by the extent of the attendant glacier (cp. Hicks et al. 1990 and references). Benn and Evans (1998) point out that besides meltwater streams as the main sediment source at temperate glaciers, non-glacial sources can play a role in sedimentation as well, as for example slope processes and fluvial processes. These factors are influenced by topography, lithology, morphology, glacial activity, and climate conditions and vary therefore from basin to basin (Benn and Evans 1998). Furthermore, already deposited sediments can be moved and re-deposited again (Summerfield 1991).

3.2 Sedimentation and affecting factors in proglacial lakes

Proglacial lakes can primarily be divided into two types: ice-contact and distal lakes (Ashley 1995). Lake Midtbotnvatn is attributed to the latter, being physically separated from the glacier ice. This characteristic may have varied in different times during the late glacial and Holocene.

Distal lakes receive most of their sediments through meltwater streams, which include suspended clay and silt particles in varying concentrations. The discharge of meltwater streams is characterized by weather fluctuations, seasonal alternations and long-term variations, which affect the nature of stratification of the lake sediments (Ashley 1995; Nesje et al. 2000a). Climate variations on annual and decadal scale have great impact on both sediment production and deposition in lakes (Nesje and Dahl 2000). Proglacial lakes are generally characterized by continuous and relatively high sedimentation, a fact indicating the high time resolution proglacial sediments can be analyzed on (Nesje et al. 2000a). Important influencing factors that affect the deposition of suspended material in a proglacial lake are among others lake type (ice-contact or distal lake), topography, bedrock lithology and vegetation cover, local climate (temperature, precipitation, wind), size, altitude and aspect of lake and catchment, lake bathymetry, water depth, water temperature, lake stratification (seasonal affected thermal stratification, sediment stratification), relative densities of lake and meltwater, the proportion of the catchment glacierized, glacier size and meltwater discharge, distance to the glacier (transport distance), number of intervening lakes located upstream that

act as sediment traps for coarser sediments, sediment sources (number and direction), position of meltwater inflow into lake water column, extent and temporal existence of an ice cover during the winter season, slope stability and avalanche activity related to slope angles around the lake (influencing mass movement at the lake margin), ice rafting, coverage of superficial deposits in the catchment, and anthropogenic impacts (Ashley 1995, 420ff; Nesje and Dahl 2000, 43; Dahl et al. 2003, 277). Birks et al. (2000) point out that the main influencing external factor on a lake catchment during late glacial and early Holocene was temperature, affecting length of the growing season and snow cover, vegetation types and soil processes; furthermore, in interaction with precipitation and wind, temperature affects glacier mass balance and water balance of the lake. In addition, there are direct effects of temperature regarding to thermal water stratification and extent and temporal existence of an ice cover (Ashley 1995; Birks et al. 2000).

With respect to paleoclimate reconstructions, variations in sedimentation rates of proglacial lakes and their origins are very complex, due to the large amount of controlling factors regarding capacity of meltwater streams and sediment disposal (Leonard 1985). In this context it is on the one hand important to differentiate between organic and minerogenic matter in the sediments, and on the other hand to distinguish and relate the different origins of the minerogenic content. Besides glacial erosion and meltwater transport also paraglacial processes can have decisive influence on glacial material dispersal, erosion and re-deposition, among other things for example erosion through slope processes, (glacio-) fluvial erosion through rivers and flood events, and runoff due to increased precipitation (Hicks et al. 1990; Ballantyne and Benn 1994; Benn and Evans 1998; Ballantyne 2002; Osborn et al. 2007).

3.3 Coring location in a proglacial lake

The selection of a proglacial site as a coring location requires the careful evaluation of several factors (Dahl et al. 2003). The area that is currently glaciated within the catchment must be adequate for recording the amplitude of glacier fluctuations in the studied time span. Also, the area/altitude distribution of the studied glacier must be taken into account; as well as the glacier type (Dahl et al. 2003). Several downstream proglacial lakes are more appropriate as study sites than one single lake; representative non-glacial control lakes in the area are advantageous (Matthews and Karlén 1992; Dahl et al. 2003). Furthermore, the proglacial lake should be dammed by a rock sill, and not by superficial deposits such as moraines, colluvial fans or rock avalanches. A flat lake bottom, gentle slopes and no mixing of the water column

to the lake base are preferable properties. On the contrary, sites located close to deltas and similar unstable sedimentary environments, must be avoided. The residence time of the water in a proglacial lake should be long enough for suspended sediment particles to settle, and short enough that some material in suspension can continue and settle in lakes further downstream. Another important factor is the existence of representative marginal moraines of known age in the catchment; these are needed for the reconstructions of fluctuations in glacier sizes and ELAs (Dahl et al. 2003). It is essential to take into account superficial deposits, climatic factors and local active geomorphologic processes within the catchment, such as landslides, debris flows and snow avalanches from adjacent valley sides, as well as turbidity currents, river floods, biological and physical mixing like bioturbation and re-suspension, and anthropogenic activity in the catchment (Nesje et al. 2000a, 1048; Dahl et al. 2003, 278ff; cp. Chapter 3.8.).

3.4 Analysis parameters

The parameters used to analyze the proglacial sediments in this study are magnetic susceptibility, loss on ignition, dry bulk density, grain-size distribution and μ -Xrf fluorescence.

3.4.1 Magnetic Susceptibility

Magnetic Susceptibility (MS) is a method used to get information about the magnetic properties of lake-sediments, their composition, magnetic grain-size and mineralogy (Sandgren and Snowball 2001). MS is defined as to what extent a material can be magnetized in a magnetic field (Blum 1997). The minerogenic composition is determining for the MS of a sample (Dahl et al. 2003). Ferromagnetic minerals, dominating the magnetic properties of lake-sediments, have comparably high magnetic moments (Sandgren and Snowball 2001). Based on a study of lake sediments in Northern Ireland, Thompson et al. (1975) came to the conclusion that downcore variations in the MS of lake sediments are positively correlated with variations in the amount of inwashed inorganic allochthonous sediment material. Sandgren and Snowball (2001) agree that variations in MS in different depths of lake sediments act as an indicator for changes in erosion and deposition. Erosion, transport and finally deposition of minerogenic sediments, in so far as they are of glacial origin, vary with the size of the glacier, and thus with climate conditions (Karlén 1976; Matthews et al. 2005). In conclusion, MS can, linked to glacial activity in the catchment of present and past proglacial lakes, be used as a relative proxy-indicator for paleoclimate changes (Karlén 1976;

Blum 1997; Dahl et al. 2003). Periods of high glacial activity induce high erosion at the glacier bed, which implies increasing meltwater-induced transport and deposition of mineral sediments at the ground of glacier lakes, resulting in higher measured MS (Karlén and Matthews 1992; Sandgren and Snowball 2001).

MS measurements can simply be performed on all materials, the method is fast and non-destructive, and the accuracy of MS is high (Blum 1997; Dearing 1999; Sandgren and Snowball 2001).

A half core surface MS scanning was performed on the cores MIP-109 and MIP-209, using a multi sensor core-logger Model MS2 (Bartington Instrument, Oxford, England) at the Paleomagnetic Laboratory of the University of Bergen. The unit of MS is SI 10^{-5} .

3.4.2 Loss on ignition

Loss on ignition (LOI) is a method used to estimate the organic content of lake sediments, expressed in percent of the total weight of the sample (Karlén 1981; Heiri et al. 2001; Nesje et al. 2001; Santisteban et al. 2004). The procedure is based on weighing samples from lake-sediment cores before and after drying and heating up to certain degrees, and then determine the weight per cent of organic matter and carbonate content through calculation (Heiri et al. 2001), based on linear relations between obtained LOI values and organic and carbonate content (Santisteban et al. 2004). For a detailed description of the procedure, see Appendix 3. Based on the assumption that the organic content of proglacial sediments is an inverse indicator for the minerogenic sedimentation rate, LOI₅₅₀ can be used as an indicator for glacial activity in the lake catchment and thus for glacial activity; peaks coincide with reduced glacier expansion (Karlén and Matthews 1992; Souch 1994; Nesje et al. 2001).

There are some factors that influence the results of the LOI method: sample size, exposure time and position of the sample in the muffle furnace during combustion. Moreover, losses of volatile salts, inorganic carbon and structural water can falsify the results of LOI₅₅₀ (Heiri et al. 2001). On drying the samples at 105°C, not only pore water is lost, but also water from the organic content of the sample and lattice water from clays and salts (Santisteban et al. 2004), which indicates that the water loss on 105°C can vary with different compositions of samples (Santisteban et al. 2004). Furthermore, some amounts of water which are bound to the inorganic content of the samples are lost by heating up to 550°C, creating inaccuracies in subsequent weight measurements. This absorbed water is dependent on grain size which varies even within one core (Karlén 1981). Diverse lithologies with varying content of clays,

salts and organic content within even one core can distort the results of the estimated carbon content (Santisteban et al. 2004). Non-glacial allochthonous organic matter within the glacier-lake sediments can corrupt the composition of the lake-sediments with non-glacial sediments (Souch 1994). When the organic content in sediment cores is throughout below 5%, the “signal-to-noise” ratio may be too low to obtain adequate LOI results for conclusions on past glacial activity in the catchment. In that case, other physical sediment parameters can be used to solve the amplitude of the glacial signal, such as dry bulk density (Bakke et al. 2005c).

3.4.3 Dry Bulk Density

When the LOI method is limited due to a too low organic component and/or high minerogenic sedimentation, dry bulk density (DBD) is an adequate substitute physical parameter to research glacier fluctuations (Bakke 2004). This was proved by Bakke et al. (2005c) in a study area at northern Folgefonna, western Norway, where LOI values below 5% for some times were insufficient to reconstruct coherent ELA fluctuations. DBD (gr/cm^3) values expressed fundamentally the same patterns as the residue after 550°C ignition (%) values, but had larger amplitude in those parts where the residue values were, due to a high minerogenic content of the sediments, very low. The two parameters showed a close relationship ($r^2=0.8$) (Bakke et al. 2005c).

Acting on the inorganic sedimentation of proglacial lake sediments as an additive parameter, DBD reflects the porosity of a sediment (Bakke 2004). More accurately, DBD indicates how powdery, fibrous, and granular sediment materials are packed and consolidated (Bakke 2004). DBD is defined as the ratio of the dry mass of the sample (after drying on 105°C minimum twelve hours) to the bulk volume (original sample volume including particle and pore volumes) of lake sediments (Blake and Hartge 1986).

Figure 3.1 shows this relationship; sediments with a large content of both organic particles and angular minerogenic particles result in low DBD values, whereas the highest DBD values are reached in fine-grained poorly sorted densely packed glaciofluvial sediments (Bakke 2004; Bakke et al. 2005c). The water content of sediment is another important property, inherently strongly related to both organic matter and DBD; water fills the pores between the sediment particles and expresses the porosity of the sediment (Menounos 1997; Bakke et al. 2005c).

DBD is a physical sediment parameter and with that depending on both the production rate of sediments through glacial activity, and on the runoff, which as well is controlled by the size of

the glacier. Applied directly on proglacial sediments, DBD is therefore a suitable method to research glacier size fluctuations (Bakke 2004).

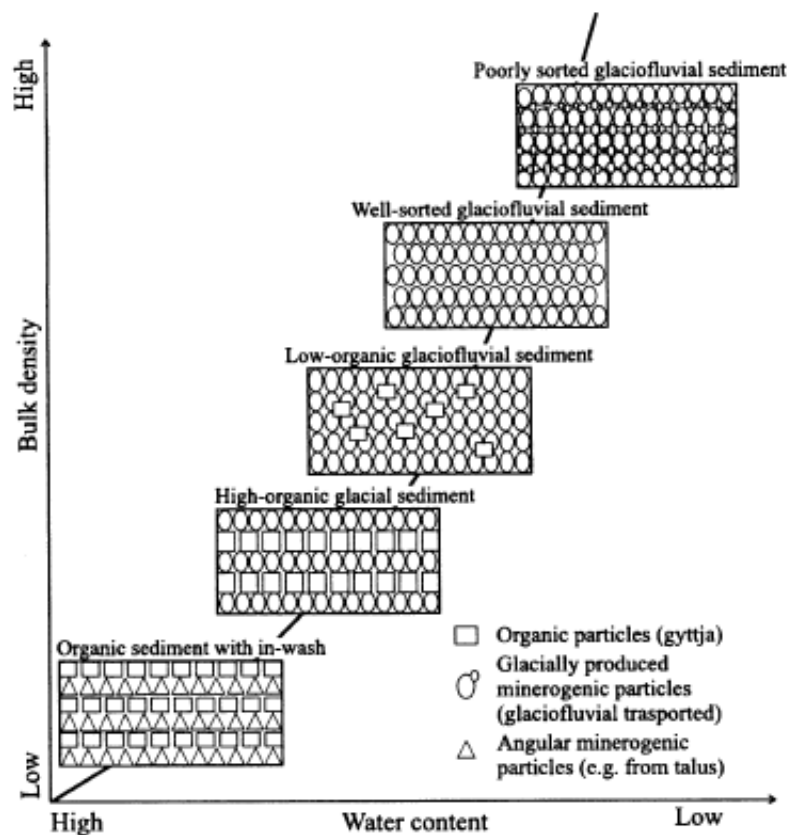


Figure 3.1 The relationship between water content and bulk density related to the type of sediment. The porosity of sediment dominated of angular minerogenic particles is higher than the one dominated of rounded glacially derived minerogenic particles; lowest bulk-density values are obtained from sediments consisting of gyttja and angular minerogenic particles (Bakke et al. 2005c, 171)

3.4.4 Grain-size distribution

Affecting the entrainment, transport and deposition of sediment particles, grain size is a fundamental property of proglacial sediments. Grain size analysis can give important information about the sediment origin, transport history and depositional conditions (Blott and Pye 2001, 1237).

Grain-size distribution is a physical sediment parameter that can be used as a proxy for high-resolution reconstructions of glacier fluctuations (Bakke et al. 2005c). In reconstructions of coherent ELA variations it is used to validate the signal (Bakke 2004).

Variations in the grain-size distribution of lake sediments, especially of the clay and silt contents, can be linked to past changes in the hydrological energy of a lake during sedimentation, which again contains information about glacial activity with regard to erosion

and water discharge (Dahl et al. 2003; Bakke et al. 2005b; Bakke et al. 2005c). Through the grain-size analysis it is thus possible, in addition to other physical sediment parameters, to obtain information about the different processes related to the minerogenic sedimentation in a glacier-fed lake, including flow competency, transport mechanism and sediment availability (Beierle et al. 2002; Bakke et al. 2005b). Depending on supply and transport of insoluble particles, the sedimentation rate in proglacial lakes is related to glacial erosion, and this association makes it possible to draw conclusions about earlier glacier size fluctuations from the properties of proglacial sediments (Beierle et al. 2002; Bakke 2004; Bakke et al. 2005b). But produced by the appropriate glacier, glacier-fed lake sediments normally contain all grain-sizes (Vorren 1977 in Bakke et al. 2005c), and variations in grain-size distribution therefore have their origin primarily in changes of lacustrine and fluvial systems (Bakke 2004; Bakke et al. 2005c), and less in the size of the producing glacier and the length of the glacial transport (Haldorsen 1981 in Bakke 2004). Glaciofluvial transport and sedimentation can be explained by the Hjulström diagram (see Figure 3.2). Whether a grain is eroded, transported or deposited depends on its grain size and the velocity of the water flow it is exposed to. To erode a grain particle already settled, more energy is needed than to transport it when it already is in motion (Nichols 1999).

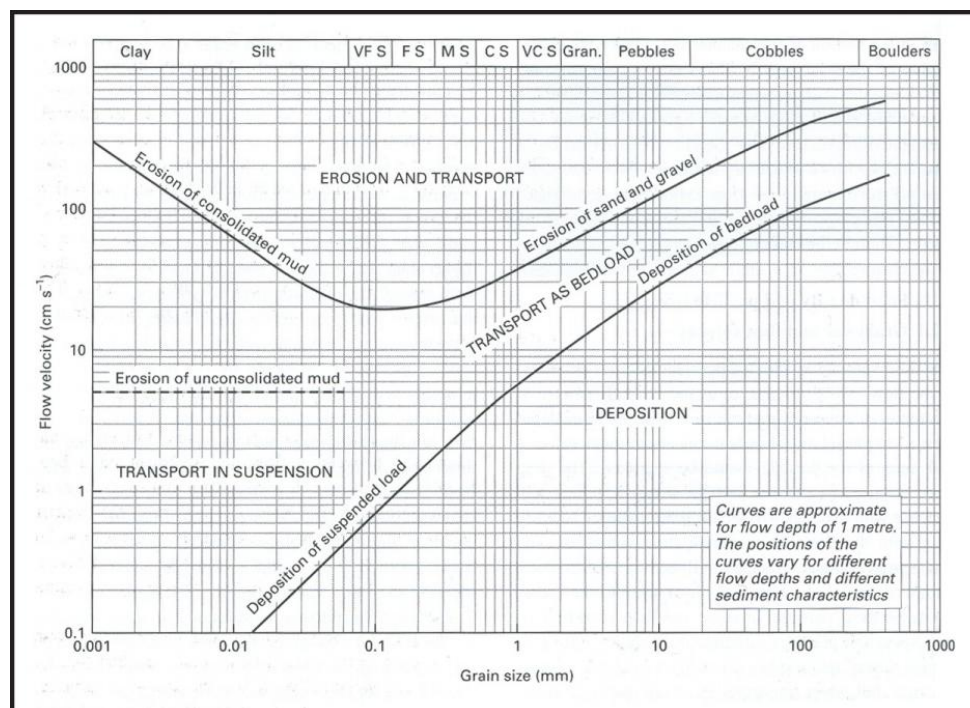


Figure 3.2 The Hjulström diagram shows the relationship between flow velocity of water and the transport of loose grains. To erode a grain particle already settled, more energy is needed than to transport it when it already is in motion (Nichols 1999, 42)

The grain-size distribution can in some parts of the sediments show clear differences from the regular sedimentation. These interruptions may be caused in supplied material by exceptionally different depositional processes, like for example major flood events or erosion from the surrounding catchment (Arnaud et al. 2002; Bakke et al. 2005c).

For a detailed description of the procedure, see Appendix 4.

3.4.5 X-radiography and X-ray fluorescence

The X-radiography and X-ray fluorescence (XRF) analyses provide highly resolved information about the optical, radiographic and elemental variations of sediment half cores (Croudace et al. 2006). The non-destructive automated multi-function core scanner ITRAX is used to perform continuous high-resolution down core geochemical, physical and textural analyses, where an intense micro-X-ray beam is used to irradiate samples enabling both X-radiography and XRF analysis (Croudace et al. 2006). From a split-sediment core, a two-dimensional optical image, a micro-radiographic image and a high-resolution micro-X-ray fluorescence spectrometry (μ -XRF) elemental profile can be obtained (Croudace et al. 2006).

The RGB digital optical image of the sediment core surface is obtained using an optical-line camera system; it can later be used to relate the radiographic image and elemental data to visual colour features of the core sediments (Croudace et al. 2006).

The radiographic image is generated by measuring and recording the intensity of X-radiation transmitted through the sediments; performed by a digital X-ray line camera. The resulting image is a “radiographic positive”, which implies that parts of the sediment core with low density appear light, and areas of higher density appear darker (Croudace et al. 2006, 54).

A high-resolution elemental profile of the sediment half core is obtained by the use of the scanning micro-X-ray fluorescence analysis of the ITRAX core scanner. Proglacial lake sediments often show annually laminated, so called “varved” layers, containing annual or even seasonal information about paleoenvironmental conditions (Shanahan et al. 2008). In this context, the μ -XRF analysis provides an adequate method for continuous reconstruction of past climate conditions (Shanahan et al. 2008).

In detail, the elemental compositions of different sediment laminations are analyzed, in order to get information about annual changes within the catchment, with respect to sedimentation factors and processes, also including individual run-off events and their sources in the drainage basin, and thus environmental and climate changes (Shanahan et al. 2008). Two approaches can be performed: elemental line-scanning of sediment cores and elemental

mapping. Both are based on the identification and quantitative determination of a wide range of major elements (Na-U) and trace element concentrations within a sample (Shanahan et al. 2008). Elemental mapping has a much greater spatial resolution, but accordingly this approach takes disproportional more time and can thus hardly be used for entire sediment cores, but may complement μ -Xrf line scans (Shanahan et al. 2008).

The exposure to a primary x-ray source, such as molybdenum, makes the sample to be analyzed emit secondary x-rays. The energy of this x-ray fluorescence varies for different elements, a fact that is used to obtain the element type. The intensity of the fluorescence at each energy level contains information about the elemental concentration, whether for example heavier elements (like Fe or Ti) or lighter elements (like Al, Ca or Si) dominate; while the elemental quantification can be obtained through theoretical calculations and/or using known standards (Shanahan et al. 2008).

Advantages of the line-scan μ -Xrf analysis are wide ranges of analyzed elements and concentrations, non-extensive sample preparation, and comparatively short measurement times (Shanahan et al. 2008).

In this work, XRF analysis was performed using an X-ray tube with a chromium target, generating incident X-rays with the energy of 30 KeV 30 and 55 mA. The radiographic image was taken from u-channels with a resolution of 60 μ m, using an X-ray tube with a molybdenum target, generating incident X-rays with the energy of 55 KeV and 45 mA.

There are some sediment properties that may negatively influence the data quality obtained from ITRAX -radiography and Xrf-scanning, for example inhomogenities within a sample such as varying density effects, mineralogy, grain-size, porosity and water content variations, packing effects, and inconstant detector-sample distance (Croudace et al. 2006; Shanahan et al. 2008). Further errors, related to the ITRAX system, may occur due to poor peak discrimination in the X-ray spectra and low count rates (Croudace et al. 2006).

3.4.6 Dating

There are two dating methods that were applied on the proglacial sediments: radiocarbon dating and lead dating. They are theoretically explained in the following.

3.4.6.1 Radiocarbon dating

^{14}C (radiocarbon) isotopes originate in the upper atmosphere due to cosmic radiation; forming $^{14}\text{CO}_2$ with oxygen, they enter the Earth's carbon cycle (Bard et al. 1990; Smart and Frances

1991; Bradley 1999). All living things contain the same concentration of ^{14}C while alive. The radioactive ^{14}C has, balanced through continuous production, a natural decay to nitrogen and a released β -particle (electron) in the global carbon reservoir (Smart and Frances 1991; Bradley 1999). After death, the ^{14}C rate lessens because no ^{14}C is absorbed anymore; the half-life of ^{14}C is 5730 ± 40 years (Godwin 1962 in Smart and Frances 1991). The upper limit of age for radiocarbon dating is 50000 years BP. The conventional techniques to measure the ^{14}C rate of a sample are based on counting emissions of β -particles. The direct method is based on measuring the concentrations of the individual ions ^{12}C , ^{13}C , and ^{14}C , using the Accelerator Mass Spectrometry (AMS) (Smart and Frances 1991; Bradley 1999). The latter can be applied in shorter time durations and on much smaller samples (Bradley 1999).

The ^{14}C rate of the atmosphere was not constant through the history of the earth, mainly due to changes in the earth's magnetic field as well as in solar activity, and furthermore changes in ocean circulations (Bard et al. 1990; Aitken 1998; Bradley 1999). That's why radiocarbon years have to be calibrated to calendar years. This is done through calibrating curves, which are mainly based on dating with help of dendrochronology, annual layers (varves) of lake sediments, and uranium (U/Th) series dating of corals (Bard et al. 1990; Stuiver and Reimer 1993; Aitken 1998). CALIB 6.0 and INTCAL09 are newest age calibration programs used to calibrate conventional radiocarbon years to calendar years (Stuiver and Reimer 1993; Stuiver et al. 2005). Before conversion to calendar years, the dated age is expressed through years BP (before present), which is before AD 1950. After calibrating, the dated age is often quoted as years cal. BP (calibrated BP) (Aitken 1998). The differences between these two vary from a few hundred to more than 40000 years, depending on the age of the sample (Aitken 1998).

A further error source is the "hard-water" effect. Some living things, for example aquatic plants and freshwater molluscs, may not be in equilibrium with the ^{14}C rate of the atmosphere due to lower $^{14}\text{C}/^{12}\text{C}$ ratios in the water they live in (Smart and Frances 1991; Bradley 1999). In those cases, the samples are dated older than they actually are (Bradley 1999). With respect to dating lake sediments with radiocarbon, Smart and Frances (1991) advise investigating the inorganic carbonate input into the lake both present and past.

Fractionation of the carbon isotopes ^{12}C , ^{13}C and ^{14}C by plants is another error source; the process of photosynthesis can cause changes in the normal carbon isotope ratio in different plant groups so it is not similar to the atmospheres ratio. Through measuring the $^{12}\text{C}/^{13}\text{C}$ ratio and correcting the ^{14}C concentration, this is taken into account (Smart and Frances 1991).

Further sources of error are the possible contamination of younger or older carbon through for example bioturbation, the dating of organic matter which is characterized by long terrestrial residence times (macrofossil types like wood and charcoal), and the “mineral carbon error”, which results from a wash-in of non-organic older carbon (Bradley 1999; Oswald et al. 2005).

3.4.6.2 Lead dating

Based on the content of ^{210}Pb , a natural radioactive isotope of lead, lead dating is used to date sediments up to 150 years back in time (Appleby 2008). The atmospheric origin and fallout of ^{210}Pb , which occurs as one of the radionuclides in the ^{238}U decay series by the natural decay of ^{222}Rn via a number of short-lived radionuclides, is seen to be constant in space in time-scales of minimum annual character (S.Krishnaswamy et al. 1971; Appleby 2008). Its flux however varies spatially, depending on precipitation and geographical location. In the northern hemisphere, there is an east to west decline in ^{210}Pb fallout, attributed to the prevailing wind directions. Supported ^{210}Pb results from in situ decay of natural ^{226}Ra within the sediment. Unsupported ^{210}Pb is transported to the lake surface by dry deposition and precipitation, and from there to the lake; it can be determined by subtracting supported from total ^{210}Pb activity. This component allows, due to known half-life, for estimation of the age of the sediments (Appleby 2001, 2008).

The main factors affecting supply of fallout ^{210}Pb to lake sediments are atmospheric flux, transport rate from the catchment, water residence time, mean particle settling velocity and transport processes after deposition (cp. Appleby 2001, 178; Appleby 2008, 85). Influencing factors on the differences between the atmospheric ^{210}Pb flux and sediment records are losses via outflow and sediment focussing. In lakes where the sedimentation rate has varied through time, the unsupported ^{210}Pb activity varies with depth, resulting in a non-linear ^{210}Pb profile, also caused by physical, chemical and biological mixing (Appleby 2001).

Three basic models are used for calculation of ^{210}Pb dates. The CIC model assumes a constant initial concentration of ^{210}Pb regardless of accumulation rates. The CRS model is based on the assumption of a constant rate of supply of atmospheric fallout ^{210}Pb (Appleby 2008). The CFCS model requires both constant flux and constant sedimentation rate (S.Krishnaswamy et al. 1971; Arnaud et al. 2002). In this study, a combined CRS and CIC model were applied.

Chronostratigraphic dates of artificial fallout radionuclides, such as ^{137}Cs or ^{241}Am , can be used to validate the results. Artificial fallout radionuclides globally dispersed have their origin mainly in the intense atmospheric testing of nuclear weapons in 1963 and the Chernobyl nuclear power plant accident in Ukraine in 1986 (Appleby 2001, 2008).

Error sources of the lead dating method are for example insecurities in sediment coring, such as losses of the uppermost layers. Calibration against ^{137}Cs can correct results falsified that way, as well as errors originated in varying sedimentation and ^{210}Pb supply rates after 1963 (Appleby 2008). Variations and changes during the late 19th until the middle of the 20th century however can only be adjusted through other chronostratigraphic approaches such as pollen, diatom and trace metal records (Appleby 2001, 2008). When the concentration of unsupported ^{210}Pb in a sample is too low due to for example a strongly increased accumulation rate caused by sediment erosion, dating cannot be performed in an adequate way, and ^{137}Cs -based resolving is essential. This also applies to enhanced ^{210}Pb supply rates due to for example sediment focusing or catchment inputs (Appleby 2008).

Flood events and earthquakes may lead to disturbances of the ^{210}Pb content with respect to the investigated age-depth-relationship; such disturbed layers should be removed (Arnaud et al. 2002). In general, it is necessary to compare calculated ^{210}Pb supply rates with an estimated atmospheric flux of the investigated area (Appleby 2008).

3.5 Lake Midtbotnvatn

Proglacial sediments of Lake Midtbotnvatn are used in this study with the goal of reconstructing Holocene glacial activity of Vestre Blomsterskardsbreen. In the following, Lake Midtbotnvatn is presented as location for proglacial sediment studies.

3.5.1 Site location Lake Midtbotnvatn

Lake Midtbotnvatn (UTM 436800, 700-770 m a.s.l., map sheet M711 1214 I Rosendal and 1314 IV Fjæra) as a site location for proglacial sediment studies, with the goal of reconstructing past glacial activity of Vestre Blomsterskardsbreen and Holocene climate variations, has been chosen for several reasons. The glacier tongue Vestre Blomsterskardsbreen and Lake Midtbotnvatn, located approximately 5 km southwest of the terminus, have not been subject to extensive investigations with respect to reconstructions of variations in glacial activity and climate in former times. Several glacier tongues located at southern Folgefonna have already been study sites for master's theses and further scientific workings with similar approaches, Møsevassbreen in the west (Bjønnes 2006), Østre Blomsterskardsbreen (cp. Tvede 1972; Tvede and Liestøl 1977; Tvede 1994) and Sauabreen (Edvardsen 2006) in the east.

The main requirements claimed of an adequate site location by Dahl et al. (2003) (cp. Chapter 3.3) are fulfilled by Lake Midtbotnvatn. The lake is surrounded by partly steep rock faces and

originally dammed by a rock sill in the north-west, where the natural outflow is located (UTM 427885, 785 m a.s.l.). There are no other lakes located upstream Lake Midtbotnvatn, but river Blådalselv flows ca. 5 km before it reaches the lake, being able to deposit coarser grain fractions in some areas where flow velocity is reduced (for example in Kjerringebotn (UTM 467917, 800 m a.s.l.), where large sandbanks could be observed). The main inflow (UTM 443280, 700-770 m a.s.l.) of glacial sediment-carrying meltwater comes from Vestre Blomsterskardsbreen (16.7 km²), and since 1970 due to a tunnel construction also from Østre Blomsterskardsbreen (14.9 km²) (Tvede and Liestøl 1977; Smith-Meyer and Tvede 1996). The proglacial sedimentation is thus mainly derived from Blomsterskardsbreen, and before 1970 only from Vestre Blomsterkardsbreen, which indicates that a clear signal of this glacier is expected to be observed in the minerogenic content of the sediments, at least before 1953, which marks the beginning of regulations of the lake in the aid of producing hydroelectric power. The present main outflow of the lake is located directly east of the dam (UTM 429011, 770 m a.s.l.), leading to Lake Blådalsvatn, and therefrom further down valley Blådalen to Matre. The regulated minimum and maximum values of elevation of Lake Midtbotnvatn are 700-770 m a.s.l. The surface area of the lake is 2 km² at maximum water level; the maximum water depth of Lake Midtbotnvatn is approximately 100 m.

Representative marginal moraines are present in the study area (for example in Insta Botnane UTM 487397, 927 m a.s.l.), and the current size of Vestre Blomsterskardsbreen indicates that the study site is adequate to investigate the amplitude of Holocene fluctuations of this glacier tongue.

The residence time of the water in Lake Midtbotnvatn is evaluated as appropriate due to the size of the lake which enables suspended sediments to settle and some material in suspension to be transported further downstream. This evaluation is also supported by the observation of the typical greyish-green colour of river Blådalselv, Lake Midtbotnvatn and Lake Blådalsvatn. With respect to the large amounts of meltwater flowing into Lake Midtbotnvatn, the sedimentation rate of the lake is estimated as high. The cores taken out for analyses may therefore be too short to cover the entire Holocene time span.

3.5.2 Core locations

The core locations were chosen with help of the bathymetric map of Lake Midtbotnvatn (Figure 3.3). This map was drawn based on water depth measurements on Lake Midtbotnvatn in August 2009, performed with an echo-sounder placed on a boat and a GPS. Twelve profiles

were established, crossing the lake in varying directions, the water depth measured every 20 m. The registered data were illustrated to a bathymetric map in Adobe Illustrator CS3.

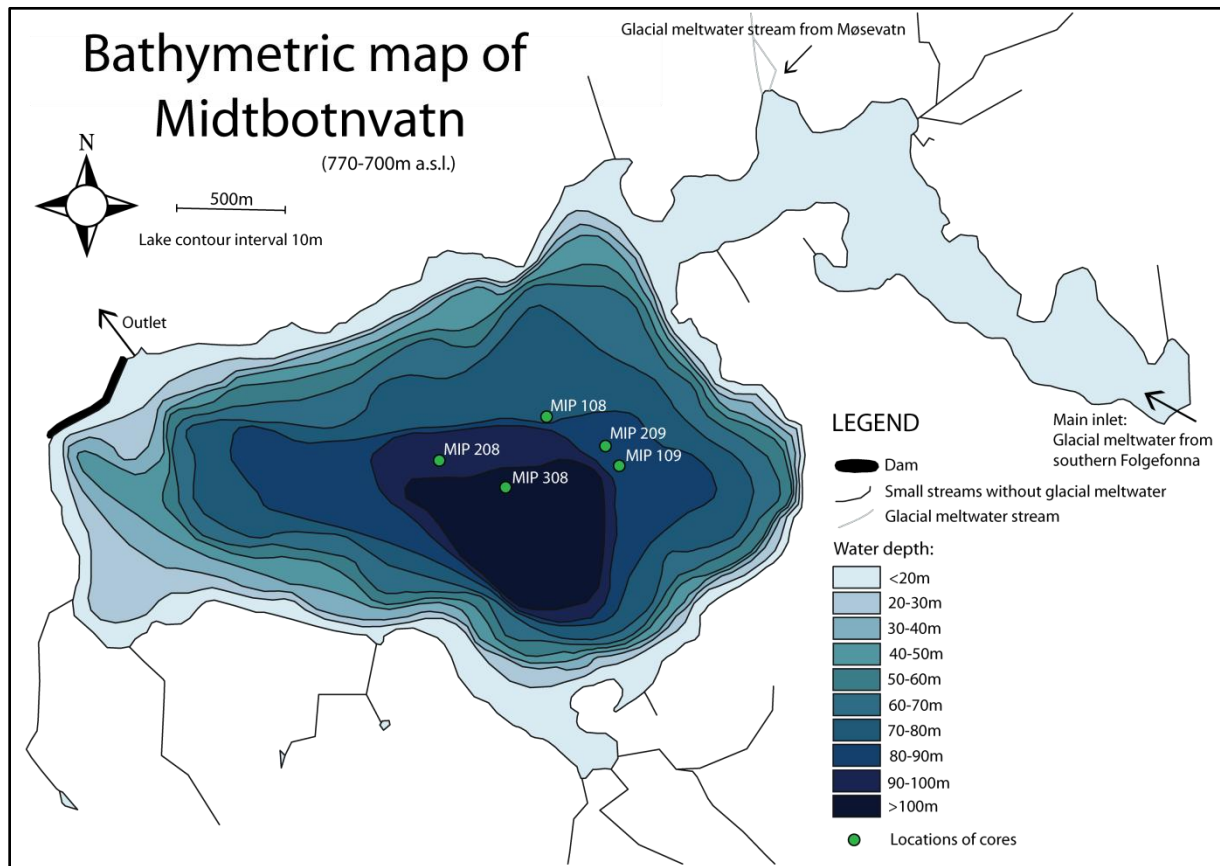


Figure 3.3 Bathymetric map of Midtbotnvatn. Water depths in colour scale, dam, coring locations, inlet, outlet, and inflowing streams are shown.

The cores were taken out in the deepest area of Lake Midtbotnvatn, in 80-100 m water depth with respect to the maximum water level. The lake bottom surrounding the coring sites is quite flat with only gentle slopes in a radius of several 100 m. The coring sites located so central within the lake were chosen to avoid the impact on sedimentation of nonglacial water streams and steep rock faces surrounding the lake, especially the one in the east; moreover the main inflow in the north-eastern part of Lake Midtbotnvatn is in appropriate distance for the cores to represent undisturbed proglacial sedimentation. According to Dahl et al. (2003), the mentioned properties of the coring locations are appropriate for further analyses and interpretations of the sediments.

3.5.3 Coring

In April 2008, three cores were taken out of Lake Midtbotnvatn: MIP-108 (UTM 440312), MIP-208 (UTM 437234), MIP-308 (UTM 439092), but large parts of the core sediments were too disturbed to be used for analyses and interpretations. Coring was performed on the ice-covered lake which was drained down to the minimum water level (700 m a.s.l., 30 m water depth); the cores had therefore to be transported up to the street at the dam with help of a snowmobile. This transport was probably the main factor for the disturbances of the cores. In August 2009, two more cores were taken out of Lake Midtbotnvatn: MIP-109 (UTM 442323) and MIP-209 (UTM 442462). Coring was performed from a float which had to be anchored; the water level was at its maximum (770 m a.s.l., 86 m water depth). A piston corer with a PVC sampling tube was used (cp. Nesje 1992). Several attempts coring a HTH-core at the coring locations in addition to the piston cores, in order to get the upper 50 cm of the proglacial sediments of Lake Midtbotnvatn, failed, due to too hard and densely packed sediments. Therefore, it was not possible to verify how many centimeters of top sediments were missed during coring of MIP-109 and MIP-209. Lead dating results meanwhile indicate a loss of 22 cm at the top of MIP-209 (cp. Chapter 3.11.).

Both MIP-109 and MIP-209 were used for the analyses, interpretations and reconstructions undertaken in this study, though the main focus is set on MIP-209 due to least disturbed core sediments (cp. Chapter 3.6). Each core has a diameter of 110 mm (Nesje 1992); MIP-109 is 209.5 cm long, and MIP-209 has a core length of 201 cm. After coring, both cores were parted into two parts and split lengthwise, to secure successful coring results and to ease the transport to Bergen, and in general to handle and work with the cores during the analyses. The cores were transported carefully and then stored in a cold storage room (4°C) at the University of Bergen, in order to prevent the sediments from being disturbed or otherwise negatively affected in quality.

3.5.4 Field observations and influencing factors on sedimentation in Lake Midtbotnvatn

Field observations in the course of quaternary mapping indicate that the sedimentation in Lake Midtbotnvatn is affected by several factors, which are presented in the following.

The main inflow of Lake Midtbotnvatn is river Blådalselv in the north-east (UTM 443280, 700-770 m a.s.l.), consisting of glacial sediment-carrying meltwater that comes from Vestre Blomsterskardsbreen. Due to the size of the adjacent glacier tongue and the huge amounts of

meltwater each year, the river is expected to have high hydraulic energy, especially during snow-melt in the spring/summer months May until September; and it is seen as the main transportation agent of the sedimentation in Lake Midtbotnvatn, causing a high sedimentation rate. The coring sites were located in appropriate distance to the river mouth to avoid disturbed sedimentation that maybe expected at the unstable sedimentary environment a river mouth causes (cp. Dahl et al. 2003).

In the course of regulations for the development of hydroelectric power since 1953, water-level regulations, including both draining and damming processes of Lake Midtbotnvatn, can have enabled erosion and re-sedimentation processes, that way affecting the proglacial sedimentation.

The Coriolis force, caused by the rotation of the Earth, has an anticlockwise impact on the flow circulation of the water coming from the main inflow in the north-east to the main outflow in the north-west. This impact is consistent, but, due to the small lake size, weak (Pye 1994).

One small glacial water stream from Lake Møsevatn (UTM 448530, 877-824 m a.s.l.) flows into river Blådalselv in the north-west (UTM 446775, 775 m a.s.l.); the existence and strength of this stream depends on precipitation and glacial- as well as snow-meltwater variations. The main outflow of Lake Møsevatn is in the south-west of the lake (UTM 445468, 870 m a.s.l.). In the 1960s, Lake Møsevatn was regulated by several dams and tunnel constructions, the main outflow until present remained, however, the one in the south-west (Bjønnes 2006). The impact of this glacial stream on the sedimentation of Lake Midtbotnvatn is estimated as small, since it is of very little extent compared to the size of river Blådalselv, and due to the facts that the majority of sediments originated from Møsevassbreen are deposited in Lake Møsevatn and that the main outflow is not leading into the catchment area of Lake Midtbotnvatn.

Besides the glacial meltwater inflows, Lake Midtbotnvatn achieves water through surface runoff and drainage streams of the area topographically constituted as the drainage area of the lake. Numerous streams of non-glacial origin flow into Lake Midtbotnvatn (for example flowing down Blådalshorga in the south-west, UTM 426777, 770 m a.s.l., and in Midtbotn in the south-east UTM 440901, 770 m a.s.l.) and into river Blådalselv (for example in Kjerringebotn UTM 465473, 780 m a.s.l.) (cp. Figure 3.3). The existence and flow conditions of the nonglacial streams are inherently depending of variations in precipitation and snow melt. The coring sites were located in some distance to the lakefront to minimize the impact

on sedimentation of water streams carrying non-glacial minerogenic material into Lake Midtbotnvatn.

Active rapid mass-movement processes at the rock faces surrounding Lake Midtbotnvatn and river Blådalselv are observed several places (cp. Quaternary map of Blomsterskardsbreen and Midtbotnvatn, Appendix 1). Both rapid mass-movement processes themselves and washing-out of rapid mass-movement deposits influence the sedimentation in the lake and moreover the glacial signal of the sediments, being minerogenic sediment sources of non-glacial origin (Matthews et al. 2005). To minimize this impact, the locations of the coring sites were therefore chosen in appropriate distance to the lakefronts.

Due to the fact that Lake Midtbotnvatn is located in the glacier foreland of southern Folgefonna, paraglacial activity is another influencing factor on proglacial lake sedimentation. Paraglacial activity is defined as nonglacial processes directly defined by glaciation and deglaciation, including both proglacial processes and processes in areas earlier glaciated, directly conditioned by former glaciation and deglaciation (Church and Ryder 1972, 3059; Ballantyne 2002, 1935). Such paraglacial processes which may affect the sedimentation in Lake Midtbotnvatn through rapid reworking, erosion and re-deposition of glacial sediment are for example slope failures and enhanced rockfall activity, debris flows, rapid snowmelt, snow avalanches and slopewash, wind erosion and frost action, and the eroding, transporting and depositing properties of rivers (Ballantyne and Benn 1994; Ballantyne 2002). The catchment area of Lake Midtbotnvatn is characterized by little superficial deposits and robust bedrock, which indicates that only few areas may have paraglacial impact on the lake sedimentation. The coring sites located distal from the lakefront were chosen to avoid this impact as far as possible.

Turbidity currents (underflows) and gravity processes due to steep areas in the lake bathymetry can cause erosion and subsequent re-sedimentation of lake sediments (Pye 1994; Benn and Evans 1998). In choosing the coring locations in the deepest and flattest area of the lake basin of Lake Midtbotnvatn, the impact of such features is avoided as far as possible.

Due to the size and water depth of the lake, the influence of wind-induced surface wave actions is estimated to not extend to the base of the water column; the influence of wind on the sedimentation of Lake Midtbotnvatn must therefore be taken into account with focus on surface flows and currents in the upper water layers; the same applies to surface heating during the summer months which in smaller and shallower lakes could cause the non-existence of stratification (Pye 1994; Ashley 1995).

During the accumulation season, the average temperature in the study area is -0.56°C , the mean annual temperature is 3.14°C (cp. Chapter 1.6.4.). There is no data available about the water temperature and the water density of Lake Midtbotnvatn, two factors which play a role for sedimentation in a lake (Pye 1994). The calculated temperatures in the study area and field observations indicate that Lake Midtbotnvatn is covered by ice several months per year, approximately from November until May.

As a consequence of the climatic conditions, there is a limited extend of vegetation in the catchment area of Lake Midtbotnvatn, mainly consisting of gramineous vegetation, mosses, and small bushes like blueberries and ling. Due to the small extend of vegetation in the area it is expected that the organic allochthonous sedimentation and the organic production in the lake are low, and only occurring during the summer months June until September, when Lake Midtbotnvatn is not covered by ice.

3.6 Presentation of data from Lake Midtbotnvatn

The sediment cores to be analyzed in this study, MIP-109 and MIP-209, were split lengthwise after coring, then the surfaces were cleaned from tube rests and disturbances that resulted from the opening procedure. The better of the two core halves was declared the working half, the one all analyses were to be performed on, while the other half, the reference part, was stored, not to be used unless the working half couldn't meet the requirements for all of the analyses anymore. Before the analyses were performed on the working half, it was photographed and logged; furthermore u-channels were taken.

The analyses performed on the cores were magnetic susceptibility, loss on ignition, dry bulk density, grain-size distribution, X-radiography and $\mu\text{-Xrf}$ fluorescence. On both cores, all analyses were performed in the central part along the core. X-radiography was performed on the u-channels, to secure a good quality of the results. Due to distinct sediment disturbances in the second part of MIP-209 (107.5-201 cm), additional measurements of LOI and DBD were performed, located ca. 2 cm to the right side along the core, in order to minimize the influence of the disturbances. For the interpretation of the proglacial sediments of MIP-209, these LOI and DBD records (central in the first half, 0-107.5 cm, and moved slightly to the right in the second half, 107.5-201 cm) were used. Since the remaining analyses were recorded in the central part along the core, some irregularities may occur, though the benefit of this measurement spreading is that larger parts of the core could be analyzed, which was an important task with respect to the disturbances of the core.

On both cores, magnetic susceptibility was performed in an interval of 0,2 cm, and loss on ignition and dry bulk density with a resolution of 0.5 cm. The grain-size distribution was measured in an interval of 1 cm on the first 50 cm of MIP-109 and the whole length of MIP-209, and every 5th cm on MIP-109 from 50 cm to 209.5 cm. μ -Xrf fluorescence was performed with a resolution of 500 μ m (0.05 cm).

On MIP-109, one radiocarbon sample was dated. On MIP-209, 18 samples at depths between 7 cm and 50 cm were dated through lead dating, and in addition, 10 radiocarbon dates were performed.

The raw data of the analysis parameters and the dating results received from the responsible laboratories are attached digitally in Appendix 2 (CD).

Both MIP-109 and MIP-209 are visually dominated of minerogen sediment, characterized by similar material compositions and homogeneous greyish colours including some lighter and darker shaded layers. Division into sections therefore is mainly based on variations in analysis parameters, and only to a minor extent on visual differences. The sections are presented from oldest to youngest in the following chapters.

The fact that both cores are disturbed in wide parts (cp. logs in Figure 3.4 and Figure 3.7) complicated the interpretations and lowered the quality of the results of the interpretation and reconstruction of glacier fluctuations and sediment transport at Vestre Blomsterskardsbreen.

3.6.1 Programs used for data handling

The computer programs used for data handling of the analysis parameters were Microsoft Office Excel 2007 and Matlab R2008b, for illustrations in addition also Adobe Illustrator CS3 and Adobe Photoshop CS3. For the SediGraph data, the program Gradistat 4.0 was used to handle and save the raw data (Blott and Pye 2001).

3.6.2 Description of MIP-109 and presentation of analysis parameters

Section D (158 cm-209.5 cm) contains minerogenic material; the dominating grain sizes are very coarse, coarse and medium silt. The mean grain size is high, reaching the highest value of the whole core in this section, as is very fine sand. The highest and lowest LOI values are 1.47% and 0.83%, the average LOI value is 1.16%. DBD values are below core average except at 193-196 cm; from 196 cm they are falling towards the end of the core. MS values are lower than in section C, though they show strong variations with several positive peaks at 158-165 cm and 184-205 cm. Ti, Si and Rb values are lower than in section C, though

strongly varying above and below core average. The highest values are reached at 197-209.5 cm.

The visual sediment structure is disturbed through coring; olive gray and dark gray diagonal, horizontal and vertical arched and disturbed layers can be observed in this section, in addition to several sediment lenses.

Section C (96 cm-158 cm) contains minerogenic material; the dominating grain sizes are medium, coarse and fine silt. The mean grain size is high; fine sand reaches the highest values of the whole core in this section. The highest and lowest LOI values are 1.2% and 0.7%, the average LOI value is 0.91%. DBD values are highest in the whole core in this section, as are MS values, except at 117.5-123 cm (change of the core halves). Ti, Si and Rb values are high except for 115-120 cm.

The visual sediment structure is affected through coring, small lenses are visible within dark gray almost structureless sediment.

Section B (71 cm-96 cm) contains minerogenic material; the dominating grain sizes are fine, medium and coarse silt; the mean grain size is lower in the upper part of the section. The highest and lowest LOI values of this section are 1.27% and 0.93%, the average LOI value is 1.07%. DBD values are varying: above core average at 76-87 cm, and below at 71-76 cm and 87-96 cm. MS values are above core average at 76.5-83 cm and 88-88.5 cm, otherwise below. Ti, Si and Rb values are high in the upper part of the section and falling downcore.

The visual sediment structure is disturbed through coring, showing single sediment lenses of different sizes within almost structureless, olive gray, gray and dark gray sediment.

Section A (0 cm-71 cm) contains minerogenic material; the dominating grain sizes are medium, fine and coarse silt. The highest and lowest LOI values of this section are 1.27% and 0.77%, the average LOI value is 1.13%. DBD values are lower than in section B and C, in the upper part of the section (12-29 cm) they rise above the core average, falling again towards the top of the core. MS values are low except for 11-22 cm and 31-37.5 cm where they are above core average. Ti, Si and Rb values are below core average at 7-21 cm and 26-36 cm, and falling from 6 cm towards the top of the core.

The visual sediment structure is affected through coring, resulting in horizontal and, in the lower part of the section, vertical arched layering with slightly varying shades of olive gray and gray, and partly more disturbed sediment.

Figure 3.4 shows the illustration of MIP-109 including core picture, x-ray picture, visual structure (log), sediment type, short description and section division.

Figure 3.5 shows a graphical illustration of the sediment parameters of MIP-109: mean, sorting, dry bulk density, magnetic susceptibility, loss on ignition, water content, titanium, silicium, rubidium, and the XRF ratios fe/ti and inc/coh.

Figure 3.6 shows the grain size distribution of MIP-109.

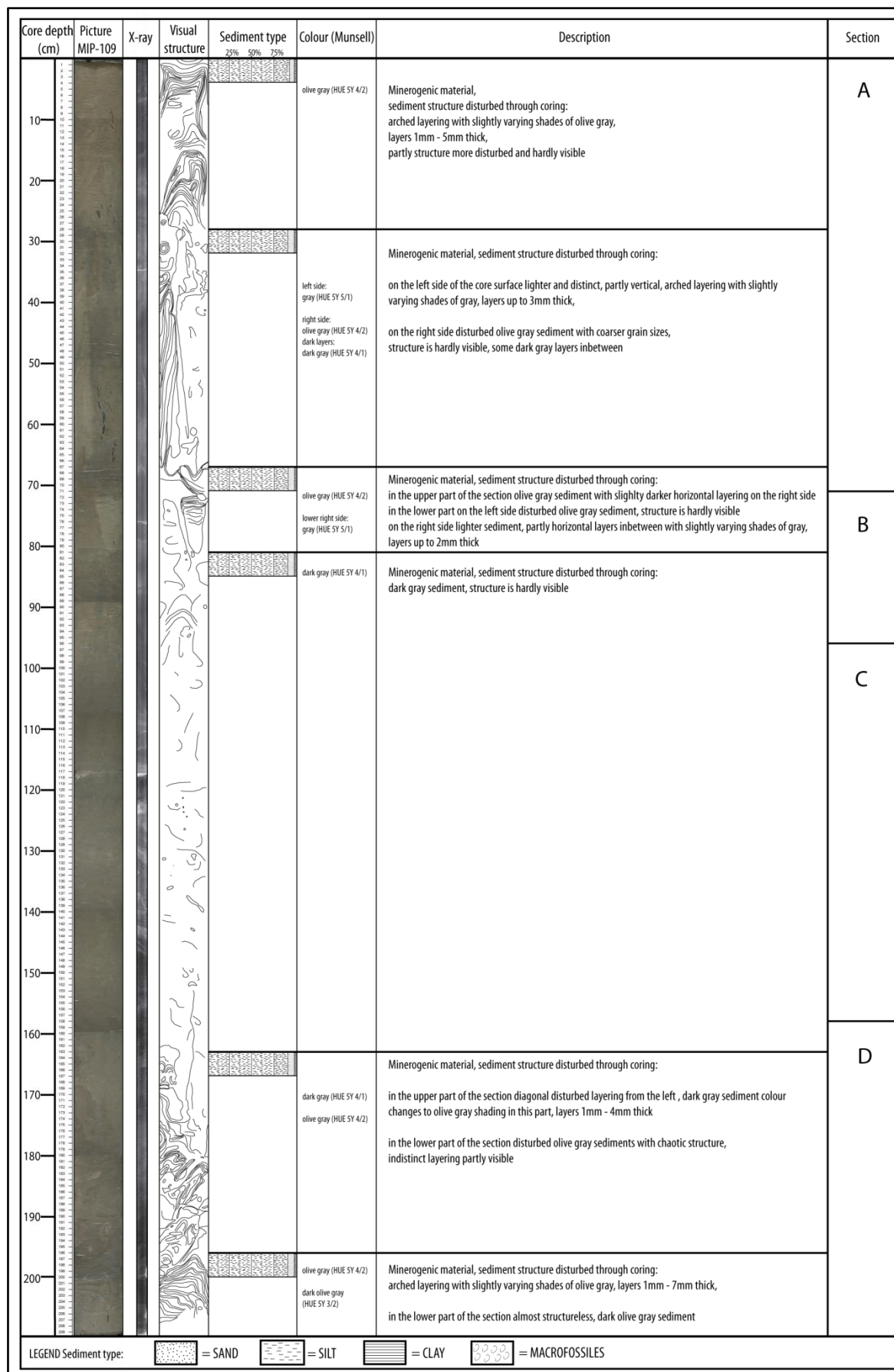


Figure 3.4 Description of MIP-109. Figure shows picture, x-ray picture, visual structure, sediment type, description and section division. The sediment structure was quite disturbed during the coring process.

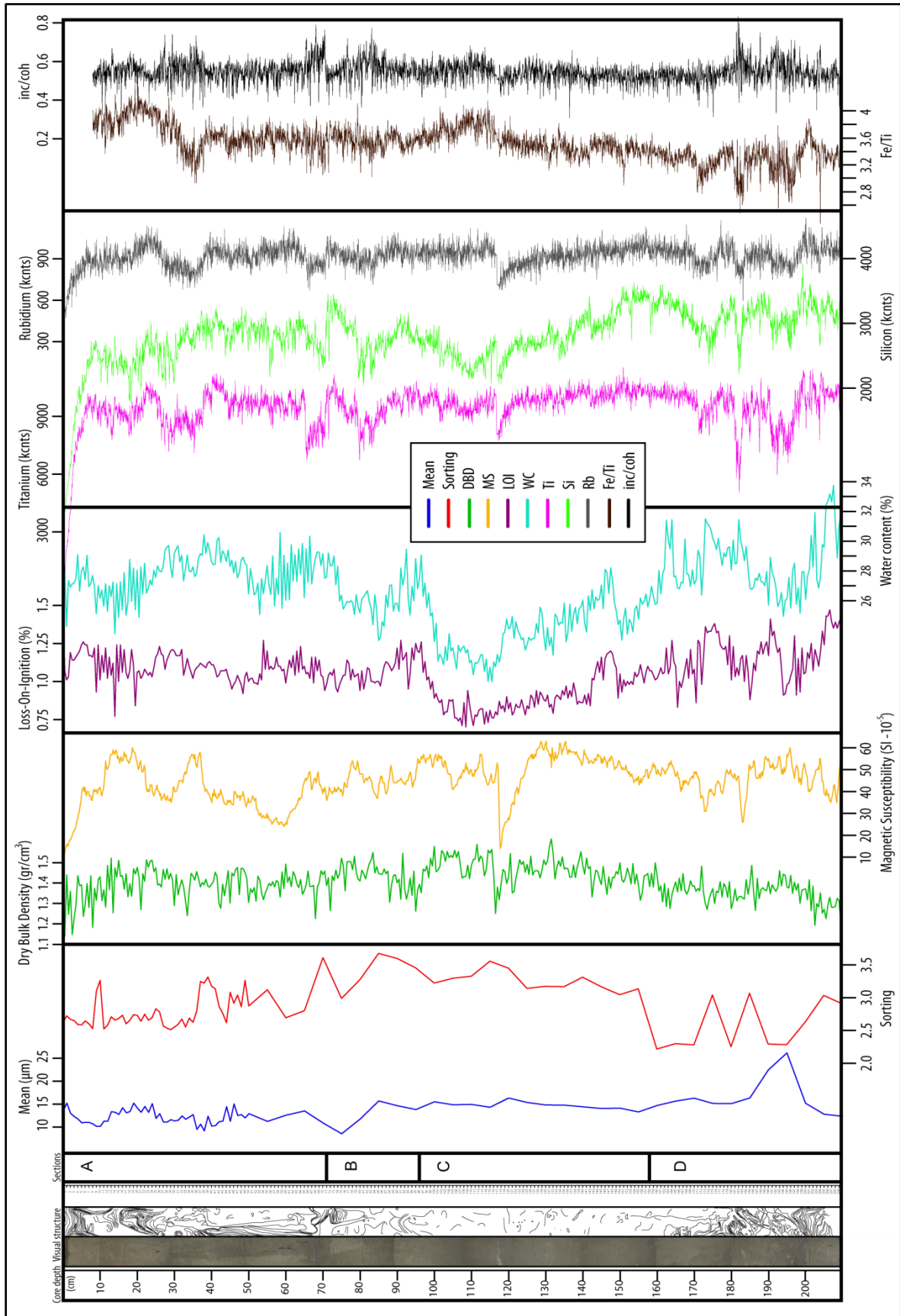


Figure 3.5 Illustration of sediment parameters of MIP-109: mean, sorting, DBD, MS, LOI, WC, Ti, Si, Rb, Fe/Ti, inc/coh. In addition, core depth, picture, visual structure and sections are included. Division into sections is mainly based on variations in analysis parameters, only to a minor extend on visual differences.

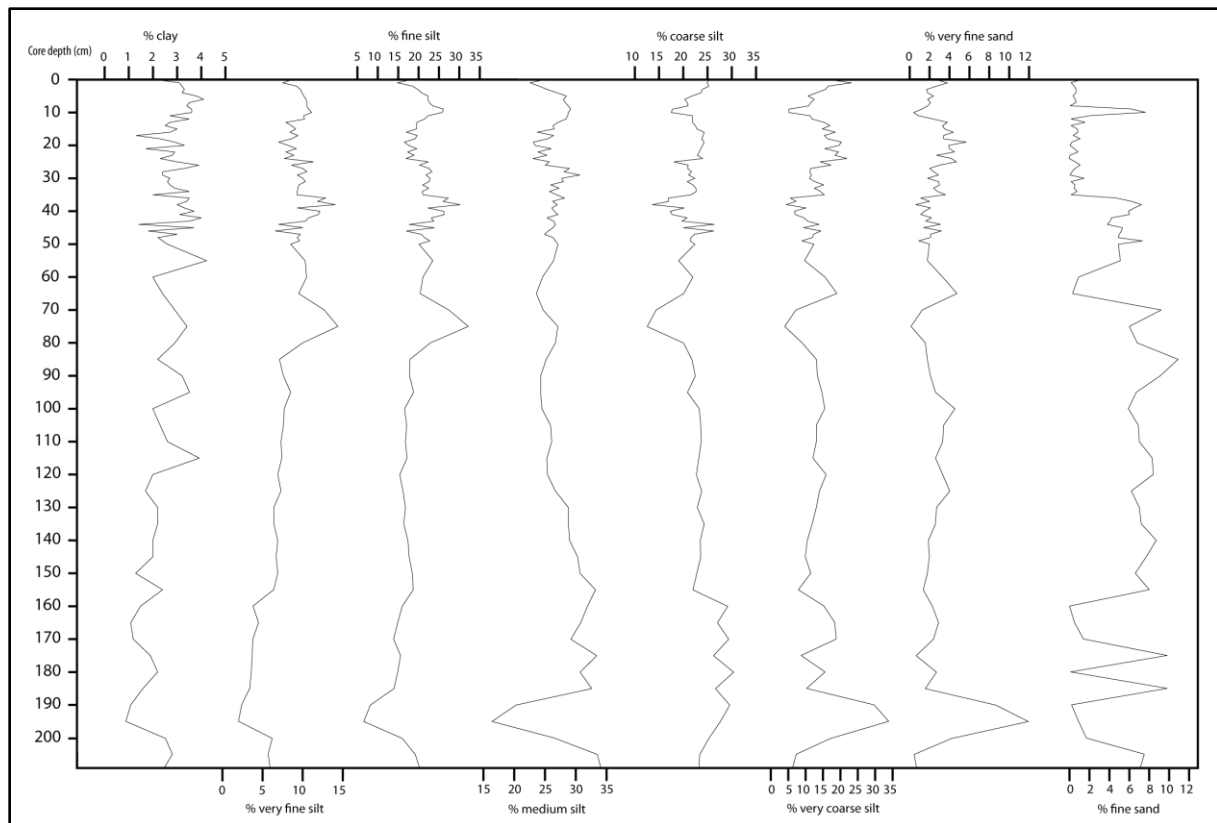


Figure 3.6 Percentage distribution of the grain sizes of MIP-109. Measurements were performed in 1 cm intervals from 0-50 cm, and thereafter in 5 cm intervals. Values of each grain size are presented in percent of the whole sample.

3.6.3 Description of MIP-209 and presentation of analysis parameters

Section E (191 cm-201 cm) contains minerogenic material; the dominating grain sizes are medium, coarse and very coarse silt. The mean grain size of this section is below core average. LOI and DBD were measured in the right part of the core, which is in contrast to the other parameters, in order to take into account the strong disturbances of this section. The highest and lowest LOI values are 1.29% and 0.99%, the average LOI value is 1.11%. DBD values are high in this section, as are MS and Ti, Si and Rb values, which all are above core average.

The visual sediment structure is disturbed through coring, horizontally and vertically, arched layers are visible with varying shades of gray and dark gray.

Section D (181.5 cm-191 cm) contains minerogenic material; the dominating grain sizes are fine, medium and coarse silt. The mean grain size and also very coarse silt are reaching the lowest values of the whole core in this section, though there is a positive peak slightly above core average at 188 cm. LOI and DBD were measured in the right part of the core, which is in contrast to the other parameters, in order to take into account the strong disturbances of this

section. The highest and lowest LOI values are 1.56% and 1.09%, the average LOI value is 1.28%. DBD values are lower than in the sections E and C, and mostly below core average. MS values are high in the upper part of the section, reaching the highest values at 183.5-187 cm, and below core average at 188.5-191 cm. Ti, Si and Rb values are varying above and below core average in this section.

The visual sediment structure is disturbed through coring, containing arched and undulated layering with varying shades of gray and dark gray.

Section C (107.5 cm-181.5 cm) contains minerogenic material and organic material; this section is very disturbed through coring, especially at 107.5-166 cm. The dominating grain sizes are very coarse silt, which reaches the highest values of the whole core in this section, coarse and medium silt, with two exceptions: at 132.5-140.5 cm fine, medium and coarse silt are prevalent, and at 144-149 cm very coarse, medium and fine silt are dominating. The mean grain size in this section is the highest of the whole core, as is very fine sand. LOI and DBD were measured in the right part of the core, which is in contrast to the other parameters, in order to take into account the strong disturbances of this section. The highest and lowest LOI values are 1.64% and 1.22%, the average LOI value is 1.07%. DBD values are the highest in the whole core in this section, though several negative peaks can be observed. MS values are low at 107.5-166 cm, except a positive peak at 136 cm, and high in the lower part of this section at 166-181.5 cm. Ti, Si and Rb values are the lowest of the whole core in this section, except for the parts 142-150 cm and below 166 cm, where they are above core average.

The visual sediment structure is strongly disturbed through coring. At 107.5-166 cm there is a disturbed dark layer containing very fine sand and macrofossils visible on the left side of the core. The sediment on the right core side is disturbed sediment with varying structures: partly there is hardly any visible structure visible in the olive gray sediment, partly vertically and horizontally arched, undulated and chaotic layers with varying shades of olive gray can be observed, and partly darker layers containing coarser grain sizes and macrofossils are visible.

Section B (65 cm-107.5 cm) contains minerogenic material; the dominating grain sizes are coarse, medium and very coarse silt in the upper part of the section, and medium, fine and coarse silt in the lower part. The mean grain size is low, and falling downcore, as is very coarse silt. The highest and lowest LOI values are 1.11% and 0.72%, the average LOI value is 0.96%. DBD values are strongly varying below and above core average, in general a downcore falling trend can be observed. MS values are above core average at 65-99.5 cm, and then lower. Ti, Si and Rb values are high in this section.

The visual sediment structure is affected through coring, arched layering with varying shades of olive gray and gray and disturbed olive gray sediment vaguely structured are visible.

Section A (0 cm-65 cm) contains minerogenic material; the dominating grain sizes are coarse silt, medium silt, very coarse silt and fine silt. The mean grain size is high in the uppermost and lowest part of the section, and below core average at 16-56 cm, as is very coarse silt. The highest and lowest LOI values are 1.42% and 0.72%, the average LOI value is 1.04%. DBD values are the lowest in the whole core, raising downcore, being above core average at 37-42 cm and 44-64 cm. MS values are generally low but varying, at 29-41 cm they are above core average. Ti, Si and Rb values are comparably high, except for the top of the core at 0-2.5 cm and 40-55 cm where they are slightly lower than core average.

The visual sediment structure is affected through coring, arched and partly undulated horizontal and vertical layering with slightly varying shades of olive gray are visible.

Figure 3.7 shows the illustration of MIP-209 including core picture, x-ray picture, visual structure (log), sediment type, short description and section division.

Figure 3.8 shows a graphical illustration of the sediment parameters of MIP-209: mean, sorting, dry bulk density, magnetic susceptibility, loss on ignition, water content, titanium, silicium, rubidium, and the XRF ratios fe/ti and inc/coh.

Figure 3.9 shows the grain size distribution of MIP-209.

Core depth (cm)	Picture MIP-209	X-ray	Visual structure	Sediment type	Colour (Munsell)	Description	Section			
				25% 50% 75%						
0-10					olive gray (HUE 5Y 4/2)	Minerogenic material, sediment structure disturbed through coring: vertical layering with slightly varying shades of olive gray	A			
10-40					olive gray (HUE 5Y 4/2)	Minerogenic material, sediment structure affected through coring: arched layering with slightly varying shades of olive gray, layers 0,5mm - 4mm thick				
40-70					olive gray (HUE 5Y 4/2)	Minerogenic material, sediment structure disturbed through coring: vertically arched and undulated layering with slightly varying shades of olive gray, layers up to 4mm thick				
70-80					olive gray (HUE 5Y 4/2), lighter layers: gray (HUE 5Y 5/1)	Minerogenic material, sediment structure affected through coring: arched layering with slightly varying shades of olive gray, inbetween lighter layers visible, layers 0,5mm - 3mm thick. Layered structure placed more to the right side of the core surface	B			
80-90					olive gray (HUE 5Y 4/2)	Minerogenic material, sediment structure disturbed through coring, partly only vaguely visible: arched layering with slightly varying shades of olive gray and disturbed sediment without visible structure				
90-110					olive gray (HUE 5Y 4/2)	Minerogenic material, sediment structure disturbed through coring: vertically arched and undulated layering with slightly varying shades of olive gray, layers up to 4mm thick				
110-160					olive gray (HUE 5Y 4/2), darker layers: dark gray (HUE 5Y 4/1)	Minerogenic material, sediment structure disturbed through coring: on the right side of the core surface disturbed sediment with varying structure: partly horizontally and vertically arched, undulated and chaotic layers with varying shades of olive gray, partly some darker layers containing coarser grain sizes and macrofossiles, partly no structure visible; on the left side of the core surface disturbed dark layer containing coarser grain sizes and macrofossiles	C			
160-170					olive gray (HUE 5Y 4/2)	Minerogenic material, sediment structure disturbed through coring: on the left side arched layering with slightly varying shades of olive gray, layers 1mm - 1cm thick, on the right side disturbed sediment with chaotic structure, in the lowest part of the section also layering with slightly varying shades of olive gray, up to 2mm thick				
170-180					gray (HUE 5Y 5/1) dark gray (HUE 5Y 4/1)	Minerogenic material, sediment structure disturbed through coring: arched, undulated and chaotic layering with varying shades of gray, in the lower part of the section sediment dark gray and partly horizontal layers visible				
180-190										D
190-200										E

LEGEND Sediment type: = SAND = SILT = CLAY = MACROFOSSILES

Figure 3.7 Description of MIP-209. Figure shows picture, x-ray picture, visual structure, sediment type, description and section division. The sediment structure was quite disturbed during the coring process.

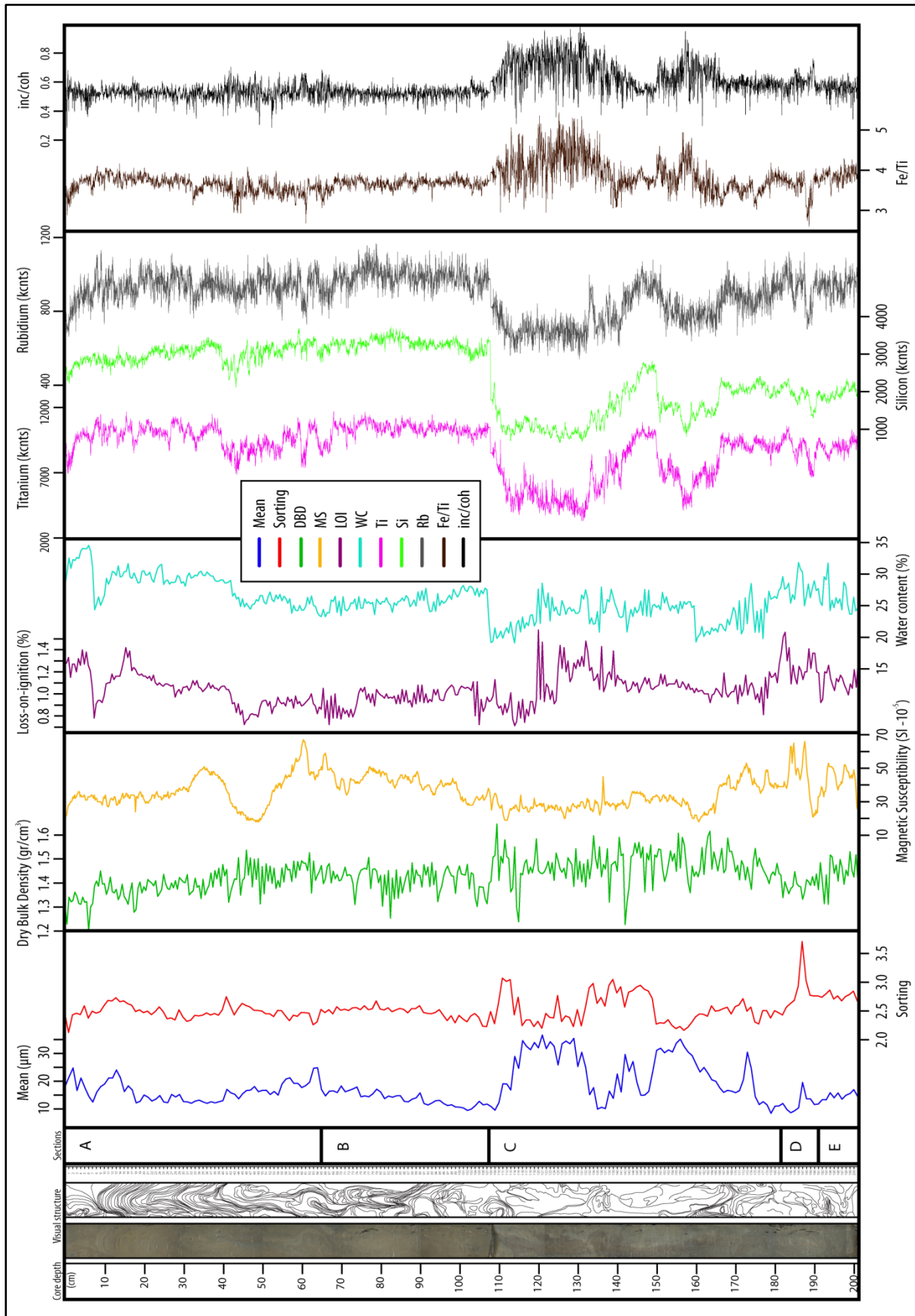


Figure 3.8 Illustration of sediment parameters of MIP-209: mean, sorting, DBD, MS, LOI, WC, Ti, Si, Rb, Fe/Ti, inc/coh. In addition, core depth, picture, visual structure and sections are included. Division into sections is mainly based on variations in analysis parameters, only to a minor extent on visual differences.

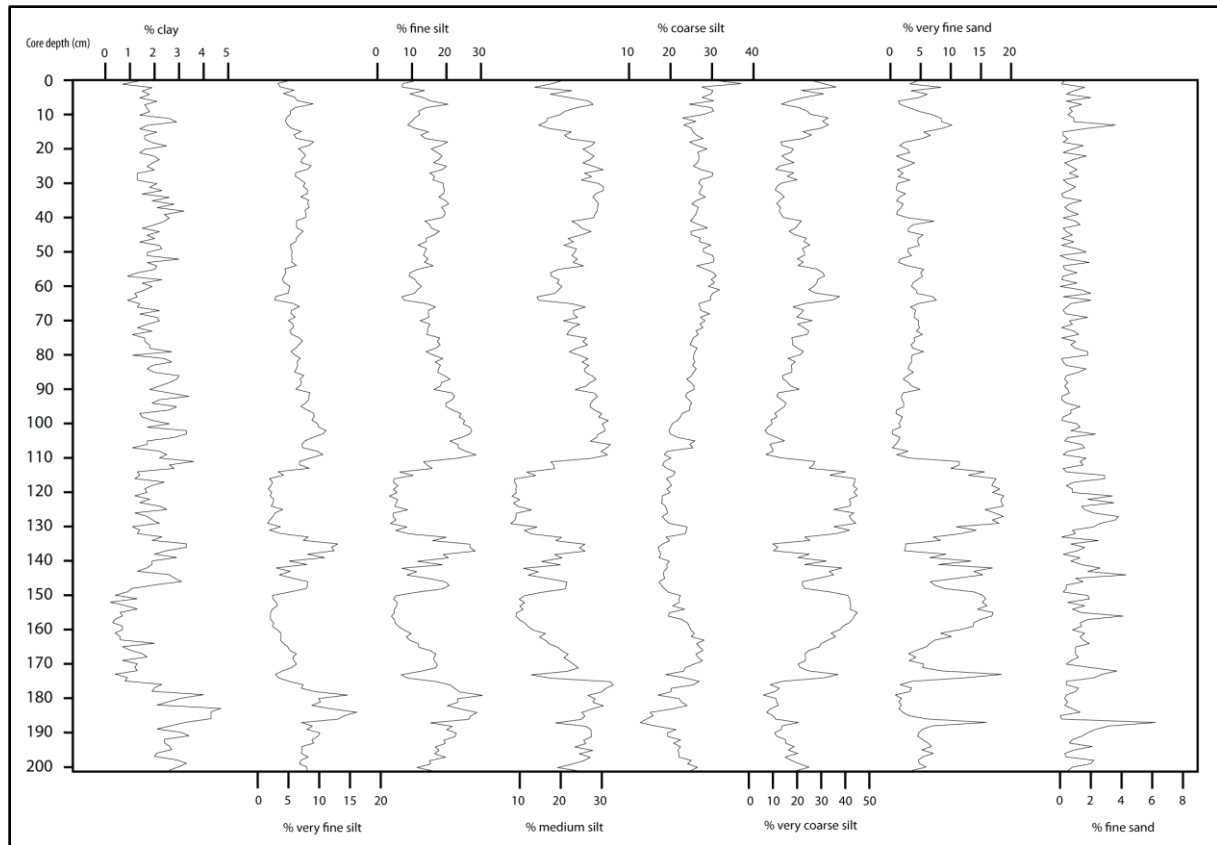


Figure 3.9 Percentage distribution of the grain sizes of MIP-209. Measurements were performed in 1 cm intervals. Values of each grain size are presented in percent of the whole sample.

3.7 Sediment parameters as proxy for glacial activity

In this study, proglacial sediments of MIP-109 and MIP-209 are analyzed with the main goal of identifying variations in several sediment parameters that reflect variations in glacial activity. Due to the high minerogenic sedimentation and a very low organic component (<5%) in Lake Midtbotnvatn, LOI is a limited parameter to represent glacial activity (Bakke et al. 2005c). In this regard, DBD is accepted as an adequate substitute physical parameter (Bakke 2004; Bakke et al. 2005c). The XRF ratio inc/coh is related to the total organic carbon content (Guyard et al. 2007); due to the high error potential of LOI in this study, inc/coh is used as a parameter for the organic content of the minerogenic sediments of the two cores.

Further important parameters that reflect increasing or decreasing glacial activity are MS, grain-size distribution (Bakke et al. 2005c), and the XRF values of elements that usually are interpreted as to be of detrital origin, such as Si, Ti and Rb. The calculated XRF ratio Fe/Ti reflects changes in minerogenic wash-in and general conditions within and around the lake not related to changes in glacial activity (Rothwell et al. 2006; Guyard et al. 2007).

The comparatively small size of Lake Midtbotnvatn (2 km²) indicates that the water residence time enables the settling of much of the glacially-derived sediments in suspension (grain sizes up to fine sand), which is transported in through river Blådalselv. Grain sizes larger than fine sand are most likely already deposited further upstream in areas where the river is shallow and flow velocity is sufficiently low, as for example in Kjerringebotn (UTM 467917, 800 m a.s.l). Due to the fact that the lake has an outflow in the northwest in addition to the inflow in the northeast, it is probable that the water flow at least in the upper third of the lake water rarely drops below $\sim 0.1 \text{ ms}^{-1}$ (Ashley 1995, 427), which indicates that some amounts of the suspended finest grain size fractions (very fine silt and clay) are not deposited, but transported further downstream. The measured grain size distributions of MIP-109 and MIP-209 are in agreement with these assumptions, since the prevailing grain size fractions are very coarse, coarse, medium and fine silt.

Table 7 and Table 8 show the correlation values of the sediment parameters used to analyze MIP-109 and MIP-209. The correlation values of both cores are partly quite poor, which is attributed to the disturbed sediment structure.

Table 7 Correlation values of the sediment parameters used to analyze MIP-109. Correlations mentioned in the text are marked bold.

MIP-109	DBD	LOI	WC	MS	Mean	Sorting	fine sand	very fine sand	very coarse silt	coarse silt	medium silt	fine silt	very fine silt	clay	Ti	Si	Rb	inc/coh	Fe/Ti
DBD	1																		
LOI	-0.56	1																	
WC	-0.6	0.76	1																
MS	0.32	-0.25	-0.25	1															
Mean	0.14	-0.15	-0.32	0.21	1														
Sorting	0.38	-0.44	-0.3	0.09	-0.14	1													
f.sand	0.27	-0.38	-0.19	0.1	-0.02	0.89	1												
v.f.sand	0.15	-0.03	-0.21	0.23	0.77	-0.36	-0.44	1											
v.c.silt	0.01	0.02	-0.21	0.06	0.79	-0.49	-0.56	0.88	1										
c.silt	-0.08	0.02	-0.19	0.05	0.74	-0.46	-0.28	0.47	0.65	1									
m.silt	-0.15	0.12	0.19	0.07	-0.37	0.01	0.27	-0.68	-0.64	-0.01	1								
f.silt	-0.08	0.12	0.36	-0.16	-0.93	0.23	0.12	-0.67	-0.77	-0.9	0.21	1							
v.f.silt	-0.02	0.07	0.21	-0.22	-0.86	0.19	-0.05	-0.45	-0.55	-0.88	-0.1	0.92	1						
clay	-0.18	0.09	0.13	-0.23	-0.66	0.23	0	-0.41	-0.43	-0.62	-0.07	0.63	0.67	1					
Ti	0.18	-0.19	0.01	0.43	-0.03	0.18	0.26	-0.08	-0.24	-0.14	0.25	0.09	-0.06	-0.06	1				
Si	-0.05	0.07	0.28	0.39	0.09	0.15	0.33	-0.05	-0.22	-0.08	0.29	0.04	-0.19	-0.21	0.71	1			
Rb	0.13	-0.07	0.07	0.37	0.06	0.14	0.17	0.02	-0.09	-0.04	0.14	-0.01	-0.13	-0.07	0.62	0.49	1		
inc/coh	0	0.16	-0.1	-0.26	0.05	-0.05	-0.12	0.08	0.18	0.06	-0.25	-0.06	0.05	0.01	0.04	0.01	-0.01	1	
Fe/Ti	-0.01	0.17	-0.17	-0.36	-0.04	-0.13	-0.21	0.02	0.15	0.09	-0.18	-0.03	0.09	0.05	-0.5	-0.63	-0.18	-0.01	1

Table 8 Correlation values of the sediment parameters used to analyze MIP-209 Correlations mentioned in the text are marked bold.

MIP-209	DBD	LOI	WC	MS	Mean	Sorting	fine sand	very fine sand	very coarse silt	coarse silt	medium silt	fine silt	very fine silt	clay	Ti	Si	Rb	inc/coh	Fe/Ti
DBD	1																		
LOI	-0.2	1																	
WC	-0.59	0.47	1																
MS	-0.07	-0.09	0.13	1															
Mean	0.26	0.02	-0.29	-0.36	1														
Sorting	0.04	0.14	-0.03	0.08	-0.26	1													
f.sand	0.12	0.14	-0.12	-0.09	0.46	0.21	1												
v.f.sand	0.3	0.11	-0.33	-0.36	0.93	0.03	0.5	1											
v.c.silt	0.28	-0.01	-0.32	-0.37	0.97	-0.18	0.37	0.89	1										
c.silt	-0.28	-0.27	0.27	0.15	-0.17	-0.4	-0.37	-0.47	-0.08	1									
m.silt	-0.29	-0.06	0.32	0.37	-0.95	0.07	-0.43	-0.92	-0.98	0.22	1								
f.silt	-0.16	0.06	0.18	0.3	-0.93	0.23	-0.35	-0.79	-0.95	-0.16	0.89	1							
v.f.silt	-0.17	0.19	0.24	0.26	-0.87	0.34	-0.32	-0.7	-0.88	-0.24	0.78	0.94	1						
clay	-0.09	0.14	0.17	0.21	-0.53	0.45	-0.1	-0.34	-0.54	-0.35	0.42	0.59	0.68	1					
Ti	-0.36	-0.17	0.42	0.52	-0.66	0.03	-0.34	-0.72	-0.63	0.45	0.68	0.5	0.4	0.18	1				
Si	-0.41	-0.32	0.43	0.47	-0.57	-0.14	-0.38	-0.7	-0.53	0.61	0.61	0.37	0.25	0.06	0.88	1			
Rb	-0.27	-0.19	0.38	0.51	-0.63	0.05	-0.3	-0.67	-0.61	0.37	0.65	0.49	0.41	0.24	0.82	0.75	1		
inc/coh	0.42	0.19	-0.48	-0.42	0.64	0.01	0.36	0.72	0.6	-0.54	-0.66	-0.43	-0.35	-0.13	-0.7	-0.69	-0.59	1	
Fe/Ti	0.2	0.3	-0.14	-0.38	0.48	-0.03	0.27	0.55	0.42	-0.47	-0.47	-0.3	-0.22	0	-0.6	-0.49	-0.32	0.38	1

DBD and very coarse silt show positive correlations (MIP-109: 0.01; MIP-209: 0.28); DBD and very fine silt are negatively correlated (MIP-109: -0.02; MIP-209: -0.17), these correlate inversely with each other (MIP-109: -0.55; MIP-209: -0.88).

To take into account the disturbed sediment structure, DBD values were correlated for several sections of MIP-109 and MIP-209. The least disturbed sediment of MIP-109 and MIP-209 are in the uppermost and lowermost parts of the cores.

The grain sizes which correlate to the highest degree with DBD values are very coarse silt (positive correlation; MIP-109 160-210 cm: 0.67; MIP-209 165-201 cm: 0.37) and very fine silt (negative correlation; MIP-109 160-210 cm -0.60; MIP-209 165-201 cm: -0.53). Therefore, the grain sizes very fine silt and very coarse silt are interpreted as to reflect glacial activity of Vestre Blomsterskardsbreen best, together with DBD and MS (MIP-109: 0.32; MIP-209: -0.07). Moreover, the detritally originated elements Ti, Si and Rb, and the ratio Fe/Ti are used in this study. Titanium has a positive correlation with DBD (MIP-109 0.18; MIP-209: -0.36), silicon values follow variations in grain sizes (correlation mean and Si MIP-109: 0.09; MIP-209: -0.57), and rubidium is connected to the clay content (MIP-109: -0.07; MIP-209: 0.24), indicating that these parameters also can be used for inferences on glacial activity (Rothwell et al. 2006; Guyard et al. 2007). The poor correlations between DBD and MS, Ti, Si and Rb in MIP-209 are attributed to the fact that DBD measurements were performed ca. 2 cm to the right, while all other parameters were measured in the central part of the core; this to take into account sediment disturbances as good as possible.

The ratio Fe/Ti is generally stable when reflecting a glacial signal only, because a glacier always produces the same ratio of these parameters. Changes in the Fe/Ti ratio (for example through oxidation) therefore indicate changes not related to the glacier, such as episodic events, or disturbed core sediments (Rothwell et al. 2006).

An increase in DBD, MS, detritally originated elements and very coarse silt and a decrease in very fine silt is interpreted to indicate increased glacial activity.

3.8 Sedimentation processes

Proglacial sediment cores do not only represent glacial activity; other processes within a drainage basin that influence the sediment yield are amongst others precipitation and runoff, topography, geology, and vegetation (Hicks et al. 1990). The successful use of proglacial sediments as proxy for glacial activity therefore requires a differentiation between depositing agents. The main focus in this study is set on the continuous glacial sedimentation in Lake Midtbotnvatn, which varies with glacial activity, in order to reconstruct glacier fluctuations at Vestre Blomsterskardsbreen. Parts of the lake sediments which were deposited by episodic events such as river flooding and gravitational processes strongly affect the sedimentation record (Hicks et al. 1990; Nesje et al. 2000a). Such single-events may deposit as much sediment within the short time period of hours or a few days as under normal circumstances is deposited within years of continuous glacial sedimentation; corresponding parts of the sediment cores must therefore be identified and isolated (Karlén 1981; Hicks et al. 1990).

The most important sedimentation processes in a proglacial lake and their main characteristics with respect to the analysis parameters used in this study are theoretically explained in the following; Figure 3.10 shows sections in MIP-209 interpreted as being deposited during different hydrological conditions in the drainage area through accordingly different sedimentation processes.

Glacial activity

Increased glacial activity

Increased glacial activity causes increased erosion at the glacier bed and increased stream power of proglacial rivers, which in turn enlarge the amount of allochthonous clastic material transported glaciofluvially, and with that the minerogenic sedimentation in the attendant proglacial lake (Summerfield 1991; Nesje et al. 2000a). Accordingly, the amount of organic material deposited decreases. Increasing DBD values and decreasing LOI and inc/coh values

thus indicate increased glacial activity in a lake catchment. Reflecting the concentration of magnetic minerals within the sediment, also increasing MS values indicate increased erosion and transport of clastic sediment (Nesje et al. 2000a; Nesje et al. 2001). An increase with increased glacial activity also applies for concentrations of elements of detrital origin (such as Ti and Si) received by μ -XRF measurements (Guyard et al. 2007). The downcore DBD and MS values, and in addition element values associated with detrital characteristics, are therefore commonly inversely correlated to the LOI values (Nesje et al. 2000a). Increased glacial erosion, minerogenic sediment input and flow conditions of proglacial rivers effect proglacial sedimentation also in terms of grain sizes; larger amounts of clastic sediments with relatively increased grain sizes are produced, transported according to the Hjulström diagram (Nichols 1999; cp. Figure 3.2) and finally deposited in a proglacial lake during periods of increased glacial activity. The grain size very coarse silt is in this study interpreted as the one with the strongest positive correlation to increased glacial activity, whereas very fine silt is negatively correlated.

Decreased glacial activity

Periods of decreased glacial activity are characterized by reduced erosion at the glacier bed, decreased hydrological energy in proglacial rivers, and hence a decreased minerogenic sedimentation rate in a proglacial lake, together with an increase of the organic content (Nesje et al. 2000a; Nesje et al. 2001). A decreased amount of glacially derived sediments, higher percentages of finer grain size fractions, a relatively decreasing amount of larger grain sizes, increasing LOI and inc/coh values, as well as decreasing values of DBD, MS and detritally originated elements indicate decreased glacial activity in proglacial sediments. In this study, very fine silt is interpreted as correlating positively with decreased glacial activity, while very coarse silt correlates negatively.

In contrast to glacially derived sediments, which commonly are deposited continuously during long time periods, are river floods and gravitational processes classified as episodic events, which may cause large amounts of sedimentation during very short time periods. To create a reliable age-depth model and successful reconstruction of the sedimentation rate of a proglacial lake, it is therefore important to isolate episodically deposited sediment sections, in order to exclusively reconstruct variations in glacial activity (cp. Hicks et al. 1990).

Floods

During flood events the hydrological energy of proglacial rivers increases abruptly, both flow velocity and stream power are then higher than normal, increasing the competence and the capacity of the river flow (Summerfield 1991; Bakke 2004). The stream power of a river is defined as the power per unit length of a stream (Summerfield 1991, 201). Moreover, the surface runoff in the drainage basin is enlarged. These characteristics enable a more extensive transport and deposition of material during river floods, affecting, according to the Hjulström diagram (Nichols 1999; cp. Figure 3.2), also relatively larger grain size fractions, compared to normal circumstances.

The “sorting” and “mean” parameters, derived through statistical analyses of the grain-size data, reflect flood events in proglacial sediments with abrupt changes to higher mean grain sizes and lower sorting values (more sorted sediment) in the beginning followed afterwards by higher sorting values (less sorted sediments) (Arnaud et al. 2002; Bakke 2004).

Floods also increase the organic erosion in a drainage basin and wash-in into a proglacial lake, resulting in higher LOI, inc/coh ratio and Fe/Ti values of flood layers within the sediment cores. Wash-in of organic material can also cause limitations concerning the radiocarbon dating technique, since such organic material may be older than the origin of the flood layer.

The thickness of a flood layer in the lake sediments depends on the capacity and the duration of the corresponding flood (Bøe et al. 2006). Floods can cause sediment layers as thick as normally deposited during several years of continuous glacial sedimentation; therefore it is of crucial importance to identify according layers and isolate them before reconstructing the sedimentation rate and age-depth model reflected in the glacial record only (Hicks et al. 1990; Bakke 2004).

Flood events in the drainage basin of Lake Midtbotnvatn are mainly triggered by extensive rainfall, snow melt and regulations.

Gravitational processes

Gravitational processes are very important mass movement and re-deposition agents, transporting large amounts of debris. Subaqueous mass flows can be differentiated into debris flows and turbidity currents (Benn and Evans 1998, 293).

Debris flows are cohesive or cohesionless high-concentration plastic slurries in subaerial and subaqueous environments. Cohesive subaqueous debris flows are characterized by the existence of clay matrix material, which, when mixed with water, can act as a fluid with

cohesive strength. Cohesionless debris flows are high-concentration, non-turbulent flows characterized by the partial or complete absence of cohesion as influencing factor for the sediment strength. The latter produce upward dispersive pressures, causing expansion of the flowing mass and forcing larger particles to the surface, the deposited sediments are therefore characterized by an inverse grading (Benn and Evans 1998, 293f).

Turbidity flows are rapidly moving turbulent underflows. The main characteristic is that grains (mainly finer fractions) within the flow body are held in turbulent suspension by fluid turbulence (Shanmugam 1997, 203ff, and references therein; Benn and Evans 1998, 294, and references therein). Turbidity currents can have erosive effect (Benn and Evans 1998). In proglacial environments, turbidity flows are mainly triggered by density differences between the lake water and sediment-laden meltwater streams that flow into the lake. The latter are commonly denser, resulting in quasi-continuous underflows at the lake bottom (Benn and Evans 1998, 295). The suspended sediment is re-deposited grain by grain through sediment fallout, larger grains are deposited first due to higher settling velocity and finer ones later, resulting in a normal size grading with an upward decline in grain size (Shanmugam 1997, 205f; Benn and Evans 1998, 294f).

All types of gravitational processes have episodic character; in the grain size distribution analyses they may be identified through the mean values changing abruptly to larger grain sizes, and the sorting values being commonly high, which indicates less sorting.

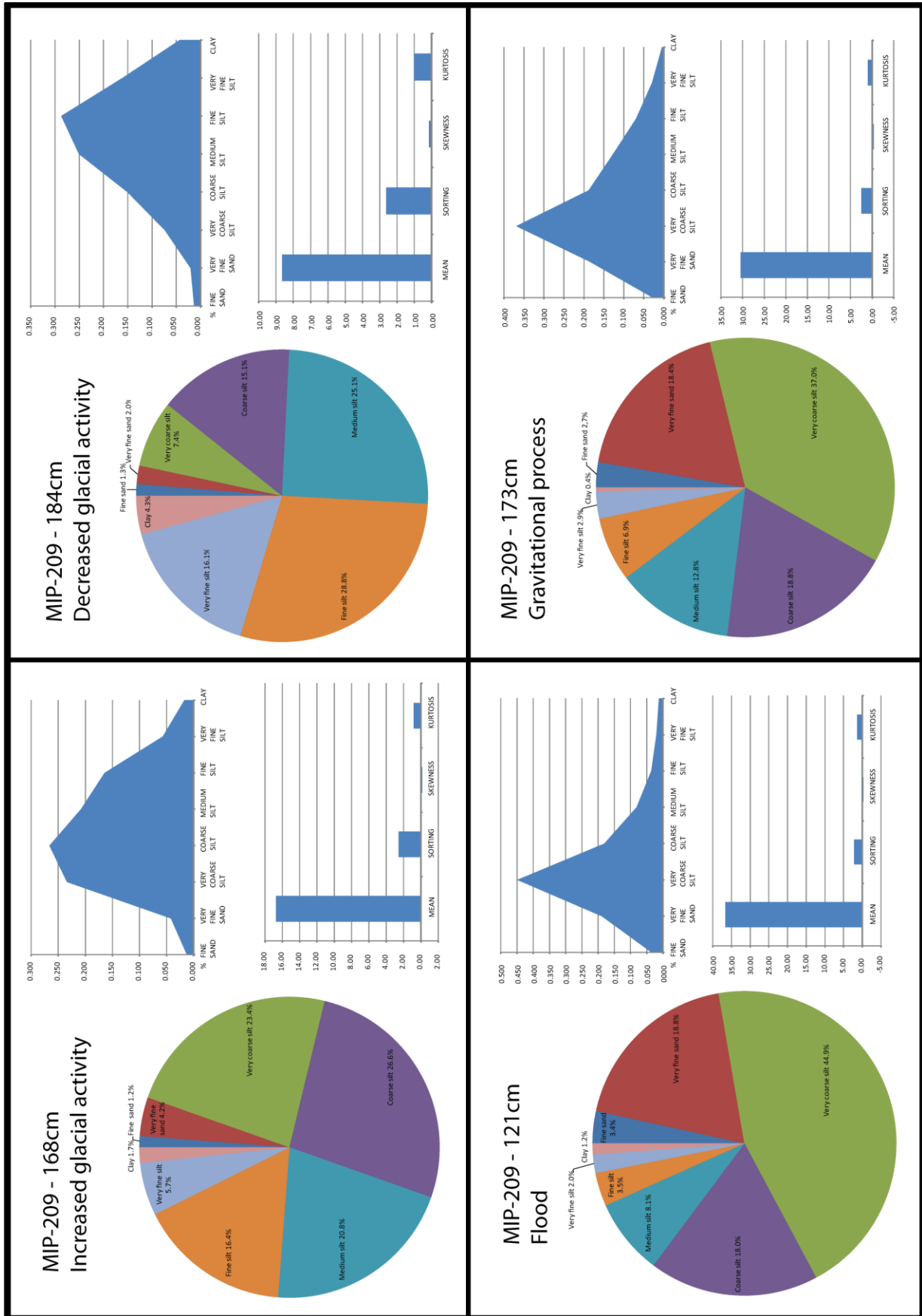


Figure 3.10 Sections in MIP-209 interpreted as being deposited during different hydrological conditions in the drainage area: increased glacial activity, decreased glacial activity, flood, gravitational process. Division presented here is according to differences in grain size distribution.

3.9 Interpretation

Based on the analyses results of the sediment parameters presented in Chapter 3.4 and 3.6, MIP-109 and MIP-209 were divided into sections, in order to identify variations in glacial activity and episodic events in the drainage basin of Lake Midtbotnvatn. The interpretations of increased and decreased glacial activity were mainly based on DBD; DBD values above core average are interpreted as to reflect increased glacial activity, and DBD values below core average reflect decreased glacial activity, respectively. Floods and gravitational processes were mainly identified via anomalies in the grain size parameters “mean” and “sorting”; their validity was approved by the normal distribution of the grain size analyses results of MIP-109 and MIP-209.

Throughout minerogenic sediments in both cores indicate that Vestre Blomsterskardsbreen has been existent in the drainage basin of Lake Midtbotnvatn the whole periods MIP-109 and MIP-209 represent. The glacier outlet is the dominating factor with respect to water discharge and sediment transport into the proglacial lake; therefore MIP-109 and MIP-209 are interpreted as to reflect the glacial signal of Vestre Blomsterskardsbreen when sediment parts originated from episodic events are excluded.

Both MIP-109 and MIP-209 being disturbed through coring, it must be stressed that the quality of the interpretations is limited by the sediment properties.

3.9.1 Interpretation of MIP-109

Section D (158-209.5 cm)

Based on DBD values, and the high mean grain size with dominating grain sizes very coarse, coarse and medium silt, section D is interpreted as reflecting a period of decreased glacial activity, including several episodic events which, due to the disturbed sediment structure, are reflected in different depths from different parameters. The grain size distribution, mainly the low peaks of the sorting parameter, the high peaks of the mean parameter and the variations of very fine sand, very coarse silt and very fine sand, indicate that flood events are reflected at the depths 158-171.5 cm, 178-181.5 cm, 187.5-198 cm. XRF parameters Ti, Si, Rb and Fe/Ti decrease abruptly at 171-173 cm, 180-183 cm, and 190-198 cm, while inc/coh increases. MS values indicate the same flood events at depths 171.5-173.5 cm, 182.5-184.5 cm, 189-197 cm where the values show strong anomalies. The fact that these events are to the most degree observable in the grain size distribution parameters is attributed to the grade of disturbances of the sediment structure; grain size distribution is performed on greater intervals (5 cm in the section), and with more sediment (1 cm) than are the other parameters, and therefore

measurements on disturbed sediment negatively affect the grain size distribution to the greatest extent, limiting the accuracy of the results.

On DBD values, these episodic events are interpreted as to be at 172.5-174.5 cm, 182.5-184.5 cm, and 190-197 cm; this assumptions are based on exceptionally lower DBD values for the upper two events and increased DBD values for the lowest one, as well as on visible sediment structures and the analyses results of the other sediment parameters.

Section C (96-158 cm)

DBD values are highest in the whole core in this section, as are MS values, except at 117.5-123 cm. Ti, Si and Rb values are high, Fe/Ti values are stabile, inc/coh values are lower than in section B and D. The mean grain size is high, with dominating grain sizes are medium, coarse and fine silt. These parameters indicate that section C represents a time period with increased glacial activity.

Both MS and all XRF values and ratios show anomalies around 115-123 cm, this is partly attributed to the change of the core halves at 117.5 cm, where the sediment surface is slightly lower, which enlarges the distance between core and sensor, resulting in falsified measurements. The anomaly is so extensive, though, and moreover also observable in the parameters DBD (115.5-122.5 cm) and grain size distribution (113-122.5 cm), which both are indepent of sediment-sector-distances, that this sediment part is interpreted as partly of artificial origin and partly episodic event. Increased mean and sorting parameters indicate that it is a gravitational process.

The sediment structure in section C is probably disturbed, though distinct structures are not visible and cannot be taken into account; this may affect the interpretation results negatively.

Section B (71-96 cm)

Based on the general trends of the sediment parameters, which is varying values of XRF, DBD and MS, and an upcore decrease of the mean grain size and contemporaneous increase in finer grain sizes, including several variations, Section B is interpreted as reflecting a period of several comparably frequent changes of increased and decreased glacial activity, with generally upcore decreasing intensity of glacial activity in either classification. DBD and MS values indicate the subsections 71-77 cm representing decreased glacial activity, 77-87 cm increased glacial activity and 87-96 cm again decreased activity.

The highly disturbed core structure in this section, including visible sediment lenses of finer grain sizes than the surrounding darker sediment, explains the missing accuracy of sediment parameter analogies for this interpretation, which therefore is mainly based on DBD values and thus has to be treated with caution.

Section A (0-71 cm)

The analyzed sediment parameters in this section do not show significant analogies that enable certain interpretation. Several anomalies of the mean and sorting parameter though may indicate episodic processes: the sorting parameter is exceptionally high at 8-11 cm, 21.5-26.5 cm and 36-42 cm. The first and the last of these episodes are two distinct abrupt increases only in the sorting parameter. Missing analogies with other sediment parameters, especially the mean parameter and other grain sizes, prevent these sorting anomalies to be interpreted as episodic events. The disturbed sediment structure, however, may have falsifying impact on the measurements and accordingly this interpretation.

The subsection 21.5-26.5 cm shows increased mean and sorting, very coarse silt, DBD, Ti, Si, Rb and Fe/Ti values, and decreased very fine silt, MS and inc/coh values. It is therefore interpreted as a gravitational process.

In the lowest part of section A, all sediment parameters show anomalies, though not in the exactly similar depths, which is attributed to the disturbed sediment structure. The mean and sorting parameters show abrupt anomalies, increase and decrease, respectively, at around 57-68 cm, indicating a flood event. This interpretation is supported by the other sediment parameters: DBD shows abruptly slightly increased values at 68.5-72 cm; MS values are abruptly increasing upcore around 69 cm. Ti, Si and Rb values are abruptly lower between 65 cm and 71 cm, inc/coh values are higher and Fe/Ti values are slightly lower, the latter in addition showing stronger variations in this interval. This flood event is interpreted as the beginning of the lake regulations in 1953.

Section A is interpreted as to represent the time period of decreased glacial activity during which Lake Midtbotnvatn has been regulated for the development of hydroelectric power. All sediment between 0 cm and 71 cm is hence influenced by the regulation, which could frequently cause both draining and damming processes of Lake Midtbotnvatn; such changes in the hydrological power of the system were capable of enabling erosion and re-sedimentation processes, and that way eliminating any certain interpretation options through sediment parameters used in this study. All interpretations of section A must therefore be seen with caution. In general, the lack of (accurate) analogies in section A are attributed to the adulterating impact of the lake regulations, and to the disturbed sediment structure.

Figure 3.11. shows MIP-109, the sections A to D with respective subsections, and their interpretations.

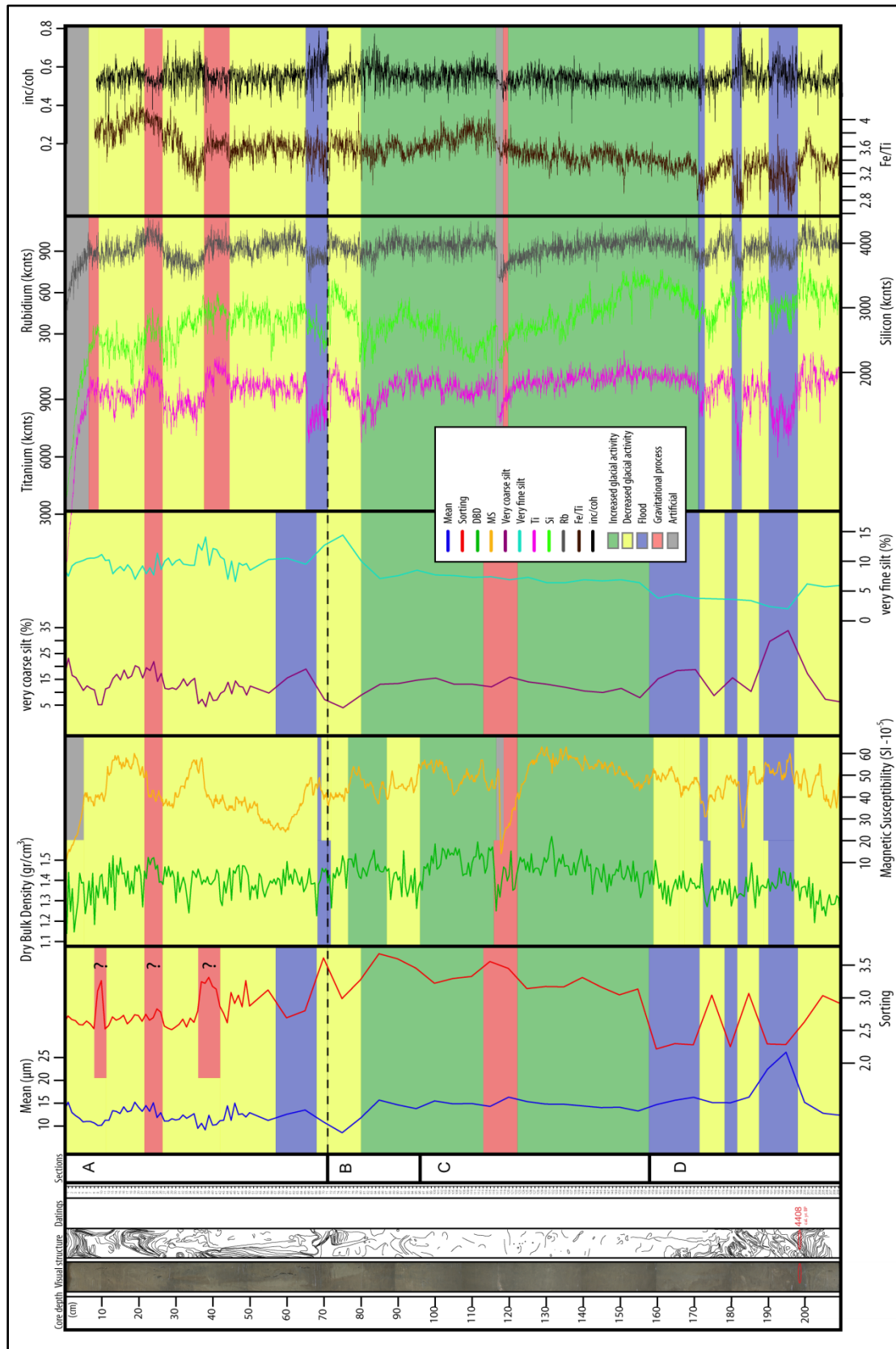


Figure 3.11 MIP-109: sections A to D with respective subsections, and their interpretations. Sections interpreted as increased glacial activity are marked green, decreased glacial activity is marked yellow, subsections interpreted as floods and gravitational processes are marked blue and red, respectively. The proglacial sediment parameters DBD, very coarse silt, very fine silt (invers indicator) and the detrital XRF parameters Ti, Si, and Rb were used to interpret glacial activity. The parameters mean and sorting as well as the XRF ratios Fe/Ti and inc/coh were used for interpretation of episodic events. In addition, radiocarbon datings are included, reliable ones are marked red.

3.9.2 Interpretation of MIP-209

Section E (191-201 cm)

DBD values in this section are above core average, as are MS, Ti, Si and Rb values. The inc/coh ratio is comparably low. These parameters indicate increased glacial activity. The mean grain size values and very coarse silt values are below core average, though, when isolating the parts identified as episodic events from the core record, both parameters are above core average. In addition, the dominating grain sizes in this section are the coarser fractions medium, coarse and very coarse silt. This supports the assumption that section E contains minerogenic sediments deposited during a time period of increased glacial activity.

There is one subsection within this part of the core, 192.5-194.5 cm, where DBD, Ti and Si values are low, while the parameters mean, sorting and MS are exceptional high. Moreover, Fe/Ti shows an anomaly. This is interpreted as an episodic event; and with respect to high sorting values identified as a gravitational process.

Section D (181.5-191 cm)

DBD values in this section are below core average, the content of very coarse silt sinks while very fine silt rises. Dominating grain sizes are fine, medium and coarse silt; the mean grain size values are lower than in section E. The ratio inc/coh is above core average, Ti, Si and Rb values are lower than in section E. Based on these analyses values, section D is interpreted as representing a time period of decreased glacial activity.

There is one subsection within this part of the core, 185.5-188.5 cm, where mean and sorting values show anomalies; the sorting parameter reaches its highest peak of the whole core. The values of MS, Ti, Si, Rb and Fe/Ti rise abruptly in this subsection, while inc/coh sinks. Very coarse silt is higher than in the surroundings, very fine silt lower. DBD is slightly lower as well. This subsection is interpreted as episodic event; the extraordinary high sorting values indicate a gravitational process. MS values are high above core average between 183 cm and 188.5 cm, reflecting anomalies in larger amplitude than the other parameters. This is attributed to the disturbed sediment structure.

Section C (107.5-181.5 cm)

The sediment structure of section C is to a high degree disturbed through coring. Therefore, this sections parameters have to be interpreted partly independent from each other.

DBD values through the whole section measured on the right side of the core are above core average, indicating a time period of increased glacial activity. Between 107.5 cm and 110.5 cm, and between 166 cm and 181.5 cm, this assumption is supported by MS values, Ti, Si, and Rb values above core average, as well as inc/coh values lower than in section D.

There are several subsections within section C that show great anomalies in several parameters, and which therefore are interpreted as episodic events.

Subsection 171.4-174.5 cm is dominated by abruptly increasing mean values, as well as strong sorting, MS, Fe/Ti as well as very coarse silt values. In contrary, DBD, Ti, Si, Rb and very fine silt values are lower than the surroundings. Accordingly, this subsection is interpreted as gravitational process.

The subsection 107.5-166 cm is visually dominated by a disturbed dark layer containing very fine sand and macrofossils visible on the left side of the core. The core parts 132.5-140.5 cm and 144-149 cm are only to a minor extent dominated by this layer, which is observable both visual and in the parameter analysis results.

The sediment on the right core side is disturbed sediment with varying structures: partly there is hardly any visible structure visible, partly vertically and horizontally arched, undulated and chaotic layers can be observed, and partly darker layers containing coarser grain sizes and macrofossils are visible.

All sediment parameters except DBD reflect the signal of the left core side, including huge anomalies of several parameters. Based on the high mean grain size with high contents of very coarse silt and fine sand and less very fine silt, a low sorting parameter, low values of MS, Ti, Si, Rb and exceptional high values of Fe/Ti and inc/coh, , the layer is interpreted as a flood event. The Fe/Ti record indicates an event or change in the drainage system not related to the glacier, the inc/coh record reveals an increased organic content. The layer was crucially disturbed through coring and is therefore dominating such large parts of it. None of these parameters can therefore be used as indicators for glacial activity; this interpretation is only based on DBD and hence cannot be strengthened or weakened by further parameters, a fact that limits the reliability of the interpretation.

It could be observed that DBD values normally are lower than the surroundings when other parameters indicate episodic events (cp. section D, E and the lower part of section C). Based on visual observations of the sediment structure and several negative peaks of DBD, several parts on the left side of section C are identified as influenced by flood events (either as part of the disturbed large layer which dominates the left side of the core, or by additional flood events): 157.5-159 cm, 158.5-159.5 cm, 146.5-147.5 cm, 141.5-143.5 cm, 137.5-138.5 cm and 112.5-115.5 cm.

Section B (65-107.5 cm)

DBD values in this section are strongly varying above and below average; in general an upcore rising trend can be observed. Dominating grain sizes are coarse, medium and very

coarse silt in the upper part of the section, and medium, fine and coarse silt in the lower part. Due to the dominating flood layer in section C, grain size distribution values of section B cannot be compared to it. Section B is interpreted as reflecting a time period of comparably frequent changes of increased and decreased glacial activity; in the upper part of the section, between 65 cm and 92.5 cm, the sediment parameters indicate generally more glacial activity both during periods of increased and decreased glacial activity.

Increased glacial activity is ascribed to the subsections 65-67.5 cm, 74-79 cm, 86-92.5 cm and 95-102.5 cm. Increased DBD values, MS values, Ti and Rb values indicate that. Based on age-depth interpolation, the subsection 66.5 cm to 67.5 cm is interpreted as to indicate the LIA maximum glacier advance in the first half of the 18th century (see Chapter 3.11.).

Decreased glacial activity is ascribed to the subsections 67.5-74 cm, 79-86 cm, 92.5-95 cm and 102.5-107.5 cm. Decreased DBD values, MS values, Ti and Rb values indicate that.

The fact that the grain size distribution values do not significantly support these interpretations is attributed to the grade of disturbances of the sediment structure; grain size distribution is performed on greater intervals and with more sediment than are the other parameters, and therefore measurements on disturbed sediment negatively affect the grain size distribution to the greatest extent, limiting the accuracy of the results. The lack of significant anomalies of the mean and sorting parameters, and of Fe/Ti, indicate that no episodic events occurred in this time period. The reliability of this interpretation is weakened by the grade of disturbances of the sediment structure.

Section A (0-65 cm)

Section A is interpreted as to represent the time period of decreased glacial activity during which Lake Midtbotnvatn has been regulated for the development of hydroelectric power. The analyzed sediment parameters do not show significant analogies that enable certain interpretation. Several anomalies of the mean and sorting parameter though indicate episodic processes: the parts 3.5-5.5 cm, 10-18 cm, 23-25 cm, 28-30 cm and 40-42.5 cm may be interpreted as sediment deposited through gravitational processes, because mean and sorting values rise abruptly. This interpretation is weakened by the fact that even layering is visible in section A especially from 0 cm to 40 cm, indicating continuous regular deposition; and moreover by the other parameters, which show variations in this section, but it is not possible to observe a certain scheme which fits to this interpretation. The missing analogies in section A are attributed to the adulterating impact of the lake regulations. The parts 0.5-2 cm, and especially 55-60 cm and 61-65 cm, show abruptly increasing mean values and abruptly decreasing sorting values, and are therefore interpreted as flood events. Observations of the

sediment structure between 56 cm and 72 cm indicate that the flood layers 55-60 cm and 61-65 cm actually represent one flood layer, disturbed through coring. This flood event is interpreted as the beginning of the lake regulations in AD 1953; all sediment between 0 cm and 65 cm is hence influenced by the regulation, preventing any certain interpretation options through sediment parameters used in this section (cp. MIP-109 section A; Chapter 3.9.1.). All interpretations of section A must therefore be seen with caution.

Figure 3.12. shows MIP-209, the sections A to E with respective subsections, and their interpretations.

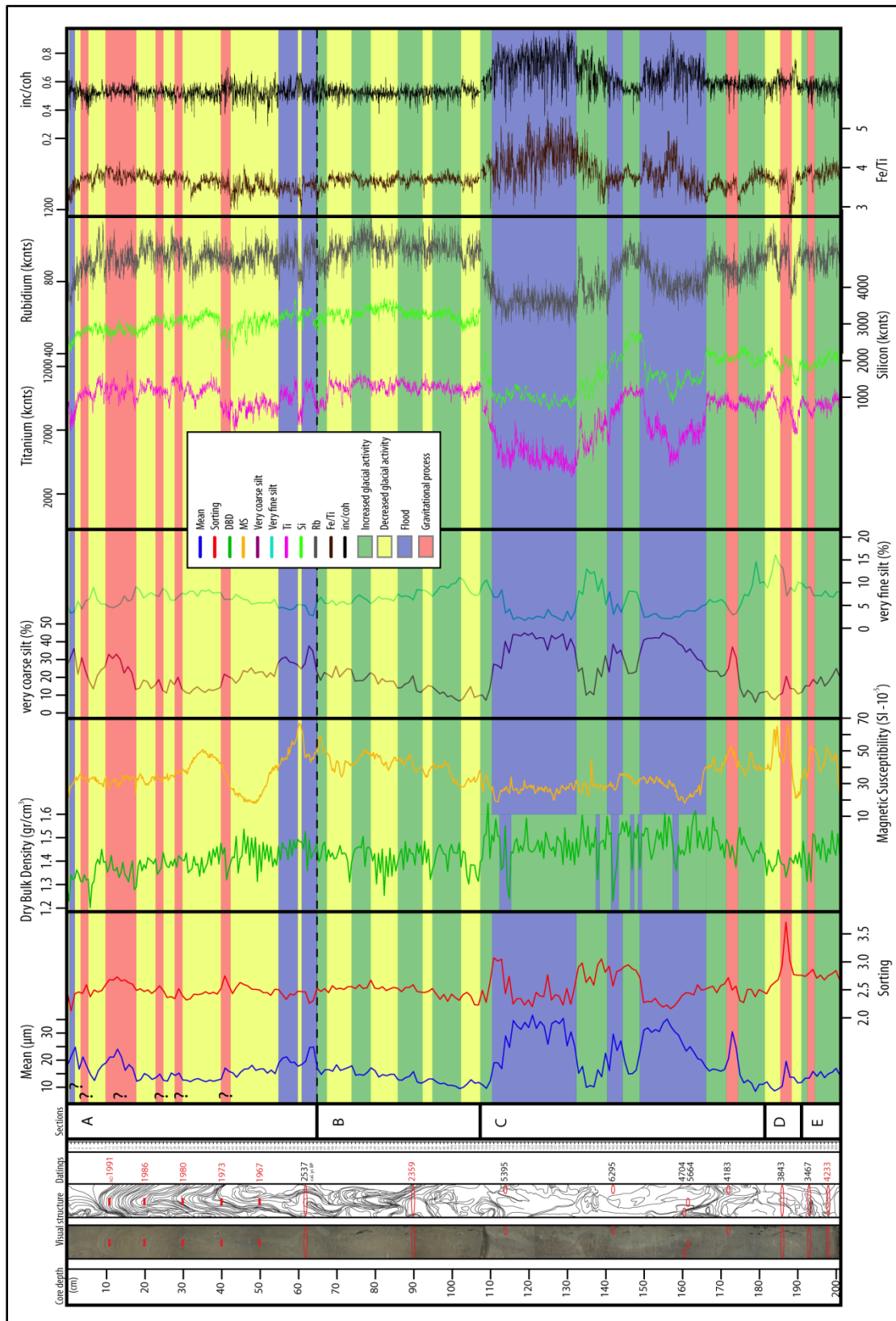


Figure 3.12 MIP-209: sections A to E with respective subsections, and their interpretations. Sections interpreted as increased glacial activity are marked green, decreased glacial activity is marked yellow, subsections interpreted as floods and gravitational processes are marked blue and red, respectively. The proglacial sediment parameters DBD, very coarse silt, very fine silt (invers indicator) and the detrital XRF parameters Ti, Si, and Rb were used to interpret glacial activity. The parameters mean and sorting as well as the XRF ratios Fe/Ti and inc/coh were used for interpretation of episodic events. In addition, radiocarbon and lead datings are included, reliable ones are marked red.

3.10 Comparison of MIP-109 and MIP-209

MIP-109 and MIP-209 are taken in very close distance from each other in Lake Midtbotnvatn. Therefore it is to be expected that the two cores basic characteristics are comparable. A comparison between two proglacial cores of the same lake can be used to draw conclusions about sedimentation differences within different areas of the lake, among other things with respect to sedimentation rate and episodic events, and furthermore there is the possibility to detect levels with special characteristics, which were dated in one core, also in the other, that way providing a better basis for the creation of an age-depth model in either of the two cores. Both MIP-109 and MIP-209 contain exclusively minerogenic sediment, indicating that Vestre Blomsterkardsbreen was permanently present in the time periods the cores represent. Figure 3.13. shows the parameters DBD and LOI of MIP-109 and MIP-209 in comparison.

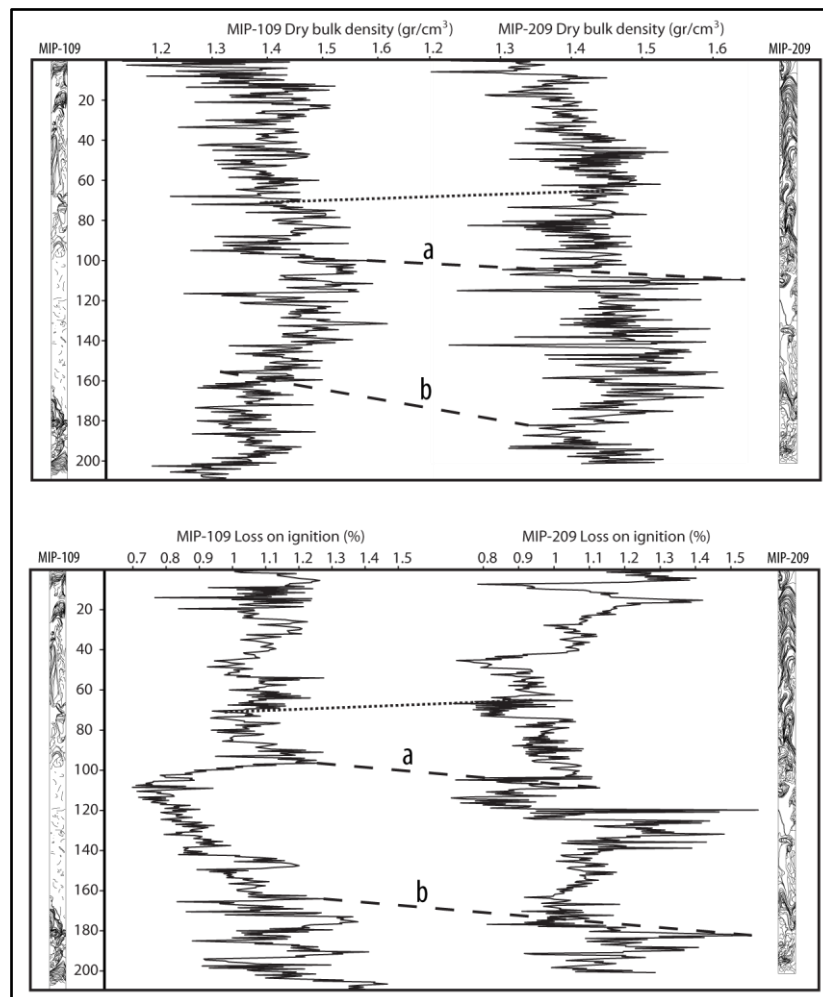


Figure 3.13 Comparison of the cores MIP-109 and MIP-209; the sediment parameters DBD and LOI are used. Dotted line indicates interpreted beginning of the regulation of Lake Midtbotnvatn, dashed lines a and b indicate interpreted changes in glacial activity observable in both cores. Visual sediment structures of both cores are included.

Due to the regulation of Lake Midtbotnvatn it is not possible to compare the uppermost sections of MIP-109 and MIP-209. In Figure 3.13, the dotted line indicates the interpreted beginning of the lake regulations.

Based on the illustrations in Figure 3.13, and the interpretations of the different sediment parameters presented in Chapter 3.9, two compared lines could be drawn (dashed):

The first dashed line (a) indicates the interpreted downcore change to increased glacial activity, in both cores DBD values increase downcore, as well as LOI values decrease. In MIP-209, LOI values increase shortly afterwards; this is attributed to the impact of the recorded flood layers in this section.

The second dashed line (b) indicates the interpreted downcore change to decreased glacial activity, DBD values decrease in both cores, and LOI values increase.

In MIP-109 there is no evidence for another section of increased glacial activity, as can be observed in MIP-209 (section E, cp. interpretation). But, a reliable radiocarbon dating to 4405 ± 130 cal. years BP at 198-199 cm in MIP-109 states that MIP-109 reaches further back in time than MIP-209, which was dated to 4235 ± 175 cal. years BP at 198 cm.

Of episodic events, only gravitational processes can occur locally, reflecting a signal only in one of the cores. Floods, in contrary, affect the whole lake, the whole hydrological system, and should therefore be observable in both cores.

None of the interpreted flood layers in the lower part of MIP-109, which is interpreted as to reflect decreased glacial activity, can be recognized in MIP-209. Furthermore, the huge flood layer in MIP-209 cannot be recognized in MIP-109 in the main section interpreted as increased glacial activity.

These controversies are attributed to the intensive sediment structure disturbances in both cores, especially in MIP-109, which may falsify interpretations. Moreover, it was not possible to correlate any radiocarbon dates between the cores.

Based on the great differences between MIP-109 and MIP-209, and the comparably higher grade of disturbance in MIP-109, only MIP-209 is used in the further course of this study.

3.11 Datings

Ten samples of terrestrial and aquatic macrofossils and one bulk sample were radiocarbon dated by accelerator mass spectrometry (AMS) at the Poznań Radiocarbon Laboratory in Poland; see in Figure 3.11 and Figure 3.12 where the dates were taken out; reliable dates are marked red. Datings were performed on one sample of MIP-109 (macrofossils) and ten samples of MIP-209 (nine macrofossils and one bulk-sediment sample, cp. Table 9).

In addition, 18 samples at depths between 7 cm and 50 cm were dated through lead dating at the Gamma Dating Center, Institute of Geography, University of Copenhagen.

For radiocarbon dating, 1 cm sections of each core depth which came into consideration were sieved in 125 μm and 63 μm sieves with distilled water. The remained organic material was determined in a microscope, in order to find adequate material for dating: mainly terrestrial plant remains. Inadequate material, such as insect remains, was taken out. The macrofossils were then dried at room temperature, put in small clean glasses of known weight, and weighed. During determination of organic material, emphasis was put on avoiding aquatic organic material as far as possible, though the characteristics of Lake Midtbotnvatn as a proglacial lake crucially limit the existence of vegetation in the surroundings (cp. Ashley 1995). To reach the minimum limit of 0.4 mg of macrofossils to date on per sample, aquatic plant remains could not be avoided completely in neither MIP-109 nor MIP-209. On one sample of MIP-209 (160-161 cm), observed macrofossils were assumed to not be sufficient; therefore a bulk-sediment radiocarbon dating had to be performed.

The data programme Calib 6.0.1., Intcal09 was used to calibrate calendar years BP from radiocarbon years BP (Stuiver and Reimer 1993). The dates obtained from radiocarbon dating are shown in Table 9. The dates used in this study are the median values of the calibrated dates with a standard deviation of two sigma (AD 1950).

Precambrian acid rocks, such as granite and gneiss, dominate the bedrock geology in the study area, which indicates that there is no substantial supply of inorganic carbon to Lake Midtbotnvatn. The “hard-water” effect, which could negatively affect the radiocarbon dates, especially the bulk-sediment date and the ones performed on aquatic plant remains (Smart and Frances 1991; Bradley 1999, cp. Chapter 3.4.6.1.), is therefore not expected to affect the radiocarbon dates of MIP-109 and MIP-209 (cp. Moore et al. 1998; Barnekow 1999). This is also supported by the measured amount of inorganic carbonate (C_i) within the two cores, which can be determined by heating the samples to a temperature of 950°C and then weigh the loss on ignition (Heiri et al. 2001, cp. Chapter 3.4.2.). LOI_{950} was performed in 5 cm-intervals on MIP-109 and MIP-209, resulting amounts of inorganic carbonate did not exceed 1.08%. This fact emphasizes the assumption that the “hard-water” effect has no sufficient impact on the sediments in Lake Midtbotnvatn.

Table 9 Radiocarbon dates obtained from the cores MIP-109 and MIP-209. Dates assumed as reliable are marked bold.

LAB.NR.	DEPTH (cm)	TYPE OF MATERIAL	WEIGHT (mg)	AGE ¹⁴ C-years BP	AGE cal. years BP (AD 1950) $\pm 1\sigma$	AGE cal. years BP (AD 1950) $\pm 2\sigma$	AGE BP (AD 1950) Median $\pm 2\sigma$
MIP-109							
Poz-32834	198-199	aquatic and terrestrial mosses	0.38	3970\pm50	4406-4522	4281-4534	4408 \pm 127
MIP-209							
Poz-33261	62	aquatic and terrestrial mosses	0.6	2460 \pm 70	2451-2544	2355-2718	2537 \pm 182
Poz-33262	90	aquatic and terrestrial mosses	0.6	2330\pm60	2307-2461	2290-2500	2359 \pm 105
Poz-33254	114	mainly aquatic mosses	0.86	4670 \pm 50	5344-5423	5306-5483	5395 \pm 89
Poz-33255	142	mainly aquatic mosses	0.8	5490 \pm 60	6267-6322	6182-6408	6295 \pm 113
Poz-32835	160-161	bulk-sediment	0.44	4170 \pm 50	4641-4762	4568-4839	4704 \pm 136
Poz-32836	161-162	aquatic and terrestrial mosses	0.59	4900 \pm 60	5588-5663	5577-5750	5664 \pm 87
Poz-33256	172	aquatic and terrestrial mosses	0.85	3790 \pm 50	4088-4243	4067-4299	4183 \pm 116
Poz-33257	186	mainly aquatic mosses	0.45	3560 \pm 70	3818-3929	3685-4000	3843 \pm 158
Poz-33259	193	aquatic and terrestrial mosses	0.55	3230 \pm 60	3381-3485	3346-3588	3467 \pm 121
Poz-33260	198	aquatic and terrestrial mosses	0.55	3790\pm70	4082-4290	4058-4408	4233 \pm 175

Of the eleven performed radiocarbon dates, the one in MIP-109 (198-199 cm, 4405 \pm 130 cal. years BP), and two in MIP-209 (90 cm, 2360 \pm 105 cal. years BP; and 198 cm, 4235 \pm 175 cal. years BP) are assumed to be reliable.

From the remaining, four are inverted (MIP-209: 114 cm, 142 cm, 160-161 cm, 161-162 cm), which is interpreted as being the results of erosion and resedimentation of terrestrial plant material from the lake surroundings during river flood events (cp. Bakke et al. 2005c); hence these dates are seen as not reliable. Another radiocarbon date of MIP-209 (62 cm) is, based on

the core sediment interpretations (cp. Chapter 3.9), taken from sediment which is assigned to have been deposited during a river flood event as well, and therefore rejected. The remaining three radiocarbon dates (MIP-209: 172 cm, 186 cm, 193 cm) are, based on the core sediment interpretations (cp. Chapter 3.9), interpreted as containing plant material deposited through gravitational processes, which, besides river floods, are important mass movement and re-deposition agents with respect to sedimentation in proglacial lakes (Benn and Evans 1998); therefore these dates are not assumed to be reliable either.

Lead dating was performed on core MIP-209; 18 samples at depths between 7 cm and 50 cm were analyzed for the activity of ^{210}Pb , ^{226}Ra and ^{137}Cs via gamma spectrometry at the Gamma Dating Center, Institute of Geography, University of Copenhagen (see Table 10).

Table 10 Lead dating results of core MIP-209

Original core depth (cm)	Corrected core depth (cm)	Age (years)	Error age (years)	Date (years)
	0.0			2009
	3.6	2	1	2007
	7.2	4	1	2005
	10.8	7	1	2002
	14.4	8	1	2001
	18.0	10	1	1999
	21.6	12	1	1997
	25.2	14	1	1995
7	29.3	15	1	1994
7	29.8	16	1	1993
9	31.8	17	1	1992
11	33.8	18	1	1991
13	35.8	20	1	1989
15	37.8	21	1	1988
18	40.0	22	1	1987
20	42.0	23	1	1986
22	44.0	24	1	1985
24	46.0	25	1	1984
26	48.0	26	1	1983
28	50.0	28	1	1981
30	52.0	29	1	1980
32	54.0	31	1	1978
35	57.0	33	1	1976
40	62.0	36	1	1973
45	67.0	39	1	1970
50	72.0	42	1	1967

The measurements were carried out on a Canberra low-background Ge-well detector. ^{210}Pb was measured via its gamma ray emissions-peak at 46.5 keV, ^{226}Ra via the granddaughter isotope ^{214}Pb , with peaks at 295keV and 352 keV, and ^{137}Cs via its peak at 661 keV.

MIP-209 shows surface contents of ^{210}Pb of around 250 Bq kg^{-1} , of this around 110 Bq kg^{-1} was supported and 140 Bq kg^{-1} was unsupported ^{210}Pb . A very weak decrease with depth was observed.

^{137}Cs showed a peak around 20 cm depth (original core depth), which is ascribed to the Chernobyl-accident in 1986. Based on this peak and using a combined CRS- and CIC-model (Appleby 2001), a chronology could be established for MIP-209, shown in Figure 3.14 and Figure 3.16. The original depths had to be corrected by 22 cm, which is ascribed to loss of material at the core top during the coring process (Thorbjørn Andersen and Jostein Bakke, personal communication, 2010; cp. Appendix 2 (CD)). All lead dates are assumed to be reliable.

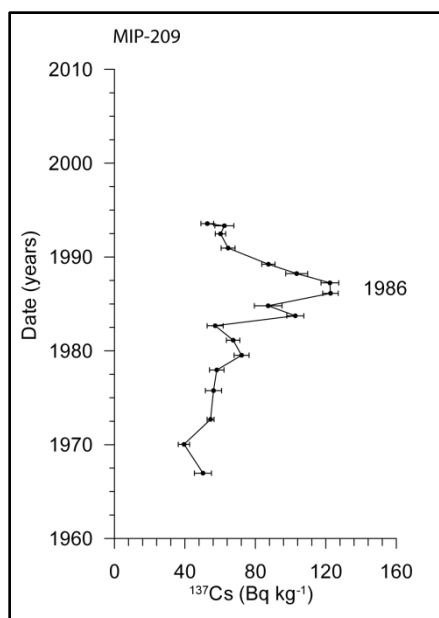


Figure 3.14 ^{137}Cs chronology of core MIP-209 with corrected core depth. The Chernobyl peak in 1986 is clearly observable.

All laboratory reports are attached in Appendix 2 (CD), as are the LOI_{950} values. Figure 3.11 and Figure 3.12 show where the dates were taken out from the sediment, reliable ones are marked red.

3.11.1 Age-depth models

The datings performed on the cores MIP-109 and MIP-209 bring up known ages of certain pointlike (one cm) levels of the core depths. To enable comparisons and correlations among one another and with other cores, and to get information about past sedimentation rates, it is essential to obtain sufficient control about the age of all core depths, not only at certain points

(Bakke 2004). Age-depth modelling is a complicated task on sediment cores of a proglacial lake, where sedimentation rates are irregular due to frequently varying meltwater inflow and sporadic episodic events such as river floods and gravitational processes (Bakke 2004). One common approach to receive an age-depth model is the use of linear interpolation between the known levels of core depth in the investigated core (Bennett 1994). To reflected the glacial record only, it is very important that sediments deposited through episodic events, such as river floods and gravitational processes, are identified and excluded from the age-depth modelling and reconstruction of the sedimentation rate, because such events can cause sediment layers as thick as normally deposited during several years of continuous glacial sedimentation, and hence would falsify the results (Karlén 1981; Hicks et al. 1990; Bakke 2004).

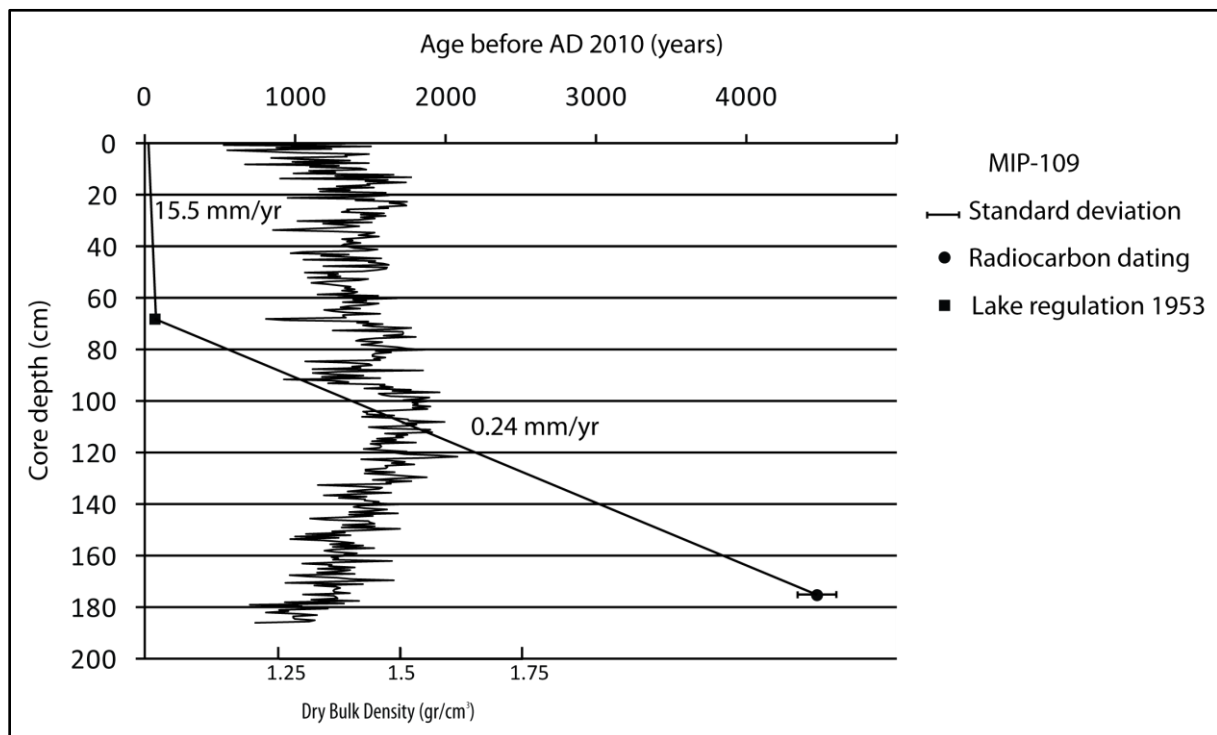


Figure 3.15 Age-depth model of core MIP-109, based on one radiocarbon date (4405 ± 130 cal. years BP) and the interpreted date of the beginning of the lake regulation in 1953. DBD values and calculated sedimentation rates are illustrated as well. A sediment loss of ca. 20 cm at the top of the core is assumed, transferred from lead dating results of core MIP-209. Episodic events are excluded before creating the model, calculating the sedimentation rates, and as well from the DBD graph.

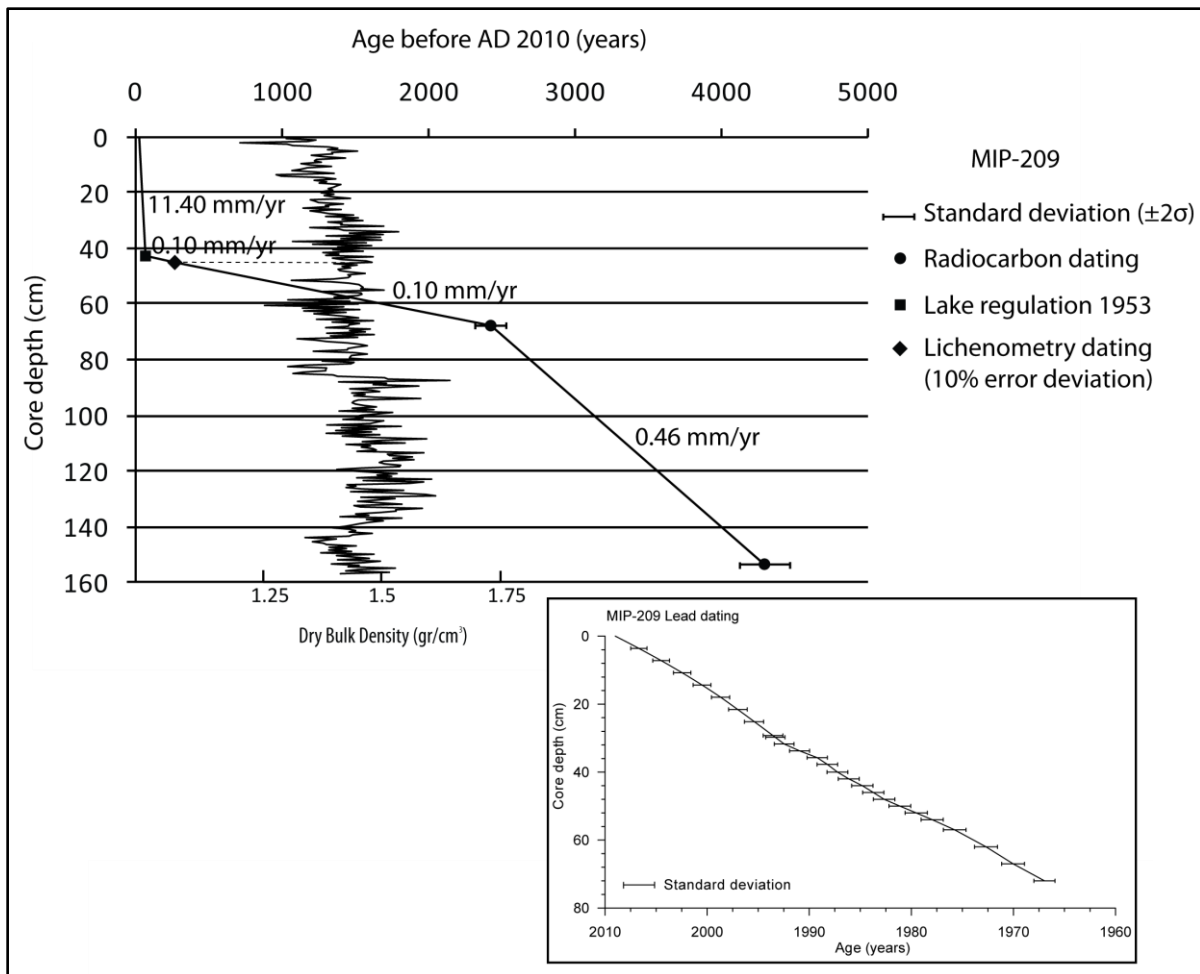


Figure 3.16 Age-depth model of core MIP-209, based on two radiocarbon dates (2360 ± 105 and 4235 ± 175 cal. years BP), one lichenometric dating of marginal moraines originated from the interpreted maximum glacier advance during the LIA (AD 1735 ± 25 ; dashed line indicates correlation to DBD) and the interpreted date of the beginning of the lake regulation in 1953. DBD values and calculated sedimentation rates are illustrated as well. A sediment loss of 22 cm at the top of the core is assumed, based on lead dating results. Episodic events are excluded before creating the model, calculating the sedimentation rates, and as well from the DBD graph. The lower figure shows the age-depth model of the upper part of MIP-209, based on 18 lead dates (2009 to 1967); core depth was corrected for a 22cm loss at the core top.

For MIP-109, an age-depth model was created based on one radiocarbon date (4405 cal. yr. BP) and the interpreted date of the beginning of the lake regulation in AD 1953. For MIP-209, an age-depth model was created based on two radiocarbon dates (2360 and 4235 cal. yr. BP, 2σ standard deviation), one lichenometric dating of marginal moraines originated during the LIA in AD 1735 (10% error deviation) and the interpreted date of the beginning of the lake regulation in AD 1953. Furthermore, an age-depth model was created for the upper part of MIP-209, based on 18 lead dates (2009 to 1967).

Age-depth models created through linear interpolation typically exhibit abrupt changes in accumulation rates around the dated levels. Due to the fact that dates often are performed at levels where other sediment parameters show changes, this feature may be caused by real changes in lithology and hence also in the sedimentation rate; but in general linear interpolation can overestimate the real accumulation rate (Bakke 2004).

The more levels of known age are used for modelling, the more accurate is the resulting age-depth model. The less dates, the greater the probability that an age-depth model does not provide a good fit to reality, and that calculated confidence intervals are over-optimistic (Telford et al. 2004).

Due to the small number of points of known age in both MIP-109 and MIP-209, the created age-depth models, especially the one of MIP-109, are assumed as to be imprecise.

3.11.2 Sedimentation rates

Sedimentation rates in proglacial lakes reflect both sediment availability and meltwater stream capacity, which in turn are controlled by numerous factors (Leonard 1985). Glacial activity in the drainage basin has huge impact on the sedimentation rates of a proglacial lake; increased ice extent causes relatively higher sedimentation rates, while low sedimentation rates mainly occur during periods of reduced ice extent (Leonard 1986b). To reflect the glacial record only, it is required that sediments deposited through episodic events, such as river floods and gravitational processes, are identified and excluded from the reconstruction of the sedimentation rate (Karlén 1981; Hicks et al. 1990; Bakke 2004).

MIP-109 is dated to an age of 4400 years BP 11 cm from the bottom of the core. MIP-209 is dated to an age of 4235 years BP 2.5 cm from the bottom of the core.

The sedimentation rates of MIP-209 and MIP-109 indicate a much higher sedimentation rate in the upper fourth of the core than in the rest of it. This is ascribed to the regulation of Lake Midtbotnvatn in the course of the development of hydrologic power since AD 1953, which resulted in an enhanced capacity of river Blådalselv and an enlarged Lake Midtbotnvatn, which enables more amounts of suspended particles to settle (cp. Ashley 1995).

MIP-109 and MIP-209 have comparatively high mean sedimentation rates, MIP-109 0.25 mm/yr before and 15.5 mm/yr after the regulation of Lake Midtbotnvatn, MIP-209 0.25 mm/yr before and 11.4 mm/yr after the lake regulation. The differences for the sedimentation rates after regulation may be caused from an overestimation of the sediment loss of the top of MIP-109; assuming no sediment loss of MIP-109 would give a sedimentation rate of 12

mm/yr since the beginning of the lake regulation. The comparatively high mean sedimentation rates of both cores are attributed to the huge size and the accordingly strong impact of the glacier tongue Vestre Blomsterskardsbreen on the sedimentation in Lake Midtbotnvatn.

The small number of dates in MIP-109 and MIP-209 limits the construction of age-depth models and the calculation of sedimentation rates, causing uncertainties and generalisations. Since being based on more dates through several different dating techniques, MIP-209 is assumed to give the more reliable results of the sedimentation rates and the age-depth models (see Figure 3.15 and Figure 3.16).

A higher sedimentation rate of 0.46 mm/yr in the lowest part of MIP-209 and a lower one of 0.1 mm/yr in the upper part before lake regulation is interpreted as to be in agreement with DBD values; increased DBD values are interpreted as to indicate increased glacial activity in the second part of MIP-209, and comparably lower DBD values reflect decreased glacial activity in the first core half. Linking the sedimentation rate to variations in DBD and thus glacial activity hence indicates that higher sedimentation rates coincidence with increased glacial activity.

Due to the facts that dates are few in both MIP-109 and MIP-209, and that both cores are disturbed to certain degrees, the created age-depth models and the calculated sedimentation rates must be seen as an inaccurate approximation; more reliable dates and less disturbed sediment cores would improve the results.

3.12 Summary

Proglacial lake sediments contain information about past glacial activity in their drainage basin. Several analysis parameters were used on two proglacial cores of Lake Midtbotnvatn. Increased values of DBD, detrital XRF elements Ti, Si, Rb, and very coarse silt, combined with decreased amounts of very fine silt, are interpreted as to reflect increased glacial activity. Anomalies in the grain size parameters “mean” and “sorting”, and the XRF ratios Fe/Ti and inc/coh, can be used to identify sediment originated from episodic events such as river floods and gravitational processes. To receive the glacial record only, such sediments must be excluded. Episodic events could be observed in both cores.

Analysis and interpretation of the proglacial sediments were complicated by the fact that the sediments were disturbed through coring.

Based on three reliable radiocarbon dates, 18 lead dates, one lichenometric date of marginal moraines correlated to DBD values, and the date of the interpreted beginning of the regulations of Lake Midtbotnvatn, age-depth models could be created and sedimentation rates reconstructed for each of the cores.

MIP-109 is dated to an age of 4400 years BP 11 cm from the bottom of the core; MIP-209 is dated to an age of 4235 years BP 2.5 cm from the bottom of the core. MIP-209 is interpreted to have a sediment loss of 22 cm at the top of the core. Both cores have comparatively high mean sedimentations rates, MIP-109 0.25 mm/yr before and 15.5 mm/yr after the regulation of Lake Midtbotnvatn, MIP-209 0.25 mm/yr before and 11.4 mm/yr after the lake regulation.

Lake Midtbotnvatn is an adequate location for proglacial sediment studies with the goal of reconstructing glacier fluctuations at Vestre Blomsterskardsbreen. The catchment area of Lake Midtbotnvatn is characterized by little superficial deposits and robust bedrock, which indicates that the paraglacial impact on the lake sedimentation is limited, as are rapid mass-movement processes. Lake Midtbotnvatn is the first proglacial lake Vestre Blomsterskardsbreen drains into; the glacier tongue covers a great part of the drainage basin. This results in a comparatively high sedimentation rate in Lake Midtbotnvatn.

The lake regulations since the early 1950s have negative impact on the analyses, causing a strong increase in sedimentation rate and altering the glacial record of the proglacial sediments during the second half of the 20th century.

4 Calculation and reconstruction of palaeoclimate: equilibrium line altitudes and relative glacial activity

This chapter contains the theoretical description of the reconstruction of equilibrium line altitudes (ELAs). Former ELAs of Vestre Blomsterskardsbreen are calculated using the presented approaches, and combined with sediment analysis parameters used to create a curve of relative glacial activity for the last 4235 cal. years BP.

4.1 Equilibrium Line Altitudes –Theory

The equilibrium line of a glacier marks the boundary between the accumulation area and the ablation area, where accordingly the net mass balance equals zero (Porter 1975; Paterson 1994). Since the elevation of the equilibrium line generally varies across the glacier due to local variations in accumulation and ablation, the ELA is defined as the average altitude of the equilibrium line (Benn and Lehmkuhl 2000, 16). The net mass balance of a glacier is the mass balance at the end of the balance year, which can be divided into positive winter balance and negative summer balance (Paterson 1994, 28). A balance year is subdivided into the ablation season (1 May – 30 September), where changes in summer air temperature are decisive, and the accumulation season (1 October – 30 April), determined by variations in winter precipitation (Paterson 1994; Dahl et al. 2003). Variations of the ELA reflect changes in the mass balance of a glacier, which in turn are caused by climate fluctuations (Porter 1975).

Both the glacier net balance and the ELA of a glacier mainly change with variations in the regional distribution of the primary climatic parameters ablation-season temperature and accumulation-season precipitation. Folgefonna, in its capacity as a maritime plateau glacier, is in existence and size mainly influenced by winter precipitation, and only to a smaller extent by summer temperature (Bakke et al. 2005c). Nesje et al. (2000b) emphasize that since the middle of the 19th century, a strong correlation has been existing between the North Atlantic Oscillation (NAO) index, winter precipitation values of the north-east Atlantic region and western Norway, and mass balance changes of maritime glaciers in southern Norway.

Further important factors that cause fluctuations in glacier net balance and ELA are local ones such as hypsometry of a glacier, topographic shading, preferential snow accumulation, avalanching, and extent of supraglacial debris cover (Benn and Gemmell 1997; Benn and Lehmkuhl 2000). Local redistribution of dry snow by wind blowing away snow from exposed surfaces to leeward topographic depressions also influences the ELA of a glacier (Dahl et al.

1997; Dahl et al. 2003). The impact of this factor depends on the glacier type, it is very important on cirque glaciers and single glacier tongues, and can be neglected on whole plateau glaciers and ice caps with glacier outlets in all aspects, where windblown snow is transported from the windward to the leeward side, accumulating again on the glacier itself and thus not influencing the mean ELA (Dahl et al. 2003) For this reason, there is a need to differentiate between the local topographic temperature-precipitation-wind ELA (TPW-ELA) of cirque glaciers and single glacier tongues and the regional temperature-precipitation-ELA (TP-ELA) of plateau glaciers and ice caps (cp. Figure 4.1) (Nesje and Dahl 2000, 58; Dahl et al. 2003, 279). Vestre Blomsterskardsbreen is a southern glacier outlet of southern Folgefonna; reconstructed ELAs will therefore be expressed as TPW-ELAs.

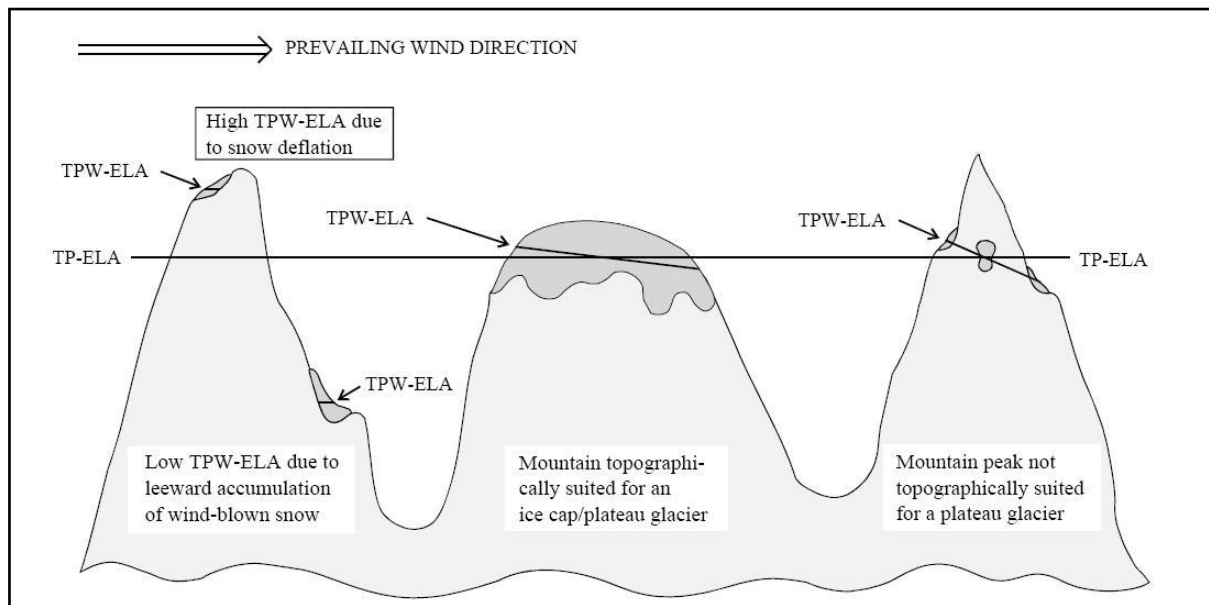


Figure 4.1 Idealized schematic overview of the differences in altitude between the regional TP-ELA of a plateau glacier and the TPW-ELAs at cirque glaciers depending on local topography (Dahl et al. 2003, 279)

The ice of a temperate glacier is at the pressure melting point throughout, except for a surface layer of several meters which is subject to seasonal temperature variations (Paterson 1994). Glacier ice being at or close to the melting point is a basic requirement for efficient glacier motion, and with that also the processes of subglacial erosion, transport and deposition sensitively depend on temperature (Benn and Evans 1998). Material transport within a glacier can take place subglacially, englacially and supraglacially (Nesje 1995). The maximum flow velocity of glacier ice, the maximum turnover of ice, and accordingly the maximum erosion related to rotational movement occur at or close to the ELA (Dahl et al. 2003). Flowlines of

glacier ice within an idealized glacier run inwards and down above the ELA (accumulation area), and outwards and up below the ELA (ablation area) (Dahl et al. 2003). (cp. Figure 4.2).

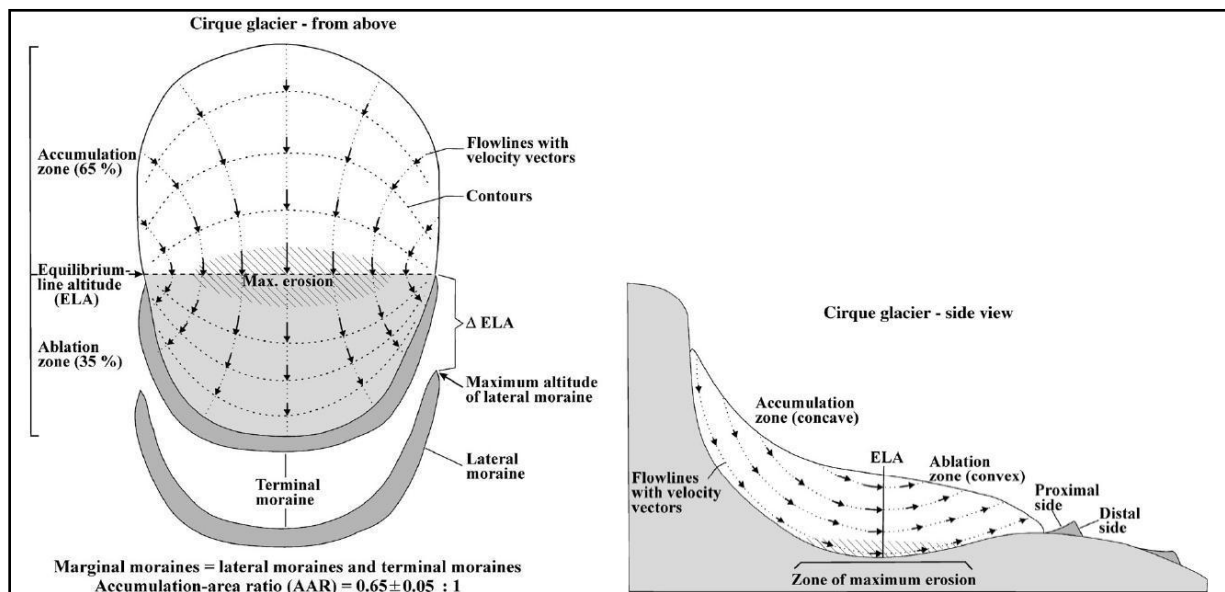


Figure 4.2 Flow lines and contours on an idealized cirque glacier seen from above and side view. Due to the fact that lateral moraines normally do not form above the steady-state ELA, they can be used to estimate former ELAs (Dahl et al. 2003, 281)

This is the reason why lateral moraines normally do not form above the steady-state ELA, and therefore their maximum elevation can be used to estimate former steady-state ELAs (Nesje and Dahl 2000; Dahl et al. 2003). Dating these moraines, for example by lichenometry, the size of the corresponding glacier at a particular time can be evaluated and via that former ELAs can be reconstructed, (Karlén 1976; Benn and Gemell 1997; Bakke et al. 2005c). At sites where for some time periods no adequate moraines can be found, or when dates are not reliable, analyzes of proglacial sediments from a proglacial lake in the catchment can be used to reconstruct former ELAs. Applying a combination of analyzes of proglacial sediments and dated moraines, continuous reconstructions of past varying glacier sizes and former ELAs can be obtained (Karlén 1976; Bakke et al. 2005c).

A limiting factor on the reconstruction of palaeoclimate via ELAs is that glaciers do react on climate changes with a delay depending on different factors.

Different methods can be applied to define the modern steady-state ELA of present glaciers and to reconstruct former steady-state ELAs, as a means to reconstruct palaeoclimates of present and past glaciated regions; these include the maximum elevation of lateral moraines (MELM), the median elevation of glaciers (MEG), the toe-to-headwall ratio (THAR), the

accumulation area ratio (AAR), and the area altitude balance ratio (AABR) (Benn and Gemmell 1997; Nesje and Dahl 2000, 59, and references therein; Dahl et al. 2003). Each method is a different approach to define ELAs; with respect to the local conditions of each study area and especially the adjacent glaciers existing in past/present, it therefore must be carefully evaluated which approach is the most appropriate one to apply (cp. Nesje and Dahl 2000). The methods adopted in this work are theoretically explained in the following.

4.1.1 Accumulation Area Ratio (AAR)

The Accumulation Area Ratio (AAR) is the ratio of the accumulation area, i.e. the area above the ELA, to the total area of a glacier (Porter 1975; Torsnes et al. 1993); based on the assumption that the former occupies a fixed proportion of the latter (Benn and Gemmell 1997).

For present glaciers in mid- and high-latitudes, steady-state AARs generally are in the range 0.5 to 0.8 (Porter 1975; Benn and Gemmell 1997). For valley glaciers and cirque glaciers under dynamic and climatic steady-state conditions, the AAR lies at 0.65 ± 0.05 (Nesje 1995; Nesje and Dahl 2000).

Generally, the AAR of a glacier varies as a function of its mass balance; values below 0.5 indicate a negative mass balance, values between 0.5 and 0.8 reflect climatic equilibrium or close to, and values above 0.8 indicate a positive mass balance (Nesje 1995, 35).

A limitation for the AAR method is the impact of the slope of the underlying surface of present and past glaciers. A steep slope can cause an overestimation of the changes in ELA, while a flat topography might lead to underestimation. The surface topography below a glacier should therefore be carefully evaluated when applying this method (Nesje 1995; Nesje and Dahl 2000). An advantage of this approach is that the glacier reconstruction is only required up to the elevation of the former ELA (Nesje and Dahl 2000).

4.1.2 Area Altitude Balance Ratio (AABR)

Unlike the AAR method, the Area Altitude Balance Ratio (AABR) takes account of the hypsometry of a glacier, which is the “detailed distribution of surface area with respect to altitude” (Osmaston 2005, 22) and the shape of the mass balance curve (Nesje and Dahl 2000). This method is based on the assumption that parts of a glacier which are far above or below the ELA have greater negative or positive spot net balances and therefore have wider influence on the total net balance and the ELA of the glacier, than parts located closer to the ELA (Osmaston 2005). Hence, detailed knowledge of the position of the glacier margin and contour data of its surface are required to be able to determine the area and mean altitude of

successive contour belts of the glaciers' surface (Osmaston 2005, 22). With respect to reconstructions of past glaciers' ELAs, these variables may accordingly cause uncertainties; though this approach is still more accurate than other morphometric methods not taking into account the hypsometry of a glacier (Benn and Lehmkuhl 2000; Osmaston 2005).

Furbish and Andrews (1984) successfully tested the operation of the AABR method, terming it the BR method, and concluded that it gave good ELA estimates of ten present valley glaciers located in geographic maritime and semi-maritime settings in Alaska, with a mean BR value of 2.01. Based on the assumption that, for glaciers in equilibrium conditions, the total annual accumulation above the ELA must balance the total annual ablation below the ELA, they multiplied the areas above and below the ELA by the average accumulation and ablation, respectively (Benn and Evans 1998, 84; Nesje and Dahl 2000, 61).

4.2 Reconstructions of former ELAs

During the past decades, several attempts were made to calculate the ELA of Vestre Blomsterskardsbreen. In 1970, the ELA of Blomsterskardsbreen was calculated to be at an elevation of 1370 m a.s.l. (Tvede and Liestøl 1977, 226). Stakes to measure snow ablation and soundings to record snow accumulation were the basis for this calculation. According to the “*Atlas of Glaciers in South Norway*”, in 1988, Vestre Blomsterskardsbreen had an ELA of 1180 m a.s.l. (Østrem et al. 1988, 39). Calculated volume changes of the southern glacier outlets of southern Folgefonna based on aerial photographs, Smith-Meyer and Tvede (1996) concluded that Vestre Blomsterskardsbreen retreated during the time period from 1959 to 1995, while Østre Blomsterskardsbreen slightly advanced. Based on core samples, measured and estimated snow densities, and snow accumulation and ablation measurements at stakes and soundings on the glacier tongue, summer, winter and net mass balances of the year 2008 at Vestre Blomsterskardsbreen were calculated. According to these calculations, the ELA of Vestre Blomsterkardsbreen lay at 1235 m a.s.l. in 2008, the AAR of the glacier tongue was 74%. The ELA of Østre Blomsterskardsbreen was assumed to lie slightly higher at 1265 m a.s.l., with an AAR of 85% (Kjøllmoen 2009, 28). An aerial photograph taken of Jan Rabben in mid-October 2005 indicates that the snow line of Blomsterskardsbreen was located at around 1300 m-1320 m at that time, which is considered quite close to the ELA of that year (see Picture 8). The differences in the calculated ELAs presented above are mainly attributed to different methods, methodological uncertainties, and variations in topography and the manually defined drainage basin of Vestre Blomsterskardsbreen, which may have been

different in the past (considered as a minor influencing factor) and within different attempts; complicated moreover by the fact that Blomsterskardsbreen is a divided glacier outlet.



Picture 8 Aerial photograph of Østre and Vestre Blomsterskardsbreen taken in mid-October 2005; snow line is located at around 1300-1320 m. (Picture: Jan Rabben)

In this study, the TPW-ELAs of Vestre Blomsterskardsbreen of today (2007), of AD 1986, of AD 1959, of the maximum glacier advance during the LIA, and of the glacier advances that deposited the marginal moraines M-20/M-21 and M-22 are calculated using the AAR and AABR method. The calculations of present and past ELAs are based on digital map data N-50 of Norway (Norwegian Mapping Authority) used in ArcGIS 9.0, digital contour intervals from laserscanning in 2007 as well as digital contour intervals of southern Folgefonna from 1959 (Sylvia Smith-Meyer, NVE, personal communication, 2010), and mapped marginal moraines dated by lichenometry (M-1, M-2, M-4, M-19, M-20, M-21, M-22).

Due to the fact that Vestre Blomsterskardsbreen is a glacier outlet of southern Folgefonna, it was necessary to define the area that topographically drains down to Lake Midtbotnvatn. This is done by drawing right angle lines on the contour intervals between Vestre Blomsterskardsbreen and the surrounding glacier outlets. The division follows the one in the “*Atlas of glaciers in south Norway*” (Østrem et al. 1988), see Figure 4.3.

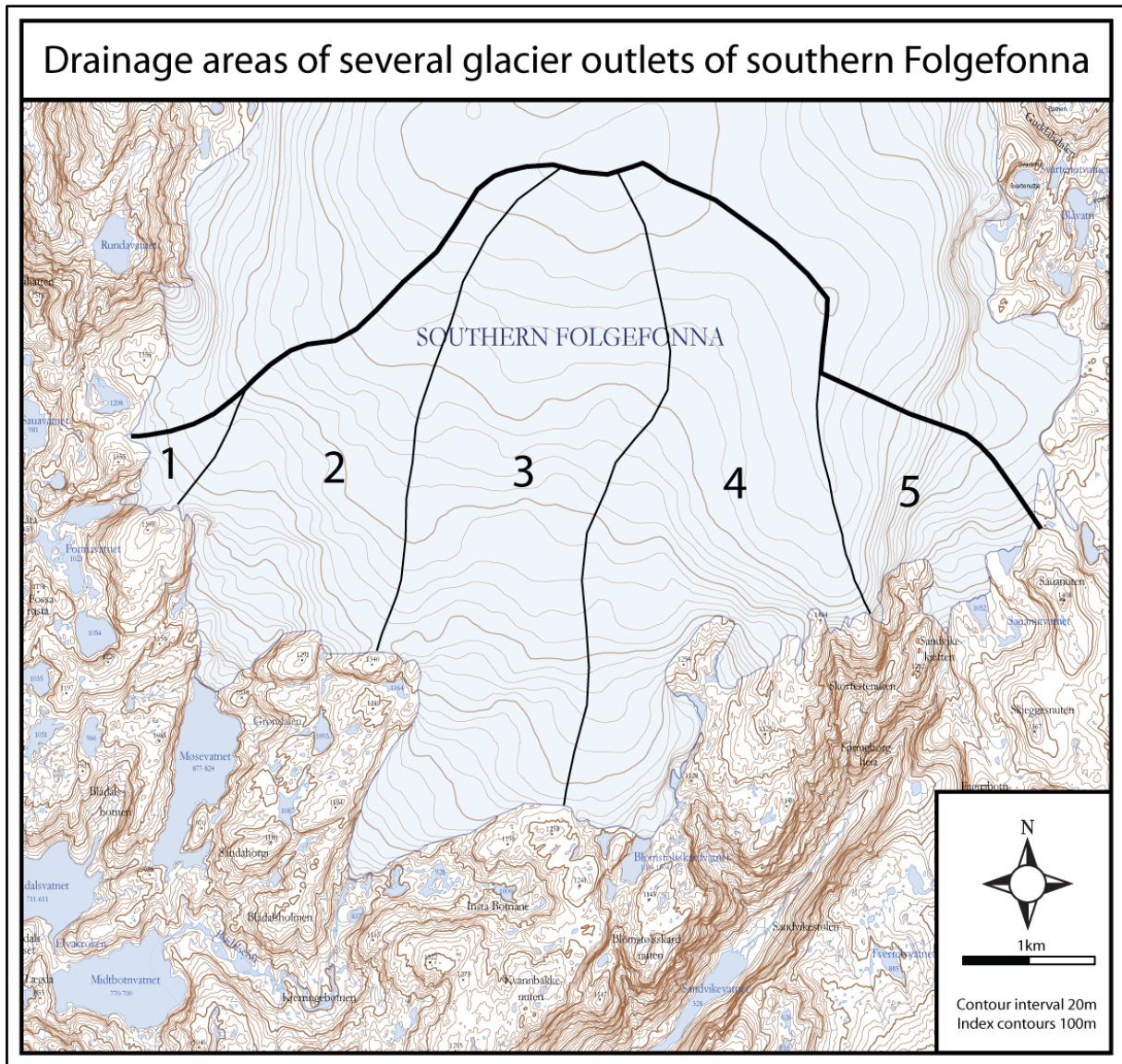


Figure 4.3 Drainage areas of several glacier outlets of southern Folgefonna; division follows the “*Atlas of glaciers in south Norway*” (Østrem et al. 1988, 38). 1= Glacier outlet draining down to Lake Fonnvatn, 2= Møsevassbreen, 3= Vestre Blomsterskardsbreen, 4= Østre Blomsterskardsbreen, 5= Sauabreen.

Areas on the glacier that are steep in reality are plotted as small areas per contour interval in the N-50 map data, which indicates that the areal distribution does not match reality in that respect. This is an error source in the reconstruction procedure; the AABR method, taking into account the hypsometry of a glacier, is in that regard assumed to be a better approach than the AAR method. It is not expected that the heights above ELA of Vestre Blomsterskardsbreen changed crucially during former advances within the time span of the reconstructions. Hence, contour intervals and area distributions above the ELA are based on the digital map data N-50 of Norway (Norwegian Mapping Authority) for all reconstructions.

4.3 Reconstructed ELAs of Vestre Blomsterskardsbreen

Past and present ELAs of Vestre Blomsterskardsbreen have been reconstructed using the AAR and AABR method (Table 11). Present and former glacier sizes of Vestre Blomsterskardsbreen were drawn in Adobe Illustrator CS3, based on older digital maps and dated marginal moraines. The areas of each of these glacier sizes were then determined in ArcGIS 9.0, including both the entire glacier size and the areas within the 100 m contour intervals. Calculations of ELAs were performed in Microsoft Excel, using special computer spreadsheets of Benn and Gemmel (1997) for the AAR method, and Osmaston (2005) for the AABR method. Reconstructed values with a balance ratio of 2.0 are considered as most reliable, since those are evaluated as to give the best results on maritime and semi-maritime glaciers (Furbish and Andrews 1984).

Figure 4.4. shows reconstructed Vestre Blomsterskardsbreen for specific times in the past: AD 2007, compared to the LIA maximum advance (based on marginal moraines M-1, M-2, M-2, M-19, all dated by lichenometry), and moreover the glacier advances that deposited moraines M-20/M-21 and M-22. Figure 4.5. shows the area distribution (hypsoetry) of Vestre Blomsterskardsbreen and the accumulative area distribution per height of Vestre Blomsterskardsbreen for the reconstructed specific times in the past: AD 2007, AD 1986, AD 1959, LIA maximum glacier advance, glacier advances that deposited M-20/M-21, and M-22. The methods AAR 0.65 and AAR 0.70 are used for the calculations.

Table 11 Reconstructed areas (km²) and ELAs (m a.s.l.) of Vestre Blomsterskardsbreen for specified times in the past, calculated using different methods, based on marginal moraines and old maps. Methods used are AAR 0.65 and 0.7 (Benn and Gemmel 1997) and AABR with a balance ratio of 1.0 and 2.0 (Osmaston 2005). ELAs calculated with a balance ratio of 2.0 are considered as the most reliable ones, the ELA lowering compared to today's ELA (2007) is based on this calculation.

Glacier	Area (km ²)	AAR 0.65	AAR 0.7	AABR 1.0	AABR 2.0	ELA lowering compared to today
Today (2007)	26.19	1378	1382	1382	1328	0 m
1986	25.98	1379	1382	1383	1328	0 m
1959	26.24	1377	1381	1382	1326	2 m
LIA max.	29.26	1362	1367	1363	1308	20 m
M-20, M-21	29.97	1352	1356	1356	1301	27 m
M-22	31.10	1333	1338	1354	1300	28 m

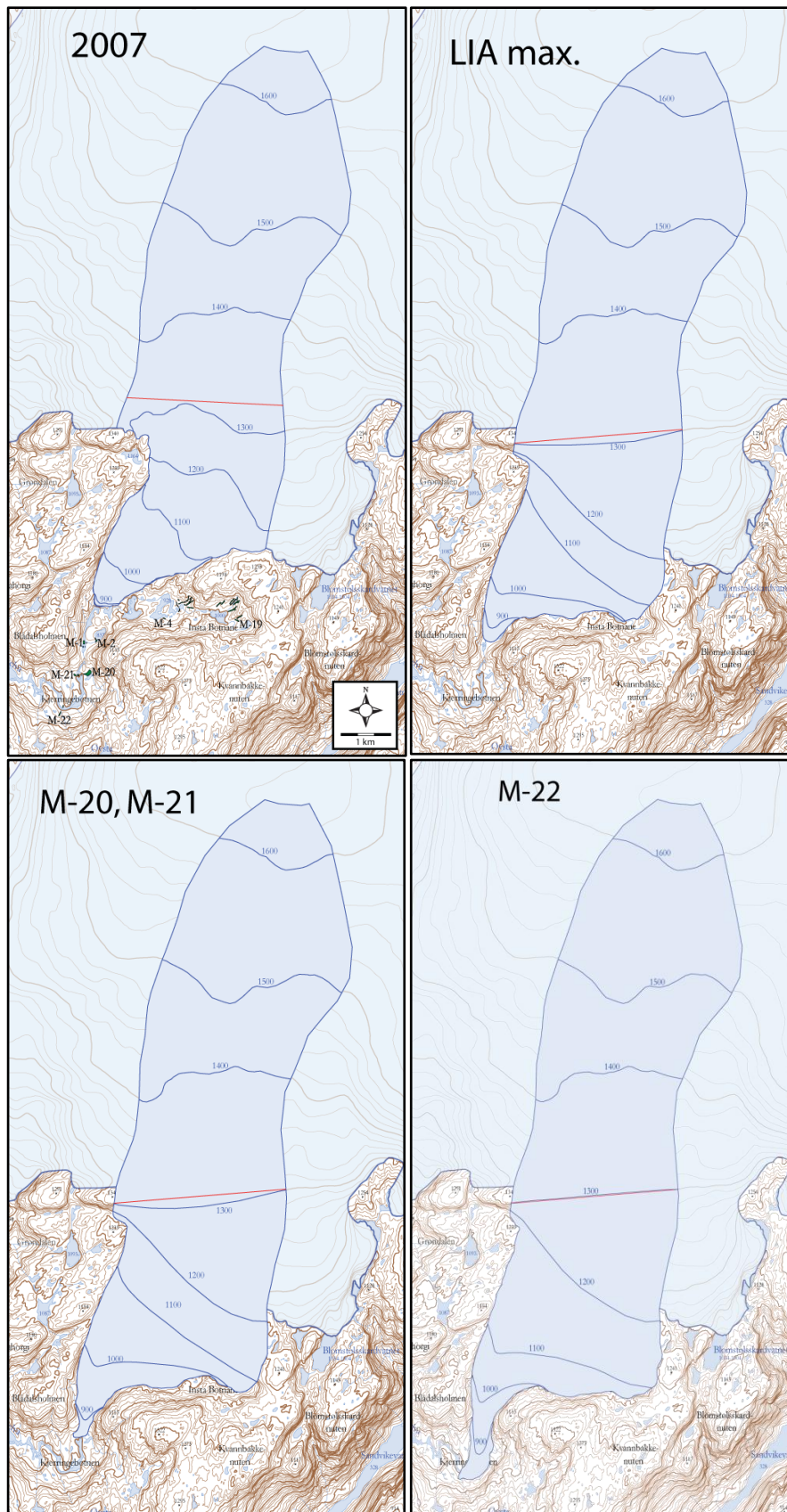


Figure 4.4 Reconstructions of Vestre Blomsterskardsbreen for specific times in the past (contour intervals 100 m; ELAs marked red): 2007 (based on digital contour intervals from laserscanning in 2007, NVE), LIA maximum advance (based on dated marginal moraines M-1, M-2, M-4, M-19), glacier advance that deposited moraines M-20 and M-21, glacier advance that deposited moraine M-22. Dated marginal moraines used for reconstructions are shown in the 2007 illustration.

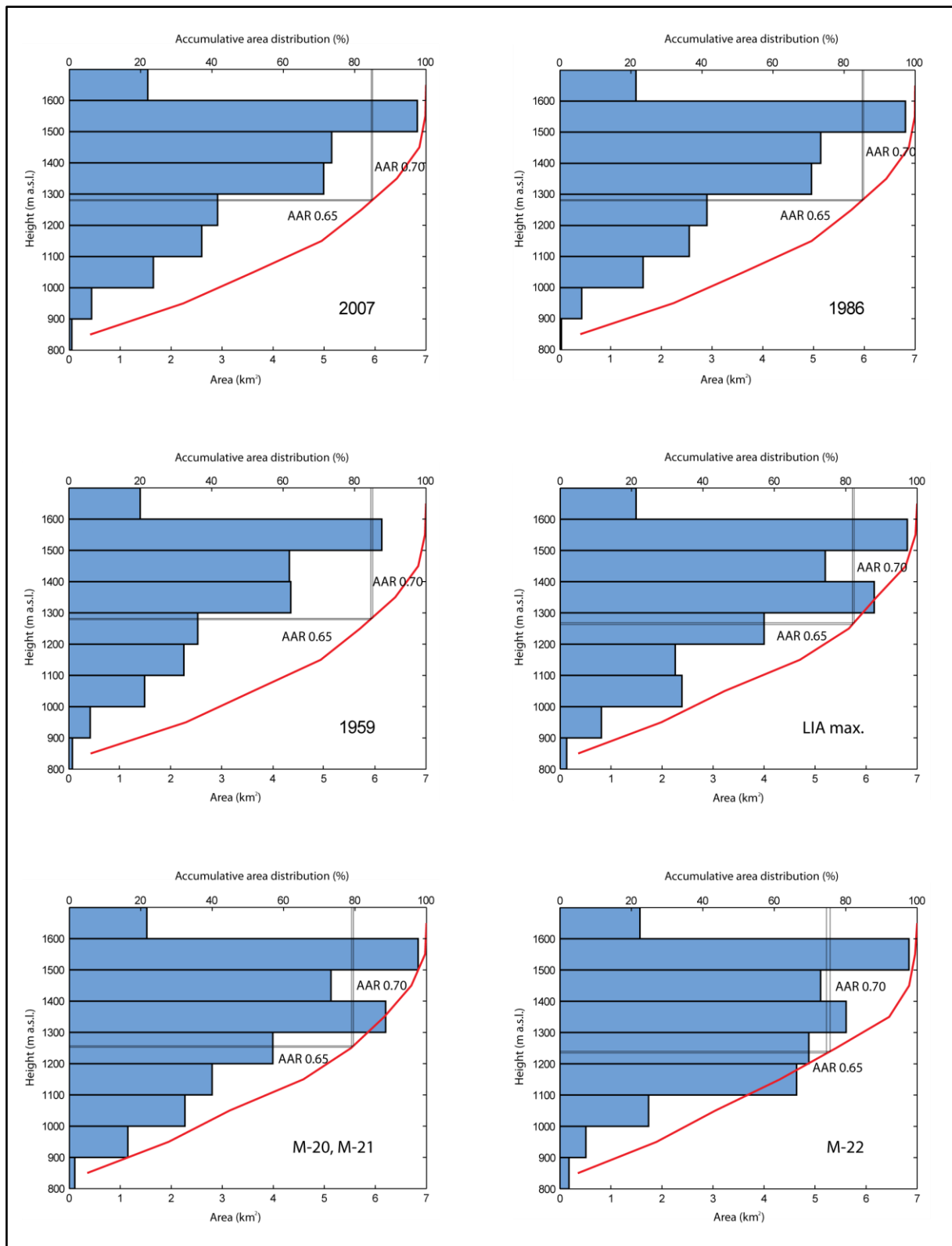


Figure 4.5 Area distribution and accumulative area distribution per 100 m contour interval of Vestre Blomsterskardsbreen for the reconstructed specific times in the past: 2007, 1986, 1959, LIA maximum glacier advance, glacier advance that deposited M-20 and M-21, glacier advance that deposited M-22. Methods AAR 0.65 and AAR 0.70 are used for the calculations (cp. Benn and Gemell 1997).

The maximum LIA glacier size and ELA of Vestre Blomsterskardsbreen was reconstructed using mapped and dated marginal moraines (M-1, M-2, M-4, M-19). Using the AABR method with a BR of 2.0 (Osmaston 2005), a lowering of 20 m compared to today's ELA (2007) could be determined. The reconstruction based on the AAR method with a BR of 0.7, in contrary, calculated an ELA lowering of 15 m. The results make it clear that there are differences in ELA reconstructions, depending on which method is used. Beside methodological uncertainties, several error sources may cause falsified area calculations and ELA results. Both the topography on the glacier and the manually defined drainage basin of the glacier may have been different during former advances, when the glacier size was unlike today's. In general, the 100 m contour intervals during reconstructed former glacier advances before AD 1959 were probably more complex than illustrated in Figure 4.4., their real positions are unknown and therefore simplified for the reconstructions. The ELAs calculated by the AABR BR 2.0 method are considered as the most reliable ones, due to the fact that this method takes the glacier's hypsometry into account (cp. Furbish and Andrews 1984).

4.4 Correction of isostatic adjustment

The melting of the ice sheet after the last ice age caused a continuous subsequent isostatic adjustment of the landmasses of Scandinavia, which is still active today, though it was most intense right after deglaciation. Thus, reconstructed ELAs have to be corrected for isostatic adjustment. This is done with help of the computer program SeaLevel Change Ver. 3.51. (Møller and Holmeslet 1998). Isobase 26 is used for the study area; Figure 4.6 and Table 12.

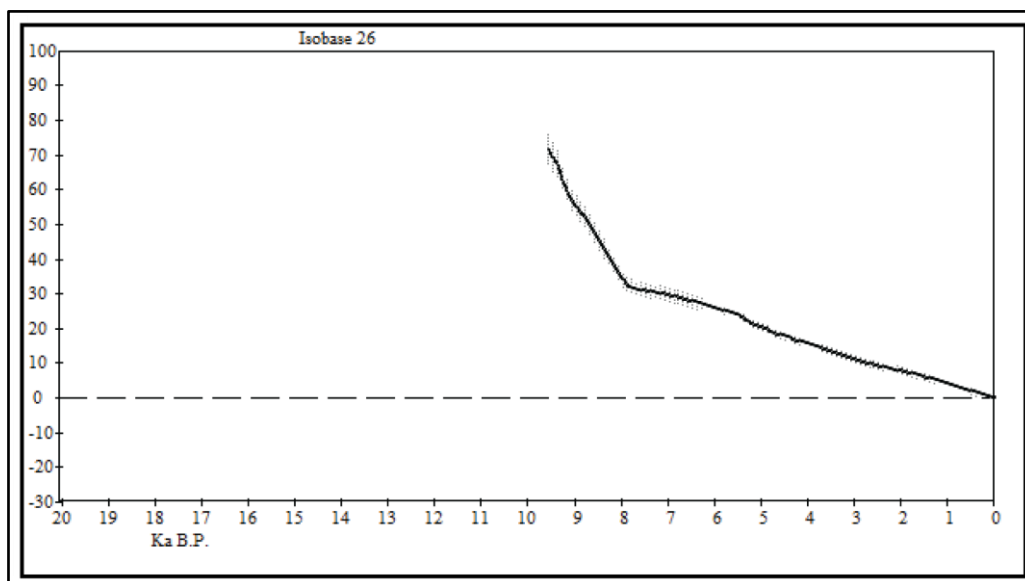


Figure 4.6 Isostatic adjustment curve for isobase 26 (Møller and Holmeslet 1998)

Table 12 Calculated ELAs corrected for isostatic adjustment; lowering of corrected ELAs compared to today. Corrections are based on isobase 26 (Møller and Holmeslet 1998).

Glacier	ELA calculated with ABBR 2.0	ELA corrected for isostatic adjustment	Lowering of corrected ELA compared to today
2007	1328	1328	0 m
1986	1328	1328	0 m
1959	1326	~1325.5	2.5 m
LIA max.	1308	~1306	22 m
M-20, M-21	1301	?	?
M-22	1300	?	?

The lowering of the ELA during the maximum LIA advance compared to 2007 was comparatively small (22 m, corrected for isostatic adjustment), as were the differences of the ELAs of the glacier advances that deposited the moraines M-20/M-21 and M-22 compared to the LIA maximum advance (cp. Table 11). The isostatic adjustment of the ELAs could not be performed for the M-20/M-21 and M-22 advances, because these moraine sets could not be dated. It is assumed, that the isostatic adjustment for both sets must be more than for the LIA, due to the fact that they are older; the influence of the isostatic adjustment is increasing with the age of reconstructed ELAs. Accordingly, the ELAs of the glacier advances that deposited M-20/M-21 and M-22 are assumed to be lower than calculated in Table 11; hence, the differences in ELA compared to the maximum LIA glacier advance must have been greater. A discussion about the deposition times of M-20/M-21 and M-22 is presented in Chapter 5.

Vestre Blomsterskardsbreen is a huge glacier outlet, which, after passing the area of Insta Botnane, flows down a comparably narrow valley. This can help to explain why the ELA differences between 2007 and the LIA maximum advance are much larger than the one between the LIA maximum advance and the ELAs reconstructed from the moraine sets of M-20/ M-21 and M-22, because a narrow valley enables greater advances of a glacier's terminus with contemporaneously comparably smaller ELA lowering. Ice thickness measurements below the glacier tongue in 1997 indicate that the bottom topography below Vestre Blomsterskardsbreen goes downwards from the glacier's terminus inwards (Elvehøy 1997). This terrain characteristic, and the existence of the high mountain area north-east of Insta Botnane may be reasons for the comparably small ELA lowering during the LIA of Vestre Blomsterskardsbreen compared to other glacial sites in Norway, such as several outlets of southern and northern Folgefonna, Jostedalbreen and Hardangerjøkulen, which had

lowerings of 100-150m (cp. Chapter 5) (Nesje and Dahl 1991a; Torsnes et al. 1993; Dahl and Nesje 1994; Bakke et al. 2005a; Bakke et al. 2005c; Bjønnes 2006; Tolo 2008).

4.5 Reconstruction of a relative glacial activity curve

Marginal moraines in front of Vestre Blomsterskardsbreen dated by lichenometry can be used to achieve knowledge about the sizes of the glacier outlet and its ELAs during specific times in the past when the glacier advanced. Combining sediment parameter records (of mainly LOI, DBD, grain size distribution) and independent dates of the proglacial sediment by radiocarbon dating with a sufficient number of reconstructed ELAs of known time points in the glacier's history, a continuous ELA curve for the glacier tongue could be reconstructed using a logarithmic regression equation (cp. Bakke et al. 2005c). Furthermore, based on the non-linear (exponential) relationship between ablation-season temperature and mean winter precipitation at the ELA, it would be possible to calculate past winter precipitation values, assumed that the ELA is known and in addition by the use of an independent proxy for summer temperature (cp. Liestøl in Sissons 1979; Sutherland 1984; Ballantyne 1989; Dahl and Nesje 1996; Dahl et al. 1997). In front of Vestre Blomsterskardsbreen only one moraine set could be dated to represent a certain specific glacier advance in the past: the maximum glacier advance during the LIA around AD 1735 \pm 10%. This is not sufficient to reconstruct a continuous ELA curve and past winter precipitation for Vestre Blomsterskardsbreen, which would require at least two reference points, ideally even more.

Due to the fact that the validity of the sediment parameter LOI in this study is limited due to a too low organic component and high minerogenic sedimentation, DBD is considered as the best parameter reflecting glacial activity of Vestre Blomsterskardsbreen during the last 4200 cal. years BP (cp. Bakke 2004; Bakke et al. 2005c). Episodic events must be isolated and excluded previously using the grain size distribution parameters "mean" and "sorting", in order to receive the glacial record only.

Based on the DBD record of MIP-209, which is the least disturbed of the two cores that were subject to investigation, combined with two radiocarbon dates in specific core depths (2360 cal. years BP and 4235 cal. years BP), and the interpreted beginning of the lake regulations in AD 1953, a relative glacial activity curve for Vestre Blomsterskardsbreen has been established, covering the past 4235 cal. years BP (Figure 4.7.). Since Lake Midtbotnvatn has been regulated since AD 1953, any conclusions on glacial activity since then and until today

(AD 2010) are not possible. Therefore, the curve starts as late as AD 1953; the glacier's extent and activity according to the DBD record of that year hence is the one past glacial activity is compared to.

Vestre Blomsterskardsbreen, with its location as the southernmost glacier outlet of southern Folgefonna, and its south-southwestern slope aspect, is considered the most maritime glacier tongue of Folgefonna. This indicates that the net mass balance of the glacier is mostly determined by the winter mass balance, which means that winter precipitation is the main controlling factor for the glacier's variations, rather than summer temperature (cp. Bakke 2004; Bakke et al. 2005c; Bjune et al. 2005; Nesje et al. 2008, see also Chapter 1). Therefore, the relative glacial activity curve of Vestre Blomsterskardsbreen (Figure 4.7.) is assumed to also be an indicator of past fluctuations of winter precipitation.

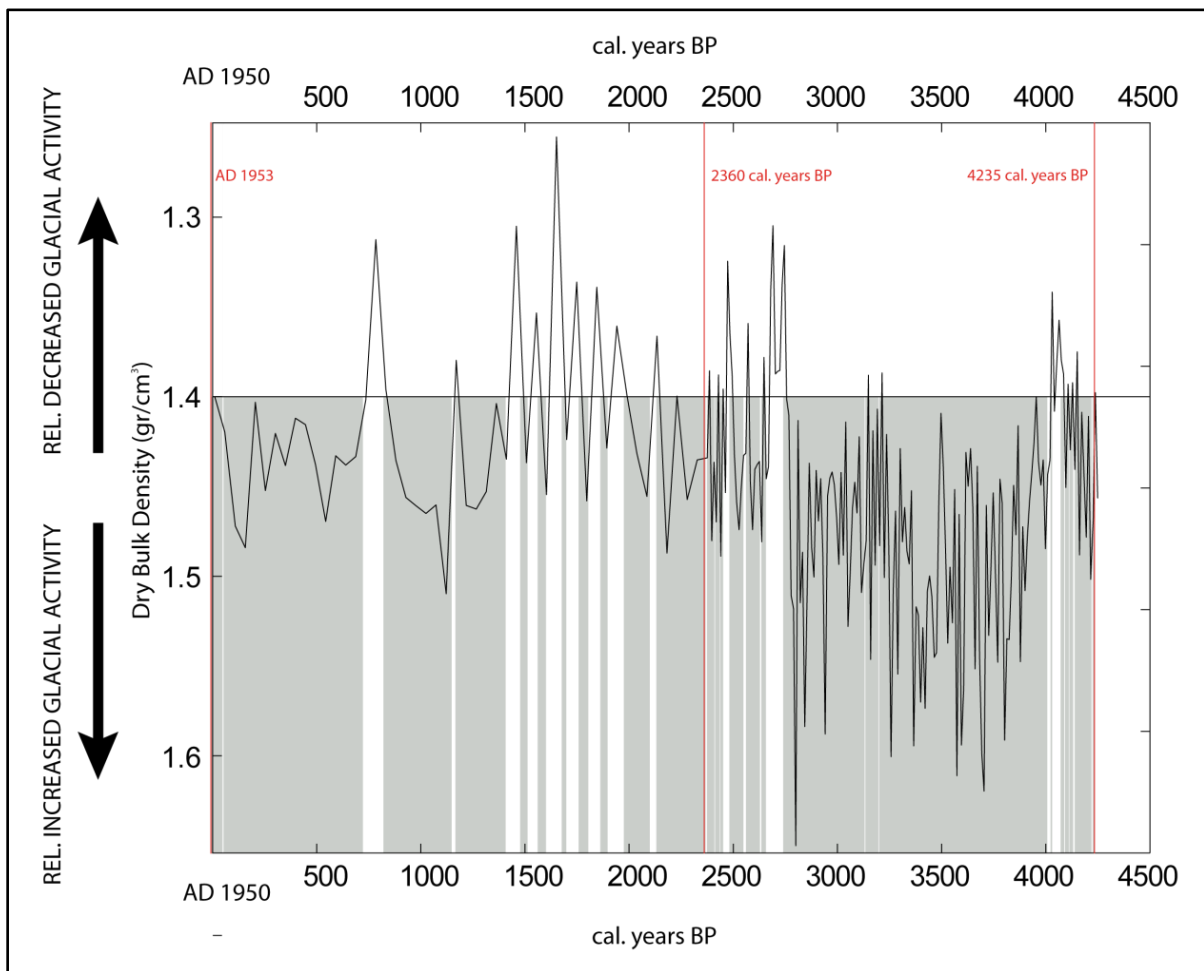


Figure 4.7 Relative glacial activity curve of Vestre Blomsterskardsbreen for the last 4235 cal. years BP. Since Lake Midtbotnvatn has been regulated since AD 1953, any conclusions on glacial activity since then are not possible. Therefore, the curve starts as late as AD 1953; the glacier's extent and activity according to the DBD record of that year hence is the one past glacial activity is compared to. Periods interpreted as increased glacial activity are marked gray. Radiocarbon dates and the beginning of the lake regulation are illustrated in red.

4.6 Variations of relative glacial activity of Vestre Blomsterskardsbreen during the Late-Holocene

The ELA of today (2007) was calculated to a height of 1328 m a.s.l., based on digital map data N-50 of Norway (Norwegian Mapping Authority) and digital contour intervals from laserscanning in 2007 (NVE).

The reconstructed relative glacial activity curve covers the past 4235 cal. years BP, which represents the oldest date of the sediment core; below this level it is not possible to draw reliable conclusions about age, sedimentation rates and hence variations in glacial activity. The curve begins in AD 1953 due to the fact that Lake Midtbotnvatn was regulated since then, which prevents any interpretations of the sediment with respect to glacial activity.

The relative curve of glacial activity of Vestre Blomsterskardsbreen shows several variations during the last 4235 cal. years BP. Especially three periods of increased glacial activity can be recognized:

- AD 1953 to 720 cal. years BP; three DBD tops indicate relative increased glacial activity interpreted as LIA glacier advances during the 17th, the first half of the 18th and since the 19th until the first half of the 20th century
- 840 cal. years BP to 1350 cal. years BP, which covers the medieval warm period; with a peak centered around 1100 cal. years BP
- 2740 cal. years BP to 3940 cal. years BP, when the glacial activity reached the maximum values during the past 4235 cal. years BP. The interpretation of this part is considered as uncertain due to the strong sediment structure disturbances in the respective core section (cp. Chapter 5).

The period 1350 cal. years BP to 2740 cal. years BP was dominated by frequent changes between relatively increased and relatively decreased glacial activity. Peaks are centered around 1600, 1800 and 2150 cal. years BP.

It must be pointed out that the relative glacial activity curve and according interpretation results are restricted by the disturbed sediment structure the curve is based on (cp. Chapter 3.6).

5 Discussion

The main purpose of this study was to reconstruct glacier fluctuations and sediment transport of Vestre Blomsterskardsbreen during the Late-Holocene.

This chapter contains a summary and discussion of the quaternary mapping, the dating of mapped marginal moraines by lichenometry, and the analyses and interpretations of proglacial sediments taken out from Lake Midtbotnvatn. The three approaches were then used to relate the proglacial lake sediments to the glacial activity of Vestre Blomsterskardsbreen. Moreover, the fluctuations of the relative glacial activity of Vestre Blomsterskardsbreen over the last 4235 cal. years BP are discussed, linked to natural climate variability and compared to other reconstructed glacier fluctuations in the Northern Hemisphere.

5.1 Sedimentation in Lake Midtbotnvatn

Five sediment cores were gained from of Lake Midtbotnvatn (2 km²), which is located ca. 5 km downstream of Vestre Blomsterskardsbreen. The glacier tongue covers almost 60% of the drainage basin and hence dominates the sedimentation within the lake. But there are always further factors that contribute to the clastic sedimentation within a proglacial lake, such as rapid mass-movement processes at the slopes surrounding the lake and sediment-laden streams of non-glacial origin (Ballantyne and Benn 1994; Ballantyne 2002), floods (natural or induced by artificial lake damming) and gravitational processes within the lake basin (Benn and Evans 1998), and paraglacial reworking (Ballantyne 2002). The latter is, however, limited due to the small content of superficial deposits of the drainage basin. With respect to coring care was taken to choose locations least affected by such processes; two of the cores were analyzed and validated to assure the glacial record.

The analyses and interpretation of the cores was carried out by the means of several sediment parameters. The main goal was to identify variations in parameters that reflect fluctuations in glacial activity. Dry bulk density (DBD) is reflecting the density/porosity of sediment; values of this parameter increase with increased glacial activity in the catchment, caused by higher production rates of all grain sizes and increased meltwater runoff, and hence higher sedimentation rates, which in turn increase the density of the proglacial lake sediments (Bakke 2004; Bakke et al. 2005c). Further important parameters that reflect increasing glacial activity are very coarse silt and very fine silt, which correlate positively/inversely with DBD in core parts not affected by disturbances through coring, and the XRF values of elements that

usually are interpreted as to be of detrital origin, such as Si, Ti and Rb (Bakke et al. 2005c; Rothwell et al. 2006; Guyard et al. 2007).

In order to get the glacial signal only, sediments deposited by episodic events had to be isolated and excluded from the core records before creating an age-depth model, calculating past and present sedimentation rates, and establishing a relative glacial activity curve. Strong contemporaneous anomalies of mean grain size and the sorting parameter, and moreover abrupt changes in the Fe/Ti ratio are interpreted as to indicate sediment deposited by floods or gravitational processes. The Fe/Ti ratio can also indicate sediment disturbances (Rothwell et al. 2006).

The interpretations of the proglacial lake sediments were complicated by the grade of disturbances that occurred during the coring process, and furthermore by the fact that Lake Midtbotnvatn has been regulated for the development of hydroelectric power since AD 1953. This crucially affected the sediment transport in the drainage basin, enlarged the sedimentation rate many times over normal and hence made it impossible to receive a reliable glacial signal for the second half of the 20th century.

5.2 Holocene variations in glacial activity of Vestre Blomsterskardsbreen

The established relative glacial activity curve reaches back to 4235 cal. years BP, based on radiocarbon dates of core MIP-209. Accordingly, Holocene glacier fluctuations at Vestre Blomsterskardsbreen earlier than this time span can not be reconstructed from proglacial sediments in this study. Moraines in front of Vestre Blomsterskardsbreen that were too old to be dated by lichenometry can possibly indicate glacier sizes and ELAs for specific times earlier than the LIA.

5.2.1 Early and mid-Holocene glacier and climate variations (earlier than 4235 cal. years BP)

Two marginal moraine sequences observed in front of Vestre Blomsterskardsbreen, M-20/M-21 and M-22 (see Chapter 2.3), had too large lichen thalli to be dated by the use of lichenometry, and were furthermore located behind the maximum LIA moraine set, consequently interpreted as to be deposited earlier than the LIA. Disregarding isostatic adjustment, the ELA of the reconstructed glacier based on M-20/M-21 was 27 m lower than today's (2007), while the M-22 ELA was 28 m lower (see Figure 4.4. and Table 11). The set M-20/M-21 is located quite close to the interpreted marginal moraines deposited during the

maximum glacier advance of the LIA; both sequences are only separated by a narrow valley (see Figure 2.1), indicating that the size of Vestre Blomsterskardsbreen was not differing excessively when lying at these positions. During the deposition of M-22, Vestre Blomsterskardsbreen is considered as comparably larger, though reconstructed ELA lowering shows only a slight difference (1 m compared to M-20/M-21 disregarding isostatic adjustment), attributed likewise mainly to the interaction of a huge glacier tongue flowing down a narrow valley.

At several places in the Folgefonna area, moraine sequences are observed that are too old to be dated by lichenometry (cp. Bakke 1999; Simonsen 1999; Bakke et al. 2005a; Bakke et al. 2005c; Bjønnes 2006; Tolo 2008), and therefore assumed to be deposited earlier than the LIA, during either the Younger Dryas (13000-11500 cal. years BP), the early Holocene (11500-8800 cal. years BP) or during the late Holocene in the time period 3000-1000 cal. years BP (Bakke et al. 2005a; Bakke et al. 2005c).

ELA lowerings during the Younger Dryas, a dry and cold period from 13000-11500 cal. years BP (Bakke et al. 2005a; Bakke et al. 2005b), are estimated to 355 m at the Northern Folgefonna ice cap (Bakke et al. 2005a).

For the time period of the Younger Dryas, the ELA lowering corrected for isostatic adjustment would be 154-177 m for M-20/ M-21, and 155-178 m for M-22. This is distinctly less than the considered Younger Dryas ELA lowering at northern Folgefonna. The close position of M-20/M-21 and M-22 to the lichen-dated LIA moraines in front of Vestre Blomsterkardsbreen, the lack of moraine sequences in-between the observed moraine sets, and the very slight lowering of the reconstructed ELAs during the specific times when the moraines were deposited, indicate that the moraine sequences M-20 to M-22 are very unlikely to be deposited during the Younger Dryas.

The Preboreal oscillation took place during the early Holocene, around 11300 to 11150 cal. years BP in the northern and eastern parts of the North Atlantic region (Björck et al. 1997). The period was characterized by cooler and humid conditions throughout north-western and central Europe (Björck et al. 1997; Bjune et al. 2005). “Jondal Event 1”, termed after a glacier readvance at northern Folgefonna, occurred within the Preboreal oscillation around 11100 cal. years BP. It was triggered by a low input of solar energy and a meltwater pulse to the North Atlantic, which resulted in a cooler and somewhat drier climate compared to today (Bakke et

al. 2005a). “Jondal Event 1” is not demonstrated at any places in western Norway other than Folgefonna (Bakke et al. 2005a; Bjønnes 2006). “Jondal Event 2”, a second glacier readvance dated to 10550-10450 cal. years BP, was on the contrary mainly caused by increased winter precipitation compared to present conditions (Bakke et al. 2005a). During “Jondal Event 1”, an ELA lowering adjusted for land uplift of 230 m was reconstructed for northern Folgefonna, while “Jondal Event 2” corresponded to an estimated ELA lowering of 220 m.

For the time period of “Jondal Event 1”, the ELA lowering corrected for isostatic adjustment for M-20/M-21 would be 148 m, for “Jondal Event 2” for M-22 140 m, respectively; this is distinctly less than the considered ELA lowerings reconstructed at northern Folgefonna. Therefore, M-20/M-21 and M-22 are not assumed to be deposited in the course of “Jondal Event 1” and “Jondal Event 2”.

“Erdalen Event 1” was a glacier readvance at northern Folgefonna dated to 10000-9900 cal. years BP, which was mainly resulting from increased winter precipitation. This event could also be demonstrated at Nigardsbreen, a south-eastern glacier outlet of Jostedalsbreen (Nesje et al. 1991). “Erdalen Event 2” was a glacier readvance caused by decreased summer temperatures recorded at Nigardsbreen, but not at the maritime ice cap northern Folgefonna, which may be explained by a shift in the atmospheric circulation resulting in relatively more winter precipitation (Dahl et al. 2002; Bakke et al. 2005a). The ELA lowering corrected for isostatic adjustment of “Erdalen Event 1” at northern Folgefonna is estimated to 210 m (Bakke et al. 2005a). The ELA lowering corrected for land isostatic adjustment for M-20/M-21 in front of Vestre Blomsterskardsbreen would be 132 m, the one for M-22 133 m, which is a great difference to the calculated ELA for this time period of northern Folgefonna. Furthermore, due to the lack of marginal moraines corresponding to “Erdalen Event 2” at northern Folgefonna, it is unlikely to have occurred at southern Folgefonna, where the glaciation threshold (defined as the mean value between the highest adequate mountain top without glacier and the lowest glaciated mountain top (Nesje 1995, 25)) is lower. Moreover Vestre Blomsterskardsbreen is the most maritime glacier outlet of Folgefonna, responding mostly on winter precipitation fluctuations and less on summer temperature variations, which probably were the main cause for moraine formation at southeastern Jostedalsbreen in that period (Dahl et al. 2002; Bakke et al. 2005a). Thus, M-20/M-21 and M-22 are interpreted as not being deposited in the course of “Erdalen Event 1” and “Erdalen Event 2”.

The Finse Event is a double glacier readvance that occurred around 8500-8300 cal. years BP, culminating at 7590 ± 120 cal. years BP, at Hardangerjøkulen, an ice cap located north-east of Folgefonna (Dahl and Nesje 1994, 1996). The Finse Event is not recorded at northern Folgefonna. A possible explanation for this is that the glaciation threshold at northern Folgefonna was not crossed during the Finse Event; Hardangerjøkulen is located higher above sea level than Folgefonna (Bakke et al. 2005c). Therefore, the Finse Event is not assumed to have occurred at southern Folgefonna either, indicating that neither M-20/M-21 nor M-22 were deposited as a result of it.

During the thermal optimum, between 9600 and 5200 cal. years BP, northern Folgefonna is assumed to not being present; estimated ELAs were above 1550 m, which is above the highest mountain of the catchment (Bakke et al. 2005c). The continuous non-existence of northern Folgefonna is in contrast to other areas in southern Norway, where several glacier advances in the time period 9960-5200 cal. years BP were demonstrated, such as for example the Finse Event. This is mainly attributed to the altitudinal range of northern Folgefonna (Bakke et al. 2005c).

Since the proglacial sediment analyzes in this study only reach back in time until 4235 cal. years BP, it is not possible to conclude about the meltdown of southern Folgefonna during the Holocene climatic optimum and when the onset of the Neoglaciation with the reformation of southern Folgefonna and Vestre Blomsterskardsbreen occurred. The thermal optimum had a very distinct time period from 8100 to 7850 cal. years BP, where summer temperatures were higher and winter precipitation rates lower. This combination is assumed to have affected all Norwegian glaciers (Dahl and Nesje 1996; Bjune et al. 2005). These conditions, combined with the facts that northern Folgefonna was demonstrated as not being present and that the glaciation threshold is higher there than at southern Folgefonna, indicate that southern Folgefonna most likely was non-existent for some time during the thermal optimum. The relative glacial activity curve of Vestre Blomsterskardsbreen reflects a permanent presence of the glacier outlet since at least 4235 cal. years BP (see Figure 5.1). A potential reformation must have occurred before this time.

The reconstruction of past ELAs of Møsevassbreen indicates that the glacier outlet was not present in the drainage basin of Lake Møsevatn during most of the mid-Holocene and parts of the late Holocene. The glacier outlet located west of Vestre Blomsterskardsbreen was reconstructed as continuously present in the drainage basin only since 1440 cal. years BP; and not present in the time span before, at least since 5790 cal. years BP, though this period was

interrupted by several temporal readvances. This glacier outlet's history is attributed to a different local glaciation threshold and especially a potential local drainage overflow gap (spillway), which both depend on the local topography below the glacier tongue. It is therefore assumed to be different compared to the general southern Folgefonna's glacial history (Bjønnes 2006).

5.2.2 Late Holocene glacier and climate variations (the last 4235 cal. years BP)

After the thermal optimum, northern Folgefonna ice cap was reformed around 5200 cal. years BP, when the ELA was lowered as a response to cooler and wetter climate conditions (Bjune et al. 2005). Between 4600 and 2300 cal. years BP a gradual build-up of northern Folgefonna towards its present size took place (Bakke et al. 2005c).

The relative glacial activity curve of Vestre Blomsterskardsbreen indicates that the glacier outlet was present in the catchment at least since 4235 cal. years BP, with relatively increased glacial activity between 4235 and 4080 cal. years BP, relatively decreased glacial activity from 4080 to 3940 cal. years BP, and relatively increased glacial activity during the time period 3940 to 2740 cal. years BP. The period 3940-2740 cal. years BP actually shows the highest relative glacial activity of the whole time span the proglacial sediment record covers. This is in contrast to reconstructed ELAs of northern Folgefonna, and of Møsevassbreen, though the latter is considered to be dominated by different local conditions (Bakke et al. 2005c; Bjønnes 2006). ELA reconstructions of Northern Folgefonna indicate that the time period with the greatest glacial activity during the late Holocene (4000 to 0 cal. years BP) occurred during the LIA, with ELAs up to 105 m lower than at present, and that the glacier was rather small in the time span between 4600 and 2200 cal. years BP (Bakke et al. 2005a; Bakke et al. 2005c; Bjune et al. 2005).

Core MIP-209, where the DBD data are taken from to compile a relative glacial activity curve, is to its most degree disturbed in this section (the first two-thirds of the second core half; cp. Chapter 3.6). The extraordinary high glacial activity reflected in the period 3940 to 2740 cal. years BP may therefore not correspond as close to reality as suggested at first. Rather, it may be interpreted as to reflect a period when the glacier outlet was present in the catchment, but that the degree of relatively increased glacial activity was strongly overestimated due to disturbed sediment structure and the influence of a dominating, greatly deformed flood layer. Between 2740 and 2650 cal. years BP, relatively glacial activity is below present (AD 1953) values; this core section is located at the bottom of the first core half, probably reflecting a more reliable estimate for the glacial activity between 3940 and

2740 cal. years BP. Consequently, the time span from 4080 to 2650 cal. years BP may be regarded as a period of rather decreased glacial activity with an increasing trend in time towards the present glacier size, given that DBD values are negatively affected by the disturbed flood layer in the second core half.

For the last 2300 cal. years BP, frequent glacier size fluctuations are recorded from northern Folgefonna, with three relatively large readvances dated to 2200, 1600 and 1050 cal. years BP (Bakke et al. 2005c). Glacier advances during these time spans are furthermore detected at several other places in southern Norway: at Hardangerjøkulen (Dahl and Nesje 1994), at Jostedalbreen (Nesje et al. 2001) and at Bøvertunsbreen (Matthews et al. 2000). Based on the fact that Folgefonna is a maritime glacier where 80% of its modern net mass balance (B_n) are controlled by changes in its winter mass balance (B_w), Bakke et al. (2005c) consider two different explanations for the 2200 cal. years BP glacier advances, when the glacier size increased significantly from small to larger than at present. First, they may be attributed to changes in winter precipitation associated with a positive NAO index corresponding to milder and wetter climate conditions in northern Europe, which was assumed less stable then compared to the period from 5200 to 2200 cal. years BP (Six et al. 2001; Bakke et al. 2005c). Second, a high-pressure field located over Russia may have had a stronger effect, resulting in variable patterns of the westerlies and hence the precipitation along the west coast of Norway (Bakke et al. 2005c and references therein).

Reconstructed relative glacial activity of Vestre Blomsterskardsbreen, southern Folgefonna, reflects major increases around 2150 and 1100 cal. years BP. In general, the time span from 2740 to 1350 cal. years BP is dominated by high-frequent changes in increased and decreased glacial activity, while the time span 1350 to 840 cal. years BP is dominated by relatively increased glacier activity interrupted by one phase of decreased glacial activity around 750 cal. years BP (see Figure 5.1.). The deposition of the marginal moraine sequences M-20/M-21 and M-22 is therefore interpreted to have taken place within the time span 3000 to 1000 cal. years BP, most likely when the relative glacial activity curve indicates peak activity around 2150 and 1100 cal. years BP. The ELA lowering corrected for isostatic adjustment for M-20/M-21 around 2150 cal. years BP would be 37 m, the one for M-22 around 1100 cal. years BP would be 33.5 m. Due to the disturbed sediment structure of core MIP-209, and since the moraine sequence could not be dated, this assumption cannot be verified independently.

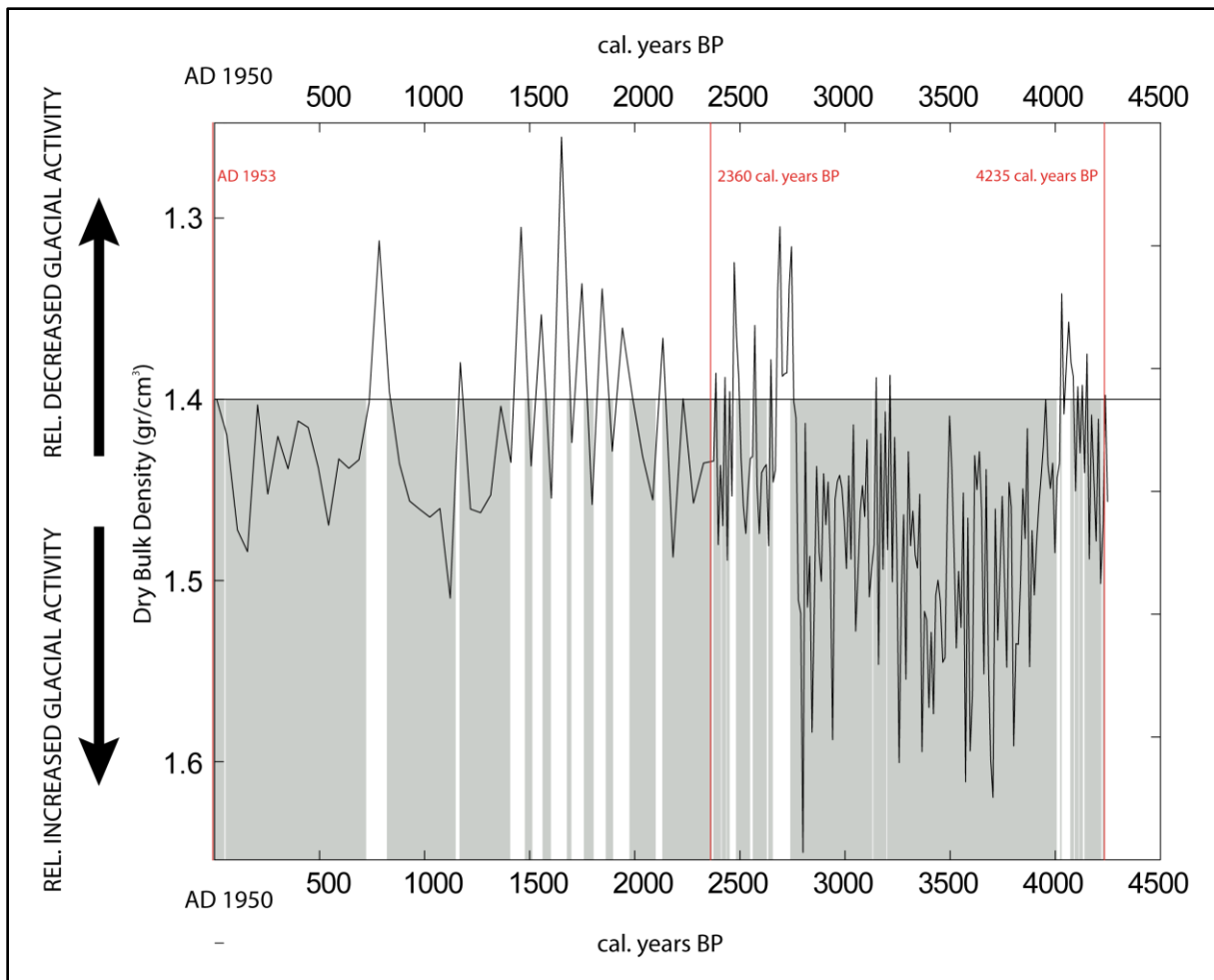


Figure 5.1 Relative glacial activity curve of Vestre Blomsterskardsbreen for the time span AD 1953 to 4235 cal. years BP. Periods interpreted as increased glacial activity are marked gray. Radiocarbon dates and the beginning of the lake regulation are illustrated in red.

5.2.2.1 The Medieval Warm Epoch

The Medieval Warm Epoch, a comparably warm period from 1200 to 700 cal. years BP (AD 800-1300) (Cronin et al. 2003), is in south Norway recognized as a period with both increased and decreased glacial activity (cp. Nesje and Dahl 1991b, 1991a; Nesje and Kvamme 1991; Nesje et al. 1991; Dahl and Nesje 1994, 1996; Bakke et al. 2005c). Reconstructions from Hardangerjøkulen indicate higher winter precipitation, higher summer temperatures and lower ELAs compared to present in this time period (Dahl and Nesje 1996). Reconstructions from Folgefonna indicate periods of both glacier expansion and decay during the Medieval Warm Epoch, attributed to a more variable pattern of the westerlies at the west coast of Norway (Bakke et al. 2005c; Bjønnes 2006). Increased winter precipitation can cause glacier expansion even though a period is characterized by generally warmer summer temperatures,

especially at maritime glaciers. When winter temperature, however, is too high, precipitation could fall as rain instead of snow, which may result in glacier decay (Bakke et al. 2005c).

Both at northern Folgefonna (Bakke et al. 2005c; Tolo 2008) and at southern Folgefonna (Simonsen 1999; Bjønnes 2006) reconstructed glacier sizes were smaller prior to the Medieval Warm Epoch. The period itself was characterized by ELA lowerings attributed to increased winter precipitation, and glacier fluctuations.

The compiled record of relative glacial activity of Vestre Blomsterskardsbreen indicates that the time span 1350 to 840 cal. years BP is dominated by relatively increased glacier activity interrupted by one phase of decreased glacial activity around 750 cal. years BP (see Figure 5.1.). Around 1100 cal. years BP, relative glacial activity values reach a peak. Large glacier readvances with distinctive ELA lowering were also recognised at several other glacier outlets of Folgefonna around that time: at Møsevassbreen, southern Folgefonna, at 1060 cal. years BP (Bjønnes 2006), Bondhusbreen at the western part of southern Folgefonna at 1080-910 cal. years BP (Simonsen 1999), Dettebreen at northern Folgefonna at 1100 cal. years BP (Tolo 2008), and glacier outlets at the northern part of northern Folgefonna at 1050 cal. years BP (Bakke et al. 2005c). Furthermore, this glacier expansion was recorded other places in southern Norway, at Hardangerjøkulen and Jostedalbreen (Dahl and Nesje 1994; Nesje et al. 2001).

The time period between 840 and 720 cal. years BP is characterized by relatively decreased glacial activity of Vestre Blomsterkardsbreen, indicating the end of the Medieval Warm Epoch.

5.2.2.2 The Little Ice Age

The term “Little Ice Age” (LIA) (introduced by Matthes 1939, cp. Grove 1988) refers to a time period of frequent climatic fluctuations and global glacier expansion attributed to lower summer temperatures and/or increased winter precipitation rates (Grove 1988; Jones and Briffa 2001; Linderholm and Gunnarson 2005; Vincent et al. 2005), which started between the 13th and 14th century and was at its peak between the mid-16th and mid-19th centuries (Porter 1986 in Grove 1988). Temperature values in the course of the LIA possessed a trend of cooling in average, but were composed of numerous fluctuations on few-years scales (Grove 1988). Glaciers reached the greatest maximum terminus positions for hundreds of years, though the LIA time period diverges in dates in different areas of the world (Grove 1988; Nesje and Dahl 2000). For northern Folgefonna, Bakke et al. (2005c) specified the time

period of lower ELAs and larger glacier sizes to between 600 cal. years BP and AD 1930, with major glacier readvances around AD 1750, 1870-1890, and 1930 (Bakke et al. 2005a; Bakke et al. 2005c). For southern Norway, the LIA maximum glacier expansion is assumed to have occurred around AD 1750 (Grove 1988; Bakke et al. 2005a), this is proven for Jostedalbreen (Nesje and Kvamme 1991), Hardangerjøkulen (Dahl and Nesje 1994) and Jotunheimen (Matthews 2005) and furthermore indicated for several glacier outlets of Folgefonna (Bakke 1999; Simonsen 1999; Bjønnes 2006). At southern Folgefonna, the glacier outlet Østre Blomsterskardsbreen is assumed to have reached its maximum LIA expansion as late as AD 1940, as a response to strong positive net balances experienced around AD 1920 (Tvede 1973; Tvede and Liestøl 1977).

In general, glaciers in southern Norway had considered ELA lowerings of 100-150 m during the LIA (Nesje and Dahl 1991a; Torsnes et al. 1993; Dahl and Nesje 1994; Bakke et al. 2005a; Bakke et al. 2005c).

The relative glacial activity curve of Vestre Blomsterskardsbreen indicates relatively increased glacial activity during the LIA for the last 720 cal. years BP, with major peaks around 530, 330, 240 and 180-95 cal. years BP, which corresponds to AD 1420, 1620, 1710 and 1770-1855.

Relative glacial activity compiled from analyses of proglacial sediment from Lake Midtbotnvatn thus indicate that Vestre Blomsterskardsbreen had relatively increased glacial activity compared to today (AD 1953) during the whole time span of the LIA, starting during the 13th century and lasting until the mid-20th century. The core sediments structure for this section, however, is quite disturbed; the interpretation must therefore be seen with caution.

Based on the lichen growth curve “Folgefonna – compiled data” (Bakke et al. 2005a, cp. Chapter 2.3.), lichen-dated marginal moraines in front of Vestre Blomsterskardsbreen indicate that the maximum LIA glacier expansion occurred during the first half of the 18th century, with several subsequent glacier readvances during the 18th and the early 19th century, as well as around AD 1945 (cp. Chapter 2.3). Reconstructed glacier sizes and ELAs indicate ELA lowerings adjusted for land uplift of up to 22 m (cp. Chapter 4.34.), which is distinctly less than observed at other glacier outlets in Norway. At northern Folgefonna, LIA ELA lowerings of 105m were determined (Bakke et al. 2005a). The differences in ELA lowerings during the LIA are attributed to the large size of Vestre Blomsterskardsbreen and local topographic conditions: the high mountain plateau located northeast of Insta Botnane, and especially the valley below the glacier tongue, which goes down to around 800-840 m a.s.l. at 1.2 km

inwards of the glacier's terminus (Elvehøy 1997), are both factors that are unfavourable for easy glacier expansion. Torsnes et al.(1993) mention two characteristics of glacier tongues that had comparatively small ELA lowerings during the LIA. First, that such glaciers have large accumulation areas compared to the ablation areas, and second, that they underwent small percentage areal increases during the LIA. Both characteristics are the case at Vestre Blomsterskardsbreen.

Lichen-dated moraines indicate that the maximum expansion of Vestre Blomsterskardsbreen during the LIA took place during the first half of the 18th century. Relative glacial activity compiled from proglacial sediment studies, however, indicates that the maximum LIA advance occurred somehow later, around AD 1770 to 1855. This may be attributed to the disturbed sediment structure and the small number of reliable dates achieved from the sediment core.

A glacier readvance around AD 1810 could be recognized in both lichen-dated moraines and the relative glacial activity curve, though the latter may be negatively influenced by disturbed sediment structure. This advance is also demonstrated at Bondhusbreen (Grove 1988), but lacks at other glacier outlets of southern Folgefonna. Vestre Blomsterskardsbreen experienced a period of relatively increased glacial activity with numerous decays and readvances during the 18th and early 19th century. This is evidenced from both lichen-dated moraines and relative glacial activity compiled from proglacial sediment analyses, and corresponds to the assumed climate conditions for this time period, which were dominated by high-frequent fluctuations (Grove 1988).

At both northern Folgefonna and several glacier outlets of southern Folgefonna including Bondhusbreen, Buarbreen, Sauabreen and Møsevassbreen glacier expansions in the time period AD 1870 to 1890 were demonstrated (Grove 1988; Bakke 1999; Bakke et al. 2005a; Bjønnnes 2006; Edvardsen 2006; Tolo 2008). This readvance could not be recognized at Vestre Blomsterskardsbreen, neither in the proglacial sediment record nor as lichen-dated moraines. Several explanations are possible: first, this advance did not occur at Vestre Blomsterskardsbreen. Second, it occurred but did not deposit marginal moraines. Third, the advance occurred, and deposited moraines were eroded afterwards, or were not found during fieldwork because they are located in difficult terrain on a mountain plateau northeast of Insta Botnane. The reliability of the relative glacial activity curve is weakened by the disturbed

sediment structure, so neither of the named possibilities can be rejected or verified. Due to the maritime setting of Vestre Blomsterskardsbreen, and the fact that both Møsevassbreen and Sauabreen advanced as a result on the climate conditions during that time span, it is assumed as likely that Vestre Blomsterskardsbreen somehow reacted as well.

The latest glacier readvance during the LIA is proven by a lichen-dated moraine from AD 1945. This expansion is not distinctly recognized in the relative glacial activity curve, though the curve indicates in general relatively increased glacial activity compared to present (AD 1953) during the whole time span of the LIA. In AD 1950, a local shepherd is cited to have experienced the position of Vestre Blomsterskardsbreen several hundred meters advanced compared to the glacier's position in AD 1915-1920 (Arve Tvede, 2010, personal communication).

At several other glacier outlets of Folgefonna readvances around AD 1930 could be demonstrated (Tvede 1972; Grove 1988; Bjelland 1998; Simonsen 1999; Bakke et al. 2005a; Edvardsen 2006). Based on comprehensive research work including fieldwork and comparison of older and up-to-date photographs, Tvede (1972, 1973, 1994) and Tvede and Liestøl (1977) proved that Østre Blomsterskardsbreen had its maximum LIA advance around AD 1930/1940. Between AD 1904, when a picture of the position of Østre Blomsterskardsbreen was taken by Rekstad (Rekstad 1905), and AD 1971, when a picture was taken from the same position (Tvede 1972), the glacier is assumed to have expanded 200-250 m, finally covering a larger area of Blomstølskardvatn (Tvede and Liestøl 1977). Since Østre and Vestre Blomsterskardsbreen are two glacier tongues of the same glacier unit, the LIA glacial history and especially the maximum LIA glacier advance at Vestre Blomsterskardsbreen would be expected to have happened analogously. But based on the observed moraine ridges in the study area and the obtained lichenometric dates, the maximum LIA glacier advance for Vestre Blomsterkardsbreen is assumed to have occurred earlier, during the first half of the 18th century. For Blomstølskardvatn, no proglacial lake sediment analyses were performed. The possibility of an earlier LIA glacier advance, such as during the 18th century, can therefore not be excluded; though such an advance must be considered as not having expanded further than the one in AD 1930/1940.

The climatic cooling since approximately AD 1200 has until recently mainly been attributed to decreased summer temperatures, as a result of variations in solar irradiance and volcanic eruptions in combination with ocean-atmosphere interactions (Nesje and Dahl 2003 and references therein). Recent research indicates, however, that increased winter precipitation

also was a main reason for rapid glacier expansion during the early 18th century. A positive NAO index caused mild and humid winters in the North Atlantic region, compensating also for significant regional variations in temperature, resulting in glacier advances demonstrated across all over southern Norway (Nesje and Dahl 2003). Assuming that winter precipitation is a decisive factor for the LIA glacial history of Folgefonna, slope aspect, prevailing wind directions and topographic conditions must be considered as important influencing factors on local precipitation rates, which mainly are characterized by the maritime grade of the glacier outlets, and on redistribution of snow between glacier outlets (cp. Nordli et al. 2005). The precipitation rate at Folgefonna is decreasing in direction northeast, which is linked to an increase in glacier decay (Tvede 1972, 1973). This may explain the lack of synchronicity for the accumulation rates on western glaciers and in general the glaciers development during the LIA in southern Norway (cp. Nordli et al. 2005). Modern annual precipitation rates of 5000 to 5500 mm/year at Blomsterskardsbreen indicate that winter precipitation is the most important factor for fluctuations of the maritime glacier outlet, rather than summer temperatures. Tvede (1972, 1973) and Tvede and Liestøl (1977) attribute the late LIA maximum advance at Østre Blomsterskardsbreen to variations in the regional distribution of winter precipitation related to variations of the NAO index, indicating increased precipitation rates during AD 1915 and 1920, which resulted in strong positive net balances experienced around AD 1920, and furthermore to the comparably longer response time of the large, long and barely steep glacier outlet. Vestre Blomsterskardsbreen reacted on these conditions as well with expansion, but reached a shorter position than during the early 18th century. The AD 1945 advance is, analogous to the AD 1940 advance of Østre Blomsterskardsbreen corresponding to Tvede (1972, 1973) and Tvede and Liestøl (1977), interpreted as a result of increased mass balance of Vestre Blomsterskardsbreen around AD 1920. This indicates that the response time of Vestre Blomsterskardsbreen can be estimated to approximately 25 years, which is 5 to 10 years more than Østre Blomsterskardsbreen; the difference is attributed to the fact that Vestre Blomsterskardsbreen is larger.

Important factors that might explain the described local differences in the glacial history of several glacier outlets of Folgefonna and other south Norwegian glaciers, and especially between Vestre and Østre Blomsterskardsbreen with respect to the maximum LIA advance, are hence interpreted to be differences in precipitation rate, combined with different local conditions with respect to slope aspect, prevailing wind direction and topographic conditions.

The ELA lowering differences between Vestre Blomsterskardsbreen and other glaciers in southern Norway during the LIA (105-150 m and 22 m, respectively) indicate that Vestre Blomsterskardsbreen is somehow different in that respect; consequently, at least “Jondal Event 1 and 2” and “Erdalen Event 1 and 2” cannot be rejected definitively with respect to the time of origin of M-20/M-21 and M-22.

5.2.2.3 Vestre Blomsterskardsbreen since the LIA

Both Østre and Vestre Blomsterskardsbreen are considered as very stable during the past 55 years, especially compared to Møsevassbreen and Sauabreen which are located in close distance and were dominated of retreat (Smith-Meyer and Tvede 1996; Arve Tvede, 2010, personal communication; Bjønnes 2006; Edvardsen 2006). This steadiness is mainly attributed to the maritime setting of the glacier outlets, where sufficient winter precipitation compensates for increasing summer temperatures, as are experienced in the course of modern climate change that is anthropogenic induced global warming (cp. Jansen et al. 2007). The strength of the westerlies in the North Atlantic region is a controlling factor for snow blow-out from Møsevassbreen to Blomsterskardsbreen (Tvede and Laumann 1996 in Smith-Meyer and Tvede 1996). The strengthened winds from west to east were, next to the precipitation rates, one of the main contributing factors to the volume steadiness of Blomsterskardsbreen during the last century (Smith-Meyer and Tvede 1996).

The precipitation amount at the Folgefonna peninsula mainly depends on the position of the atmospheric polar front with respect to quantity and strengths of the cyclones within the westerlies, and on the temperature of sea surface (SST) of the North Atlantic Sea (Bakke 2004; Nesje et al. 2004). The intensity of the westerlies is strongly related to the North Atlantic Oscillation index (NAO index), as are consequently the winter precipitation rates and the mass balances of maritime glaciers in south-western Norway (cp. Chapter 1.6.) (Six et al. 2001; Hurrell et al. 2003; Bakke 2004; Bjune et al. 2005; Nesje et al. 2008).

5.3 Natural climate variability

The Earth's climate history is characterized by natural variabilities, depending on several factors (Nesje 1995; Bradley 1999; Nesje et al. 2005).

With respect to long-term Holocene climate variability, orbital forcings, such as changes in precession, obliquity, and eccentricity, are dominating factors, since they affect the overall solar insolation (Nesje et al. 2005). Moreover, variations in the total insolation are enlarged by redistribution between seasons and latitudes (Nesje 1995).

The causes of more high-frequent climate changes are less understood, though mainly ascribed to variations in sunspots, which cause changes in the Sun's output of solar energy, volcanic eruptions, which bring gasses and silicate particles into the stratosphere absorbing parts of the incoming short-wave sunrays and thus changing the Earth's input in solar energy, changes in the thermohaline circulation, and sea level changes (Nesje 1995; Bradley 1999).

Solar magnetic activity variability is considered an important influencing factor on high-frequent natural climate variability. During most of the last millennium, total solar irradiance was usually lower than at present, suggesting a millennial-scale cooling trend, except a period centered around AD 1200 (Bard et al. 2000).

Briffa et al. (1998) examined the influence of volcanic eruptions on Northern Hemisphere summer temperatures over the past 600 years, concluding that large explosive volcanic eruptions caused different extents of Northern Hemisphere summer temperature cooling during the past 600 years. It is difficult to link the results to relative glacial activity of Vestre Blomsterskardsbreen over the same time span, but with respect to natural climate variability volcanic eruptions must be considered.

The thermohaline oceanic circulation (THC) consists of deep ocean currents, generated by the sinking of cold salty water within the North Atlantic, that circulate sea water slowly around the globe. The THC is assumed to be slowed down or stopped by sudden, large fresh water inputs of huge meltwater lakes into the North Atlantic, which may have occurred during the end of the last Ice Age. Fresh water decreases the salt content and density of sea water, what could prevent it from sinking. A slowed or interrupted THC would affect the heat transfer between the equatorial and northern latitudes, with rapid climatic changes as possible results of such events (Strahler and Strahler 2006).

The winter NAO index, characterized by mild and humid winter conditions in Northern Europe when positive, and cold and dry conditions when negative (Six et al. 2001; Hurrell et al. 2003), is an important indicator of winter precipitation at the south-western coast of Norway, dominating the (winter) mass balances of the maritime glaciers located there (Nesje et al. 2000b; Hurrell et al. 2003; Bakke 2004; Bjune et al. 2005; Nesje et al. 2008) (cp. Chapters 1.6.1 and 5.2.2.3.). Vestre Blomsterskardsbreen is to a large extent a maritime glacier outlet of southern Folgefonna; annual precipitation rates exceed 5000 mm/year (Tvede 1973; Tvede and Liestøl 1977; Nesje et al. 2004), which indicates a strong potential correlation between the glaciers' net (winter) mass balance and the winter NAO index.

Surface air temperatures and sea surface temperatures (SST) are highly correlated with NAO variability, both factors are in turn related to precipitation rates and storminess (Hurrell et al. 2003). Warmer surface waters in the North Atlantic result in increased evaporation and hence increased orographically enhanced front precipitation values in western Norway when combined with stronger, warm, south-westerly winds (westerlies) corresponding to a positive winter NAO index (Bakke et al. 2005a; Bakke et al. 2005c and references therein).

Climate variations during the Late Holocene are observable in many different climate archives, both terrestrial and marine (cp. Andersson et al. 2003; Cook 2003; Bjune et al. 2005; Nesje et al. 2005; Bakke et al. 2008; Bakke et al. 2010).

Figure 5.2. shows the relative glacial activity curve compiled for Vestre Blomsterskardsbreen compared to several natural climate archives; the comparisons are based on the presented curves, and not on mathematical correlations.

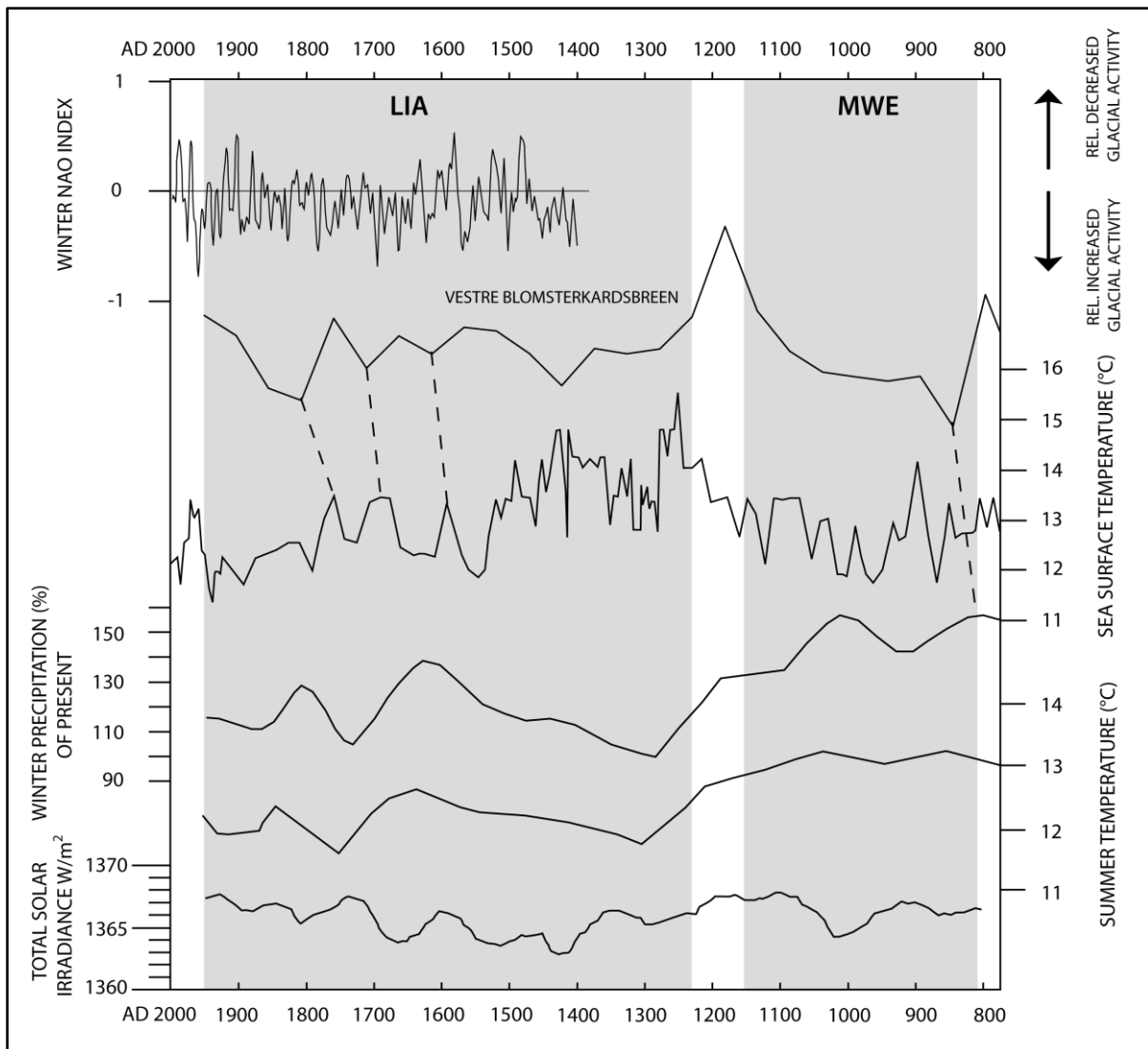


Figure 5.2 The relative glacial activity curve compiled for Vestre Blomsterskardsbreen over the past 1200 years compared to the multi-proxy reconstruction of the winter NAO index back to AD 1400 (Cook 2003, 73), sea surface temperature in °C (August) at the Vøring Plateau in the North Atlantic (Andersson et al. 2003, 22.5), winter precipitation in % of present (AD 1961-1990) at Folgefonna (Bakke et al. 2008, 34), summer temperature in °C (July) at Vestre Øykjamyrtjørn in south-western Norway (Bjune et al. 2005, 184) and the total solar irradiance in W/m^2 (Bard et al. 2000, 989). The time periods of the Little Ice Age (LIA) and the Medieval Warm Epoch (MWE) are marked gray, for comparisons of the parameters during these times see text. Dashed lines indicate peaks in winter precipitation and SST followed by subsequent peaks in relative glacial activity; according to this the reference time of Vestre Blomsterskardsbreen averages out around 30 years.

4235 cal. years BP to 2650 cal. years BP

During this time period, Vestre Blomsterskardsbreen is interpreted as present in the catchment of Midtbotnvatn, but with rather decreased glacial activity compared to the present with an increasing trend in time towards the present size; though relative glacial activity indicates the highest Late-Holocene record of glacial activity in this section (cp. Chapter 5.2.2 and Figure 5.1.). The interpretation is based on research results of Holocene glacier fluctuations at

Northern Folgefonna, and on the compiled relative glacial activity curve of Vestre Blomsterskardsbreen from proglacial sediment records in this study, which is characterized by disturbed sediment structure in the respective section, dominated by a greatly deformed flood layer and therefore classified as rather unreliable.

While the Holocene Climatic Optimum (8500 to 5500 cal. years BP) was characterized by the warmest sea surface temperature (SST) values during the Holocene, a clear cooling tendency has been registered during the late Holocene towards the present cooler values (Calvo et al. 2002). The late Holocene SST cooling responds to decreasing summer insolation attributed to orbital changes and changes in the oceanic heat transport (Calvo et al. 2002 and references therein). Marked drops of the SST around 5400 and 2500 cal. years BP correspond to distinct changes in glacier size at Northern Folgefonna (Bakke et al. 2005c); a marked change in relative glacial activity is as well recognized in the record of Vestre Blomsterskardsbreen around 2650 cal. years BP (Figure 5.1.). This indicates that atmospheric and oceanic variations have strong impact on the precipitation distribution in the North Atlantic region (Bakke et al. 2005c, 172). Reconstructed summer temperature values in south-western Norway indicate lower temperatures since 4500 cal. years BP (Bjune et al. 2005); and reconstructed winter precipitation values indicate increased values since then, with marked peaks centered around 5500 and 1800 cal. years BP, which is interpreted as a response to an increase in strength of the westerlies in the North Atlantic Realm (Bakke et al. 2008). The 5500 cal. years BP increase in glacier size cannot be linked to Vestre Blomsterskardsbreen due to the fact that the compiled curve only covers the past 4235 cal. years BP.

According to Bakke et al. (2008), the onset and general development of the Neoglacial along the west coast of Norway has been depending on a combination of lower summer insolation and a gradually weakening of the seasonal amplitude as aphelion changes throughout the Holocene.

2650 cal. years BP to 1350 cal. years BP

During this time period, Vestre Blomsterskardsbreen is interpreted to have experienced frequent fluctuations of relatively increased and decreased glacial activity, with peaks centered around 2150, 1800 and 1600 cal. years BP (cp. Chapter 5.2.2 and Figure 5.1.).

SSTs at the Vøring Plateau were warmer compared to present values throughout the past 3000 cal. years BP, though highly variable (Andersson et al. 2003). Between 2500 and 1600 cal. years BP SSTs were relatively warm with the highest SSTs recorded around 2000 cal. years BP, a cooling trend of SSTs started which culminated around 1550-1500 cal. years BP (Andersson et al. 2003). A climate characterized as cooler and wetter during the last 2200 cal.

years BP is assumed to have been favourable for glacier growth on the Folgefonna peninsula (Bakke et al. 2005c; Bjune et al. 2005); high-amplitude variations in glacier sizes and ELAs during that time span are attributed to a more variable mode of the westerlies at the west coast of Norway (Bakke et al. 2005c). A significant peak in winter precipitation around 1800 cal. years BP is attributed to an overall increase in the strength of the westerlies (Bakke et al. 2008), based on the assumption that regional precipitation and winter accumulation at glaciers in western Norway depends on the strength of the western airflow, which in turn commonly corresponds to a positive NAO weather mode (Nordli et al. 2005; Bakke et al. 2008).

1350 cal years BP to 720 cal. years BP (AD 600-1230) – The Medieval Warm Epoch

This time period is characterized by relatively increased glacial activity compared to present (AD 1953) at Vestre Blomsterskardsbreen, interrupted by one phase of relatively decreased glacial activity centered around 750 cal. years BP (see Figure 5.1. and 5.2.). Around 1100 cal. years BP, relative glacial activity values reached a peak. The time period between 840 and 720 cal. years BP reflects relatively decreased glacial activity of Vestre Blomsterkardsbreen, indicating the termination of the Medieval Warm Epoch.

The total solar irradiance curve over the past 1200 years (Bard et al. 2000) indicates that the total solar irradiance has been lower than at present for the most parts of this time span. The period AD 1000 to 1200 is characterized by higher values, similar to present ones; this time period may be linked to the Medieval Warm Epoch (AD 800-1300). Vestre Blomsterskardsbreen shows both sections of relatively increased and relatively decreased glacial activity during that time period; with rather increased glacial activity in the beginning of the Medieval Warm Epoch, and decreased glacial activity towards the end, where total solar irradiance is high-valued. High summer temperatures which correspond well to increased total solar irradiance values contradict relatively increased glacial activity of Vestre Blomsterskardsbreen during the Medieval Warm Epoch (Bjune et al. 2005; Mann et al. 2009), which therefore is mainly attributed to extraordinary high winter precipitation values as a response to unstable westerlies (Bakke et al. 2005c; Bjune et al. 2005). In the reconstruction of Bakke et al. (2008), winter precipitation values exceed 150% of present (AD 1961-1990) rates during the Medieval Warm Epoch. Glacier decay around 750 cal. years BP despite increased precipitation rates may be explained by precipitation falling as rain instead of snow due to too warm temperatures (Bakke et al. 2005c). Surface ocean conditions were highly variable during the Medieval Warm Epoch, as were SSTs. The time period 800 to 550 cal.

years BP (AD 1450-1200) was characterized by comparably warm conditions at the Vøring Plateau (Andersson et al. 2003)

720 cal. years until present (AD 1230-1953) – The Little Ice Age and until present

During this period, the relative glacial activity curve of Vestre Blomsterskardsbreen indicates relatively increased glacial activity, with major peaks around 530, 330, 240 and 180-95 cal. years BP, which corresponds to AD 1420, 1620, 1710 and 1770-1855.

Low values of total solar irradiance were recognized around AD 1900, 1810 (corresponding to the “Dalton”-minimum) and 1690 (corresponding to the “Maunder”-minimum) (Bard et al. 2000). Low total solar irradiance values occurred furthermore in the time period AD 1450 to 1750. During the “Maunder”-minimum (AD 1645-1715), almost no sunspots were observed, this period and the one from AD 1450 to 1750 are together interpreted as to correspond to the determined low temperature values during the LIA (Bard et al. 2000). During the LIA, reconstructed summer and mean temperature values were comparably low (Bjune et al. 2005; Mann et al. 2009). The relative glacial activity curve of Vestre Blomsterskardsbreen seems to correlate well with the observations of the total solar irradiance curve and reconstructed summer temperature values, where low irradiance and temperature values correspond to periods of relatively increased glacial activity, such as in the beginning of the 15th and 19th centuries, and vice versa. There are variations in the relative glacial activity curve, though, which may not exclusively be explained by variations in the total solar irradiance, such as during the first half of the 18th century, where increased glacial activity and moreover lichen-dated moraines indicate the maximum LIA advance of Vestre Blomsterskardsbreen, and during which, however, solar irradiance values are comparably high.

During the 15th and 16th centuries, the winter NAO index is persistently positive (Cook 2003; cp. Figure 5.2.), indicating that in general, the glacier expansion of Vestre Blomsterskardsbreen during the LIA must be a result of increased winter precipitation in combination with decreased summer temperature values due to lower solar irradiance. This can be seen in Figure 5.2., where relatively increased glacial activity is accompanied by a positive winter NAO index during the 15th and 16th centuries followed by reduction in the strength of the NAO attributed to the climate cooling in the North Atlantic region between AD 1640 to 1880 (Cook 2003). The climate cooling during that time period is mainly interpreted as the result of lower summer temperatures compared to the Medieval Warm Epoch linked to a reduction in solar irradiance (Bard et al. 2000; Bjune et al. 2005; Mann et al. 2009). The reconstructed winter precipitation curve for Folgefonna (Bakke et al. 2008)

shows analogously a strong increase until the mid-17th century, and strong variations in the time period afterwards, with a distinct peak in the beginning of the 19th century, when also Vestre Blomsterskardsbreen is interpreted to have a peak in relatively increased glacial activity.

SSTs indicate a cooling trend leading to the onset of the LIA around 700 cal. years BP, with two marked cold periods centered around 400 and 100 cal. years BP (Andersson et al. 2003).

The maximum expansion of Vestre Blomsterskardsbreen during the LIA in the first half of the 18th century is accordingly interpreted as a result of lower ablation-season temperatures rather than increased accumulation-season precipitation rates; while the onset of the LIA is interpreted as a combined result of increasing winter precipitation values linked to a positive winter NAO index and a contemporaneous decrease in summer temperatures and SSTs linked to decreasing total solar irradiance.

A direct comparison of the curves of SST, winter precipitation and relative glacial activity of Vestre Blomsterskardsbreen makes it evident that, during the Medieval Warm Epoch and the LIA, peaks in winter precipitation and SST, respectively, were coincident with or followed by subsequent peaks in relative glacial activity. Disregarding any eventualities with respect to sediment structure disturbances of core MIP-209, this indicates that the response time of Vestre Blomsterskardsbreen averages out around 30 years.

5.4 Vestre Blomsterskardsbreen in comparison with other glacier records in the Northern Hemisphere

The relative glacial activity curve of Vestre Blomsterskardsbreen is in the following compared to other glacier records in the Northern Hemisphere (Figure 5.3.).

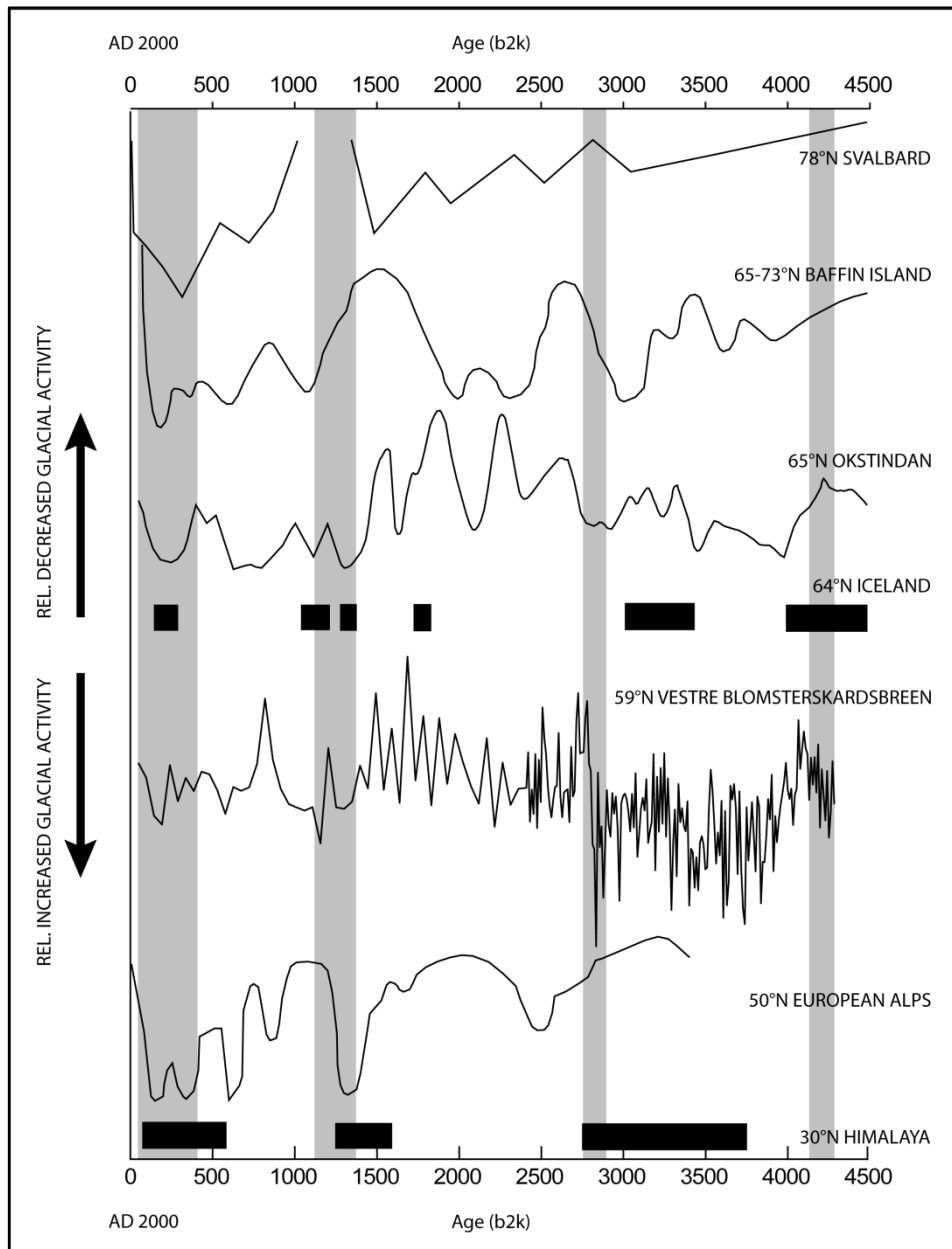


Figure 5.3 The relative glacial activity curve compiled for Vestre Blomsterskardsbreen compared to selected reconstructions of relative glacier extents and phases with major moraine formations from the Northern Hemisphere: 78°N Svalbard (Humlum et al. 2005; Jansen et al. 2007, 461), 65-73°N Baffin Island (Briner et al. 2009, 2084), 65°N Okstindan (Bakke et al. 2010, 1259), 64°N Iceland (Kirkbride and Dugmore 2008 in Bakke et al. 2010; Geirsdóttir et al. 2009 in Bakke et al. 2010), 50°N European Alps (Ivy-Ochs et al. 2009, 2143), 30°N Himalaya (Owen 2009 in Bakke et al. 2010). Gray marking indicates common glacier advances mentioned in the text. Figure based on Bakke et al. (2010, 1260).

The onset of the Neoglacial at Vestre Blomsterskardsbreen must have occurred prior to 4285 years b2k, due to the fact that the proglacial sediment record since then is exclusively minerogenic, and hence glacier-fed. Generally colder climate conditions compared to the Holocene Thermal Optimum caused glacier expansions in the European Alps around 3300 years b2k, indicating the onset of the Neoglacial there; especially in the time period 3300 to 2600 years b2k, glaciers advanced markedly (Ivy-Ochs et al. 2009). Okstindan in northern Norway, in contrary, experienced a major glacier advance already around 4200 years b2k, as did glaciers on Svalbard and Iceland (Humlum et al. 2005; Kirkbride and Dugmore 2008 in Bakke et al. 2010; Geirsdóttir et al. 2009 in Bakke et al. 2010). This event may as well be recognized in the record of Vestre Blomsterskardsbreen, though the proglacial sediment structure was exceedingly disturbed and is therefore considered as not reliable.

Around 2700 years b2k, an abrupt glacial event occurred both at Okstindan, in Baffin Island, in the Himalaya and at Vestre Blomsterskardsbreen (Briner et al. 2009; Owen 2009; Bakke et al. 2010).

The Neoglacial maximum glacier expansion occurred around 1150 years b2k at Vestre Blomsterkardsbreen. At Okstindan, in the European Alps and in the Himalaya, the maximum Neoglacial advance is recognized somewhat later, around 1300 years b2k (Ivy-Ochs et al. 2009; Owen 2009; Bakke et al. 2010). On the contrary, glaciers on Svalbard reached their Neoglacial minimum during this time (Humlum et al. 2005; Jansen et al. 2007).

The time period of the LIA is characterized by the greatest Holocene glacier advances in Baffin Island, and great glacier expansions in Svalbard, at Okstindan in northern Norway, Iceland, at Vestre Blomsterskardsbreen in southern Norway, the European Alps and in the Himalaya.

In general, the Late Holocene is characterized by four synchronous glacier advances in the Northern Hemisphere around 4200 years b2k, 2700 years b2k, around 1300 years b2k, and during the LIA (Figure 5.3.) (Bakke et al. 2010). The overall general relative glacial activity record of Vestre Blomsterskardsbreen corresponds to this pattern, though smaller high-frequency fluctuations in relative glacial activity at Vestre Blomsterskardsbreen are not reflected in the other glacier history reconstructions in the Northern Hemisphere, and vice versa. This may, in addition to minor differences in time of the four common glacier advances, be attributed to differences in local climatic and topographical conditions, and special characteristics of each glacier, such as the grade of maritimity, and moreover the disturbed sediment structure the relative glacial activity curve of Vestre Blomsterskardsbreen was compiled from.

6 Conclusion

In this study, the catchment of Lake Midtbotnvatn was quaternary mapped. Marginal moraines deposited by the glacier outlet Vestre Blomsterskardsbreen were dated by lichenometry. Proglacial sediment cores were gained from Lake Midtbotnvatn, analyzed and interpreted by the means of several parameters. A combination of the lichen-dated moraines and the analyses of the radiocarbon-dated proglacial sediments were used to compile a relative glacial activity curve of Vestre Blomsterskardsbreen for the past 4235 cal. years BP.

Based on the results and discussion in this study, the following conclusions can be drawn:

1. Lake Midtbotnvatn appeared to be an adequate location for proglacial sediment studies with the goal of reconstructing past glacier fluctuations and sediment transport. Limiting factors in this study were the grade of disturbances of the sediment cores, and the fact that Lake Midtbotnvatn has been regulated since AD 1953, which enlarged the sedimentation rate many times over normal and hence prevents any interpretation of the sediment with respect to glacial activity since then.
2. The sediment parameter Dry Bulk Density (DBD) is interpreted to reflect fluctuations in glacial activity of Vestre Blomsterskardsbreen. The grain size distribution analysis was used to isolate episodic events such as floods and gravitational processes, in order to receive the glacial record only.
3. Vestre Blomsterskardsbreen has been present in the catchment the whole time period covered by the proglacial sediment cores. The presumed reformation of the glacier outlet after the Holocene Thermal Optimum (8500 to 5500 cal. years BP) hence is interpreted to have occurred before 4235 cal. years BP. A period of relatively increased glacial activity is interpreted to have occurred from 4235 to 4080 cal. years BP.
4. During the period 4080 to 2650 cal. years BP, Vestre Blomsterskardsbreen is interpreted to have relatively decreased glacial activity; probably with an increasing trend towards the present size. These assumptions are complicated due to the strong disturbed sediment structure in this part of the core

5. The period 2650 to 1350 cal. years was characterized by high-frequent fluctuations in relative glacial activity of Vestre Blomsterskardsbreen; with peaks centered around 1600, 1800 and 2150 cal. years BP.
6. During the Medieval Warm Epoch (AD 800-1300), the relative glacial activity of Vestre Blomsterskardsbreen fluctuated. In general, higher values compared to present (AD 1953) were determined, culminating around 1100 cal. years BP.
7. The LIA (13th to mid-20th centuries) was characterized with increased relative glacial activity of Vestre Blomsterskardsbreen. Several moraine ridges were lichen-dated. The maximum glacier expansion during the LIA occurred during the first half of the 18th century. Further glacier advances occurred during the second half of the 18th and the first half of the 19th century. The latest glacier advance was dated to AD 1945.
8. Marginal moraine ridges that were too old to be dated by lichenometry are interpreted to most likely be deposited in the time period 3000-1000 cal. years BP, when the compiled relative glacial activity curve indicates peak activity around 2150 and 1100 cal. years BP. ELA lowerings of 37 m and 33.5 m would correspond to these deposition times of the two moraine sets. Depositing in the course of “Jondal Event 1 and 2” or “Erdalen Event 1 and 2”, however, cannot be excluded definitively, since the moraines could not be dated.
9. The comparison of reconstructed relative glacial activity of Vestre Blomsterskardsbreen and natural climate variability reconstructions of the NAO index, SST, winter precipitation, summer temperature and total solar irradiance indicates that Vestre Blomsterskardsbreen is mainly forced by variations in winter precipitation. Accordingly, the glacier outlet is considered an indicator for winter climate variability, and hence the NAO weather modes and the strengths of the westerlies at the southwestern coast of Norway. Four main common glacier advances at selected glacier sites in the Northern Hemisphere were compared to Vestre Blomsterskardsbreen; the overall relative glacial activity of the glacier outlet corresponds to this pattern.

7 Closing remarks

The Blådalen area at southern Folgefonna turned out to be an adequate location for proglacial sediment studies with the goal of reconstructing glacial activity. Several glacier outlets drain into numerous proglacial lakes. A limiting factor is the development of hydroelectric power in the area, which causes anthropogenic damming and tunnel constructions for a most effective use of the meltwaters. Artificial increased sedimentation rates, as well as eroded and re-deposited sediment falsified the glacial record in the proglacial sediments during the last five decades.

The proglacial sediment cores analyzed in this study were greatly disturbed in the course of the coring procedure. The reliability of the interpretation and discussion results were limited by this, especially with respect to the correlation of the two cores and the DBD record, which the continuous relative glacial activity curve of Vestre Blomsterskardsbreen was compiled from. An increased number of reliable radiocarbon dates could have improved the age-depth models and the calculated sedimentation rates. With that, comparisons to natural climate archives and other glacier reconstructions in the Northern Hemisphere would have been more reliable.

The difficultness of the terrain, especially north-west of Insta Botnane, prevented fieldwork in that area. Possible marginal moraines could therefore not be observed. A closer investigation of this area could be helpful to understand the LIA glacial history of Blomsterskardsbreen, especially with regard to the differences between Vestre and Østre Blomsterskardsbreen. In that respect, comparable proglacial sediment studies of Lake Blomstølskardvatn would be reasonable.

Proglacial sediment studies of the small lake in front of Vestre Blomsterskardsbreen (837 m a.s.l.) could give more specific knowledge about the LIA history of the glacier outlet with respect to the local overflow gap (spillway) which must have caused draining through this lake during periods of the LIA.

References

- AHNERT, F.** (2003): *Einführung in die Geomorphologie*. Verlag Eugen Ulmer, Stuttgart.
- AITKEN, M.J.** (1998): *An Introduction to Optical Dating: The Dating of Quaternary Sediments by the Use of Photon-stimulated Luminescence*. Oxford University Press, Oxford.
- ANDERSSON, C., B. RISEBROBAKKEN, E. JANSEN and S.O. DAHL** (2003): Late Holocene surface ocean conditions of the Norwegian Sea (Vøring Plateau). *Paleoceanography* **18**(2): 22.1-22.13.
- APPLEBY, P.G.** (2001): Chronostratigraphic techniques in recent sediments. In: W. M. Last and J. P. Smol (eds.): *Tracking Environmental Change Using Lake Sediments. Volume I: Basin Analysis, Coring, and Chronological Techniques*. Kluwer Academic Publishers, Dordrecht.
- APPLEBY, P.G.** (2008): Three decades of dating recent sediments by fallout radionuclides: a review. *The Holocene* **18**(1): 83-93.
- ARNAUD, F., M. LIGNIER, M. REVEL, M. DESMET, C. BECK, F. POURCHET, F. CHARLET, A. TRENTESAUX and N. TRIBOVILLARD** (2002): Flood and earthquake disturbance of ^{210}Pb geochronology (Lake Anterne, NW Alps). *Terra Nova* **14**: 225-232.
- ASHLEY, G.M.** (1995): Glaciolacustrine Environments. In: J. Menzies (eds.): *Modern Glacial Environments: Processes, Dynamics and Sediments*. Butterworth-Heinemann, Oxford.
- ASKVIK, H.** (1976): Hordalands berggrunnsgeologi. In: G. H. Hartvedt (eds.): *Bygd og by i Norge. Hordaland og Bergen*, Oslo.
- ASKVIK, H.** (1995): Oversikt over Norges Prekambriske og Paleozoiske berggrunn. Tekst til G 103 Historisk geologi, Department of Geology. University of Bergen.
- BAKKE, J.** (1999): Rekonstruksjon av bre- og klimavariasjoner på Nordre Folgefonna med kringliggende botnar. Master's thesis in physical geography, Department of Geography. University of Bergen.
- BAKKE, J.** (2004): Late Weichselian and Holocene glacier fluctuations along a south-north coastal transect in Norway: Climatic and methodological implications. Dissertation, Department of Geography. University of Bergen.
- BAKKE, J., S.O. DAHL and M. DIESEN** (2000): Folgefonna nasjonalpark: Oppfølgende utgreiingar 2000 Kvartærgeologi. Rapport, Department of Geography. University of Bergen.
- BAKKE, J., S.O. DAHL and A. NESJE** (2005a): Lateglacial and early Holocene palaeoclimatic reconstruction based on glacier fluctuations and equilibrium-line altitudes at northern Folgefonna, Hardanger, western Norway. *Journal of Quaternary Science* **20**(2): 179-198.
- BAKKE, J., S.O. DAHL, Ø. PAASCHE, R. LØVLIE and A. NESJE** (2005b): Glacier fluctuations, equilibrium-line altitudes and palaeoclimate in Lyngen, northern Norway, during the Lateglacial and Holocene. *The Holocene* **15**(4): 518-540.
- BAKKE, J., S.O. DAHL, Ø. PAASCHE, J.R. SIMONSEN, B. KVISVIK, K. BAKKE and A. NESJE** (2010): A complete record of Holocene glacier variability at Austre Okstindbreen, northern Norway: an integrated approach. *Quaternary Science Reviews* **29**: 1246-1262.
- BAKKE, J., Ø. LIE, S.O. DAHL, A. NESJE and A.E. BJUNE** (2008): Strength and spacial patterns of the Holocene wintertime westerlies in the NE Atlantic region. *Global and Planetary Change* **60**: 28-41.

- BAKKE, J., Ø. LIE, A. NESJE, S.O. DAHL and Ø. PAASCHE** (2005c): Utilizing physical sediment variability in glacier-fed lakes for continuous glacier reconstructions during the Holocene, northern Folgefonna, western Norway. *The Holocene* **15**(2): 161-176.
- BALLANTYNE, C.K.** (1989): The Loch Lomond Readvance on the Isle of Skye, Scotland: glacier reconstruction and palaeoclimatic implications. *Journal of Quaternary Science* **4**(2): 95-108.
- BALLANTYNE, C.K.** (2002): Paraglacial geomorphology. *Quaternary Science Reviews* **21**: 1935-2017.
- BALLANTYNE, C.K. and D.I. BENN** (1994): Paraglacial Slope Adjustment and Resedimentation Following Recent Glacier Retreat, Fåbergstølsdalen, Norway. *Arctic and Alpine Research* **26**(3): 255-269.
- BARD, E., B. HAMELIN, R.G. FAIRBANKS and A. ZINDLER** (1990): Calibration of the ¹⁴C time scale over the past 30,000 years using mass spectrometric U-Th ages from Barbados corals. *Nature* **345**: 405-409.
- BARD, E., G. RAISBECK, F. YIOU and J. JOUZEL** (2000): Solar irradiance during the last 1200 years based on cosmogenic nuclides. *Tellus* **52B**: 985-992.
- BARNEKOW, L.** (1999): Holocene tree-line dynamics and inferred climatic changes in the Abisko area, northern Sweden, based on macrofossil and pollen records. *The Holocene* **9**(3): 253-265.
- BEIERLE, B.D., S.F. LAMOUREUX, J.M.H. COCKBURN and I. SPOONER** (2002): A new method for visualizing sediment particle size distributions. *Journal of Paleolimnology* **27**: 279-283.
- BENN, D.I. and D.J.A. EVANS** (1998): *Glaciers and Glaciation*. Arnold, London.
- BENN, D.I. and A.M.D. GEMMELL** (1997) Calculating equilibrium-line altitudes of former glaciers by the balance ratio method: a new computer spreadsheet. *Glacial Geology and Geomorphology*, From <http://ggg.qub.ac.uk/ggg/> (02.12.2009).
- BENN, D.I. and F. LEHMKUHL** (2000): Mass balance and equilibrium-line altitudes of glaciers in high-mountain environments. *Quaternary International* **65/66**: 15-29.
- BENNETT, K.D.** (1994): Confidence intervals for age estimates and deposition times in late-Quaternary sediment sequences. *The Holocene* **4**(4): 337-348.
- BERGSTRØM, B., A. REITE, H. SVEIAN and L. OLSEN** (2001): Feltrutiner, kartleggingsprinsipper og standarder for kvartærgeologisk kartlegging/løsmassekartlegging ved NGU. *NGU Intern Rapport 2001.018*.
- BESCHEL, R.** (1950): Flechten als Altersmaßstab rezenter Moränen. *Zeitschrift für Gletscherkunde und Glazialgeologie* **1**: 152-161.
- BICKERTON, R.W. and J.A. MATTHEWS** (1992): On the accuracy of lichenometric dates: an assessment based on the "Little Ice Age" moraine sequence of Nigardsbreen, southern Norway. *The Holocene* **2**(3): 227-237.
- BICKERTON, R.W. and J.A. MATTHEWS** (1993): "Little Ice Age" variations of outlet glaciers from the Jostedalsbreen ice-cap, southern Norway: a regional lichenometric-dating study of ice-marginal moraine sequences and their climatic significance. *Journal of Quaternary Science* **8**(1): 45-66.
- BIRKS, H.H., R.W. BATTARBEE and H.J.B. BIRKS** (2000): The development of the aquatic ecosystem at Kråkenes Lake, western Norway, during the late-glacial and early-Holocene – a synthesis. *Journal of Paleolimnology* **23**: 91-114.
- BJELLAND, T.** (1998): Rekonstruksjon av Holocen skredaktivitet og brefluktuation i Buerdalen, Hardanger, Sør-Norge. Master's thesis in physical geography, Department of Geography. University of Bergen.

- BJUNE, A.E., J. BAKKE, A. NESJE and H.J.B. BIRKS** (2005): Holocene mean July temperature and winter precipitation in western Norway inferred from palynological and glaciological lake-sediment proxies. *The Holocene* **15**(2): 177-189.
- BJØNNES, E.** (2006): Rekonstruksjon av brefluktasjoner og klimavariasjon på Møsevassbreen, Folgefonna gjennom Holosen med hovedvekt på neoglasial tid og "Den Vesle Istida". Master's thesis in physical geography, Department of Geography. University of Bergen.
- BJÖRCK, S., M. RUNDGREN, Ó. INGÓLFSSON and S. FUNDER** (1997): The Preboreal oscillation around the Nordic Seas: terrestrial and lacustrine responses. *Journal of Quaternary Science* **12**(6): 455-465.
- BLAKE, G.R. and K.H. HARTGE** (1986): Bulk density. In: A. Klute (eds.): *Methods of Soil Analysis Part 1: Physical and Mineralogical Methods*. American Society of Agronomy Inc., Soil Science Society of America Inc., Wisconsin, USA: 363-375.
- BLOTT, S.J. and K. PYE** (2001): Gradstat: a grain size distribution and statistics package for the analysis of unconsolidated sediments. *Earth Surface Processes and Landforms* **26**: 1237-1248.
- BLUM, P.** (1997): *Reflectance, Spectrophotometry and Colorimetry*. In: PP Handbook: 4.1.-4.10.
- BOULTON, G.S.** (1979): Processes of glacier erosion on different substrata. *Journal of Glaciology* **23**: 15-38.
- BRADLEY, R.S.** (1999): *Paleoclimatology: Reconstructing Climates of the Quaternary*. Academic Press, San Diego, California.
- BREKKE, N.G., S. NORD, J. BAKKE, S. INDRELID, I. AARSETH and A. HAALAND** (2008): *Folgefonna og Fjordbygdene*. Bergen Museum and University of Bergen, Nord 4, Bergen.
- BRIFFA, K.R., P.D. JONES, F.H. SCHWEINGRUBER and T.J. OSBORN** (1998): Influence of volcanic eruptions on Northern Hemisphere summer temperature over the past 600 years. *Nature* **393**(4): 450-455.
- BRINER, J.P., P. THOMPSON DAVIS and G.H. MILLER** (2009): Latest Pleistocene and Holocene glaciation on Baffin Island, Arctic Canada: key patterns and chronologies. *Quaternary Science Reviews* **28**: 2075-2087.
- BROECKER, W.S.** (1991): The great ocean conveyor. *Oceanography* **4**: 79-89.
- BØE, A., S.O. DAHL, Ø. LIE and A. NESJE** (2006): Holocene river floods in the upper Glomma catchment, southern Norway: a high-resolution multiproxy record from lacustrine sediments. *The Holocene* **16**(3): 445-455.
- BØRRESEN, J. A.** (1987): *Wind Atlas for the North Sea and the Norwegian Sea*. The Norwegian Meteorological Institute, Oslo.
- CALVO, E., J. GRIMALT and E. JANSEN** (2002): High resolution U_{K37} sea surface temperature reconstruction in the Norwegian Sea during the Holocene. *Quaternary Science Reviews* **21**: 1385-1394.
- CHURCH, M. and J.M. RYDER** (1972): Paraglacial Sedimentation: A Consideration of Fluvial Processes Conditioned by Glaciation. *Geological Survey of America Bulletin* **83**: 3059-3072.
- COOK, E.R.** (2003): Multi-Proxy Reconstructions of the North Atlantic Oscillation (NAO) Index: A Critical Review and a New Well-Verified Winter NAO Index Reconstruction Back to AD 1400. In: J. W. Hurrell, Y. Kushnir, G. Ottersen and M. Visbeck (eds.): *The North Atlantic Oscillation: Climatic Significance and Environmental Impact*. Geophysical Monograph 134, American Geophysical Union, Washington, D.C.
- CRONIN, T.M., G.S. DWYER, T. KAMIYA, S. SCHWEDE and D.A. WILLARD** (2003): Medieval Warm Period, Little Ice Age and 20th century temperature variability from Chesapeake Bay. *Global and Planetary Change* **36**: 17-29.

- CROUDACE, I.W., A. RINDBY and R.G. ROTHWELL** (2006): ITRAX: description and evaluation of a new multi-function X-ray core scanner. In: R. G. Rothwell (eds.): *New Techniques in Sediment Core Analysis*. Geological Society, Special Publications, London. **267**: 51-63.
- DAHL, S.O., J. BAKKE, Ø. LIE and A. NESJE** (2003): Reconstruction of former glacier equilibrium-line altitudes based on proglacial sites: An evaluation of approaches and selection of sites. *Quaternary Science Reviews* **22**: 275-287.
- DAHL, S.O. and A. NESJE** (1992): Paleoclimatic implications based on equilibrium-line altitude depressions of reconstructed Younger Dryas and Holocene cirque glaciers in inner Nordfjord, western Norway. *Palaeogeography, Palaeoclimatology, Palaeoecology* **94**(87-97).
- DAHL, S.O. and A. NESJE** (1994): Holocene glacier fluctuations at Hardangerjøkulen, central southern Norway: a high-resolution composite chronology from lacustrine and terrestrial deposits. *The Holocene* **4**(3): 269-277.
- DAHL, S.O. and A. NESJE** (1996): A new approach to calculating Holocene winter precipitation by combining glacier equilibrium-line altitudes and pine-tree limits: a case study from Hardangerjøkulen, central southern Norway. *The Holocene* **6**(4): 381-398.
- DAHL, S.O., A. NESJE, Ø. LIE, K. FJORDHEIM and J.A. MATTHEWS** (2002): Timing, equilibrium-line altitudes and climatic implications of two early-Holocene glacier readvances during the Erdalen Event at Jostedalbreen, western Norway. *The Holocene* **12**(1): 17-25.
- DAHL, S.O., A. NESJE and J. ØVSTEDAL** (1997): Cirque glaciers as morphological evidence for a thin Younger Dryas ice sheet in east-central southern Norway. *Boreas* **26**: 161-180.
- DEARING, J. A.** (1999): *Environmental Magnetic Susceptibility. Using the Bartington MS2 System*. Chi Publishing, Kenilworth, England.
- DET NORSKE METEOROLOGISKE INSTITUTT** (2008): Climate data from The Norwegian Meteorological Institute (DNMI). From http://shimmer.oslo.dnmi.no/portal/page?_pageid=35,96278,35_96303&_dad=portal&_schema=PORTAL (16.03.2008).
- DET NORSKE METEOROLOGISKE INSTITUTT** (2009a): Map over precipitation values 1960-1991 of Norway from The Norwegian Meteorological Institute. From <http://met.no/Klima/Klimastatistikk/Klimanormaler/?module=Articles;action=ArticleFolder.publicOpenFolder;ID=651> (08.12.2009).
- DET NORSKE METEOROLOGISKE INSTITUTT** (2009b): Map over temperature values 1960-1991 of Norway from The Norwegian Meteorological Institute. From <http://met.no/Klima/Klimastatistikk/Klimanormaler/?module=Articles;action=ArticleFolder.publicOpenFolder;ID=390> (08.12.2009).
- EDVARDSSEN, I.** (2006): Paleoklimatisk rekonstruksjon av Sauabreen. Master's thesis in physical geography, Department of physical geography. University of Bergen.
- ELVEHØY, H.** (1997): Istykkelsesmålinger på Kjerringbotnbreen, Søndre Folgefonna. *Norwegian Water Resources and Energy Directorate (NVE), Rapport 22*.
- ELVEHØY, H.** (1998): Samanlikning av massebalanse på Hardangerjøkulen og Folgefonna. *Norwegian Water Resources and Energy Directorate (NVE), Rapport 5*.
- EMBLETON, C. and C.A.M. KING** (1975): *Glacial Geomorphology*. Arnold, London.
- ERIKSTAD, L. and J.L. SOLLID** (1986): Neoglaciation in South Norway using lichenometric methods. *Norsk Geografisk Tidsskrift* **40**: 85-105.
- FOLLESTAD, B.A.** (1970): Deglasiasjonsforløpet på den sydvestlige del av folgefonna. Master's thesis in quaternary geology and geomorphology. University of Bergen.

- FOSSEN, H.** (2004a): Hordaland på Høyde med Himalaya. In: W. Helland-Hansen (eds.): *Naturhistorisk Vegbok Hordaland*. Bergen Museum, Nord 4, Bergen.
- FOSSEN, H.** (2004b): Urtiden og grunnfjellet. In: W. Helland-Hansen (eds.): *Naturhistorisk Vegbok Hordaland*. Bergen Museum, Nord 4, Bergen.
- FURBISH, D.J. and J.T. ANDREWS** (1984): The Use of Hypsometry to indicate long-term stability and response of valley glaciers to changes in mass transfer. *Journal of Glaciology* **30**(105): 199-211.
- GEIRSDÓTTIR, Á., G.H. MILLER, Y. AXFORD and S. ÓLAFSDÓTTIR** (2009): Holocene and latest Pleistocene climate and glacier fluctuations in Iceland. *Quaternary Science Reviews* **28**: 2107-2118.
- GJESSING, J.** (1978): *Norges landformer*. Universitetsforlaget, Oslo.
- GODWIN, H.** (1962): Half-life of radiocarbon. *Nature* **195**: 984-984.
- GROVE, J.M.** (1988): *The Little Ice Age*. Methuen, London.
- GUYARD, H., E. CHAPRON, G. ST-ONGE, F.S. ANSELMETTI, F. ARNAUD, O. MAGAND, P. FRANCUS and M. MÉLIÈRES** (2007): High-altitude varve records of abrupt environmental changes and mining activity over the last 4000 years in the Western French Alps (Lake Bramant, Grandes Rousses Massif). *Quaternary Science Reviews* **26**: 2644-2660.
- HAAKENSEN, N.** (1989): Akkumulasjon på breene i Norge vinteren 1988-89. *Norwegian Water Resources and Energy Directorate (NVE), Publication no. 70 of the Department of Hydrology*.
- HAGEN, J.O., O. LIESTØL, J.L. SOLLID, B. WOLD and G. ØSTREM** (1993): Subglacial investigations at Bondhusbreen, Folgefonna, Norway. *Norsk Geografisk Tidsskrift* **47**: 117-162.
- HALDORSEN, S.** (1981): Grain-size distribution of subglacial till and its relation to glacial crushing and abrasion. *Boreas* **10**: 91-105.
- HALDORSEN, S.** (1983): Mineralogy and geochemistry of basal till and their relationship to till-forming processes. *Norsk Geologisk Tidsskrift* **63**: 15-25.
- HEIRI, O., A.F. LOTTER and G. LEMCKE** (2001): Loss on ignition as a method for estimating organic and carbonate content in sediments: reproducibility and comparability of results. *Journal of Paleolimnology* **25**: 101-110.
- HELLAND-HANSEN, W.** (2004): *Naturhistorisk Vegbok Hordaland*. Bergen Museum , Nord 4, Bergen.
- HELLELAND, B.** (2008): Namnelandskapet. Enn om vi kledde fjellet - med stadnamn? In: N. G. Brekke, S. Nord, J. Bakke, S. Indrelid, I. Aarseth and A. Haaland (eds.): *Folgefonna og Fjordbygdene*. Nord 4, Bergen.
- HICKS, D.M., M.J. MCSAVENEY and T.J.H. CHINN** (1990): Sedimentation in Proglacial Ivory Lake, Southern Alps, New Zealand. *Arctic and Alpine Research* **22**(1): 26-42.
- HOPKINS, T.S.** (1991): The GIN-Sea-a synthesis of its physical oceanography and literature review 1972-1985. *Earth-Science Reviews* **30**: 175-318.
- HUMLUM, O., B. ELBERLING, A. HORMES, K. FJORDHEIM, O.H. HANSEN and J. HEINEMEIER** (2005): Late-Holocene glacier growth in Svalbard, documented by subglacial relict vegetation and living soil microbes. *The Holocene* **15**(3): 396-407.
- HURRELL, J.W., Y. KUSHNIR, G. OTTERSEN and M. VISBEK** (2003): An overview of the North Atlantic Oscillation. In: J. W. Hurrell, Y. Kushnir, G. Ottersen and M. Visbeck (eds.): *The North Atlantic Oscillation. Climatic Significance and Environmental impact*. Geophysical Monograph 134, American Geophysical Union, Washington, DC.
- INNES, J.L.** (1985a): Lichenometry. *Progress in Physical Geography* **9**: 187-254.

- INNES, J.L.** (1985b): A standard *Rhizocarpon* nomenclature for lichenometry. *Boreas* **14**: 83-85.
- INNES, J.L.** (1986): The Use of Percentage Cover Measurements in Lichenometric Dating. *Arctic and Alpine Research* **18**(2): 209-216.
- IVY-OCHS, S., H. KERSCHNER, M. MAISCH, M. CHRISTL, P.W. KUBIK and C. SCHLÜCHTER** (2009): Latest Pleistocene and Holocene glacier variations in the European Alps. *Quaternary Science Reviews* **28**: 2137-2149.
- JANSEN, E., J.T. OVERPECK, K.R. BRIFFA, J.-C. DUPLESSY, F. JOOS, V. MASSON-DELMOTTE, D. OLAGO, B. OTTO-BLIESNER, W.R. PELTIER, S. RAHMSTORF, R. RAMESH, D. RAYNAUD, D. RIND, O. SOLOMINA, R. VILLALBA and D. ZHANG** (2007): Palaeoclimate. In: S. Solomon, D. Qin, M. Manning, Z. Chen, M. Marquis, K. B. Averyt, M. Tignor and H. L. Miller (eds.): *Climate Change 2007: The Physical Science Basis. Contribution of Working Group I to the Fourth Assessment Report of the Intergovernmental Panel on Climate Change*. Cambridge University Press, Cambridge, United Kingdom and New York, NY, USA.
- JONES, P.D. and K.R. BRIFFA** (2001): The "Little Ice Age": Local and Global Perspectives. *Climatic Change* **48**: 5-8.
- KARLÉN, W.** (1976): Lacustrine Sediments and Tree-Limit Variations as Indicators of Holocene Climatic Fluctuations in Lappland, Northern Sweden. *Geografiska Annaler Series A Physical Geography* **58**(1/2): 1-34.
- KARLÉN, W.** (1979): Glacier Variations in the Svartisen Area, Northern Norway. *Geografiska Annaler. Series A, Physical Geography* **61**(1/2): 11-28.
- KARLÉN, W.** (1981): Lacustrine Sediment Studies. A Technique to Obtain a Continuous Record of Holocene Glacier Variations. *Geografiska Annaler Series A Physical Geography* **63**(3/4): 237-281.
- KARLÉN, W. and J.A. MATTHEWS** (1992): Reconstructing Holocene Glacier Variations from Glacial Lake Sediments: Studies from Nordvestlandet and Jostedalbreen-Jotunheimen, Southern Norway. *Geografiska Annaler Series A Physical Geography* **74**(4): 327-348.
- KARLÉN, W. and G. ROSQVIST** (1988): Glacier Fluctuations Recorded in Lacustrine Sediments in Mount Kenya. *National Geographic Research* **4**(2): 219-232.
- KENNETT, M. and A.C. SÆTRANG** (1987): Istykkelsesmålinger på Folgefonna. *Norwegian Water Resources and Energy Directorate (NVE), Rapport 18*.
- KIRKBRIDE, M.P. and A.J. DUGMORE** (2008): Two millenia of glacier advances from southern Iceland dated by tephrochronology. *Quaternary Research* **70**: 398-411.
- KJØLLMOEN, B.** (2009): Folgefonna. In: B. Kjøllmoen (eds.): *Glaciological investigations in Norway in 2008. Report No. 2*. The Norwegian Water Resources and Energy Directorate (NVE), Oslo.
- LEEDER, M.R.** (1982): *Sedimentology*. George Allen & Unwin, London.
- LEEMANN, A. and F. NIESSEN** (1994): Holocene glacial activity and climatic variations in the Swiss Alps: reconstructing a continuous record from proglacial lake sediments. *The Holocene* **4**(3): 259-268.
- LEONARD, E.M.** (1985): Glaciological and climatic controls on lake sedimentation, Canadian Rocky Mountains. *Zeitschrift für Gletscherkunde und Glazialgeologie* **21**: 35-42.
- LEONARD, E.M.** (1986a): Use of Lacustrine Sedimentary Sequences as Indicators of Holocene Glacial History, Banff National Park, Alberta, Canada. *Quaternary Research* **26**: 218-231.
- LEONARD, E.M.** (1986b): Varve Studies at Hector Lake, Alberta, Canada, and the Relationship between Glacial Activity and Sedimentation. *Quaternary Research* **25**: 199-214.

- LINDERHOLM, H.W. and B.E. GUNNARSON** (2005): Summer temperature variability in central Scandinavia in the last 3600 years. *Geografiska Annaler* **87A**: 231-241.
- LUTRO, O.** (2005): *Geological map of the Folgefonna Peninsula*. Geological Survey of Norway (NGU), unpublished.
- MANN, M.E., Z. ZHANG, S. RUTHERFORD, R.S. BRADLEY, M.K. HUGHES, D. SHINDELL, C. AMMANN, G. FALUVEGI and F. NI** (2009): Global Signatures and Dynamical Origins of the Little Ice Age and Medieval Climate Anomaly. *Science* **326**: 1256-1260.
- MATTHES, F.E.** (1939): Report of Committee on Glaciers, April 1939. *Transactions of the American Geophysical Union* **20**: 518-523.
- MATTHEWS, J.A.** (1975): Experiments on the reproducibility and reliability of lichenometric dates, Storbreen gletschervorfeld, Jotunheimen, Norway. *Norsk Geografisk Tidsskrift* **29**: 97-109.
- MATTHEWS, J.A.** (1994): Lichenometric dating: a review with particular reference to "Little Ice Age" moraines in southern Norway. In: C. Beck (eds.): *Dating in exposed and surface contexts*. University of Mexico Press, Albuquerque.
- MATTHEWS, J.A.** (2005): "Little Ice Age" glacier variations in Jotunheimen, southern Norway: a study in regionally controlled lichenometric dating of recessional moraines with implications for climate and lichen growth rates. *The Holocene* **15**(1): 1-19.
- MATTHEWS, J.A., M.S. BERRISFORD, P.Q. DRESSER, A. NESJE, S.O. DAHL, A.E. BJUNE, J. BAKKE, H.J.B. BIRKS, Ø. LIE, L. DUMAYNE-PEATY and C. BARNETT** (2005): Holocene glacier history of Bjørnbreen and climatic reconstruction in central Jotunheimen, Norway, based on proximal glaciofluvial stream-bank mires. *Quaternary Science Reviews* **24**: 67-90.
- MATTHEWS, J.A., S.O. DAHL, A. NESJE, M.S. BERRISFORD and C. ANDERSSON** (2000): Holocene glacier variations in central Jotunheimen, southern Norway, based on distal glaciolacustrine sediment cores. *Quaternary Science Reviews* **19**(16): 1625-1647.
- MATTHEWS, J.A. and W. KARLÉN** (1992): Asynchronous neoglaciation and Holocene climatic change reconstructed from Norwegian glaciolacustrine sedimentary sequences. *Geology* **20**(11): 991-994.
- MCCARROLL, D.** (1994): A new approach to lichenometry: dating single-age and diachronous surfaces. *The Holocene* **4**: 383-396.
- MCCARROLL, D.** (2001): Enhanced Rockfall Activity during the Little Ice Age: Further Lichenometric Evidence from a Norwegian Talus. *Permafrost and Periglacial Processes* **12**: 157-164.
- MENOUNOS, B.** (1997): The water content of lake sediments and its relationship to other physical parameters: an alpine case study. *The Holocene* **7**: 207-212.
- MENZIES, J.** (1995): Hydrology of glaciers. In: J. Menzies (eds.): *Modern Glacial Environments: Processes, Dynamics and Sediments*. Butterworth-Heinemann, Oxford.
- MOORE, T.C. JR., D.K. REA and H. GODSEY** (1998): Regional variation in modern radiocarbon ages and the hard-water effects in Lakes Michigan and Huron. *Journal of Paleolimnology* **20**: 347-351.
- MØLLER, J. and B. HOLMESLET** (1998): SeaLevel Change Ver.3.51. *University of Tromsø*. From www.imv.uit.no/english/science/sealev/index.htm (10.04.2010).
- NESJE, A.** (1992): A Piston Corer for Lacustrine and Marine Sediments. *Arctic and Alpine Research* **24**(3): 257-259.
- NESJE, A.** (1995): *Brelære*. Høyskoleforlaget AS, Kristiansand.
- NESJE, A., J. BAKKE, S.O. DAHL, Ø. LIE and J.A. MATTHEWS** (2008): Norwegian mountain glaciers in the past, present and future. *Global and Planetary Change* **60**: 10-27.

- NESJE, A. and S.O. DAHL** (1991a): Holocene Glacier Variations of Blåisen, Hardangerjøkulen, Central Southern Norway. *Quaternary Research* **35**: 25-40.
- NESJE, A. and S.O. DAHL** (1991b): Late Holocene glacier fluctuations in Bevringsdalen, Jostedalbreen region, western Norway (ca 3200-1400 BP). *The Holocene* **1**(1): 1-7.
- NESJE, A. and S.O. DAHL** (2000): *Glaciers and Environmental Change*. Arnold, London.
- NESJE, A. and S.O. DAHL** (2003): The "Little Ice Age" - only temperature? *The Holocene* **13**(1): 139-145.
- NESJE, A., S.O. DAHL, C. ANDERSSON and J.A. MATTHEWS** (2000a): The lacustrine sedimentary sequence in Sygneskardvatnet, western Norway: a continuous, high-resolution record of the Jostedalbreen ice cap during the Holocene. *Quaternary Science Reviews* **19**(11): 1047-1065.
- NESJE, A., S.O. DAHL and R. LØVLIE** (1995): Late Holocene glacier and avalanche activity in the Alftobreen area, western Norway: evidence from a lacustrine sedimentary record. *Norsk Geologisk Tidsskrift* **75**(2-3): 120-126.
- NESJE, A., S.O. DAHL, A.M. TVEDE and J. BAKKE** (2004): Breen. Klimaindikator og landskapsskulptør. In: W. Helland-Hansen (eds.): *Naturhistorisk Vegbok Hordaland*. Bergen Museum, Nord 4, Bergen.
- NESJE, A., E. JANSEN, H.J.B. BIRKS, A.E. BJUNE, J. BAKKE, C. ANDERSSON, S.O. DAHL, D. KLITGAARD KRISTENSEN, S. LAURITZEN, Ø. LIE, B. RISEBROBAKKEN and J SVENDSEN** (2005): Holocene Climate Variability in the Northern North Atlantic Region: A Review of Terrestrial and Marine Evidence. In: H. Drange, T. Dokken, T. Furevik, R. Gerdes and W. Berger (eds.): *The Nordic Seas: An Integrated Perspective. Oceanography, Climatology, Biogeochemistry, and Modeling*. Geophysical Monograph 158, American Geophysical Union, Washington, D.C.
- NESJE, A. and M. KVAMME** (1991): Holocene glacier and climate variations in western Norway: Evidence for early Holocene glacier demise and multiple Neoglacial events. *Geology* **19**: 610-612.
- NESJE, A., M. KVAMME, N. RYE and R. LØVLIE** (1991): Holocene glacial and climate history of the Jostedalbreen region, western Norway; evidence from lake sediments and terrestrial deposits. *Quaternary Science Reviews* **10**(1): 87-114.
- NESJE, A., Ø. LIE and S.O. DAHL** (2000b): Is the North Atlantic Oscillation reflected in Scandinavian glacier mass balance records? *Journal of Quaternary Science* **15**: 587-601.
- NESJE, A., J.A. MATTHEWS, S.O. DAHL, M.S. BERRISFORD and C. ANDERSSON** (2001): Holocene glacier fluctuations of Flatebreen and winter precipitation changes in the Jostedalbreen region, western Norway, based on glaciolacustrine sediment records. *The Holocene* **11**: 267-280.
- NICHOLS, G.** (1999): *Sedimentology and Stratigraphy*. Blackwell Science, London.
- NORDLI, Ø., Ø. LIE, A. NESJE and R.E. BENESTAD** (2005): Glacier mass balance in southern Norway modelled by circulation indices and spring-summer temperatures AD 1781-2000. *Geografiska Annaler Series A Physical Geography* **87A**(3): 431-445.
- OSBORN, G., B. MENOUNOS, J. KOCH, J.J. CLAGUE and V. VALLIS** (2007): Multi-proxy record of Holocene glacial history of the Spearhead and Fitzsimmons ranges, southern Coast Mountains, British Columbia. *Quaternary Science Reviews* **26**: 479-493.
- OSMASTON, H.** (2005): Estimates of glacier equilibrium line altitudes by the Area x Altitude, the Area x Altitude Balance Ratio and the Area x Altitude Balance Index methods and their validation. *Quaternary International* **138-139**: 22-31.
- OSWALD, W.W., P.M. ANDERSON, T.A. BROWN, L.B. BRUBAKER, F.S. HU, A.V. LOZHKIN, W. TINNER and P. KALTENRIEDER** (2005): Effects of sample mass

- and macrofossil type on radiocarbon dating of arctic and boreal lake sediments. *The Holocene* **15**(5): 758-767.
- OWEN, L.A.** (2009): Latest Pleistocene and Holocene glacier fluctuations in the Himalaya and Tibet. *Quaternary Science Reviews* **28**: 2150-2164.
- PATERSON, W.S.B.** (1994): *The Physics of Glaciers*. An imprint of Elsevier Science Ltd., Butterworth-Heinemann, Oxford.
- PORTER, S.C.** (1975): Equilibrium-Line Altitudes of Late Quaternary Glaciers in the Southern Alps, New Zealand. *Quaternary Research* **5**: 27-47.
- PORTER, S.C.** (1986): Pattern and forcing of the northern hemisphere glacier variations during the last millenium. *Quaternary Research* **26**: 27-48.
- PYE, K.** (1994): *Sediment Transport and Depositional Processes*. Blackwell Scientific Publications, Oxford.
- PYTTE, R.** (1969): Glasiologiske undersøkelser i Norge 1968. *Water Resources Directorate, Department of Hydrology, Rapport 5/69, Oslo*.
- REKSTAD, J.** (1905): Iagttagelser fra Folgefonnens bræer. *Norges geologiske Undersøkelse, Aarbog for 1905*, **43**.
- RISAN, K. Å.** (1950): Om Kvinnherads Kwartærgeologi. Master's thesis in physical geography. University of Oslo.
- ROLAND, E. and N. HAAKENSEN** (1985): Glasiologiske undersøkelser i Norge 1982 (with English summary). *Norwegian Water Resources and Energy Directorate (NVE), Department of Hydrology, Rapport 1*: 1-102.
- ROSQVIST, G., C. JONSSON, R. YAM, W. KARLÉN and A. SHEMESH** (2004): Diatom oxygen isotopes in pro-glacial lake sediments from northern Sweden: a 5000 year record of atmospheric circulation. *Quaternary Science Reviews* **23**(7-8): 851-859.
- ROTHWELL, R.G., B. HOOGAKKER, J. THOMSON, I.W. CROUDACE and M. FRENZ** (2006): Turbidite emplacement on the southern Belearic Abyssal Plain (western Mediterranean Sea) during Marine Isotope Stages 1-3: an application of ITRAX XRF scanning of sediment cores to lithostratigraphic analysis. In: R. G. Rothwell (eds.): *ITRAX: description and evaluation of a new multi-function X-ray core scanner*. Geological Society, Special Publications, London. **267**: 79-98.
- RYVARDEN, L. and B. WOLD** (1991): *Norges isbreer*. Universitetsforlaget, Oslo.
- S.KRISHNASWAMY, D., J.M. MARTIN and M. MEYBECK** (1971): Geochronology of Lake Sediments. *Earth and Planetary Science Letters* **11**: 407-414.
- SANDGREN, P. and I. SNOWBALL** (2001): Application of Mineral Magnetic Techniques to Paleolimnology. In: W. M. Last and J. P. Smol (eds.): *Tracking Environmental Change Using Lake Sediments, Volume 2, Physical and Chemical Methods*. Kluwer Academic Publishers, Dordrecht.
- SANTISTEBAN, J.I., R. MEDIAVILLA, E. LÓPEZ-PAMO, C.J. DABRIO, M.B.R. ZAPATA, M.J.G. GARCÍA, S. CASTAÑO and P.E. MARTÍNEZ-ALFARO** (2004): Loss on ignition: a qualitative or quantitative method for organic matter and carbonate mineral content in sediments? *Journal of Paleolimnology* **32**: 287-299.
- SEXE, S.A.** (1864): *Om Sneebræen Folgefon*, Christiania.
- SHANAHAN, T.M., J.T. OVERPECK, J.B. HUBENY, J. KING, F.S. HU, K. HUGHEN, G. MILLER and J. BLACK** (2008): Scanning micro-X-ray fluorescence elemental mapping: A new tool for the study of laminated sediment records. *Geochemistry, Geophysics, Geosystems* **9**(2): 1-14.
- SHANMUGAM, G.** (1997): The Bouma Sequence and the turbidite mind set. *Earth-Science Reviews* **42**: 201-229.
- SIMONSEN, J.R.** (1999): Rekonstruksjon av Holocene brevariasjoner for vestre del av Søndre Folgefonna. Master's thesis in physical geography, Department of Geography. University of Bergen.

- SISSONS, J.B.** (1979): Palaeoclimatic inferences from former glaciers in Scotland and the Lake District. *Nature* **278**: 518-521.
- SIX, D., L. REYNAUD and A. LETRÉGUILLY** (2001): Bilans de masse des glaciers alpins et scandinaves, leurs relations avec l'oscillation du climat de l'Atlantique nord. *Earth and Planetary Sciences* **333**: 693-698.
- SKAAR, E.** (2004): Nedbør. Regn og Snø i Noregs våtaste fylke. In: W. Helland-Hansen (eds.): *Naturhistorisk Vegbok Hordaland*. Bergen Museum, Nord 4, Bergen.
- SMART, P.L. and P.D. FRANCES** (1991): *Quaternary Dating Methods – A User's Guide. Technical Guide 4*. Quaternary Research Association, Cambridge.
- SMITH-MEYER, S. and A.M. TVEDE** (1996): Volumendringer på Søndre Folgefonna mellom 1959 og 1995. *Norwegian Water Resources and Energy Directorate (NVE), Rapport 36*.
- SOUCH, C.** (1994): A Methodology to Interpret Downvalley Lake Sediments as Records of Neoglacial Activity: Coast Mountains, British Columbia, Canada. *Geografiska Annaler Series A Physical Geography* **76**(3): 169-185.
- STATENS VEGVESEN, NORSK INSTITUTT FOR SKOG OG LANDSKAP and STATENS KARTVERK** (2006): Norge i bilder. From <http://www.norgebilder.no/> (19.03.2008).
- STRAHLER, A. and A. STRAHLER** (2006): *Introducing Physical Geography*. John Wiley & Sons, Inc., Hoboken.
- STUIVER, M. and P.J. REIMER** (1993): Extended ^{14}C data base and revised CALIB 3.0 ^{14}C age calibration program. *Radiocarbon* **35**(1): 215-230.
- STUIVER, M., P.J. REIMER and R. REIMER** (2005): Calib Radiocarbon Calibration CALIB 5.0. From <http://calib.qub.ac.uk/calib/> (04.05.2008).
- STØREN, E. NAGEL** (2006): Rekonstruksjon av sen-holosene brevariasjoner og skråningsprosesser. En studie av innsjøsedimenter fra Russvatn i Øst-Jotunheimen. Master's thesis in physical geography, Department of Geography. University of Bergen.
- SULEBAK, J.R.** (2007): *Landformer og prosesser. En innføring i naturgeografiske tema*. Fagbokforlaget, Bergen.
- SUMMERFIELD, M.A.** (1991): *Global Geomorphology. An introduction to the study of landforms*. Longman Scientific and Technical, Harlow, England.
- SUNDBORG, A.** (1956): The River Klarälven, a study of fluvial processes. *Geografiska Annaler* **38**: 125-316.
- SUTHERLAND, D.G.** (1984): Modern glacier characteristics as a basis for inferring former climates with particular reference to the Loch Lomond Stadial. *Quaternary Science Reviews* **3**: 291-309.
- TELFORD, R.J., E. HEEGAARD and H.J.B. BIRKS** (2004): All age-depth models are wrong: but how badly? *Quaternary Science Reviews* **23**: 1-5.
- THOMPSON, R., R.W. BATTARBEE, P.E. O'SULLIVAN and F. OLDFIELD** (1975): Magnetic Susceptibility of Lake Sediments. *Limnology and Oceanography* **20**(5): 687-698.
- THORESEN, M.K.** (1991): *Kvartærgeologisk kart over Norge, tema: Jordarter*. Norges Geologiske Undersøkelse, Statens Kartverk, Trondheim.
- TJELMELAND, S.** (1992): *Blåfalli Anleggsarbeid i Martre i 45 år*. Sunnhordalands Kraftlag, Stord.
- TOLO, A. JØRDRE** (2008): Brefluktuasjoner og klimaendringer på Dettebrea, Folgefonna, gjennom Sein-Holosen. Master's thesis in physical geography, Department of Geography. University of Bergen.
- TORSNES, I., N. RYE and A. NESJE** (1993): Modern and Little Ice Age Equilibrium-line Altitudes on Outlet Valley Glaciers from Jostedalsbreen, Western Norway: an

- Evaluation of Different Approaches to their Calculation. *Arctic and Alpine Research* **25**(2): 106-116.
- TVEDE, A.M.** (1972): En glasio-klimatisk undersøkelse av Folgefonni. Master's thesis in physical geography. University of Oslo.
- TVEDE, A.M.** (1973): Folgefonni – En glasiologisk avvikar. *Naturen* **1**: 11-16.
- TVEDE, A.M.** (1994): Blomsterskardbreen, Folgefonni. En oversikt over breens variasjoner i nyere tid. *Norwegian Water Resources and Energy Directorate (NVE), Rapport 22*.
- TVEDE, A.M.** (2008): Den store Fonna. Om glasiologi, hydrologi og klima. In: N. G. Brekke, S. Nord, J. Bakke, S. Indrelid, I. Aarseth and A. Haaland (eds.): *Folgefonna og Fjordbygdene*. Bergen Museum and University of Bergen, Nord 4, Bergen.
- TVEDE, A.M. and T. LAUMANN** (1996): Glacial variations on a meso-scale: examples from glaciers in the Aurland Mountains, southern Norway. *Annals of Glaciology* **24**: 130-134.
- TVEDE, A.M. and O. LIESTØL** (1977): Blomsterskardbreen, Folgefonni, mass balance and recent fluctuations. *Reprint from Norsk Polarinstitutt Årbok 1976*: 225-234.
- UTAAKER, K.** (2004): Vestavêt. Vêr og klima på vestkysten. In: W. Helland-Hansen (eds.): *Naturhistorisk Vegbok Hordaland*. Bergen Museum, Nord 4, Bergen.
- VINCENT, C., E. LE MEUR and D. SIX** (2005): Solving the paradox of the end of the Little Ice Age in the Alps. *Geophysical Research Letters* **32**: 1-4.
- VORREN, T.O.** (1977): Grain-size distribution and grain-size parameters of different till types on Hardangervidda, south Norway. *Boreas* **6**: 219-227.
- VOSTER, J.V.** (2007): Raunsdalen - en dal i endring. Arealbruk og klima som årsaker for endringer i fjellvegetasjonen. Master's thesis in physical geography, Department of Geography. University of Bergen.
- WEBB, P.A.** (2004): The Perseverance of the Sedigraph Method and Particle Sizing. From http://www.micromeritics.com/Repository/Files/sedigraph_method.pdf (20.12.2009).
- WINKLER, S.** (2003): A new interpretation of the date of the “Little Ice Age” glacier maximum at Svartisen and Okstindan, northern Norway. *The Holocene* **13**(1): 83-95.
- WINKLER, S.** (2004): Lichenometric dating of the “Little Ice Age” maximum in Mt Cook National Park, Southern Alps, New Zealand. *The Holocene* **14**(6): 911-920.
- ØSTREM, G.** (1975): Sediment transport in glacial meltwater streams. In: A. Jopling and B. Mc Donald (eds.): *Glaciofluvial and glaciolacustrine sedimentation*. Society of Economic Palaeontologists and Mineralogists, Special Publication: 101-122.
- ØSTREM, G., K. DALE SELVIG and K. TANDBERG** (1988): Atlas over breer i Sør-Norge (Atlas of glaciers in south Norway). *Norwegian Water Resources and Energy Directorate (NVE), Publication no. 61 of the Department of Hydrology*.

Appendix

1.) Quaternary map of Blomsterskardsbreen and Midtbotnvatn (see end of the thesis)

2.) Analyses raw data and dating results:

CD (at the paperback of the thesis) including

- DBD, LOI₅₅₀, LOI₉₅₀, WC
- MS
- Grain size distribution (Sedigraph)
- XRF
- X-ray
- Radiocarbon dating reports
- Lead dating report
- Digital copy of Quaternary map of Blomsterskardsbreen and Midtbotnvatn

3.) Procedure LOI:

The first step after taking out samples of 1 cm³ volumes at intervals of 0.5 cm of core length is to dry those minimum twelve hours in an oven at 105°C, in order to remove all water and to reach constant weight of each sample. The weight loss through the drying process at 105°C indicates the quantity of water within the sample, which is a degree for the dry bulk density (DBD) (gr/cm³) (cp. Chapter 3.4.3). The LOI in per cent after drying at 105°C (LOI₁₀₅) can be calculated through Equation 2:

$$LOI_{105} = \left(\frac{WS - DW_{105}}{WS} \right) * 100$$

Equation 2 LOI in per cent after drying at 105°C (Santisteban et al. 2004, 289)

WS is the weight in g of the air-dried sample and DW₁₀₅ is the dry weight in g of the sample heated at 105°C.

The second step is to heat the dried samples in a muffle furnace up to 550°C. At that heat, organic matter is oxidised to ash and carbon dioxide. After ignition, the samples are cooled down under vacuum in an exsiccator (in order to avoid moisture absorption during cooling) and finally weighed. The amount of weight loss after combustion is proportional to the

amount of organic content in the original sample (Heiri et al. 2001). The LOI in per cent after heating up to 550°C (LOI_{550}) can be calculated through Equation 3:

$$LOI_{550} = \left(\frac{DW_{105} - DW_{550}}{DW_{105}} \right) * 100$$

Equation 3 LOI in per cent after heating up to 550°C (Heiri et al. 2001, 102)

DW_{105} is the weight in g of the dried sample at 105°C, and DW_{550} is the weight in g of the sample after heating up to 550°C.

The third step of the LOI procedure it to heat the samples (5 cm intervals) up to 950°C, which destroys most carbonate minerals, leaving oxide (Heiri et al. 2001; Santisteban et al. 2004). Equation 4 shows how the LOI in per cent after heating up to 950°C (LOI_{950}) is calculated:

$$LOI_{950} = \left(\frac{DW_{550} - DW_{950}}{DW_{105}} \right) * 100$$

Equation 4 LOI in per cent after heating up to 950°C (Heiri et al. 2001, 102)

DW_{105} is the weight in g of the dried sample at 105°C, DW_{550} is the weight in g of the sample after heating up to 550°C, and DW_{950} is the weight in g of the sample after heating up to 950°C (Heiri et al. 2001). The amount of inorganic carbonate (C_i) in the original sample is then obtained through Equation 5:

$$C_i = 1.36 * LOI_{950}$$

Equation 5 Amount of carbonate (C) in the sample (Heiri et al. 2001, 102)

4.) Procedure grain size distribution:

A Micromeritics SediGraph III 5120 Particle Size Analyzer was used to perform the grain-size distribution analysis. During preparation for the analysis, each sample (6 to 7g) was sieved through a 125 μm sieve and mixed with 70 ml of calgon 0.05 % solution.

The SediGraph measures the settling velocity of gravitational sedimentation by relative absorption of a horizontally collimated beam of low-energy X-rays, and uses the percentage of particle mass and calculated particle falling rates to determine the grain size distribution. The relationship between settling velocity and particle diameter is described by Stokes' law,

which states that the terminal settling velocity of a spherical particle in a fluid medium is proportional to the square of the particle diameter (Webb 2004, 1ff).

The program Gradistat 4.0 was used to handle and save the raw data (Blott and Pye 2001). The size scale adopted in the Gradistat program with respect to the grain sizes is as follows: Very fine sand (63-125 μm), very coarse silt (31-63 μm), coarse silt (16-31 μm), medium silt (8-16 μm), fine silt (4-8 μm), very fine silt (2-4 μm) and clay (<2 μm) (Blott and Pye 2001). Besides this grain sizes, the parameters mean grain size and sorting were used to classify depositional processes (cp. Arnaud et al. 2002).